Isothermal microcalorimetry as a novel microbiological tool for industrial production process control: A case study of a commercial probiotic

MIROSLAV CABADAJ

Thesis submitted to University College London
for the degree of Doctor of Philosophy

2025

Department of Pharmaceutics
UCL School of Pharmacy
29-39 Brunswick Square
London WC1N 1AX

Declaration

I, Miroslav Cabadaj, confirm that the work presented in this thesis is my own. Where information has been derived from other sources, I confirm that this has been indicated in the thesis.

Signed: M. Cabadaj

Date: 07.03.2025

Abstract

Safety and quality assurance testing must be an integral part of any industrial fermentation production process. It is challenging to find a method that is fast, reliable and simple to perform and which can deal with samples containing very high initial bacterial loads and that can be incorporated easily into an in-house testing procedure. Isothermal microcalorimetry (IMC) can possibly fulfil all the above.

The work reported in this thesis investigated the suitability and applicability of IMC in real-world problem-solving. An industrially produced commercial probiotic was taken for a model study. The approach taken was two-phased: pragmatic and theoretical.

The pragmatic phase consisted of a proof of concept that IMC has the capacity to determine, consistently and with a high degree of reproducibility, that the fermentations resulted in a good product, as precisely or better than traditional microbiological plating methods. Samples taken directly from the real fermentation process were tested using IMC and resulted in much faster turnaround testing times; higher reproducibility of the experiments; and better sensitivity in observing good versus contaminated samples.

The theoretical phase consisted of developing simple equations describing exponential bacterial growth and deriving quantitative parameters such as growth rate, intercept and area under curve.

The two phases complemented each other resulting in the practical application of the developed theory. This was done by studying *L. rhamnosus* in a controlled growth medium (MRS broth) and establishing standard references (these did not exist previously). The IMC test designed was to rapidly get permission from the management of the company to bottle the finished product and save as much time as possible from the end of the fermentation to bottling and sale with a demonstrated better accuracy that the traditional microbiological plating methods (these methods required up to two weeks of testing time). IMC was shown to be a fast (10-15 hours) and accurate method (± 3%) to get accept/reject result for the selected microbiological system with potential to be employed in other similar processes.

Impact statement

The main aim of this industrially based project was concerned with the improvement of turnaround testing times from fermentation completion of commercial probiotic to release to sale, using isothermal microcalorimetry (IMC). The work on this pragmatic aim resulted in a remarkably successful outcome which meant that the testing time was reduced from 7-15 days to 11-12 hours. The method developed here is in principle applicable to any industry where fermentation takes place, and or contamination detection is important.

This success also involved extension of this IMC based project into the theoretical area; equations describing the exponential growth of microorganisms were developed in order to advance the matrix of data (parameters) and the theoretical interpretation of the power-time curve to yield more secure decisions about fermentation success. As a part of the theoretical success a publication (Cabadaj *et al*., 2021) was released, which also dealt with the prospect of automatisation of data processing — a black-box solution.

There are a lot of situations in which it would be rational and plausible to explore the utility of the systems developed here (microorganisms in a growth medium with resulting matrices of comparable quantitative parameters) for example, real time analysis of the kinetics of drug cell interactions (an unexplored area in calorimetry).

Through the work presented herein the field of calorimetry and its crossover with practical and fundamental microbiology have been advanced. Future publications will result from data gathered during this work, both based on theory and on the practical developments in industrial as well as academic settings. These will significantly contribute to the fields of calorimetry, microbiology and biotechnology at large.

UCL Research Paper Declaration Form

referencing the doctoral candidate's own published work(s)

Please use this form to declare if parts of your thesis are already available in another format, e.g., if data, text, or figures:

- *have been uploaded to a preprint server*
- *are in submission to a peer-reviewed publication*
- *have been published in a peer-reviewed publication, e.g., journal, textbook.*

This form should be completed as many times as necessary. For instance, if you have seven thesis chapters, two of which containing material that has already been published, you would complete this form twice.

1. **For a research manuscript that has already been published** (if not yet published, please skip to section 2)

   a) **What is the title of the manuscript?**

   Kinetic analysis of microcalorimetric data derived from microbial growth: Basic theoretical, practical and industrial considerations

   b) **Please include a link to or doi for the work**

   https://doi.org/10.1016/j.mimet.2021.106276

   c) **Where was the work published?**

   Journal of Microbiological Methods

   d) **Who published the work?** (*e.g.*, OUP)

   Elsevier

   e) **When was the work published?**

   30.06.2021

   f) **List the manuscript's authors in the order they appear on the publication**

   Miroslav Cabadaj, Shazia Bashir, David Haskins, Jawal Said, Laura McCoubrey, Simon Gaisford, Anthony Beezer

   g) **Was the work peer reviewed?**

   Yes

   h) **Have you retained the copyright?**

   Yes

   i) **Was an earlier form of the manuscript uploaded to a preprint server?** (*e.g.*, medRxiv). If 'Yes', please give a link or doi)

   Click or tap here to enter text.

   If 'No', please seek permission from the relevant publisher and check the box next to the below statement:

   ☐

*I acknowledge permission of the publisher named under **1d** to include in this thesis portions of the publication named as included in **1c**.*

2. **For a research manuscript prepared for publication but that has not yet been published** (if already published, please skip to section 3)

   a) **What is the current title of the manuscript?**

   Click or tap here to enter text.

   b) **Has the manuscript been uploaded to a preprint server?** (*e.g.*, medRxiv; if 'Yes', please give a link or doi)

   Click or tap here to enter text.

   c) **Where is the work intended to be published?** (*e.g.*, journal names)

   Click or tap here to enter text.

   d) **List the manuscript's authors in the intended authorship order**

   Click or tap here to enter text.

   e) **Stage of publication** (*e.g.*, in submission)

   Click or tap here to enter text.

3. **For multi-authored work, please give a statement of contribution covering all authors** (if single-author, please skip to section 4)

Miroslav Cabadaj:	conceptualisation, principal investigator, manual data analysis, theoretical analysis
Shazia Bashir:	data assessment, English proofreading
David Haskins:	coding
Jawal Said:	microbiology, culture preparation
Simon Gaisford:	manuscript editing, corresponding author
Anthony Beezer:	conceptualisation, principal investigator, theoretical analysis, manuscript drafting

4. **In which chapter(s) of your thesis can this material be found?**

   Chapter 3, Chapter 4

5. **e-Signatures confirming that the information above is accurate** (this form should be co-signed by the supervisor/ senior author unless this is not appropriate, *e.g.*, if the paper was a single-author work)

Candidate	*Supervisor/ Senior Author (where appropriate)*
Miroslav Cabadaj	Simon Gaisford/ Anthony Beezer
Date:	*Date:*
22.04.2024	22.04.2024

Dedication

To Carolina, David and those who already left us.

Rest in peace.

Acknowledgements

This was the last page that I wrote before submitting the thesis contained within these pages. The endeavour of getting here was not fast nor easy. However, my journey was comfortable and secure, without any doubts whether it was possible to reach its successful end because I was lucky enough to meet some remarkable and beautiful people, whose friendship and trust I have had.

Tony, thank you for sharing your wealth of knowledge and lifelong experience in the field of biological microcalorimetry.

Manuela, thank you for all your support, reflections and always fruitful discussions, you are a wonderful being. You were always there, for me, selflessly determined to help.

Thank you both for your unbreakable personal and professional integrity, especially during hard times. You inspired me to do my best. The inspiration keeps on going.

David, thank you for your enthusiasm and high spirit during our work on coding.

Vivien, thank you for introducing me to microbiological calorimetry, I wish you stayed.

Cornelius, thank you for your kind attitude when I was just learning how to deal with data. I hope we meet again.

Sebastian, thank you for helping me to understand the mathematics of this project.

Jawal, thank you for our discussions about calorimetry, microbiology, life in general and nice coffee. It was pleasure to work in your lab and learn so much about microbiology from you.

Asma, thank you for our discussions about calorimetry and sharing your experience at the School of Pharmacy.

Shazia, thank you for the time we spent in the lab together trying to work out what was going on with the bacteria.

Thank you to all my family members for their encouragement and support.

Wifi, last but not at all least, thank you for your purring whilst I write.

Vicky and Jennifer thank you for agreeing to read and examine the work presented herein. I am looking forward to our discussions.

Table of Contents

List of figures

Figure 4.45 Slope *k* analysis. (Same detail as above Figure 4.42.) Data derived from logarithmically transformed p-t curves.

Figure A5 P-t curves of the individual Symprove organisms (*L. acidophilus*, *L. rhamnosus*, *L. plantarum* and *E. faecium*) tested in a batch of MRS (without Tween).

List of tables

Abbreviations

AD	- Alzheimer's disease
AUC	- area under curve
BB	- Black-box solution
BCAA	- branched chain amino acids
BHI	- brain and heart infusion
CDM	- chemically defined medium
CFU	- colony forming unit
CMM	- cooked meat medium
DLW	- Dohler wort
DSC	- differential scanning calorimetry
FAO	- Food and Agriculture Organisation
FDA	- Food and Drug Administration
FG047/psd	- Wickham labs internal document for plate testing
FMT	- faecal microbiota transplantation
FV1	- fermenting vessel one
FV2	- fermenting vessel two
GG	- good growth
GIT	- gastrointestinal tract
GMP	- good manufacturing practice
GLP	- good laboratory practice
HACCP	- hazard analysis and critical control point
Hz	- Hertz [s^{-1}]
IBD	- inflammatory bowel disease

IBS	- irritable bowel syndrome
ID	- identification
IMC	- isothermal microcalorimetry
ISAPP	- International Scientific Association for Probiotics and Prebiotics
LCFA	- long chain fatty acids
log	- logarithm
MALDI-TOF	- matrix-assisted laser desorption/ionization time-of-flight mass spectrometry
MSR	- De Man–Rogosa–Sharpe broth
NCIMB	- The National Collections of Industrial, Food and Marine Bacteria
OOS	- out of specification
PCR	- polymerase chain reaction
PD	- Parkinson's disease
pH	- −log 10 (Hydrogen ion concentration)
p-t curve	- power-time curve
PUFA	- polyunsaturated fatty acids
QA	- quality assurance
QC	- quality control
R-squared, (R^2)	- coefficient of determination
SCFA	- short chain fatty acids
SD	- standard deviation
SHIME	- Simulator of the Human Intestinal Microbial Ecosystem
TAM	- Thermal activity monitor (calorimeter)
TSA	- Tryptone Soya Agar
TSB	- Tryptone Soya Broth

TYMC	- total yeast and mould count
UCL	- University College London
VBNC	- viable but non-culturable cells
WHO	- World Health Organisation
Wort	- barley extract
µW	- micro-Watt
16s rDNA	- ribosomal deoxyribonucleic acid amplification method

Chapter 1 Introduction

1.1 Overview of this project

Globally, the probiotic industry is growing rapidly and has become hugely important and commercially competitive with a predicted market value of over USD 80 Billion by the end of 2025 ((R and M Report, 2018) It is influencing how agriculture, feed, food, food supplement, medicine, and other sectors choose to incorporate probiotics into their portfolios. Locally, this trend has been experienced by Symprove Ltd., manufacturer of the eponymous probiotic food supplement where I was employed as a production manager from 2012-2019 and as a research and development manager from 2019-2022. I do not hold any stock options nor had other interest in the company. Symprove has seen a growth of approximately 100-fold in the last decade, 2010-2020, with a further growth predicted for 2024 and beyond. I was in charge of the production of Symprove during the major growth of the company, later in charge of the research and development department. Quality and safety assurance testing was done exclusively on the final product using microbial culture methods (**see 1.4.1**).

This posed challenges because the testing procedures introduced significant time delays (up to two weeks) to the final product release for sale, whilst also shortening its shelf life. We needed a faster method for qualitative and quantitative assessment of both the production process and the final product. Having an in-house capacity to get a Yes/No answer (*i.e.*, is the product fit for sale or not?) would be greatly advantageous. Shortening the testing turn-around times would have a significant impact on the production timelines, with significant cost benefits. Additionally, the heterogeneous production process of Symprove was affected by variations in the growth medium (barley extract) that could, in turn, impact the behaviour of the fermenting bacteria (**see 1.4.1**). These challenges required a method which could also investigate metabolic processes during the fermentation.

A variety of methods was available and, after comparative evaluation isothermal microcalorimetry (IMC) was selected (**1.4.5**). IMC is a method that can measure the rate of heat produced by biological, chemical, and physical processes (Wadsö and Galindo, 2009). Consequently, it can be used to study biological systems such as bacteria during fermentation because these produce heat detectable by calorimeters. The information so captured by a calorimeter in the form of power (Js^{-1} or W) as a function of time can be analysed qualitatively and quantitatively to provide details about the quality of the

fermentation, with the potential for detecting contaminants at the same time. Furthermore, given that IMC had been used previously to assess the efficacy of the Symprove product against other commercial probiotics with success (Fredua-Agyeman and Gaisford, 2015), the idea of exploring its utility in the production of Symprove came to mind naturally. IMC method, if successfully developed, could provide a timely, accurate and repeatable tool, central for quality assurance of the final product with a great potential (if developed further, which was not the scope of this project) for being also implementable as a real-time monitoring method. Additionally, the content of IMC ampoules could be analysed after the IMC tests were completed using either molecular or traditional microbiological methods if required given the non-destructive nature of IMC sample analysis.

This research investigated the suitability and advantages of IMC as a testing method for microbiological quality assurance and its potential for product development in an industrial biotechnological manufacturing process (exemplified by studying Symprove probiotic product). It set out to develop a testing, safety and quality monitoring, method that incorporated data collected by IMC from an industrial-production-batch sample, providing information about microbial growth characteristics and metabolisms of the bacteria, that would support the decision to either accept or reject a new batch. The data collected by the calorimeter, although complex, should ideally be analysed through a black-box solution (BB), where the input would be the data, processed by an algorithm specifically developed for this purpose, and the output would be yes/no an indication of which parameters were in/out of specification. This method therefore would speed up the process of analysis as, once established, it could be used by anybody regardless of their understanding of the mathematics and theory behind it. The output provided specifications (a matrix of parameters) that a good product needed to be within. Good product was defined as a product that was released for sale after it passed all quality assurance (QA) testing.

The proposal to explore the potential of IMC in an industrial setting as set out in this thesis required pursuit of two further objectives. Firstly, to provide a set of references that were new in our field and would be needed, in future, if a BB for data processing was to be developed. The testing method was designed to test bacterial growth during fermentation in order to establish whether this growth was good or not and needed to be contrasted with an ideal growth (the references). This was done by creating as perfect scenarios as possible where all experimental parameters were as defined and as controlled as possible *e.g.*, bacteria were pure, growth media were as consistent as possible, timings of experiments were consistent. The research was conducted on a product produced by Symprove Ltd

(hereafter Symprove), a water-based food supplement containing live and active bacteria. Symprove was made by fermenting four strains of lactic acid bacteria (in pairs in 2 separate fermenting vessels: FV1 and FV2) in an extract of germinated barley. The focus of this project was FV1. Symprove provided the perfect opportunity for exploration of the calorimetric analysis since it was made in a simple closed batch production process.

Secondly, developing the mathematical background for data processing and analysis that could be incorporated into the coding for the BB was undertaken. This was done only as a proof of feasibility on a limited basis. The coding was done in a general-purpose programming language c and the algorithm for an automatic data processing was available online until the code developer's death. A number of mathematical models to obtain information on bacterial systems from IMC data have been developed in recent years by different researchers in the field. For this project, some of those equations were manually developed considering the particularities of the bacteria involved in Symprove.

In summary, this was a study which had two main areas of investigation (one —pragmatic *i.e.*, suitability and applicability into an industrial process control; and the other one — theoretical *i.e.*, exploring and developing the theoretical background) and was about an application of calorimetry in an industrial setting, exemplified through Symprove. The complexity that Symprove presented was a real test of calorimetry. The IMC test was designed to get the permission, after the fermentation was finished, to go ahead and bottle to save as much time as possible from the end of the fermentation to bottling and sale.

1.2 The gut

1.2.1 The relevance of the gut for this project.

Since this research investigated the suitability and advantages of IMC as a testing method for quality assurance and product development in the probiotic manufacturing process, we needed to operate with a notion of what an efficient probiotic ass, and this relied on an understanding of the gut in the human body. While the development of a testing method might seem like a mere technical matter, it necessarily relied on the appropriate contextual knowledge being applied properly. For example, the gastrointestinal tract environment affects the fitness of any microorganisms entering it; therefore, it will have an impact on the metabolic activity of a product containing live bacteria and these effects can be evaluated

by IMC. The background knowledge about the gut is also useful for the application, to its full potential, of the testing method being developed for evaluating the production of probiotics. For example, selecting new strains of bacteria and testing them in specific combinations could be done by IMC. Furthermore, the fact that probiotics are now being used for rebiosis (the reversal of dysbiosis) strengthens the importance of having a method such as IMC. It can measure all metabolic processes, non-destructively, without any sample treatment, with high sensitivity, enabling them to be studied in detail, qualitatively as well as quantitatively, and can be applied in an industrial setting to optimise production processes and their final products. The main limitation of the IMC method is that the obtained data are non-specific.

1.2.2 Description

The alimentary canal (gastrointestinal tract , or gut in short), is a system of organs beginning with the mouth, passing through the stomach, and ending with the anus, all connected with muscular tubes, such as the pharynx, oesophagus, small and large intestines, and rectum (Gray, 1977). The whole gut is a home to and is colonised by a diverse and populous community of microorganisms dominated by bacteria as seen in **Figure 1.1** (Qin *et al*., 2010) but also including archaea, bacteriophages, viruses, unicellular eukaryotes, and fungi (Dieterich *et al*., 2018), collectively referred to as the gut microbiota (Cani *et al*., 2016) *i.e.*, a community of microorganisms (Berg *et al*., 2020), residing in the gut. The microbiota has a significant role, both in health and disease of several other organs, for example the pancreas (Zhang *et al*., 2021), gall bladder (Urdaneta and Casadesús, 2017), and liver (Tranah *et al*., 2021) and remains an area of intensive scientific and clinical research efforts. Newly discovered functions like brain-gastric coupling offer insights into how different organs of the body are interconnected and affect each other (Rebollo *et al*., 2021).

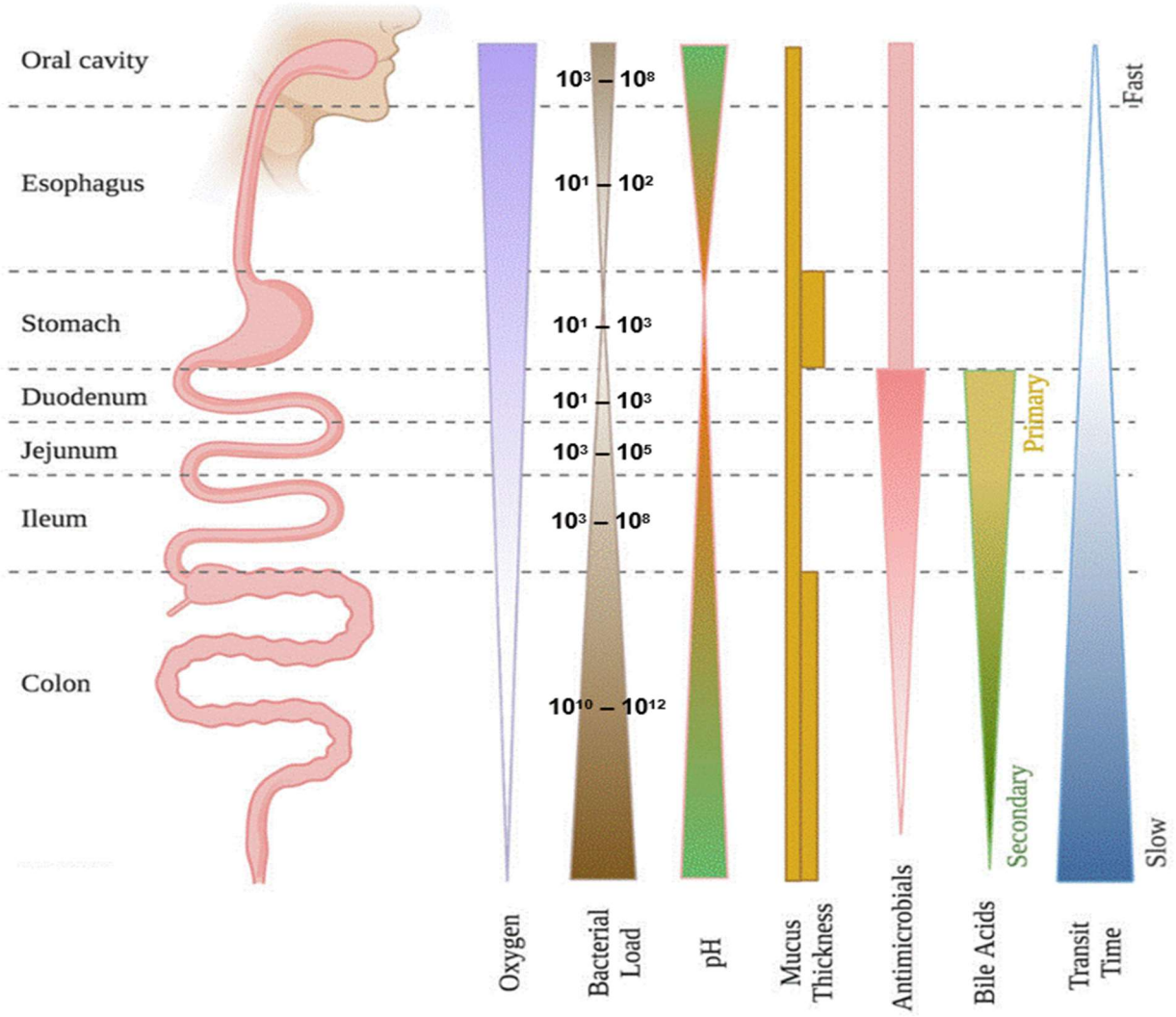

Figure 1.1 A visual diagram of the GIT noting bacterial loads in each part with ecologically relevant spatial gradients. (Adapted from Kennedy and Chang, 2020; oesophagus load estimated from Gorkiewicz and Moschen, 2018)

The mouth contains the oral microbiota, a diversely composed ecosystem of microorganisms (Zaura *et al*., 2014; Baker *et al*., 2024). The oral microbiota of healthy humans contains approximately 1 x10^8/mL bacterial cells based on saliva analysis (Curtis *et al*., 2011), however, when dental plaque is analysed, this can yield around 1 x10^{11}/mL bacterial cells (Sender *et al*., 2016). The oral microbiome (a microbiome in general is defined as “the microbiota and their theatre of activity” (Berg *et al*., 2020)) is relatively stable despite its highly dynamic nature, where constant perturbations are caused by frequent changes in acidity, temperature, oxygen and carbohydrate availability, with occasional disturbances caused by antibiotic therapies (Shaw *et al*., 2017).

In a healthy state, the oesophagus has its own resident microbiota, dominated by *Streptococcus* species in healthy state (Di Pilato *et al*., 2016; Zou *et al*., 2023). The intermediate areas connecting the oesophagus to the pharynx and the oral cavity at the proximal end influence the bacterial composition in that location (Snider *et al*., 2018), and the same effect can be expected at the distal end by the stomach (Di Pilato *et al*., 2016). This region of the gut is a particularly unexplored area. However, as more studies are being conducted, new evidence suggests that a normal healthy oesophagus microbiota is diverse and complex, dominated by Gram-positive bacteria with higher diversity, whereas Gram-negative bacteria with lesser diversity dominate in some disorders (Corning *et al*., 2018; Okereke *et al*., 2019).

The stomach, a food processing and storing organ, secretes hydrochloric acid, pepsinogen, mucus, gastric lipase and intrinsic factor (Feher, 2012). It has an acidic environment ranging from pH 1.5 to pH 5 (Walter and Ley, 2011), where only a few bacterial species are able to survive (Lopetuso *et al*., 2014). The chance of microorganisms to enter the lower parts of the gut and cause infection or disease is limited because of this extreme environment (Hunt *et al*., 2015). The stomach antibacterial property can be appreciated from the estimated 1 $x10^{10}$ microorganisms entering it per day (Riedel *et al*., 2014), while the residential bacterial load in the healthy stomach is approximately 1 $x10^{1}$ – 1 $x10^{3}$ CFU/mL (O'Hara and Shanahan, 2006). The microbial diversity and abundance of different species increases again beyond the stomach with the highest concentration of bacteria being found in the colon (McCallum and Tropini, 2024).

The small intestine is divided into three parts: duodenum, jejunum, and ileum. The bacterial load increases from about 1 $x10^{2}$ microorganisms/mL in the duodenum, up to around 1 $x10^{8}$ microorganisms/mL in the terminal ileum. It is suggested that the short retention time together with the bile salts and antimicrobial peptides secreted here results in the relatively low bacterial load compared with the colon (Riedel *et al*., 2014).

The large intestine, sometimes referred to as "the microbial organ" (Byndloss and Bäumler, 2018) or simply as "colon", is the home to the most populous microbial community, reaching some 10^{12} cells per gram of the intestinal content (Riedel *et al*., 2014; Di Domenico *et al*., 2022). The colon is divided into several regions starting at the ileocecal sphincter, continuing with the caecum, ascending, transverse, descending and sigmoid colon finishing in the rectum with the anus (Feher, 2012). Given that the colon is the most densely colonised part of the human body, it plays a major role in shaping the overall gut microbiota through

epithelial cells and their metabolism (Litvak *et al*., 2018). Among its functions are for example sensing for nutrients and metabolites, initiating a hormonal cascade needed for nutrient absorption, production of short chain fatty acids (SCFA) and other by-products such as long chain fatty acids (LCFA) and polyunsaturated fatty acids (PUFA), thus regulating dendritic and T-cells and other functions in the body (Ratsika *et al*., 2021). The ecosystem of the colon can also be understood as a production facility for the vitamins and substrates needed for stimulating the immune system and building defence mechanisms against invading exogenous bacterial species (Bakken, 2009; Maciel-Fiuza *et al*., 2023).

1.2.3 Function and significance

The main function of the gut is to digest food, turning it into energy and different compounds. These include vitamins, and other chemicals such as SCFA, all of them needed for a properly functioning body. The waste of the digestion is disposed during bowel movement. The ability of the gut microbiota to influence and shape different systems of the body is of great importance and an area of intensive research (Vogel *et al*., 2020). For example, a bidirectional relationship has been established between the gut microbiota and the immune system (Ralli *et al*., 2023), where the quality and shape of the second is affected by the former, and vice versa (Grigg and Sonnenberg, 2017). Another area of recent interest is the so-called microbiota-gut-brain axis (hereafter we understand by “axis” both the connections and interactions between different systems in the body), which is understood as a two-way communication channel between the central nervous system and the microbes in the gut (Michels *et al*., 2019).

There are several aspects to this complex relationship, microbial diversity, microbial imbalance and psychiatric disorders being just three of them (Ahmed *et al*., 2024). As Callaghan *et al*. (2020) have recently suggested, there is a correlation between early life stress levels and gut microbiota diversity. These authors have also indicated a correlation, between irritable bowel syndrome (IBS), gastrointestinal distress and higher levels of mood disorders and anxiety symptoms (Callaghan *et al*., 2020). There is also evidence pointing at the association between a mother’s mental wellbeing and proper neurodevelopmental process of the baby through the mother’s milk. Breast milk can be altered as a result of stress, psychopathologies and other factors such as diet, hence influencing the macro/micronutrients, bioactive compounds and other constituents of it entering the GI tract of the baby (Ratsika *et al*., 2021; Weerth *et al*., 2023). Another interesting correlation

between the gut microbiome and the brain has to do with mechanosensitive and nutrient sensing pathways. Hunt *et al*., (2015) have stressed that the gut also serves as a means of information transmission, and this is fundamental for “gastric nutrient sensing in the perception of gastric filling and control of hunger and satiation” (Hunt *et al*., 2015).

A well-functioning gut microbiota plays a significant communication role in health and disease states (**Figure 1.2**). The communication with other organs in the body through, for example gut-heart axis, gut-lung axis, gut-skin axis, gut-bone axis, gut-muscle axis, gut-liver axis and gut-kidney axis influences processes such as serotonin metabolism, insulin secretion, lipogenesis, thermogenesis, gene expression, body growth and energy expenditure (Schroeder and Bäckhed, 2016; Saxami *et al.*, 2023; Chakraborty *et al.*, 2024; Olteanu *et al.*, 2024). All the gut-organ axes are also linked to the relevant systems of the body such as cardiovascular system, respiratory system, integumentary system, skeletal system, muscular system, digestive system, urinary system and immune system therefore will play a major role in therapeutic strategies (Saxami *et al.*, 2023; Gao *et al.*, 2024; Nie *et al.*, 2024; Olteanu *et al.*, 2024).

The relevance of the gut microbiome has been further emphasised recently by the suggestion that various factors influencing the constitution of the intestinal microbiota during the first thousand days are critical for important developmental stages with likely functional and systemic effects for the rest of the life (Cusick and Georgieff, 2016; Robertson *et al*., 2019; Ratsika *et al*., 2021; Toubon *et al*., 2023).

1.2.4 Acquisition and composition of the gut microbiota

The gut microbiota evolves through three stages starting with a boom in early childhood, relative stability in adulthood, and decline in old age (Costea *et al*., 2018). The development of the gut microbiota and its resilience to perturbations are affected by a number of factors, relating to both host genotype and environment (Fassarella *et al*., 2021). The latter include mode of delivery, diseases, use of antibiotics, geography, type of feeding and lifestyle (Laursen *et al*., 2017; Ratsika *et al*., 2021), and bacterial-host symbiotic interactions (Lee *et al*., 2013; Pickard and Chervonsky, 2015; Aminov and Aminova, 2023).

There is still some controversy over whether the gut microbiota starts establishing (a) before birth in the uterus with low levels of bacteria (Funkhouser and Bordenstein, 2013; Milani *et*

al., 2017); or (b) during and after the birth (Koenig *et al*., 2011; Vogel *et al*., 2020; Ratsika *et al*., 2021; Kennedy *et al*., 2023), however, it is clear that the microbiota is there from a very early stage in the life of the host. The gut microbiota varies between preterm and full-term infants, where the facultative anaerobes are more representative than strict anaerobes in preterm compared with full-term infants (Arboleya *et al*., 2012). Another significant factor in the development of the gut microbiota is associated with the mode of birth, vaginal or C-section delivery; for example, Ratsika *et al*., (2021) contend that the development of the infant's microbiota is affected by the mother's nutrition prior to birth as well as by the mode of delivery. Furthermore, recent research suggests that communities in all body habitats of newborns are dominated by *Bifidobacterium*, *Lactobacillu*s and *Bacteroides* when delivered vaginally in contrast to C-section delivered newborns, whose microbiota in all body habitats are characterised by higher levels of *Staphylococci* (Ratsika *et al*., 2021), reflecting the mother's skin and hospital bacterial communities (Dominguez-Bello *et al*., 2010).

Breast milk provides the baby with over 200 different bacterial genera, including *Lactobacilli*, *Staphylococci*, *Streptococci* and *Bifidobacteria* (Murphy *et al*., 2017; Ratsika *et al*., 2021), however, the composition of breast milk can vary as a result of for example mother's diet (Padilha *et al*., 2019). The first three years of life are key in establishing a healthy gut microbiome which will influence the long-term health of the host (Nagpal *et al*., 2017). There is evidence suggesting that during the transition period from milk-based feeding to family diet, the abundance of the species *Lactobacillaceae*, *Bifidobacteriaceae*, *Enterococcaceae*, and *Enterobacteriaceae* decrease, while at the same time the species of *Lachnospiraceae*, *Ruminococcaceae*, and *Bacteroidaceae* increase (Laursen *et al*., 2017). The low diversity of microbiota in infants is considered healthy (Laursen *et al*., 2017), and the shift from low to high microbial diversity in later age had been attributed to the cessation of breastfeeding (and the bacteria coming from the mother) as well as to the inclusion of new foods with higher protein and fibre content (Laursen *et al*., 2016).

1.2.5 Balance and imbalance in the gut environment

The healthy gut microbiome is composed of different and interacting types of microorganisms such as bacteria, archaea, viruses, and fungi. There are more than 1000 different bacterial species residing in the gut (Quin *et al*., 2010), having a specific function in maintaining health and the proper function of the gut (Guo *et al*., 2020). This bacterial diversity is important as some bacteria act as hosts for viruses and may be indicative of the

human microbial health state (Reyes *et al*., 2010). Some important characteristics of the gut microbiota for human health are its stability, resistance, and resilience to change, and this is where the notion of “gut balance” or “homeostasis” plays a key role with the commensal bacteria being a critical component (Thriene and Michels, 2023). When the whole intestinal microbial ecosystem is in a homeostatic state, this is called eubiosis, which is a basic principle of health of the host as previously suggested by, for example Hippocrates (Iebba *et al*., 2016).

The wide array of microorganisms coexisting in the human gut creates a balance, in which the microorganisms both compete and cooperate in order to thrive while the host benefits as a result. The basic principle of a competing adaptation is through direct and geographical site-specific access to nutrients (Guo *et al*., 2020). Commensal bacteria are able to develop a cross-feeding or cooperation mechanism with other bacteria, whereby both depend on each other for survival and successful colonisation in the gut (Guo *et al*., 2020). An example of the cross-feeding situation can be illustrated when an increase in genes for maltose utilisation in *Escherichia coli* is observed in bi-colonized mice with *Escherichia coli* + *Bacteroides thetaiotaomicron* (*E. coli* + *B. thetaiotaomicron*) compared with mono-colonised mice just with *E. coli* (Li *et al*., 2015).

The stability of the gut microbiota in healthy individuals shows little change over time (Clemente *et al*., 2012) and is associated with a highly diverse microbial population (Bonsack *et al*., 2020). However, it is important to stress that stability here implies a dynamic state in which the gut is in an ecological equilibrium and other factors such as diet and environment do not fluctuate. The healthy gut will fluctuate (**Figure 1.2**) around a stable equilibrium, and the same is true for the unhealthy gut (this time, the new stable equilibrium is an unhealthy one). This is because the resilience of the gut makes it resistant to change in the long term without interventions such as medications or probiotics (Fassarella *et al*., 2021). The ecological equilibrium in the healthy gut is a function of the microbial diversity within it. There is a link between this diversity and resilience during perturbations because the diversity of microorganisms can compensate for missing strains (Fassarella *et al*., 2021).

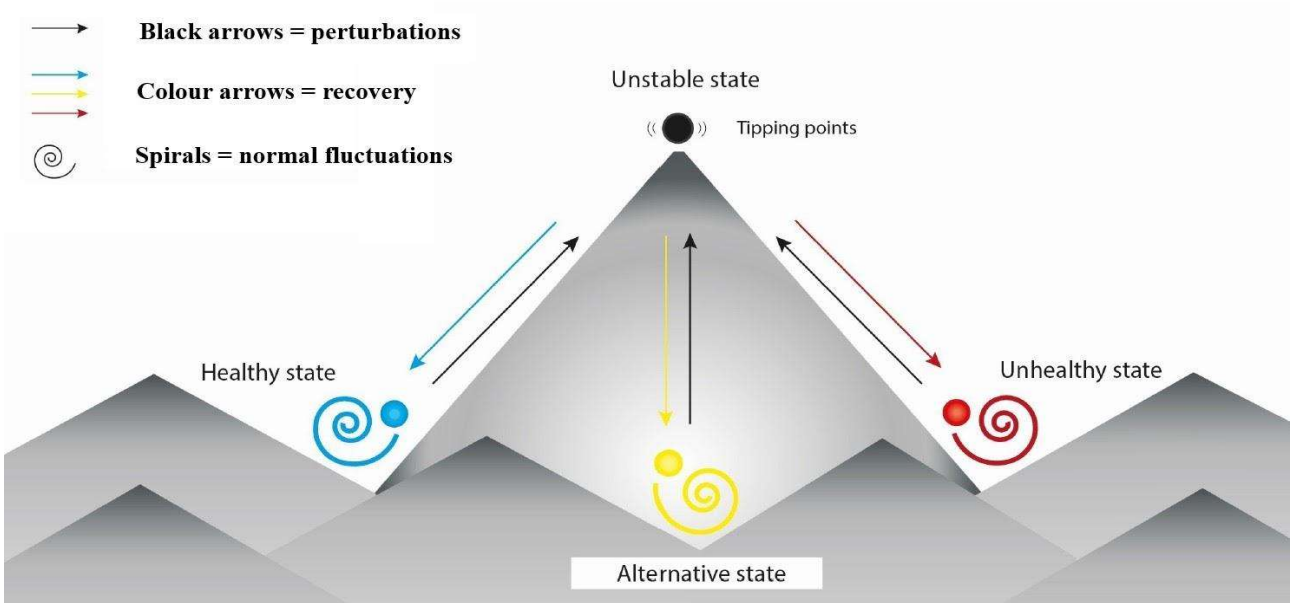

Figure 1.2 The gut microbiota fluctuations in health and disease. (Adapted from Fassarella *et al*., 2021.)

The gut ecosystem can be disrupted by a number of factors, for example the use of antibiotics, injury or surgery, psychological stress, radiation and diet (Prakash *et al*., 2011), amongst others. When these factors change the composition and the functional properties of the gut microbiota, this leads to gut imbalance (*i.e.*, dysbiosis). Dysbiosis can be characterised by any of the three following states, which often appear concurrently: loss of beneficial commensal microbes; expansion of pathobionts (members of the commensal microbiota that have the potential to cause pathology); and loss of diversity (Petersen and Round, 2014). The resulting change in microbial functional capacity, which can include microbial pathways for oxidative stress tolerance, immune evasion, metabolite uptake, carbohydrate or amino acid biosynthesis, has been shown to be upregulated (Buttó *et al*., 2015). Dysbiosis is normally caused by: (a) enteric infections and resulting inflammation that reduces the commensal bacteria's ability to resist colonisation by pathobionts or other pathogens; (b) diet and xenobiotics (chemical compounds not naturally present or produced in the host, such as drugs or pollutants); (c) genetic and familial transmission (*e.g.*, mode of birth) (Levy *et al*., 2017).

This state of imbalance can, in turn, affect health in other parts of the body, because of the bidirectional relationship between the gut and other systems described earlier. For example, Sadler *et al*. (2020) have demonstrated that having a stroke, results in alteration of the gut microbiota composition, creating a dysbiosis that thereafter affects the recovery after stroke

through lowering the amounts of SCFA normally produced by gut microbiota (acting as recovery mediators). Similarly, SCFA producing bacteria in the gut were decreased (Mowat, 2021) as a result of increased population of proinflammatory invasive adherent pathogen *Escherichia coli,* and other invasive adherent *Proteobacteria* (*Campylobacter concisus* and enterohepatic *Helicobacter*) leading onto developing Inflammatory Bowel Disease (IBD) (Mukhopadhya *et al*., 2012; Wiredu Ocansey *et al*., 2023). The metabolic inflammation so fuelled by dysbiosis (Tilg *et al*., 2020) causes dysbiosis associated abnormal gut metabolism (Liu *et al*., 2021) and metabolic reprogramming enabling pathogens to adapt to the inflammatory milieu (Guo *et al*., 2020). This situation can develop into colorectal cancer, one of the most commonly diagnosed and fatal cancers worldwide (Sung *et al*., 2021). Other conditions associated with dysbiosis, such as autoimmune disease, atopy, metabolic syndrome, obesity, cardiovascular disease, neurodegenerative conditions, and behavioural disorders can be managed better by determining both which bacteria are present in the normal intestine and their functions. Furthermore, it is also important to understand their interactions with the immune system and to find ways to modulate the gut and thus prevent infections and diseases triggered, aggravated or associated with dysbiosis (Mowat, 2021). Additionally, a deeper understanding of brain functions involved in maintaining homeostasis is essential, as the same are also involved in the regulation of dysbiosis (Bonsack *et al*., 2020).

As discussed previously, diet has a significant effect on the composition of the microbiota (Clemente *et al*., 2012) and is key in maintaining homeostasis together with a healthy lifestyle, regular physical activity, and food hygiene (Ferreira *et al*., 2022). However, if dysbiosis takes place, leading to a disease state, other ways will be required to restore the homeostasis (Petersen and Round, 2014). The effectiveness of altering diet as a prevention of infections caused by opportunistic pathogens appears higher in the steady-state gut. The same intervention was shown to be ineffective in people at advanced stages of disease *e.g.* (Guo *et al*., 2020). This process of restoration and rebalancing microbial communities back to a healthy state has been called “rebiosis” (Petersen and Round, 2014).

Recent advances in the field of microbiome research and the next generation multi-omics (Park *et al*., 2022; Gao *et al*., 2023; Chetty *et al*., 2024; Wu *et al*., 2024) offer new approaches to understanding the restoration of gut health pointing toward more personalised interventions (Sadowsky and Khoruts, 2016; Fassarella *et al*., 2021). These advances allow to determine which strains of bacteria might be needed in a specific case, a prerequisite to personalised treatment. For example, bacterial diversity in IBD patients is

decreased, while at the same time the bacteriophages (viruses that infect bacteria) increase significantly. Such effects need to be taken into consideration when a strategy for restoration of homeostasis is planned (Gogokhia *et al*., 2019).

For implementing a dysbiosis treatment strategy successfully, one needs to: (1) identify the most beneficial microbiome (including the diversity, amount and metabolic activity of, microbes), (2) analyse the microbiota colonizing specific areas of interest in an individual (*e.g.*, skin, oral cavity, respiratory tract, gastrointestinal tract, urogenital tract), and (3) modify the patient's microbiome to achieve effective rebiosis (Dietert and Dietert, 2015).

Traditionally, there have been two main treatment strategies for rebiosis. They include intensively researched faecal microbiota transplantation (FMT), and biotics administration, together with specific pathogen metabolic inhibitors (Guo *et al*., 2020). The term "biotics" includes prebiotics, probiotics, symbiotic, postbiotics and others. This type of treatment will be further illustrated in section **1.3**. FMT approach is common in clinical practice and offers a full range of microorganisms from a healthy donor. The biotics field is growing rapidly and applications in clinical practice are also becoming widespread. More recently, predator-prey strategies have also been advanced. These use predatory bacteria, bacteriophages or protists that are more aggressive than those causing the imbalance (Mosca *et al*., 2016; Fujiki and Schnabl, 2023).

Older FMT modes of delivery such as nasogastric intubation, or the use of lower endoscopy are gradually giving way to a novel colon specific delivery FMT oral capsules containing minimally processed donor material which are coated externally with a blend of bacterially triggered polysaccharide and pH-responsive polymer which dissolves in the colon (Allegretti *et al*., 2019). The risks and adverse events arising from FMT can be broadly categorised into two (Vrieze *et al*., 2013): procedure related complications, such as bowel perforation, or donor related complications, such as transmission of unknown pathogens (Cammarota *et al*., 2014; Yu *et al*., 2023). For this reason, despite the implementation of FMT into clinical practice becoming more common, some emerging risks connected to this procedure, including multidrug-resistant organisms, enteropathogenic or Shiga toxin-producing *Escherichia coli*, require better donor screening and safety protocols (Gupta *et al*., 2021).

For the sake of succinctness, only a few examples of the way in which these strategies operate in restoring balance will be drawn. There are incipient results pointing towards fixing dysbiosis in ageing, which contributes to neurodegenerative diseases, through strategies

that encompass diet and biotics (*e.g.*, fibre-rich foods or indigestible-carbohydrates that help short-chain fatty acids production, prebiotics, probiotics, and polyphenol) or FMT (Castelli *et al*., 2021). Similarly, there is evidence suggesting that in patients with advanced chronic liver disease the three strategies, biotics, FMT, and predator-prey strategies are promising, although more data are still needed (Tranah *et al*., 2021; Bajaj *et al*., 2022). Ma *et al*., (2021) have recently provided a further example of rebiosis achieved through biotics (psychobiotics) having an important impact on relieving stress and anxiety and hence showing the neuro potential of the gut microbiota.

1.3 The Biotics Family

1.3.1 Description

"Biotics" is an umbrella term that has been adopted recently to describe an array of new terminology generally referring to new areas in the development of the "application of microbes with technological, agro-industrial, ecological, or health purposes" (Vinderola and Burns, 2021). This is an emerging and rapidly expanding field; knowledge is being generated so fast, that the WHO had to publish guidelines so not all producers can say their products are pre-pro-syn-biotics and as such having the health benefits which are an ultimate goal.

1.3.1.1 Probiotics

A report issued in 2002 by a Joint Food and Agriculture Organization (FAO) / World Health Organization (WHO) Working Group on Drafting Guidelines for the Evaluation of Probiotics in Food (FAO, WHO, 2002), recommend the adoption of the definition of probiotics as "Live microorganisms which when administered in adequate amounts confer a health benefit on the host" (Nutrition Division FAO/WHO, 2006). This definition was reviewed in 2013 by the International Scientific Association for Probiotics and Prebiotics (ISAPP) Expert Panel and they concluded that it is still accurately broad and precise (Hill *et al*., 2014). There are several activities that should be carried out to deem products to be probiotics, including bacterial strains identification, functional characterisation of the strains, validation of the attributed health benefits, and proper labelling (Pandey *et al*., 2015).

1.3.1.2 Prebiotics

Prebiotics are currently defined as “a substrate that is selectively utilized by host microorganisms conferring a health benefit” (Gibson *et al*., 2017). The previous definition “a non-viable food component that confers a health benefit on the host associated with modulation of the microbiota” (Pineiro *et al*., 2008) was based on the first definition of prebiotics by Gibson and Roberfroid (1995), and their subsequent updated versions (Gibson *et al*., 2004; Roberfroid, 2007). These successive updates illustrate the dynamic nature of this field and the need for an agreement on the breadth of the definition and on the relevant criteria needed for it (Gibson *et al*., 2004). As the field of biotics advances the need for regulation increases and as a result The Joint FAO/WHO Food Standards Programme proposed international guidelines for prebiotics (Codex Alimentarius Commission. FAO/WHO, 2018).

1.3.1.3 Synbiotics

The current definition of synbiotics, as by ISAPP 2019, states that they are “a mixture comprising live microorganisms and substrate(s) selectively utilized by host microorganisms that confers a health benefit on the host” (Swanson *et al*., 2020). It is worth noting that resident as well as externally added microorganisms, are considered as integral parts of the host microbiota despite some being present only temporarily (Swanson *et al*., 2020). Also, we should bear in mind that an alternative definition of second-generation synbiotic agents has been put forward (Vinderola and Burns, 2021), in which “prebiotic agents could be defined based on their physiological effects or functional capacities in the host rather than their specific microbial targets” (Sharma and Padwad, 2020).

1.3.1.4 Postbiotics

Postbiotics used to be referred to as bioactive compounds produced during a fermentation process (Malagón-Rojas *et al*., 2020) that did not fit into the category probiotics, prebiotics or synbiotics (Collado *et al*., 2019), while still having the health beneficial effects on the host (Mayorgas *et al*., 2021). In other words, postbiotics could have been any bioactive bacterial metabolites with beneficial effects on the host (Person and Keefer, 2021). The definition of postbiotics was rather tentative (Malagón-Rojas *et al*., 2020; Morniroli *et al*., 2021), until

ISAPP's consensus was reached on the definition of postbiotics as "a preparation of inanimate microorganisms and/or their components that confers a health benefit on the host" (Salminen *et al*., 2021). Having properly defined biotics both current as well as emerging is imperative given that there is a great interest, in this field from the industry, health and clinical application and growing evidence of efficacy (Vinderola *et al*., 2022).

1.3.2 Probiotics and their role in health and disease

The general principle at work when understanding the role of probiotics in health is that microbial diversity is beneficial to the host's wellbeing (Chaluvadi *et al*., 2015). As discussed previously (**1.2.4**), the notion of balance linked to a healthy gut is related to the commensal bacterial diversity. Since the gut is connected to many other systems of the body, as exemplified by the brain-gut axis, the healthy gut has an impact on the health of the rest of the body. Hence, the diversity promoted by probiotics translates into general health. Currently, research on the health benefits of probiotics covers a wide scope of diseases, such as gastrointestinal diseases (Liu *et al*., 2018), neurodevelopmental and neuropsychiatric disorders (Vaghef-Mehrabany *et al*., 2020; Sharma *et al*., 2021; Vasiliu, 2023), dermatological/topical problems (Notay *et al*., 2017; Whiting *et al*., 2024), immune system modulations (Singh *et al*., 2021), pain management and treatment (Rea *et al*., 2021), to mention some of them. One prominent function of the gut microbiota is its modulating capacity. For that reason, it has a key role in controlling metabolic and inflammatory pathways in the above mentioned and other diseases (Nguyen *et al*., 2019; Palade *et al*., 2022). Consequently, developing new and innovative strategies and treatments for dealing effectively with disease prevention and disease treatment will inevitably include probiotics. Studying and understanding the many different axes is proving to be an invaluable tool in designing and developing innovative strategies for dealing effectively with disease prevention and treatment. A few examples of how understanding the axes are bringing a new array of approaches to health and disease are outlined below.

The first example comes from the so-called brain-gut-microbiota-diet axis. The ability to tailor interventions, such as treatments in synchrony with diets, using postbiotics (Person and Keefer, 2021), relies on placing the focus of our understanding of the psychiatric, neurological, and neurodegenerative diseases on the proper development and maintenance of the brain through the gut (Cryan *et al*., 2019). **Figure 1.3** illustrates interconnectedness axes that could be drawn for other systems in the body's holobiont.

There are several communication channels. For instance, the immune system, the vagus nerve, and the enteric nervous system are used by the gut microbiota to “talk” to the brain and vice versa, entailing SCFA, branched chain amino acids (BCAA), and bile acids (Cryan *et al*., 2019). Yet, the full implications of biotic therapies in the management of different diseases associated with the gut remains to be elucidated (Deleu *et al*., 2021).

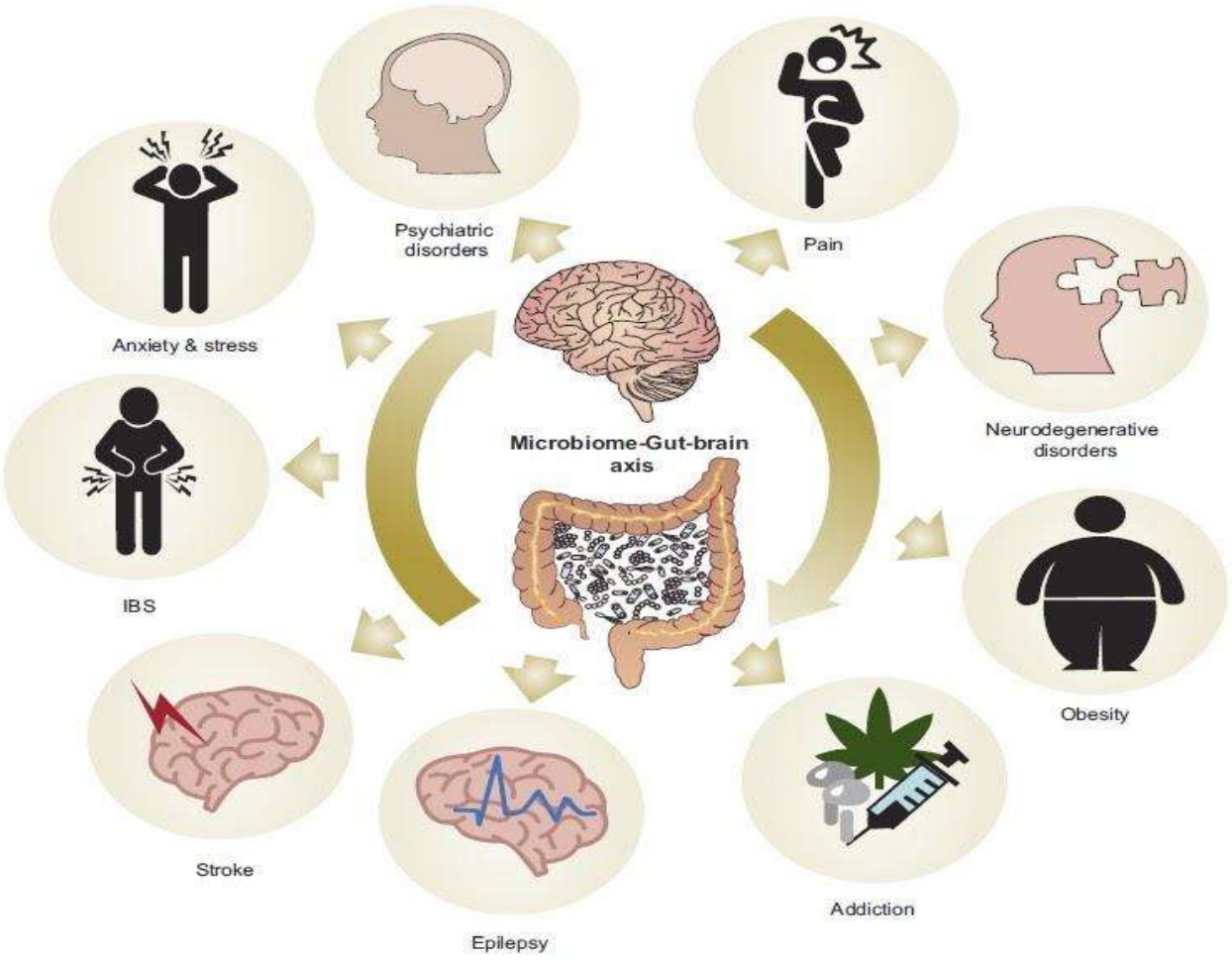

Figure 1.3 A non-exhaustive illustration of the scope for gut microbiota-brain axis to influence different health conditions. Image taken from Cryan *et al*. (2019).

The second example is the brain-gut-skin axis. Skin protects the body from all external elements, including microorganisms, and plays a vital role in maintaining the body’s homeostasis. The resident microorganisms constitute the skin microbiome (Sfriso *et al*., 2020). Dysbiosis in the skin microbiome can cause pathological disorders for example, acne, eczema and allergies (Sfriso *et al*., 2020). Often these conditions are reported to have psychological effects especially in young people with insomnia, depression, or anxiety being

the most common ones. It is likely that some of the psychological effects might originate from just having the illness itself rather than having a gut-brain molecular mechanism. However, there are only limited treatment options, therefore, the potential for exploring the utility of probiotics is appealing (Goodarzi *et al*., 2020).

The third example is the brain-gut-endocannabinoid axis. The endocannabinoid system can be defined as a metabolic pathway implicated in the communication between the gut microbiota and the host, regulating the intestinal barrier function (Jansma *et al*., 2021). For instance, decreased activity of the endocannabinoid system has been reported in gut inflammatory disorders (Jansma *et al*., 2021), whereas obesity, while also being linked to inflammation in the gut, showed an increased endocannabinoid system activity (Muccioli *et al*., 2010). Probiotic and prebiotic interventions to manipulate the endocannabinoid system activity have been investigated with encouraging results (Cani, 2012; Chevalier *et al*., 2020; Pinapati *et al*., 2024). The potential for the biotic therapies, as adjunct therapies for certain pain modalities (including IBS or other gut related pains), is encouraged because the endocannabinoid system can be modulated via the gut microbiota (Rea *et al*. 2021).

1.3.3 Where probiotics go

The use of probiotics can be traced back to the Neolithic period, in the form of fermentation, as a food preservation technique (Bourdichon *et al*., 2012). Fermentation evolved to have many different uses in food preservation and safety, being also used for improving the organoleptic (taste and smell) and nutritional quality of foods (Bourdichon *et al*., 2012). This is in part because fermentation helps biofilm and pathogen control through, for example an inhibition and reduction of toxic compounds (Moradi *et al*., 2020; Shao *et al*., 2021).

Probiotics, and the biotics family in general, have been developed to have applications in pharmaceuticals, food industry, and other areas. They have been receiving increased attention in recent years as the availability of scientific and clinical evidence of their effectiveness and versatility is growing. Many new bioactive compounds produced by probiotic bacteria are finding their uses in restoring and maintaining hormonal and metabolic homeostasis; immunity enhancement; cancer prevention and cancer therapy (Maleki *et al*., 2016); mitigation of adverse effects of neurodegenerative diseases, such as Parkinson's disease (PD) and Alzheimer's disease (AD); replacement and fortification of antibiotics;

personalised treatments; adjunct therapies for gut conditions, and other areas (Novik and Savich, 2020).

1.3.4 Types of probiotics available

There are three main areas where probiotics are currently being applied in humans, namely food and beverage, drugs, and dietary supplements. The most commonly used probiotic species across all three sectors are *Lactobacilli* and *Bifidobacteria* (Market Watch, 2021; GMI, 2023). Other lactic acid bacterial species that are frequently used include *Enterococci, Lactococci* and *Streptococci* (Patro *et al*., 2016), *Bacillus* species (Cutting, 2011; Soares *et al*., 2023), *Escherichia coli* strain Nissle 1917 (Pandey *et al*., 2015) and yeasts such as *Saccharomyces* (Czerucka *et al*., 2007; Suez *et al*., 2019) have also established their presence in the food and pharmaceutical industries.

Commercially, dairy products (cheese, fermented milk and yoghurts) and non-dairy products (juices, meat, fruits and vegetables) have been used as delivery systems for probiotics (Freitas *et al*., 2014). Furthermore, extensive efforts have been made to understand how best to protect probiotic bacteria from the harsh environment of the digestive tract with encapsulation leading the way (Romano *et al*., 2016).

1.3.5 Commercial importance of probiotics

In 1994, the Dietary Supplement Health and Education Act in the USA was passed, and it was this legislation that enabled an exponential boom in the global probiotic market which was worth approximately USD 14.9 billion in 2007. The legislation allowed probiotic agents to be marketed as dietary supplements without the strict regulatory requirements necessary for sale and marketing of prescription drugs (Gogineni *et al*., 2013). Currently, it is predicted that the global market for probiotics will generate revenue of around USD 81.8 billion by the end of 2025 (R and M Report, 2018). The probiotics dietary supplements segment alone (where Symprove currently belongs) was estimated at USD 4.6 billion in 2020 and was projected to reach USD 7.1 billion by 2027 (R and M Report 2021), however, the newest report indicates that the estimated market value for 2022 was already at USD 8.1 billion and is to increase to USD 12.3 billion by 2030 (R and M Report, 2024).

Probiotic products, which are designed to deliver live beneficial bacteria into the host, face unique challenges with regard to design and development of the formula, manufacturing process, scaling-up production volumes, quality and safety assurance, and marketisation. To meet these challenges, the industry, regulatory bodies, testing laboratories and research institutes converge in the process of achieving a set of requirements and standards for control and validation (Jackson *et al*., 2019). For example, the increasing demand for probiotic products stresses the need for fast and reliable quality assurance testing methods (Patro *et al*., 2016; Ziyaina *et al*., 2020; Manoj *et al*., 2021). There are several new ways in which probiotics are being used. For example, to prevent foodborne illnesses (Likotrafiti and Rhoades, 2016); to manufacture bioactive edible packaging (Moradi *et al*., 2021); to biofortify foods (Banik *et al*., 2020) and to develop non-lactic plant-based matrices (Sethi and Anurag, 2021). These new applications and production methods require new approaches to testing the safety and quality of probiotic preparations (Zawistowska-Rojek *et al*., 2022; Boyte *et al*., 2023). The need for further development is amplified as the existing methods either do not work well or are not fit for purpose in all areas of the probiotic industry (Marinova *et al*., 2019; Capozzi *et al*., 2020).

From a commercial perspective, there is a growing need to establish a number of parameters relating the effect of probiotics on the host (Qi *et al*., 2020). Some of these parameters comprise indications and contraindications with medicines and recommendation for specific health conditions (Gogineni *et al*., 2013; Purdel *et al*., 2023). They also include knowledge of how probiotic supplementation can affect the gut microbiome recovery after antibiotic treatment (Suez *et al*., 2018) and understanding of the interactions between individual components within a given product (Fredua-Agyeman *et al*., 2017b). All these parameters will have an impact on how the products are formulated and recommended for use to achieve optimal effects.

1.3.6 Outline of the essential components of a good/functional probiotic

There is some consensus that the following properties should be present in an ideal probiotic strain for oral administration : non-pathogenic, acid and bile tolerant, genetically stable, fast generation time, effective adhesion to gut lining, anti-genotoxic and able to survive production processing (Pandey *et al*., 2015). Therefore, it is important to understand the gut's environment with its changing spatial gradients as outlined in **Figure 1.1**. This will aid in development of new probiotics and optimisation of existing probiotics to make sure these

are functioning as intended and highly efficacious. However, there are also several other criteria in order to classify a potential microorganism as probiotic in foods and food supplements. For instance, the strain must be sufficiently characterised according to the International Code of Nomenclature of Prokaryotes (Parker *et al*., 2019). It also should be safe for the intended use (for example, for human consumption). The strain should qualify for either being on the Qualified Presumption of Safety list on grounds of historical evidence (Koutsoumanis *et al*., 2020; Koutsoumanis *et al*., 2022) or being subject to the Novel Food Regulation (European parliament and the Council, 2015), or its equivalent in other countries. It is also recommended for the probiotic to be supported by at least one positive human clinical trial, and to be alive in the product at an efficacious dose throughout shelf life (Binda *et al*., 2020).

Additional characteristics that are considered beneficial for consumer satisfaction and acceptance include delivery system (tablets, capsules, liquid formats), organoleptic palatability, the story behind the product (being eco-friendly, organic, ethically sourced and produced).

Having outlined the main characteristics of probiotics, both from a theoretical and a commercial perspective, the discussion will now be placed on the specific probiotic product, Symprove, which is the focus of this research.

1.3.7 General description of Symprove

Symprove is a liquid food supplement. Considering the definitions of the different members of the biotics family illustrated above (**1.3.1**), Symprove is a combination of all of them. It consists of prebiotic in the form of an extract of germinated barley that contains simple and complex sugars, including fructo-oligosaccharides. The probiotic part is the four live and active lactic acid bacteria. These bacteria produce a postbiotic, a lactate that is present in the product throughout its shelf life (Marzorati *et al*., 2020). Since the product contains four species of lactic acid bacteria in a water-based extract of germinated barley, it also meets the definition of a symbiotic.

Symprove was initially formulated for people to maintain and support their digestive health as well as to manage symptoms of IBS. As will be discussed below, the product helps build up and balance the gut microbiota with friendly bacteria. Symprove can be used by people

who are lactose and gluten intolerant. The product is ready to use and is suitable for most vulnerable groups including children, pregnant women, elderly people, and people with food allergies. The product should be stored and consumed as recommended by the manufacturer, with additional advice from a health care professional if needed. The functionality of the product lies in modifying the colon environment through the production of lactic acid and related lactate that serves as a food source for other beneficial microbes. They turn the lactate into different compounds, such as SCFA, within the gut environment. The full description of the product and the production process will be given in section **1.4.**

Given the scope of this research (specific probiotic food supplement production), a brief summary of studies and clinical trials where Symprove was used is below. In general, two types of studies (*in vitro* and *in vivo*) were conducted.

In vitro studies focused on two main areas: product efficacy in some diseases and product formulation quality. Product efficacy investigations are detailed in a *Clostridium difficile* infection model (Fredua-Agyeman *et al*., 2017a; Van den Abbeele *et al*., 2018), common gut pathogens model (Dodoo *et al*., 2019), ulcerative colitis model (Ghyselinck *et al*., 2020), Parkinson's disease model (Ghyselinck *et al*., 2021), and in modulating effects on the gut microbiota (Marzorati *et al*., 2018; Moens *et al*., 2019; Marzorati *et al*., 2020). Product formulation quality was assessed in a simulated gastric model (Fredua-Agyeman and Gaisford, 2015) and from studying the interactions between the individual bacterial species within Symprove (Fredua-Agyeman *et al*., 2017b).

In vivo studies, in humans, which used Symprove examined the effects of the product on IBS (Sisson *et al*., 2014), IBD (Sisson *et al*., 2015; Bjarnason *et al*., 2019), Diverticular disease (Kvasnovsky *et al*., 2017) and Infection and inflammation (Hassan, 2020).

1.4 Symprove production process and quality assurance

1.4.1 Background

The initial research into formulating Symprove conducted in the 1990s set the ground for the proposed solution and a patent filed by Thurlby (2006). Although the formulation and the production process developed and described in the patent was the foundation for the current production process, it has gone through several alterations since then to accommodate the demand for an increased production volume. Symprove formulation was based on the

growth parameters of its constituent bacteria, their metabolites and the speed of delivery of it when passing through the digestive system, specifically the stomach, to safely arrive in the large intestine for maximum host benefit.

The production process started with germinating barley, the base growth substrate for the subsequent fermentation of the four lactic acid bacteria. The subsequent steps after the completion of the germination included: milling the germinated barley; mashing-in using water; separation of spent barley from the barley extract (wort); and boiling of the extract. The fermentation stage and a subsequent blending of the final product is described in more detail in the next two paragraphs.

Fermentation was done using two fermenting vessels (FV1 and FV2) filled with pasteurised barley extract, each vessel was inoculated with equal parts (ratios) of two strains of lactic acid bacteria (NCIMB stands for The National Collections of Industrial, Food and Marine Bacteria. FV1: *Lactobacillus acidophilus* NCIMB 30175 + *Lacticaseibacillus rhamnosus* NCIMB 30174 (1:1) and FV2: *Lactiplantibacillus plantarum* NCIMB 30173 + *Enterococcus faecium* NCIMB 30176 (1:1)). The selection of the bacteria for FV1 and FV2 was based on their basic ability to lower the pH during the growth (fermentation) phase and their individual interactions with one another. These four organisms were kept at -80°C, two of which were in a powder form and two were in a frozen liquid slush form. Organisms, thawed before use, were added directly to the fermenting vessels. Both FVs could be considered a biological semi-closed (meaning formally non-sterile; in other words, not as an attempt to make medicine) system with defined organisms and a controlled medium (containing only 2 strains of bacteria each and a growth substrate / medium of limited variability, therefore controlled to some extent).

The final product was made up by blending FV1 and FV2 in equal proportions with added antioxidant (ascorbic acid), preservative (potassium sorbate) and flavours (only in flavoured versions of the final product) while being cooled down from 37ºC to approximately 10ºC. The cooling stage during blending of FV1 and FV2 was designed to slow down the fermentation process and bring the final mix close to an equilibrium state –minimal bacterial activity within the product to ensure long shelf life and optimal performance of the product. The final product could be refrigerated at 4ºC to prolong its stability further. The optimal blending ratios of individual bacterial components was not scientifically established and offers an opportunity for improvements of the current product formulation in terms of efficacy and stability over its shelf life.

Safety and quality testing of the final product was done via an accredited (Food and Drug Administration (FDA), Good Laboratory Practice (GLP), Good Manufacturing Practice (GMP)) contract microbiology laboratory. This testing included checking for the presence and levels of the individual beneficial bacterial strains, basic screening for contaminants such as *Salmonella* species, *Escherichia coli,* total yeast and mould count (TYMC) and annual screening for endotoxins. Microbial culture methods as detailed in standard operating procedures (Green *et al*., 2013) were used. Samples were taken from all vessels (FV1, FV2 and all mixes), and then sent to the contract microbiology laboratory. This testing was done on each new batch according to the patent and relevant legislation specifications (European Commission, 2005; Handbook of microbiological criteria for foods, 2020). The final product was also evaluated by trained staff members for organoleptic properties of smell and taste. It took between one to two weeks (the exact time to get a full set of results could be even longer (see for example, **Chapter 2, Table 2.4**) if the basic screening for contaminants yielded a positive result and a further identification was required) to get the microbiology tests results, after which the product was either approved or rejected for subsequent bottling and sale. This long waiting time introduced delays in production and this limited the performance of the whole operation especially during busy periods.

Each step in the production process aimed at ensuring that a safe and good quality product was made and shipped to consumers. The need for managing the process and the product was of increasing importance especially since the company was planning to expand its manufacturing capacity while also looking into outsourcing the barley processing. The company adopted a quality management system ISO 9001, hazard analysis critical control point (HACCP) and was preparing to have good manufacturing practice (GMP) standards incorporated during 2022 production expansion planning stage.

1.4.2 Challenges in production process and quality assurance (QA)

There were several challenges presently identified either in the production process itself or concerning QA procedures. Production challenges included: processing of raw barley on site which was time and labour intensive; the current manufacturing capacity was limited to producing one batch per day; the production process was only partially controlled through temperature and time limits; the fermentation was only checked by measuring pH at the end of the process; the fermentation was self-regulating and not controlled by the operator. QA challenges were concerned with the speed of testing and the accuracy of the microbial

culture techniques. Therefore, a closer-to-real-time analysis would be commercially (and potentially theoretically) important.

1.4.2.1 Description of the problem

Fermentation is, as any biological process, highly complex. This means that creating models that can be used in industry is a challenging task. As described in **1.4**, the production of Symprove was carried out in two different vessels, FV1 and FV2, whose contents were mixed in equal proportions after the fermentation stage was completed, resulting in Mix (FV1 +FV2). FV1 contained two strains of lactic acid bacteria, making it the simplest possible system to study within the Symprove production process. This provided an excellent opportunity to investigate and model the behaviour of two strains of bacteria, interacting with the growth medium and with each other, in a sufficiently controlled way. The two bacteria used in FV1 were pure strains (pure means there was only the desired strain of microorganism and no microbiological contaminants present in the inocula, also see **4.2.2** for further details). It was not always the case that pure cultures were used, as in the past the bacteria used were of lower purity allowing up to 5 x10^4 of total aerobic contaminants. There was only one supplier of inocula whose specifications allowed non-pathogenic aerobic contaminants up to this level (5 x104 / g) in their final product. Symprove co accepted these batches as there was no alternative at that time and there was no obvious or detectable contamination by Lab 1 (Wickham labs, UK) either in the inocula themselves or Symprove final product. Studying those potentially contaminated cultures compared with pure ones introduced an extra complexity, especially when all the components/contaminants were not known. The switch from lower purity inocula to pure strains made the composition of FV1 an ideal system to study because any contaminants detected would not be originating from the inocula themselves.

The growth medium used was barley wort. The analysis of the chemical composition of the wort was very limited and varied from batch to batch as well as from variety to variety and seasonality of the barley used for its manufacture. It was therefore reasonable to assume that any metabolic changes detected during fermentation could be attributed to the variations resulting from the heterogeneity of the growth medium or external contaminants and not from the variations of the controlled inocula, providing all other production parameters such as timings and temperatures were consistent.

Quality Assurance (QA) methods as described in **1.4** posed challenges and delays to the final product release procedure. These QA methods were time consuming , the accuracy of the microbiological culture techniques varied significantly (a contract microbiological laboratory used by Symprove company, had ±0.5 log result accuracy which was consistent with the literature (Jarvis *et al*., 2007; Jarvis *et al*., 2012)) and these methods could not be implemented on-line (such as a spectroscopic or calorimetric probe located directly in a fermenting vessel monitoring the processes in real time). Additional problems associated with the QA methods included: high cost of testing per sample; loss of approximately 2-3 weeks of shelf life whilst the quarantined batches awaited results for release; and the need for a large storage capacity to keep several (up to 2 weeks' worth of produced batches) in quarantine before release for subsequent bottling and sale was allowed. Furthermore, the microbiological methods did not capture sufficient information about the process of metabolism as it happened or the progress of the same metabolism of the growing culture. Additionally, the metabolism of bacteria could be affected by being plated onto a semi-solid matrix of agar plates as this did not represent closely the liquid planktonic type of growth that happened in FV1. The lack of these insights into metabolism was particularly challenging in decision making. For example, if the final pH of FV1 was within the specified range and *L. rhamnosus* count was outside of the specified range the acceptance or rejection of this particular batch was in question. Therefore, a fit-for-purpose method that could provide more detailed information about the state of the fermentation process was needed. Ideally, this new method should be a standalone one or alternatively a complementary one to the existing microbiological method.

Historically, most problems in the production process were experienced during the fermentation phase, particularly in FV1 (Symprove database of test results). Additionally, cross-contaminations of FV1 by FV2 was experienced, specifically by *E. faecium*, and these were not reliably and consistently detected by the contract laboratories. There were many reasons why this was the case. The fermentation took place in non-sterile vessels, using a non-sterile growth medium (wort). It relied on the overloading of the non-sterile growth medium with high concentrations of viable good bacteria (*L. acidophilus* + *L. rhamnosus*) that, it was hoped, would outgrow anything else that could be present. Other equipment such as transfer hoses, pumps and heat exchangers were used interchangeably throughout the production process, and this provided an opportunity for the whole system to be cross-contaminated. There was a rather long lag phase in FV1 (approximately 1.5 hour when tested in TSB) compared with FV2 (no lag phase observed when tested in TSB) and this

was a significant problem in FV1, as both of its bacterial components grew much slower than one of the FV2 components —*E. faecium.* This meant the *E. faecium* could take hold in the FV1 and alter its final composition.

Lowering the pH faster through faster growth and increasing the concentration of metabolic by-products of the good bacteria meant lowering the chances of establishment of a potential contaminant. Relying on this ability of the FV1 and FV2 bacteria to naturally outcompete other potential contaminants could work, in principle, if the contaminating organisms were not high in numbers, did not grow much faster than the correct inoculum, did not persist in the final product, did not metabolise (or degrade the target compounds such as lactic acid) metabolic by-products of the inoculum, and were non-pathogenic. However, if there was a contaminant (assuming non-pathogenic, as pathogen contamination would result in disposal of the batch in question), this could still have a detrimental effect on the fermentation process, for example change in metabolic pathways, resulting in faster nutrient depletion or gas formation, affecting organoleptic properties and stability of the final product. Detection of a contaminating organism might be challenging with microbiological methods used at the time, as the final product already contained high concentrations of beneficial microorganisms (I demonstrated this previously by testing a freshly made batch of *L. acidophilus* inocula by a contract manufacturer. I discovered, using IMC (isothermal microcalorimetry), that the new batch of *L. acidophilus* was contaminated during the manufacture with *E. faecium* (different strain from the one used in Symprove formula) that was produced for another customer on the same line. The initial IMC findings were confirmed later by genetic sequencing of the contaminating isolate. Despite the contaminant not being pathogenic, the composition and therefore the functionality of the final product, its shelf life and stability could be affected. This was most likely because of nutrient exhaustion by competing bacteria as well as by their metabolite build up in the final product.

In short, the main problems with the testing procedure were: long time to results; accuracy varies significantly from batch to batch; end point analysis only (could not be implemented on-line); laborious sample preparation reflected in high cost per sample. Hence, the method needed, should ideally have the following characteristics; rapid compared with the current microbiological method; reproducibility of the method (better than the microbiological method: *e.g.*, agar plate analysis of identity and number); have the potential to be implemented directly into the fermenting process monitoring; the interpretation of data obtained should be simple (*e.g.*, yes/no answer) and the implementation into the production process should be easy. Yet, this was only considering the pragmatic aims. For the

theoretical one, the method needed should ideally allow for: having data analysis and interpretation of the results carried out automatically (*e.g.*, a matrix of parameters worked towards vs. observed parameters); industrial exploitation of the capacity for interpretation of data from microbiology (data from a chosen method); kinetic analysis of the data available, consequently offering quantitative assessments.

1.4.3 Opportunities for improvements

There was only a modest confidence in the production of a successful end product until a full set of test results was received from the contract analytical laboratory a week or more later. The product was stored on site over this period. Faster turn-around or a quicker method for QA and analysis would offer increased production rates, money saving and confidence in the process itself. There were two main areas where improvements could be made. One related to the production process and the other one related to QA. Both are detailed below in **1.4.3.1** and **1.4.3.2**.

1.4.3.1 Production process opportunities

The germination process and some other key variables such as smell, taste and colour of the barley and the extract thereof were controlled by pragmatic knowledge and experience only. Consequently, nutritional variations could occur in the barley extract, affecting the fermentation and quality of the final product. Types and quantities of sugars and other nutrients within the germinated grains could be further optimised by introducing precise temperature, moisture and aeration monitoring. Kilning (heat drying of the germinated grains) would offer a large storage quantity of ready to use grains. Alternatively, ready to use extract or synthetically prepared growth medium offered a suitable substitute to barley extract produced onsite. Working together with a suitable extract producer was a feasible way to tailor the properties of the extract to the exact requirements as set in the patent. Additionally, I discovered, during the course of this project, a new way of preparing the growth medium, wort, and IMC played a critical role in assessing its suitability (see **4.3.2**).

Monitoring of the pH in real time presented a chance to suitably buffer or stop the fermentation at a precisely defined value and this could help to optimise the production process and the quality of the final product. In addition, the shelf life of the product could be

extended by maintaining storage conditions for example temperature at a recommended value (Thurlby, 2006) and by addition of suitable nutrients.

The viability and purity management of the bacterial cultures used in the production process could be improved by customising the format of each one as a single dose only. For example, the need to dispense bulk bacteria into smaller units onsite required multiple defrosting and freezing cycles, introducing a potential for contaminating the stock and impacting the viability of the cultures.

This method of inoculation introduced a long growth lag time, leaving some potential for opportunistic pathogens to take hold and prolonging the fermentation stage of the production process. Time could be saved by pre-preparing these as liquid based starting culture inocula. A significant improvement in time and confidence could be achieved by using frozen liquid based pure inocula (Beezer *et al*., 1976). This would also limit the opportunity of pathogens and other contaminating organisms to take hold in the wort during the initial lag time of the production organisms. Production strains had a limited viability and purity maintenance because of a bulk storage on site and a subsequent dispensing into smaller dosing units.

Lastly, to establish comprehensive parameters of a good growth (GG), would mean all was going well during the fermentation stage, and was essential from a quality and safety perspective. When the fermentation proceeded as expected, the timing of the pH downshifting was as expected based on the standard operating procedure, the smell and the taste of the product at the end of the fermentation was acceptable and finally the test results were within the specified limits. More advanced parameters for example bacterial growth rates, lag phase, maximum growth, gas analysis, interspecies interactions and other metabolic variables during fermentation could offer insights into the process which would enable fine tuning and optimising the quality and safety of the product.

1.4.3.2 Quality assurance opportunities

Microbial culture techniques used for QA by the contract laboratories introduced significant time delays to the final product release and might not be sensitive or accurate enough to detect unwanted contaminants (see **2.6.1**, **2.6.2** and **2.6.3**). The accuracy of these methods could create a large degree of variability between batches (Sutton, 2011; Weitzel *et al*.,

2021). Other methods with real time or near real time monitoring capabilities could optimise the whole QA procedure. One such method is isothermal microcalorimetry and is discussed in in this thesis.

Additional methods which could quantify live and dead bacteria suitable for implementing into Symprove QA are detailed hereafter: staining and quantification of bacteria by microscopic enumeration, electronic enumeration or fluorescence activated cell sorting; viable bacteria quantification by molecular methods for example quantitative polymerase chain reaction, ribonucleic acid analysis and genomic cell number estimations and quantification of viable bacteria by physicochemical parameters for instance adenosine triphosphate, heat flow by calorimetry or foam formation (Mauerhofer *et al*., 2019).

1.4.4 Available production process monitoring methods

Industrially, a significant commercial interest lies in knowing which method is best suited and convenient to assess the quality and safety of both final products and production processes involving microbial growth. When it comes to fermentation monitoring, control and assessment are imperative for ensuring safe and efficient production processes. Although there was a range of methods available to that end, most of the available options for Symprove company would impose either additional cost to modifying the existing equipment (*e.g.*, on-line testing method) or significant time delays and relatively high cost because of external lab testing. Given that UCL was interested in developing the IMC method for a wider industry use and Symprove company wanted to have their own rapid batch-release test for production, they decided to partner in developing a batch-release test for Symprove production.

There were different methods for monitoring industrial processes suitable for the Symprove production process. Specifically, fermentation monitoring could be done using either off-line (*e.g.*, microbiological methods used by Symprove), at-line (Guo *et al*., 2012) or on-line methods (Feng *et al*., 2021). It is fundamentally important to understand and control the fermentation process in order to optimise parameters such as biomass quantification, nutrient utilisation, metabolite build up, desired bacterial concentrations and pH during the production process (Macaloney *et al*., 1996).

On-line methods offer monitoring of the fermentation process in real time using optical or spectroscopic sensors, and electrodes which are located directly in the fermenting vessel (Slouka *et al*., 2016). This method is preferred over off-line methods as the measurements are collected directly in the vessel without the need for sampling and transfer of samples into a different analysing device (Mauerhofer *et al*., 2019). However, the technical issues and the cost associated with the installation into already commissioned equipment is not currently feasible for Symprove.

At-line spectroscopic methods are advantageous over off-line methods because the sampling is done almost in real time, automatically in defined intervals (Mauerhofer *et al*., 2019). In addition to viable cell concentrations, these methods offer the possibility to measure other parameters such as available nutrients, metabolite build up, dissolved oxygen, and pH during the fermentation process (Leme *et al*., 2014). Here again the cost of retrofitting into an already commissioned system would require calibrations and validations for the specific process of Symprove fermentation and rather high cost and are presently not feasible.

Off-line methods include direct cell counting, most probable number, biomass measurement and light scattering (Mauerhofer *et al*., 2019). These are generally end-point analyses where samples are taken at the end of the fermentation process from the final bulk product. The contamination risks can be lowered if sampling is done at the end of the whole process compared with intermittent sampling for off-line testing during the fermentation. Symprove production process parameters (colony counting, monitoring of growth through temperature and pH and nutrient analysis) were conducted off-line, using microbial culture methods, away from the fermenters. Despite recent advances in industrial bioprocess control, this method of monitoring was still routinely used because it was reliable (Gomes *et al*., 2019), easy to perform and relatively cheap. The main disadvantages of any off-line method, especially microbial culture method are the time delay from taking the samples to getting the results and the potential for contaminating the samples during sampling and testing.

There are a number of methods investigated by the food industry to assess how to incorporate the best option for a fast and reliable quality assurance system. It is likely the final method will be a combination of several methods exploiting the advantages of currently investigated methods, including IMC, quantitative polymerase chain reaction and whole genome sequencing. While the methods are being developed, customised, and validated in light of the past challenges, future research in areas like viable but non-culturable cells

(VBNC), persistence of bacterial biofilms and their virulence factors in food production plants, interspecies interactions in multispecies formulations, and safety concerns related to new biological and non-biological innovation technologies (Suzzi and Corsetti, 2020) needs to be monitored with care.

1.4.4.1 Method selection

The Symprove company carried out an analysis to assess the suitability of readily available methods for production process monitoring and to authenticate the final product for sale. This was done through consideration of several factors including the following: speed of testing (*e.g.*, turnaround times); cost per sample; sample preparation complexity; potential for real time monitoring of the fermentation process; previous experience with the testing method and simplicity to implement the method into QA procedure. The range of methods considered was not an exhaustive one, but rather a practical one reflecting the factors outlined earlier. To achieve what Symprove envisaged in this regard, the methods considered are presented in **Table 1.1** below. The method selected was to be developed further to specifically suit the purpose for which it will be used.

It needs to be mentioned here that the company was aware of other methods (such as flow cytometry) potentially suitable for production process monitoring or the final product testing at the time of decision making. However, various reasons such as a very limited budget at the time, process design and the company growth stage (too early to pursue more than one new objective in research and development) had an impact on the general scope of this project which could have been broader.

Method	Time to results	Cost/sample (£)	Sample preparation	Can it be installed on-line?	Previously used on Symprove
Microbial culture	7-15 days	150 – 300	Serial dilutions (labour intensive)	No	Yes
IMC	0*-48 hours	10 - 50	Minimal	Yes	Yes
PCR	5-48 hours	150 - 450	DNA extraction	No	No
Spectroscopy (SERS Raman)	12-48 hours	100 - 200	Nanoparticles Sample drying	No	No

Table 1.1 Summary of different methods considered for QA and QC assessments of Symprove. * Assumes being fitted on-line.

According to the prospective method's ideal characteristics to solve the problem described in section **1.4.2.1** (last paragraph) and the established parameters evaluated in **Table 1.1**, IMC was chosen as the testing method to be developed. IMC was also chosen because there was a well-developed understanding of how to derive kinetic parameters for chemical systems and this could be developed for the studied biological problem of fermentation. Further elaboration on kinetics is given in **3.2.1.1**. Moreover, thermal analysis was superior compared with the other methods assessed, because it allowed monitoring of metabolic activities including the progress of metabolism (*e.g.*, how well the organisms grew) as well as the process of the same metabolism (*e.g.*, how the growth developed over time) directly. Calorimetry offered numerous advantages to study biological systems such as the Symprove fermentation process. Simplicity of the test method which could monitor processes inside opaque suspensions (and not just opaque systems but as long as the sample could be contained in, say, an ampoule then it could be studied via IMC), the possibility to obtain real time data, when installed on-line and the capacity for data analysis automation offered extra advantages.

The decision to pursue IMC as an experimental method with a real potential to be implemented into the Symprove production process was made based on the assessment mentioned earlier in this section. Additionally, this decision was supported by University College London (UCL) researchers who carried out some of the previous studies concerning

IMC and Symprove (Fredua-Agyeman and Gaisford, 2015; Fredua-Agyeman et. al., 2017a; Fredua-Agyeman et. al., 2017b; Dodoo et. al., 2019) and were especially interested in developing the theoretical aim (see **1.4.5.1**). Their experience and expertise in IMC enabled the conception of the project presented herein. Moreover, UCL had an active interest in developing IMC techniques for wider probiotic industry applications. The initial assessment of the feasibility of the proposed project revealed several challenges as there was no funding, no equipment or even any laboratory facility onsite at Symprove, nor a calorimetrist or other expert scientist available within Symprove at the time of the assessment. The possibility of collaboration between Symprove and UCL was very appealing to both parties as Symprove was eager to introduce science into their portfolio and UCL was keen to further their knowledge base regarding IMC. Both Symprove and UCL appreciated the potential benefits of this cooperation and the groundwork began in 2015 with identifying the budget needed to conduct the research, appointing the right candidate to carry out the research (myself), setting up a basic laboratory space suitable for IMC within Symprove facilities in 2016 and the preliminary experiments began in late 2016. However, there was no suitable microbiology laboratory space available to enable performing microbiological plating or other microbiological techniques. As a result, it was not going to be possible to supplement any IMC data with *e.g.*, microbial cell numbers, substrate concentrations *etc*., reported within this thesis.

Furthermore, several parameters needed consideration before choosing calorimetry because data quality (validity and utility) collected by a calorimeter depend on a proper use of the instrument and defining any potential pitfalls. For example, the experiment duration should reflect the length of the studied process (*e.g.*, fermentation timescale); the instrument should be sensitive enough to detect sufficient power allowing these to be distinguishable from the baseline; multiple peaks (events) taking place at the same time might need deconvolution or the individual events causing multiplicity would need to be determined experimentally (Kaletunc, 2009).

The IMC method when fully developed should be the only method needed and could be implemented whenever basic laboratory space suitable for IMC was available onsite, with no need for a specialist to process the samples or the results of the testing. In other words, the pragmatic outcome was to ensure a simple, batch to batch, analysis of Symprove production that accounts both for natural variation between batches and reproducibility. The operational simplicity could be achieved by implementing an algorithmic tool whose output

would provide the relevant information to establish the “yes/no” (or “pass/fail”) answer desired.

Additional advantages of exploring IMC were discovered as the previously published calorimetric studies involving Symprove, mentioned earlier, generated quantitative data that could be further analysed. For example, the effects of gut transit on the fitness of the microorganisms within the product arriving in the colon could be simulated and assessed.

1.4.5 Isothermal microcalorimetry (IMC)

“Calorimetry” is a hybrid word combining “calor” (the Latin for heat) and “metron” (the Greek for measure) to denote a heat measuring technique. The first experiment using calorimetry as a new quantitative means to measure heat generated by a living organism was carried out by Lavoisier and Laplace ([1783] 1994). Their early design was a simple ice calorimeter inside which a live guinea pig was placed. The principle was straightforward: in a closed system at constant temperature and pressure, the body heat of the guinea pig melted a portion of the ice, allowing them to establish that the volume of melt water was directly proportional to the heat generated by the guinea pig. From this relationship and knowledge of the latent enthalpy of fusion of pure water it was possible to determine the enthalpy of metabolism. The outcomes of the experiment proved to be very useful despite its rudimentary nature. However, it would take almost eighty years for the first true industrial scale calorimetric experiment to be conducted. It was Dubrunfaut, who in 1856 studied yeast fermentation in a large wooden wine vat (Battley, 2013). Detailed description of this rather macro calorimetric experiment (it involved 21400L of molasses solution with a great amount of yeast inoculum) is given by Battley (1998).

Calorimetry has been developed enormously since Lavoisier and Dubrunfaut, being applied to many different biological systems and sciences (Calvet and Prat, 1963; Brown, 1969; Beezer, 1980; Wadsö, 1986; James, 1987; Okada *et al*., 1998; Wadsö and Galindo, 2009; Maskow, 2013; Morozova *et al*., 2017; Braissant *et al*., 2020; Cabadaj *et al*., 2021). In this project, calorimetry is used to investigate the heat generated by living organisms (bacteria) using a calorimeter in order to implement it into a 1000L fermentation vat —small by comparison with the Dubrunfaut design, however much improved in terms of sensitivity (microcalorimetry) and repeatability.

Microcalorimetry (calorimetry where measurement of heat is expressed on a microwatt scale) is able to detect changes in heat generated by microorganisms. This technique is fast, accurate and nonspecific, suitable for direct measurements of metabolic activity of bacteria. The method has high reproducibility within 3% compared with 5-10% of agar plate diffusion method (Beezer, 1977). It can be used with either opaque or transparent growth media and metabolic rates and biomass can be determined from data collected by a calorimeter (Ashby and Beezer, 1996).

Isothermal microcalorimetry (IMC) is an experimental technique where sealed samples are kept at a constant temperature inside a calorimeter during measurement (Wadsö, 2002). The stable temperature environment in the calorimeter is usually achieved by using a heat sink such as a thermostatted water bath in which calorimetric measuring channels are submerged (Thermometric, 1996). It implies, therefore, that the thermal power that flows between the sample and the heat sink will produce (exothermic) or absorb (endothermic) heat from the heat sink. Hence, the thermal power comes from any physical, chemical, and biological processes happening within the sample itself. The heat sink is connected to thermoelectric modules which convert temperature differences into an electric signal and this signal is recorded as power-time data, ready for further analysis (Braissant *et al*., 2010a).

1.4.5.1 Calorimetry and its use in industry

The account of calorimetry uses in industry offered here is by no means an exhaustive one, however it was structured to lay grounds for the specificity of this project. Since the advent of calorimetry in the late 18th century, calorimetry has been tried and applied in many different fields. Whilst little changed since then in the basic principle of measuring heat changes, calorimeter design and development have been greatly improved and expanded with the revolution in advances in computer sciences and microelectronics (Sarge *et al*., 2014). This enabled researchers and scientists to implement calorimetry in wider and novel kinds of investigations for example in pharmaceutical industries (Gaisford and O'Neill, 2006), biological sciences (Beezer, 1980; Wadsö, 1986; James, 1987), environmental sciences (Wadsö, 2009; Maskow, 2013), microbiology (Braissant *et al*., 2010a; Nykyri *et al*., 2019; Braissant *et al*., 2020; Feng *et al*., 2021) and food industry (Wadso and Galindo, 2009; Kaletunc, 2009; Stulova *et al*., 2015).

Other sectors where calorimetry has been implemented and proved to be useful include biomaterials testing (Zimehl *et al*., 2002); biochemical and clinical analysis (Grime, 1980); chemical industry (de Buruaga *et al*., 1997; Leiza and McKenna, 2014); material sciences (Sheng *et al*., 2021) and many other areas.

Calorimetry is suitable for analysis of chemical, physical and biological processes and as such is specifically suitable for analysing foods, food production processes and food systems. This is because many processing methods involved in food production and food processing are thermal processing techniques which are either heating, cooling or freezing and their physicochemical effects are detectable by calorimeters. For example, exothermic processes such as fermentation, oxidation or crystallisation as well as endothermic processes such as melting, denaturation and vaporisation can be studied. Traditionally, differential scanning calorimetry (DSC) is the method of choice in the food industry as this method is well suited to deal with different transformation processes such as melting, oxidation, crystalisation or denaturation. The ranges of temperatures occurring during these processes vary significantly therefore DSC has great utility (Le Parlouër and Benoist, 2009). Nevertheless, many food production processes involve mixtures of different liquids and powders and for this reason IMC offers a much better analytical tool that can deal with diluted solutions or bulk materials isothermally (Le Parlouër and Benoist, 2009). In contrast to DSC, IMC measures heat processes occurring directly in samples at constant temperature - the samples do not need heating or cooling; these heating and cooling cycles could interfere with the studied processes (Law and Zhou, 2017).

The industrial production process of Symprove described in **1.4** is just one practical example where calorimetry can be implemented. Calorimetry, and more precisely isothermal microcalorimetry, is well suited to the purpose of on-line (real time) process monitoring through heat change measurements because it can mimic processes which need constant temperature for optimal yields such as fermentation (Schäffer and Lorinczy, 2005). This makes IMC a specifically suitable method for fermentation process monitoring. Data obtained by a calorimeter contains kinetic parameters and these can be analysed in order to gain insights into the dynamics of the system under investigation (Riva and Schiraldi, 1993).

There are many benefits for using calorimetry to enhance quality and safety in the food industry as outlined by Kaletunc (2009) and others, for example:

1. It can be implemented in various pure components of foods or complex food matrices (or raw materials);

2. It does not require optical transparency, unlike spectroscopic methods or gas liberation or precipitation of a sample during the analysis (Kitzinger and Benzinger, 1960);

3. Uniformity and homogeneity of studied materials is not required;

4. The results are model independent;

5. It directly measures the energetics of transition;

6. Interactions of individual components in a complex food matrix (Aguilera, 2019) can be studied;

7. Sample preparation is usually simple and non-destructive in ampoule batch IMC;

8. It is a well-established technique in the food industry and has a solid theoretical basis.

9. Highly advanced instruments are available and the measurements can be correlated to more traditional methods such as microbial culture techniques (Burlett, 2008);

10. Major safety as well as quality issue - microbial spoilage, can be assessed by calorimetry (Burlett, 2008). IMC specifically, is a well-suited method for bacterial monitoring because it can measure heat changes non-destructively on a microwatt scale (Braissant *et al*., 2010a), whilst it is implementable as an on-line monitoring method as mentioned in **1.4.4**;

11. Thermal behaviours of individual components as well as the final products can be studied (Raemy *et al*., 2009);

12. Shelf life of complex food matrices can be predicted using calorimetry (Gaisford *et al*., 2009).

As outlined in the introduction (**1.1)**, this project has two objectives, one pragmatic and one theoretical. Both objectives considered a biological semi-closed (meaning formally non-sterile; in other words, not as an attempt to make medicine) system with defined organisms and controlled medium, which constitute FV1. The pragmatic aim was to develop a reliable method for the Symprove company that allowed them to discern in very simple terms (a

Yes/No answer) if the product could be released for sale. Ideally, the method should be a standalone method whose requirements were: an instrument; a competent technician and implementability in an industrial environment with minimal laboratory provision. The theoretical aim, on the other hand, was to contribute to theory at large and so develop the theory behind the pragmatic one enough as to make this approach applicable to different industrial settings as well as making contribution to microbiological theory and calorimetry. This theoretical development worked towards a mathematical framework for quantitative interpretation of exponential bacterial growth. The analysis would ambitiously also enable other future investigations. These could include: organisms' history (*i.e.*, inoculum variation caused by the medium it was grown in, when produced); suitability of other bacteria to be added into the product; designing new formulations or generations of the product; suitability assessments of new growth substrates; compatibility and fitness of additives such as buffers or prebiotics. The theoretical development involved modifying existing equations that describe bacterial systems so they could be used to obtain information from the various processes occurring during bacterial growth.

The method envisioned as the pragmatic outcome, the one that could authenticate the production and the product, should also contribute to a theoretical analysis. It would, hopefully, enable the establishment of growth phase parameters (and their numerical values including confidence ranges, to maximise the extraction of information from data collected). A potential expansion of the method to include the continuing metabolism of the organisms in the product post exponential phase (*e.g.*, stationary phase and death phase parameters of the bacterial culture) could be achieved. This would enable testing the stability of the product over its shelf life.

One of the ambitions of this project was to solve a major industrial production process challenge, namely shortening the testing time. The method should be simple enough so as to ensure that when put to everyday use, it would not require in-depth knowledge of fermentation processes or laborious sample preparation. Data processing and interpretation should be done using a BB as to minimise the subjectivity arising from a manual operator-dependent analysis. In order to choose the most adequate method, it was first important to outline the nature of the problem and the range of methods under consideration.

1.5 Conclusion

Symprove production was a heterogeneous, closed system process. It had limited variability because it involved only two bacterial components and one growth medium in each fermenter and temperature fluctuations during the fermentation stage were limited. The final product was an equal mixture of FV1 and FV2. It was opaque in appearance and contained suspended particulate material from barley and bacteria and bacterial metabolites. Calorimetry as used in this project offered an elegant approach to reach both pragmatic outcome (Yes/No release for sale answer) as well as theoretical outcome (quantitative data analysis). IMC was fast, simple, repeatable and could monitor processes inside opaque suspensions whilst they were happening. Calorimetry enabled the study of real time behaviours of the individual bacterial components (*L. acidophilus and L. rhamnosus*) of the fermentation, separately and in pairs. The samples could be set up without any treatment and non-destructively by a technician. The interpretation of the results could be easy, assuming the black-box approach to analysis, however, this required that the mathematical background to data processing was completed (**1.5.1, objective 3**). Further developments were ongoing to enhance the formulation with more nutritious substrates in order to extend the shelf life and quality of the final product.

In sum, this project aimed at developing a reliable, science-based, and timely method for the biotechnology industry. By determining basic parameters of a successful fermentation process, its ambition was to contribute to the understanding of bacterial growth characteristics, cell numbers, and the interactions between different bacteria fundamental for developing new formulations of probiotics and potentially assist in designing disease appropriate/specific probiotics.

1.5.1 Aims and objectives

The overarching aim was to find out whether IMC can be useful for Symprove's product quality and safety assurance testing. The following objectives were set to achieve the overarching aim:

1. To determine whether IMC had the capacity as a batch to batch release method and as a production process monitoring tool for Symprove.

2. To provide a set of calorimetric bacterial references, new in this field, which were needed to determine the repeatability of the IMC method.

3. To develop the mathematical background (equations) required for data processing and analysis that would enable a future BB approach incorporation into a piece of coding for an automated data processing (only a proof of concept is offered).

4. To introduce scientific methodology into the industrial production processes of Symprove

5. To enable fast and precise decision making about bottling and selling the finished product by having an extended range of production control parameters.

Chapter 2 Exploratory phase

2.1 Introduction

The initial exploratory phase of this project lasted 18 months during which approximately 500 calorimetric experiments were conducted in order to explore the behaviour of the product in a variety of media; to explore the reproducibility of the system selected; and to establish a protocol which allowed for a sufficiently sensitive insight into the performance of the product in the calorimeter.

IMC as used in this project was proposed to Symprove co. as a novel technique for QA. For IMC to be useful as a QA method for Symprove, it had to be demonstrated that it could show what was considered (when doing this project) a good final product. A good product in this context was the product which was authenticated by an independent laboratory as having the right distribution of organisms at the right densities (concentrations) without contaminants. The standard QA testing done by a contract independent laboratory usually took between 7-15 days from receiving samples of the product. It also needed to be demonstrated that the images (p-t curves) coming from the calorimeter were consistent and reproducible for each new batch of a good product when compared with previous ones. This first task is presented in section **2.3**.

There was no theory behind determining whether consistency and reproducibility were possible, except the observation that it was necessary to have a controlled experiment. This first step was done simply on a reproducibility and similarity of patterns basis; in other words, taking a sample of the final product and testing it in the calorimeter in a variety of growth media (including barley worts, Cooked Meat Medium (CMM), Brain-Heart Infusion (BHI), chemically defined media (CDMs), Tryptone Soya Broth (TSB), De Man, Rogosa and Sharpe broth (MRS)) to observe what would happen. Whilst all media supported growth of the full product well, it was decided that TSB and MRS were the media of choice for this project as these two media were also used by the contract QA laboratory. This would minimise any discrepancies between results obtained from the laboratory and IMC because of media differences.

The first test in this situation (Symprove) was to discover whether a good product was revealed in IMC tests as a consistent outcome. That meant, looking at the shapes (**2.3** and **2.5**) and say everything seems to occur at the same time within small differences which were expected in this semi controlled system, where there was an expected variation in the

medium (wort) composition and there was an ambitious view that the inoculum should be controlled.

2.2 Materials and methods

2.2.1 Instrumentation (TAM)

A Thermometric Thermal Activity Monitor (TAM) 2277 (TA Instruments Ltd., UK) was used for all microcalorimetric experiments reported in this thesis. The model used contained 4 individual and independently working measuring cylinders, each of which had a twin cup form (sample and reference), accepting 3 mL glass ampoules. The reference ampoule should be of similar heat capacity as the sample tested, and this was achieved by choosing the same medium and its volume in the reference ampoule as in the sample ampoule, for example, sterile MRS or TSB. TAM's functional description, installation requirements, calibration, operation and maintenance are detailed in the Thermometric instruction manual (Technical specifications, Thermometric). The TAM used in all experimental work was located in an air-conditioned room at stable temperature 22°C ±1°C. Calibration of the instrument was performed according to the TAM instruction manual (Thermometric, 1996).

2.2.2 Media

De Man, Rogosa and Sharpe (MRS) broth, from Sigma-Aldrich, was prepared according to the manufacturer's recipe and used in all experiments involving MRS. To avoid fluctuations in the composition of MRS, a sufficient quantity of the same batch was acquired from one supplier only. This is referred to as a controlled medium in this thesis. Similarly, any other medium could be controlled in this way if its composition and its individual components were not chemically defined.

Tryptone Soya Broth (TSB) from Thermo Fisher Scientific, was prepared according to the manufacturer's recipe and used in all experiments involving TSB.

Selection of appropriate growth medium and its composition control was critical. Minimal changes in the TAM testing medium composition *e.g.*, weighing error during a growth medium batch preparation, autoclaving or manufacturer's batch-to-batch variation of the

same medium could have a significant effect on the growing culture and lead to significant differences between p-t curves as demonstrated by Perry *et al*. (1979). Evaluation of growth medium could also be studied microcalorimetrically (Perry *et al*., 1981).

2.2.3 Test samples

The initial exploratory experiments were done using either the final (full) product (equal mix of FV1 and FV2 without flavouring) or FV1 only (the focus on FV1 was because most batches which failed were the result of problems in this vessel). 500 mL samples were drawn directly from the fermenting vessels or the mixing vessels, taken to the TAM laboratory where 30 µL from each 500 mL sample were tested following **2.2.4** protocol.

2.2.4 IMC experiment protocol

The operation of the calorimeter was according to the TAM instruction manual and in outline consists of the following steps. Sterile glass ampoules (3 mL) were filled with pre-warmed (37°C) sterile MRS or TSB (2.97 mL) and inoculated with an appropriate sample (30 µL of either full product or FV1 sample). The ampoules were immediately sealed under aseptic conditions, vortexed for 1 minute and then inserted into the thermal equilibration position inside of the TAM for 30 min before data capture began. TAM temperature was set to 37°C. Data were collected using the software package Digitam 4.1. Digitam 4.1 collects data every 10 seconds. This method has the effect of smoothing the power data (Cabadaj *et al*., 2021). Data were recorded for as long as it took the signal to return back to baseline. Care needed to be taken when sealing the ampoules as if the samples were not sealed completely, high moisture content (water activity) of the samples could create evaporation during testing, causing data corruption deeming the experiments invalid.

2.3 IMC curves of good product

Not all samples reached peak powers at the same time or to the same extent as seen in **Figure 2.1**. This could have been caused by different cell densities in the individual batches. This phase of exploration of suitability of IMC for the purpose of this project demonstrated that the IMC was a reliable indicator of a good product, and the images (p-t curves) obtained via IMC were highly reproducible. However, the complexity of data obtained for the full product (4 bacteria in a complex medium) might present a challenge, for example in identifying a contaminant present at a very low concentration or indeed if the growth of a particular contaminant was not supported by the testing medium of choice (TSB, MRS). In this instance, more specific media (such as antibiotic supplemented or discriminating nutrient supplemented media) might be required for testing or the system itself could be simplified (e.g., deconstructing the full product into its individual components FV1 and FV2). The latter, simplifying the complexity of the full product was explored in more detail in **Chapter 4**. It appeared that MRS supported the growth of full product better by observing higher peak power and total area under the curve compared with TSB results (**Table 2.1** and **Table 2.2**). The greater lag time observed in MRS experiments showed that the organisms grew much faster in TSB (suggesting more favourable nutrient composition of TSB for the initial growth, or MRS not supporting growth of one or more of the bacteria as well as TSB did).

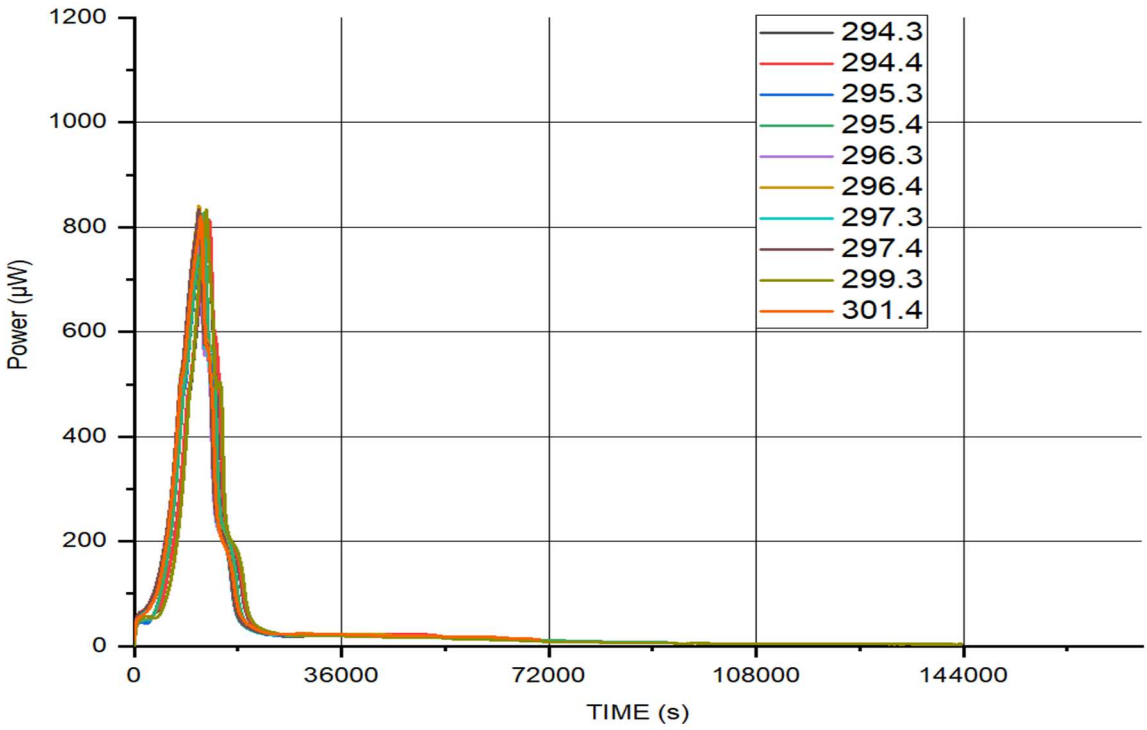

a)

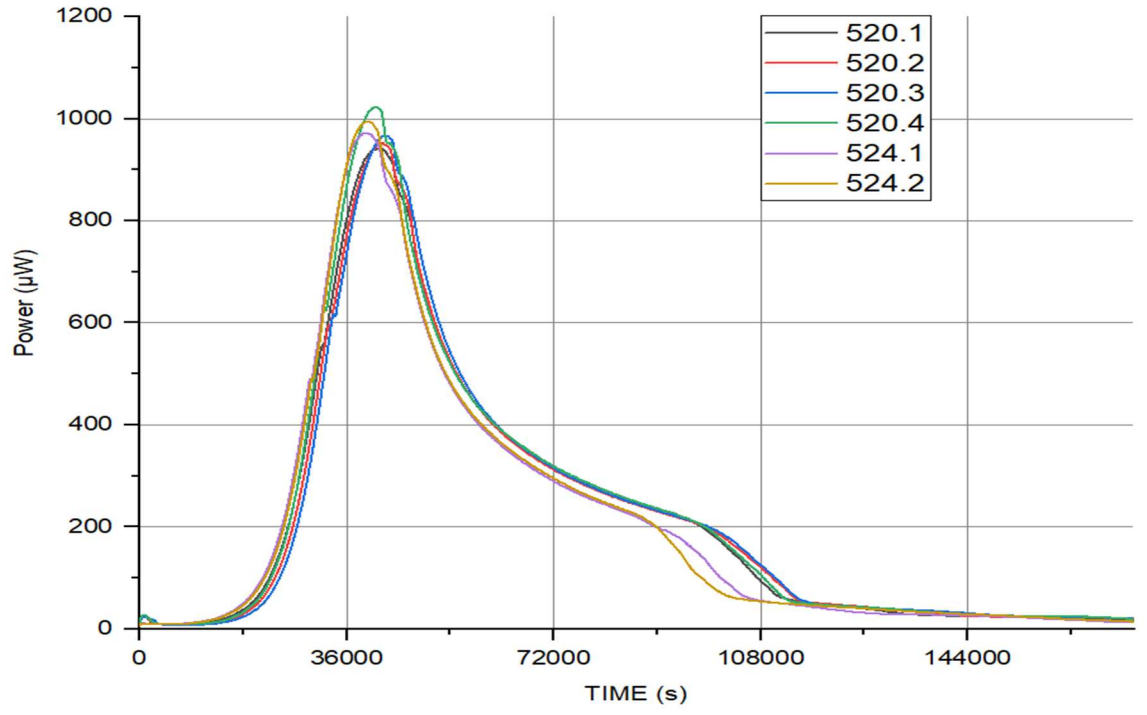

b)

Figure 2.1 Repeatability demonstration on a good final product, 10 individual batches of Symprove tested in TSB a); and 6 individual batches of Symprove tested in MRS b).

Exp number	Peak height time [s]	Peak height [µW]	AUC
294.3	12970	777.4	5.50×10^6
294.4	13040	812.7	5.81×10^6
295.3	11870	796.5	5.52×10^6
295.4	12010	825.9	5.78×10^6
296.3	11150	805.1	5.40×10^6
296.4	11240	840.7	5.68×10^6
297.3	11290	806.1	5.36×10^6
297.4	11200	833.4	5.75×10^6
299.3	12550	833.4	5.95×10^6
301.4	11580	820.9	5.73×10^6
SD	696	18.5	1.84×10^5
mean	11890	815.2	5.65×10^6
1% of mean	118.9	8.2	5.65×10^4
x% of SD = repeatability	5.9	2.3	3.2

Table 2.1 Basic shape analysis parameters, Symprove good batches full product tested in TSB.

Exp number	Peak height time [s]	Peak height [µW]	AUC
520.1	41891	941.6	3.52×10^7
520.2	42201	952.4	3.55×10^7
520.3	42601	967.0	3.60×10^7
520.4	40661	1022.0	3.73×10^7
524.1	39401	972.5	3.44×10^7
524.2	39411	995.3	3.44×10^7
SD	1290	26.8	9.99×10^5
mean	41028	975.1	3.55×10^7
1% of mean	410.3	9.8	3.55×10^5
x% of SD = repeatability	3.1	2.8	2.9

Table 2.2 Basic shape analysis parameters, Symprove good batches full product tested in MRS.

2.4 Consistency and reproducibility

Excellent consistency and reproducibility were seen between individual real batches of the final product in **Figure 2.1** —images of a good product. The consistency was confirmed by the main contract laboratory (Lab 1) for each batch by having the right distribution of

organisms at the right densities, without any detectable contamination. It is important to state here that there was an agreement between Lab 1 results and the IMC curves in terms of consistency (Lab 1 results and p-t curve shapes).

Consistency of IMC traces in a good product was very important. The consistency indicated that calorimetry had the possibility and capacity of being used to identify, in principle, a good product. If there was no consistency, this could be indicative of, for example, some problem in the product, such as presence of a contaminant, occurrence of different metabolisms or IMC not being suitable for this purpose.

Subsequently, the majority of new batches of product was analysed via IMC although IMC was not used for the release for bottling and sale as Lab 1 results were still the gold standard. This routinised IMC testing served to establish a good statistical base (more than 100 experiments) for a good product.

It was established in this chapter so far that calorimetry has the possibility and potential to be useful. The first task to see whether a good product could be seen reliably and consistently in a calorimeter was successful. The confidence to see a good product was established (**Figure 2.1**) and strengthened by investigating the majority of subsequent products. The same approach was taken to study a simplified system (FV1) to determine whether IMC is sensitive enough to detect problems. These are presented in **Chapter 4**.

Consequently, when anomalies from the expected p-t curve appeared, these were investigated and are reported in the following sections. However, since these events were random, individual and unique events by definition, therefore these were not analysed in the same way as the rest of the experiments with multiple repeats.

Basic shape analysis could be done by overlaying subsequent shapes (p-t curves) on top of an established working reference shape (in principle everything should be the same - peak height, time to peak height, area under curve if the investigated batch was good). There was an understanding that quantitative data was available and could be measured, however shape was what was relied on at the time.

After confidence in IMC was established, the majority of subsequent real production scale batches were tested by IMC using a routine protocol IMC was not used to accept/reject a new batch at this point. It did however, complemented the standard microbiological methods. Symprove company still relied on the Lab 1 for batch release. However, as it became clear

that having additional IMC data was greatly advantageous, all samples started to be routinely inspected by IMC. Even though the whole p-t curve needed to be recorded (to be able to perform a visual shape analysis) a dramatic reduction of testing time was envisaged if IMC was used.

2.5 Establishing working reference curve

The term “working reference curve” refers to an average p-t curve obtained as a simple mean of ten p-t curves from good FV1 batches (good growths). **Figure 2.2** shows the establishment of a working reference curve. It was immensely rewarding that consistency and high reproducibility of the p-t curves seen with the full product could be seen again in FV1 batches. **Figure 2.2c** shows a range of ± 2x standard deviation (SD) of the mean of 10 batches to set 95% probability a good batch fell within this range. Moreover, there was also an agreement between the external QA laboratory (Lab 1) and the p-t curves as detailed in **Table 2.3.** Therefore, it should be, in principle, possible to see contaminated batches through distortions in the resultant observed p-t curves (assuming the additional heat from a contaminant would be sufficiently high and the IMC testing medium would support the growth of a potential contaminant). The mean time to get results using Lab 1 was more than 14 times greater with SD (standard deviation) approximately 100 times greater compared with IMC (**Table 2.3**). This demonstrated again how satisfactory IMC was.

After determining a mean TAM output of 10 individual FV1 real batches tested in TSB, this mean was compared with a real production batch (294.1, referred in this chapter as FV1-real-pure batch) in which pure rather than production inocula were used. Production inocula (as noted earlier in **1.4.2.1**) could contain ≤ 5 x10^4 of total aerobic contaminants as per supplier’s raw material specifications (set by the supplier) and this could contribute to anomalies in the p-t curves.

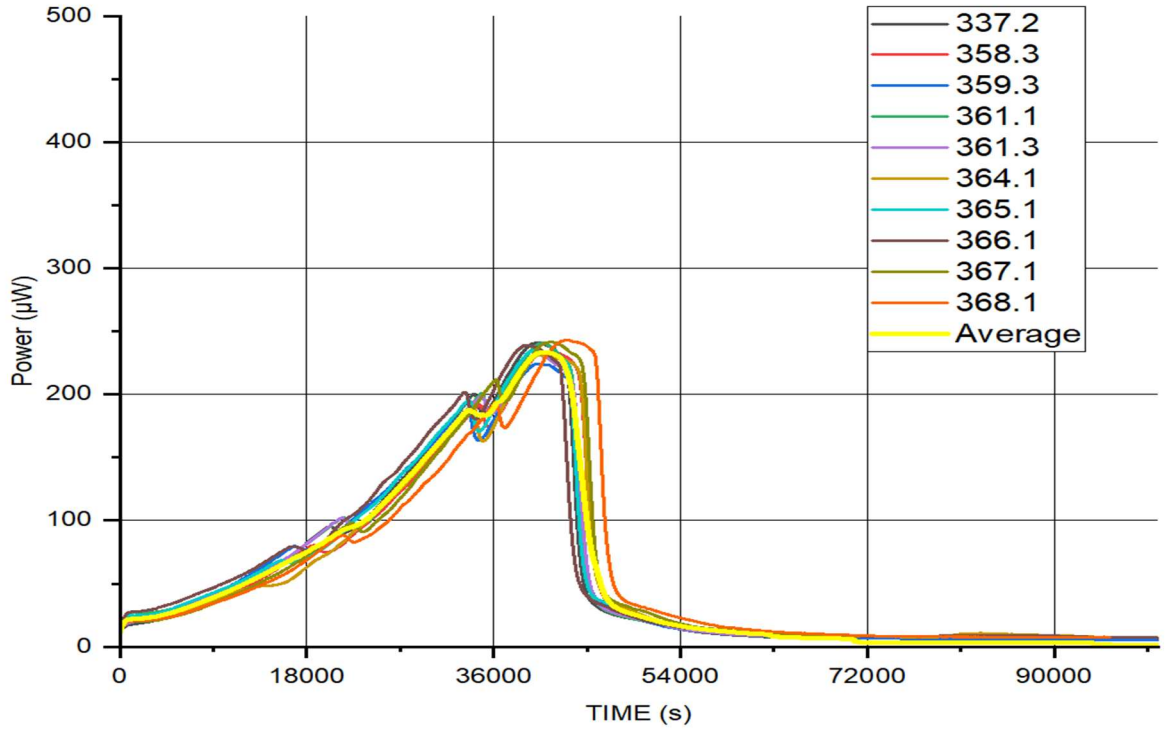
337.2
358.3
359.3
361.1
361.3
364.1
365.1
366.1
367.1
368.1
Average
Power (µW)
TIME (s)
0
100
200
300
400
500
0
18000
36000
54000
72000
90000

a)

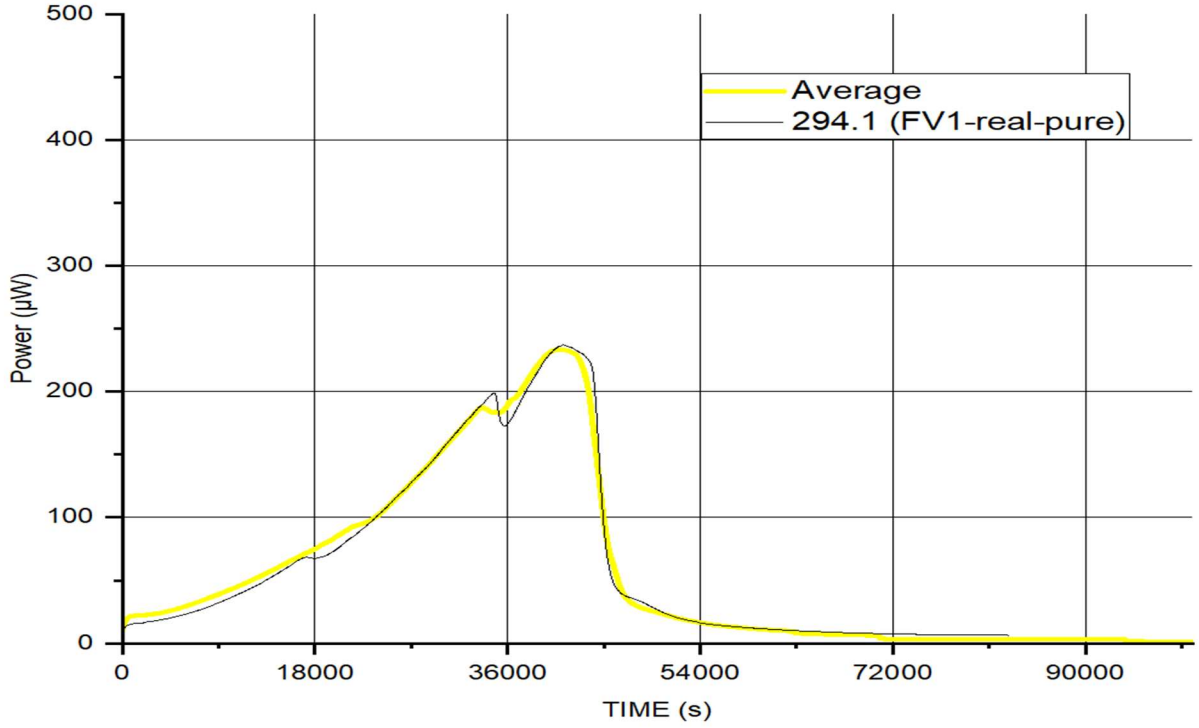
Average
294.1 (FV1-real-pure)
Power (µW)
TIME (s)
0
100
200
300
400
500
0
18000
36000
54000
72000
90000

b)

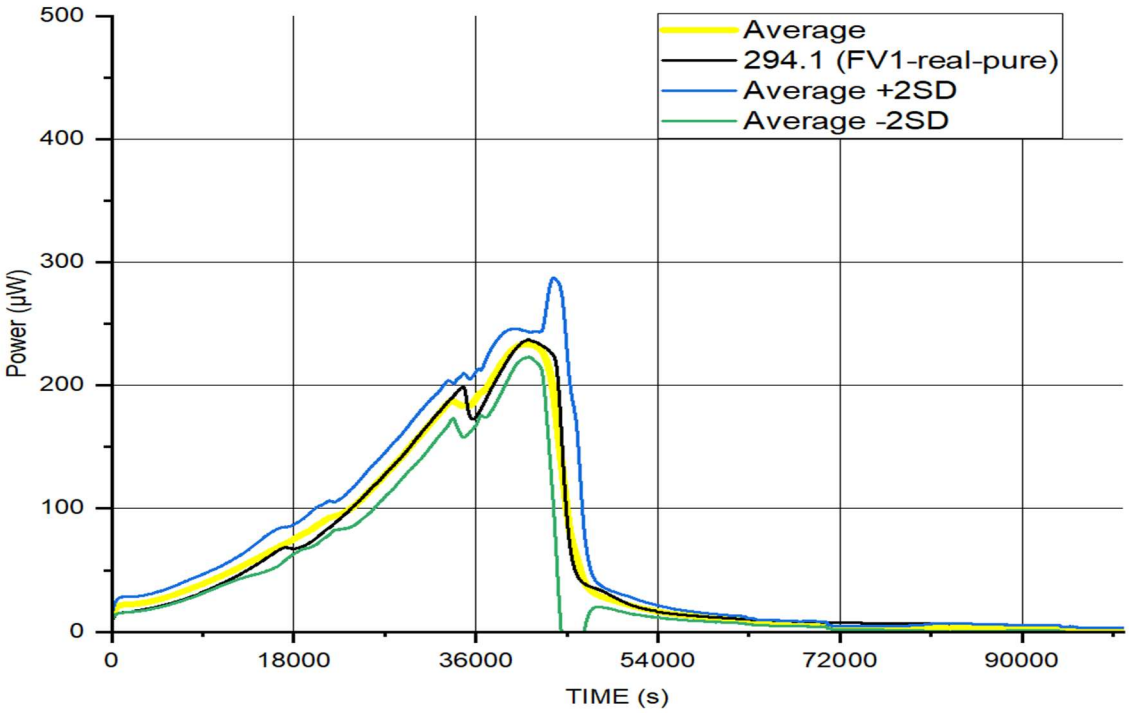

c)

Experiment number	Peak height time [s]	Peak height [µW]	AUC
337.2	39993	240.7	4.78×10^6
358.3	41003	234.1	4.81×10^6
359.3	40013	223.8	4.77×10^6
361.1	40693	240.7	4.72×10^6
361.3	40213	231.2	4.89×10^6
364.1	40263	231.2	4.54×10^6
365.1	40243	234.9	4.62×10^6
366.1	39233	238.9	4.85×10^6
367.1	41313	241.5	4.85×10^6
368.1	42823	242.9	4.85×10^6
SD	927	5.8	1.05×10^5
mean	40579	236.0	4.77×10^6
1% of mean	405.8	2.4	4.77×10^4
x% of SD = repeatability	2.3	2.4	2.2

d)

Figure 2.2 Determination of a mean p-t curve (working reference) from 10 independent good batches of FV1 a). Comparison between the working reference and a single FV1-real-pure batch made using pure inocula b). Outlining ± 2x standard deviations c). Details of the shape analysis parameters are tabulated in d).

Establishing the working reference curve relied on shape analysis —overlaying p-t curves of new batches onto the working reference p-t curve (though not done herein) to assess whether the new batches were good or not. This meant that shape derivable parameters such as peak height, area under curve and the time to reach peak height of the working reference curve and a new batch p-t curve should be equivalent providing the new batch was good. So, the p-t curve shape was what the shape analysis relied on whilst understanding that there was measurable quantitative data contained within it. To measure these quantitative data other type of analysis needed to be developed and is discussed in **Chapter 3** and **Chapter 4**.

Batch no	Time (hrs) IMC	Time (hrs) Lab 1	IMC anomaly detected	Lab contamination detected
337.2	11.1	168	No	No
358.3	11.4	144	No	No
359.3	11.1	216	No	No
361.1	11.3	144	No	No
361.3	11.2	168	No	No
364.1	11.2	168	No	No
365.1	11.2	144	No	No
366.1	11.5	192	No	No
367.1	11.5	168	No	No
368.1	11.9	144	No	No
294.1	11.4	144	No	No
Mean	11.3	163.6	-	-
SD	0.22	22.46	-	-

Table 2.3 Comparison between IMC and Lab 1 turnaround testing times.

The consistency between the contract laboratory (Lab 1) and IMC was seen in the majority of cases. IMC was consistently seen to accord with a good product as specified by the Lab 1. However, IMC studies reported in the following sections showed anomalous results which were not consistent with the data presented by Lab 1. These IMC results prompted additional microbiological testing in order to discover the reasons of the anomalies.

2.6 Practical applications of IMC

Historically, almost all production contaminations were detected in FV1, therefore, after demonstrating the potential of IMC on full product, FV1 became the focus of the work and is reported in this chapter. Another reason to study FV1 in depth was to break down complexity of the full product. Studying FV1 separately had a further advantage, as, if there was a problem detected prior to mixing the two vessels (FV1 and FV2), the mixing could be postponed, a fresh batch of FV1 made, and FV2 saved. After the establishment of a good FV1 (working reference) the flow of the next three sections is organised from obvious problems (*e.g.*, smell or taste issues in **2.6.1**), through to not so obvious problems (contract laboratory tests showed in-specification results and no smell or taste issues —the only indicators of a problem were anomalous p-t curves when compared with the working reference curve in **2.6.2**) to more specific issues of raw materials contamination (**2.6.3**).

Sourcing top quality ingredients from reputable suppliers is the first step in ensuring safe and high-quality end products. This first step is even more important when some of the ingredients are bacteria and part of the product is a growth medium supporting growth of many different bacteria including pathogenic bacteria. Section **2.6.3** shows an excellent practical application of IMC into real world industrial problem solving.

2.6.1 Obviously spoiled product

The events of spoiled batches were rather random in nature, therefore difficult to investigate. When they occurred, the priority was to rectify the lost volume by discarding the affected batch and producing a new one. Eventually, as the production volume increased, more focus was given to find the root cause of these events to prevent their occurrence. Samples of the spoiled batches were already routinely tested by IMC to capture any potential anomalies that could be analysed at a later stage. The reason to test spoiled batches was my curiosity about what they would look like in the calorimeter, as well as a simplicity and low cost of performing an IMC experiment in the laboratory with the calorimeter immediately next to the production unit on site. When I realised that having a comparison between IMC and contract laboratory would be beneficial (examining the sensitivity of the contract laboratory to detect a problem in a clearly poor product), the same samples of spoiled batches were tested via IMC as well as sent to the contract laboratory for analysis. Previously, spoiled batches were not analysed by the contract laboratory as the cost of testing was prohibitive for a batch that

was not to be used. For comparison, the cost of performing IMC experiments on one batch was approximately £25 and the cost of microbiological testing of one batch of product was approximately £500, if there was no issue detected.

To confirm the question of the ability to see anything unusual in the calorimeter, obviously spoiled batches of FV1 were tested and compared with good batches of FV1. A starting point was as previously shown in **Figure 2.1**, a good product, however this time the complexity of the full product was reduced into its first component FV1 and 1 medium (TSB in this case), as this was a logical thing to do when dealing with the problems occurring in FV1.

2.6.1.1 Results

Bad FV1 batches (these were one offs, not repeatable as by definition they are unique events, not planned nor predictable) are represented by individual experiments only. P-t curves of the bad batches whose quality was obviously compromised, because they were organoleptically unacceptable for any further processing either because of their smell, taste or fizziness at the end of fermentation are shown in **Figure 2.3.** Comparison with the working reference and its ±4 x SD —99.9% of all p-t curves of good batches should fall within this range.

There was significantly shorter time needed for the IMC experiments relative to the contract laboratory timings (**Table 2.4**). Extended tests were prompted by anomalous IMC results.

Batches that were clearly bad (defined as either smelly, fizzy or otherwise organoleptically compromised, therefore not suitable for human consumption or further processing) are shown in **Figure 2.3a.** It was obvious that the p-t curves differed notably when compared with the expected p-t curve. The expected p-t curve was previously established as the working reference in **2.5**. This expected p-t curve was then compared against the p-t curves of the bad FV1 batches, see **Figure 2.3b**. IMC did reveal problems, likely contaminants, because the patterns (shapes of the resulting p-t curves) were different whereas the Lab 1 did not detect any problem with their standard testing (except in 1 case —batch 201.2 see **Table 2.4**) while there were obvious problems with the batches. Additionally, the IMC detected anomalies much faster (more than 10 times) than Lab 1. Moreover, IMC was shown to be capable of identifying contamination with greater sensitivity (as compared with Lab 1).

Four examples of Lab 1 not detecting a contaminant in their standardised Symprove specific tests (240.1, 243.4, 327.2 and 333.4) are summarised in **Table 2.4.** As seen in **Figure 2.3b**, all 5 batches in question were identified by IMC as out of the expected FV1 p-t curve shape (working reference). 100 % problem detection was achieved by IMC as opposed to only 20% problem detection by Lab 1's standard test package.

IMC results, interpretation and implementation into production decision making offers a fast, cheap (the calorimeter used in this project was a second hand one and its cost was £400 to purchase) and reliable warning tool as demonstrated above. If the p-t curves seem similar as illustrated in **Figure 2.3c** (purple 333.4 and yellow mean curves), it would be prudent to perform further analysis especially if the batch in question is not obviously compromised by odd organoleptic parameters. This is demonstrated in the next section **2.6.2.**

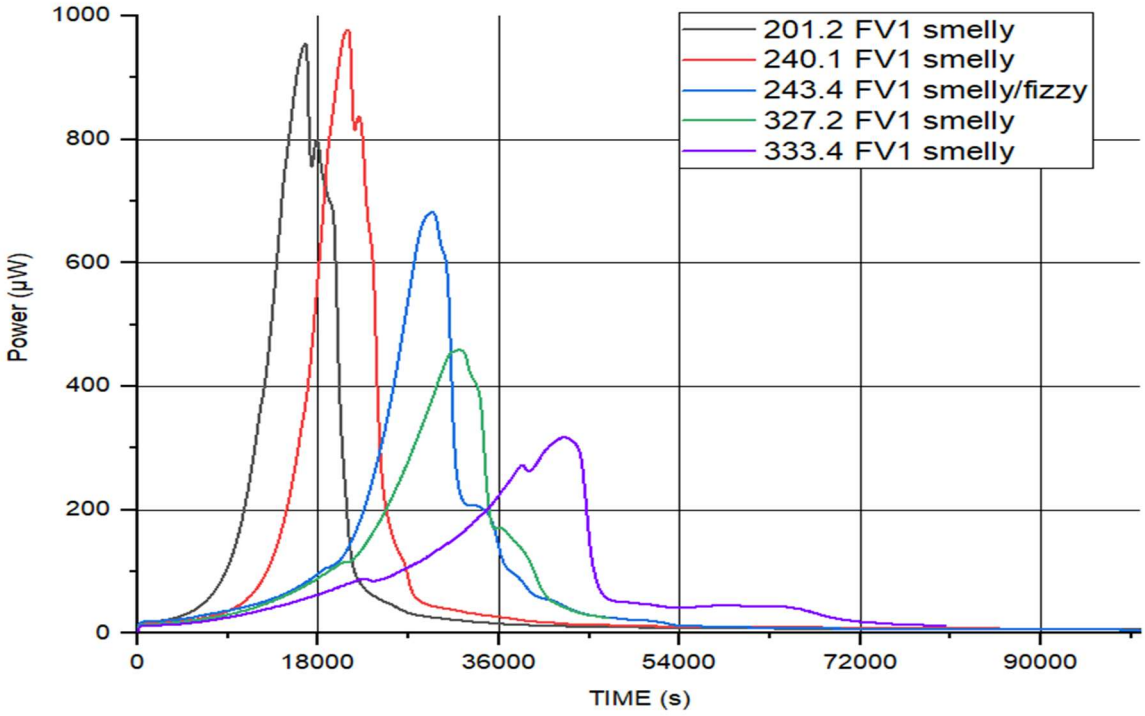

a)

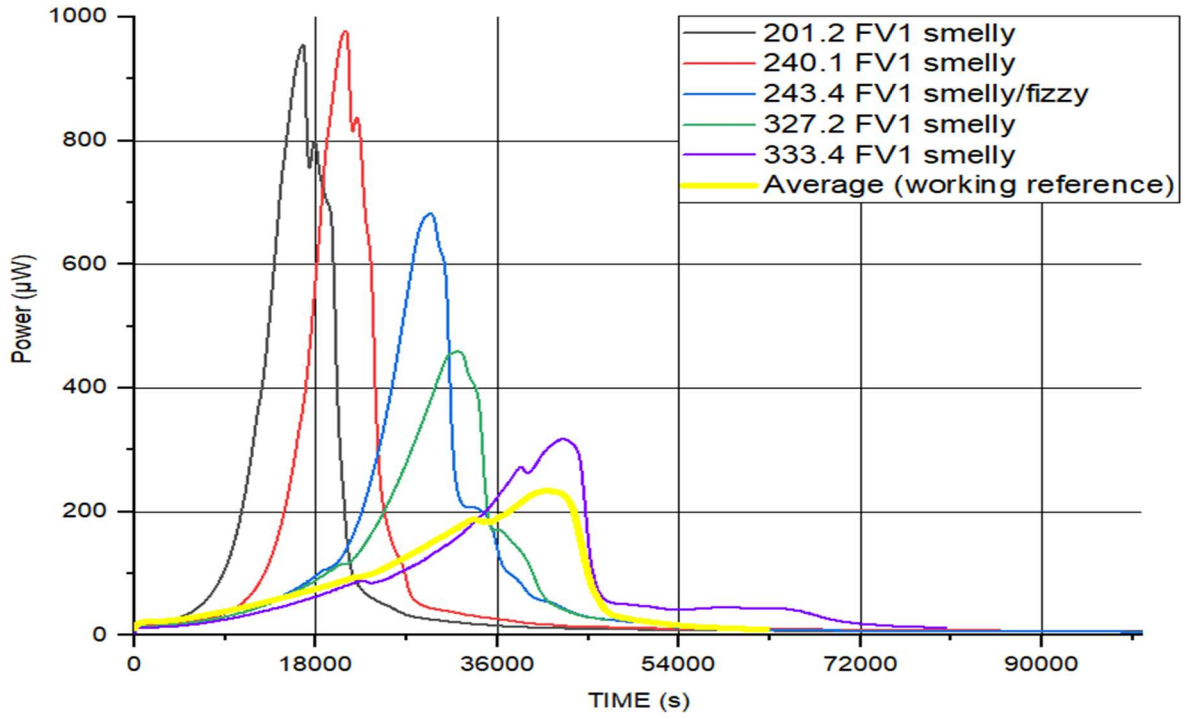

b)

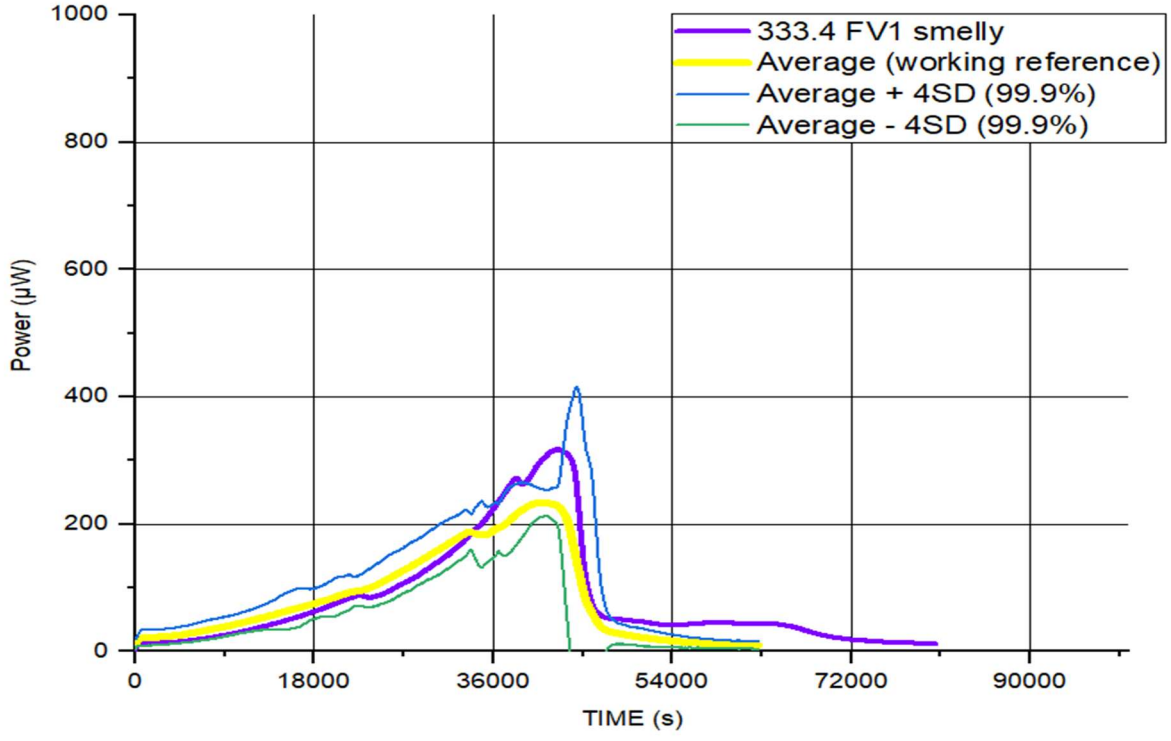

c)

Figure 2.3 Illustrations of contamination perception in 5 different batches of FV1 using IMC a); the same 5 batches in comparison with the working reference b); and c) represents more detailed analysis of batch 333.4. All tested in TSB.

Batch no	Time (hrs) IMC	Time (hrs) Lab 1	IMC anomaly detected	Lab contamination detected
201.2	5	144	Yes	Yes
240.1	6	144	Yes	Yes, on extended tests, not on standard tests
243.4	8	336	Yes	Yes, on extended tests, not on standard tests
327.2	9	312	Yes	Yes, on extended tests, not on standard tests
333.4	11.8	168	Yes	Yes, on extended tests, not on standard tests
Working reference (see **2.5**)	11.3	163.6	No	No
Detection success			100%	20%

Table 2.4 Comparison of contamination detection using IMC and Lab 1 methods

2.6.1.2 Discussion

Standard Lab 1 tests were routinely used to test the individual components FV1 and FV2 as well as the final mix with any additives (such as flavour, antioxidants, and preservatives) for product release for bottling and subsequent sale. These tests included the following: presence/absence and enumeration of *L. plantarum, L. acidophilus, L. rhamnosus, E. faecium*, *Escherichia coli, Salmonella species,* Yeasts and Moulds, and pH – denoted as standard test package provided by Lab 1. The results usually took between 7-15 days to be received by Symprove. If any extra testing was required, this added more time and cost to receiving the final results (it depends on the type of tests required how long before the results were available, however, in some instances this could be two or more weeks). If the main contract laboratory (Lab 1) did not successfully identify a contaminating organism using their in-house MALDI-TOF instrument, they sent a slope of the isolate to another certified laboratory. Their primary sub-contracting laboratory was based in France and this would add up to 2 extra weeks to getting results.. There were only a few reasons such as rancid smell or unusual fermentation for which extra tests would be requested. A basic assessment of the organoleptic properties (taste and smell) was done by the production staff. This assessment was essential for requesting the extra tests. Samples of any batch were tested immediately after being taken. It took approximately 40 minutes to prepare samples to start data capture by IMC. Regularly it took 24 hours for a standard IMC experiment to complete.

If there was an issue, as seen for example in **Figure 2.3**, the IMC experiment would reveal the issue even faster. Subsequent data analysis would take no longer than 30 minutes. However, based on the expected p-t curve, this particular batch (333.4) would not be released for subsequent processing (bottling and sale) as its p-t curve was outside of the mean (yellow) p-t curve even when ± 4 x SD was applied. In other words, it was observed with 99.99 % confidence that there were other/different processes happening which derailed the observed p-t curve (purple) from its expected path (yellow curve).

The images presented in **Figure 2.3a** were those of FV1 batches which were undoubtedly bad as their quality and potentially safety was compromised. Organoleptic properties of bad smell, foul taste and fizziness of these batches confirmed the batches as not being suitable for further processing. There were two possibilities regarding the examining laboratory:

1. The examining laboratory saw the contamination in their standard tests and reported as such or;

2. The examining laboratory did not see the contamination in their standard tests.

The case just presented, where it was reasonable to assume that if there were no obvious problems with the FV1 batches, standard Lab 1 test package would not reveal problems in 80% of compromised batches and these batches would end up bottled and sold on the market.

The examining laboratory did not identify any issues in 4 out of 5 batches. The question for IMC to answer in this context was: can the IMC alert the production staff and the management of the company that there was a problem with a particular batch, faster and more reliably than the standard laboratory testing? And the answer was yes. The results presented in this chapter spurred the curiosity to enquire more about the utility and implementation of IMC into regular batch to batch screening. It will be further elucidated in the next sections **2.6.2** and **2.6.3** where IMC tests revealed anomalous results whilst the main laboratory Lab 1 did not.

2.6.2 Seemingly-good product

As presented in **2.5**, a working reference curve obtained as the mean of 10 good FV1 batches was a fast and reliable way to assess a new FV1 batch for quality and safety by

detecting contaminants or other problems, therefore prompting extra testing if the measured p-t curves diverged from the expected one.

2.6.2.1 Results

The batches of product with conflicting laboratory results are shown in **Figure 2.4** where the yellow curve is the working reference curve. These results are individually compared with the working reference in **Figure 2.5a-j** for a better visual presentation.

When an anomaly from the working reference curve was seen these anomalies were one offs. Confidence based on consistency and reproducibility (see **2.4**) previously developed provided a basis for what a p-t curve of a good product should look like (see **2.5**). The reason for doing microbiological identification of contaminants was to get an indication whether the source of the contamination was at the supplier's facility or on site. Furthermore, a comparison of two independent laboratories (**Table 2.5**) provided additional confirmation that IMC was sufficiently sensitive to recognise that there was something different between the good curve (working reference) and suspicious p-t curves.

It is also important to note that Symprove did rely on the standard package of tests to release every new batch of the final product for bottling and sale, previously deemed sufficient to detect most contaminants. Extended testing would be requested only for an obviously "spoiled" batch, whilst a not obviously problematic batch such as only a p-t curve out of expected range would not necessarily trigger extra testing to keep the already high cost of QA procedures manageable by the limited resources of the growing start-up company. Additionally, the nature of the product itself (high bacterial load in the product) could mask the actual contaminant. This could happen if the contaminant's growth rate was much slower than the beneficial bacteria's growth rates, or the growth medium (wort) did not support the growth of the contaminant sufficiently in the mixed culture with the beneficial bacteria. It was reasonable to assume that the laboratory procedure might not be sensitive enough to detect the contaminant, which would not be high enough in numbers in the samples when diluted using serial dilutions method.

All the presented results come from batches which did not show any issues post-fermentation (e.g., smell, taste and pH in specifications (Symprove, 2021) —as assessed by production staff). IMC measurements that appeared out of specification based on the working reference mean of 10 (**Figure 2.2**) prompted the Symprove company to rethink the quality and safety testing procedures used up to that point (and provided solely by Lab 1).

Lab 1 had developed their standard testing procedures to suit Symprove product, which was complex in microbiological composition, hence posing a specific challenge in terms of microbiological quality and safety assessment. This specificity (such as high initial bacterial load as opposed to common food microbiology testing, which focuses on presence or absence of contamination detection) needed to account for example, for diluting a sample and therefore diluting any potential contaminants to non-detectable levels (this can be seen in **Table 2.5**, Exp 380.1 where Lab 1 was not able to detect any contamination even on their extra tests, whereas Lab 2 was able to detect a low level contamination on their standard *Enterococci* test and this was in agreement with the out of specification (OOS) IMC result (**Figure 2.5c**). The unusual activity in Exp 380.1 sample was detected by the IMC towards the end of the experiment, when the average reference curve metabolic activity was finished, however in that particular case (Exp 380.1) there was a secondary peak observed at the time when the reference curve was back to the baseline. The OOS IMC result prompted the additional testing of the same sample by Lab 2.

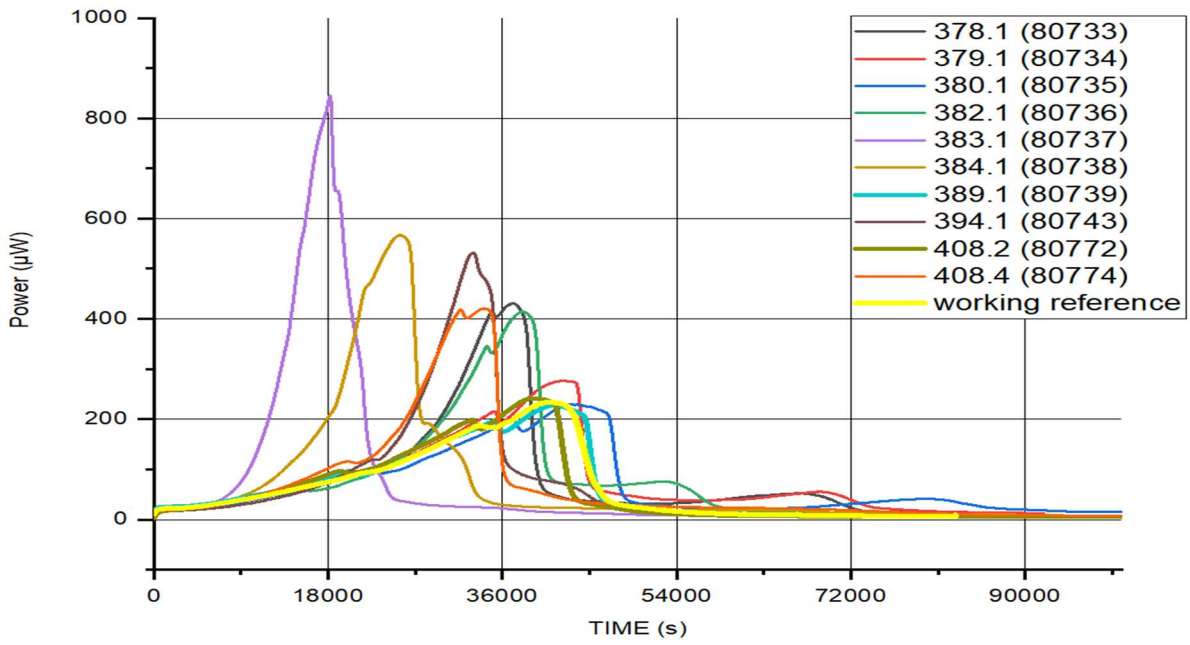

Figure 2.4 P-t curves of 8 batches with conflicting lab results and 2 batches (curves in bold) in agreement with both laboratory results

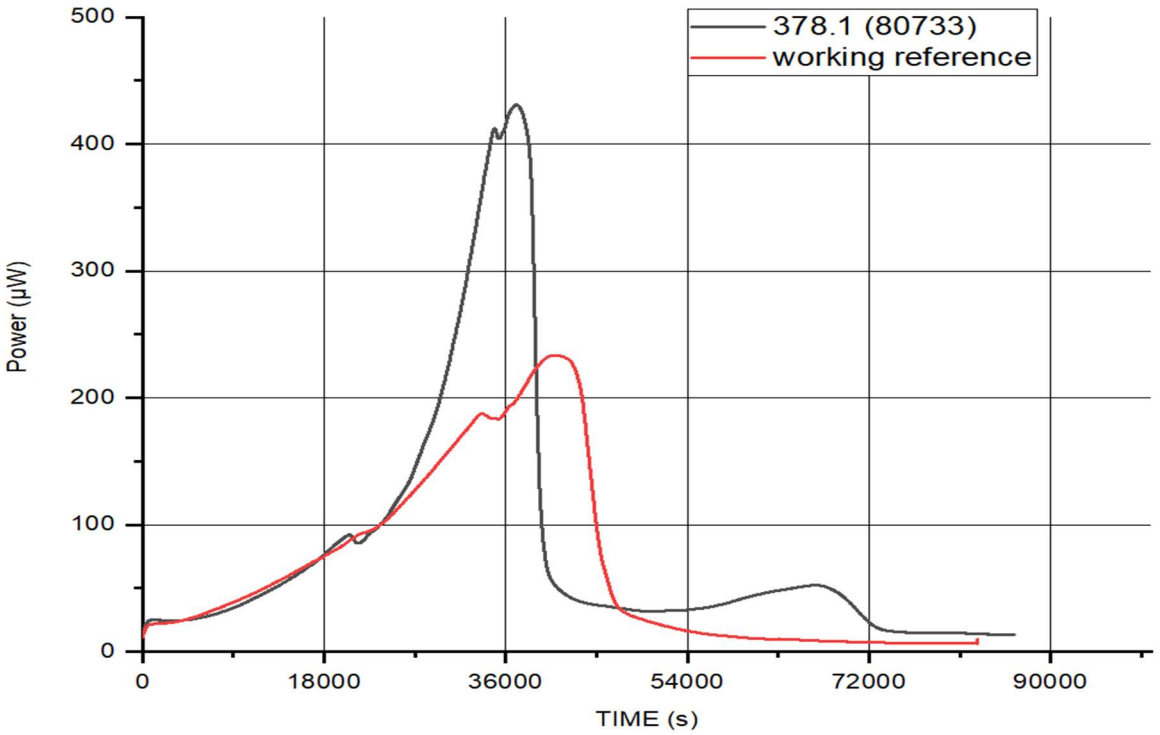
378.1 (80733)
working reference
Power (µW)
TIME (s)
0
100
200
300
400
500
0
18000
36000
54000
72000
90000

a)

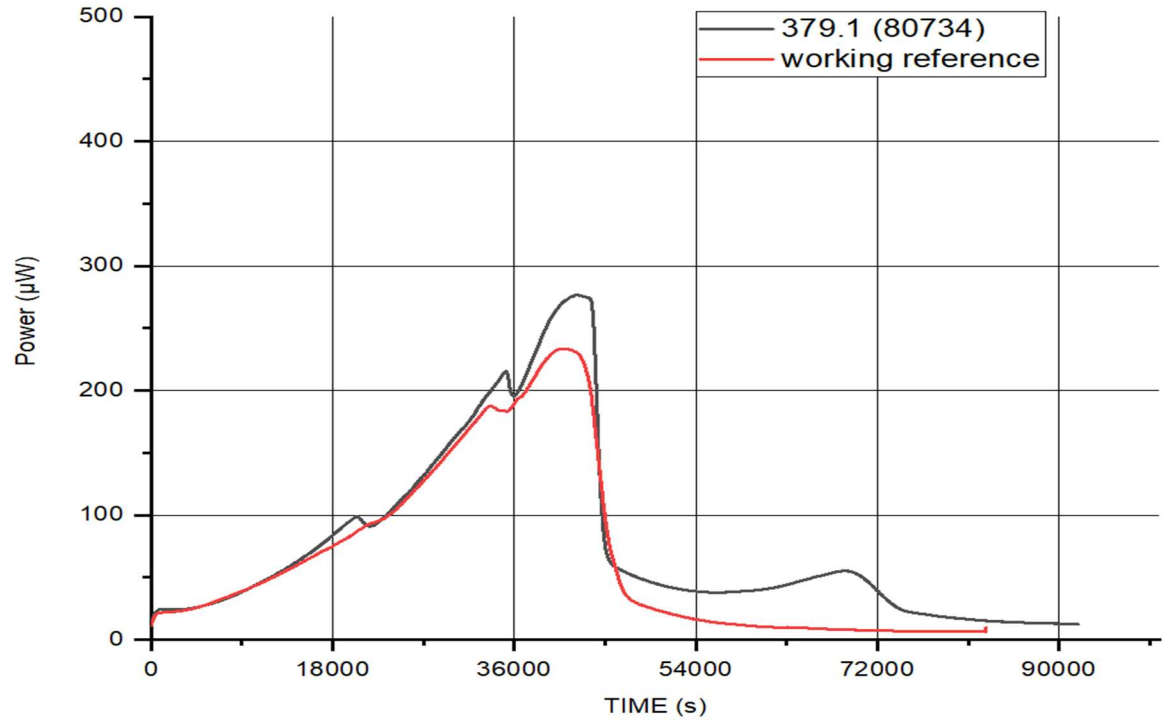
379.1 (80734)
working reference
Power (µW)
TIME (s)
0
100
200
300
400
500
0
18000
36000
54000
72000
90000

b)

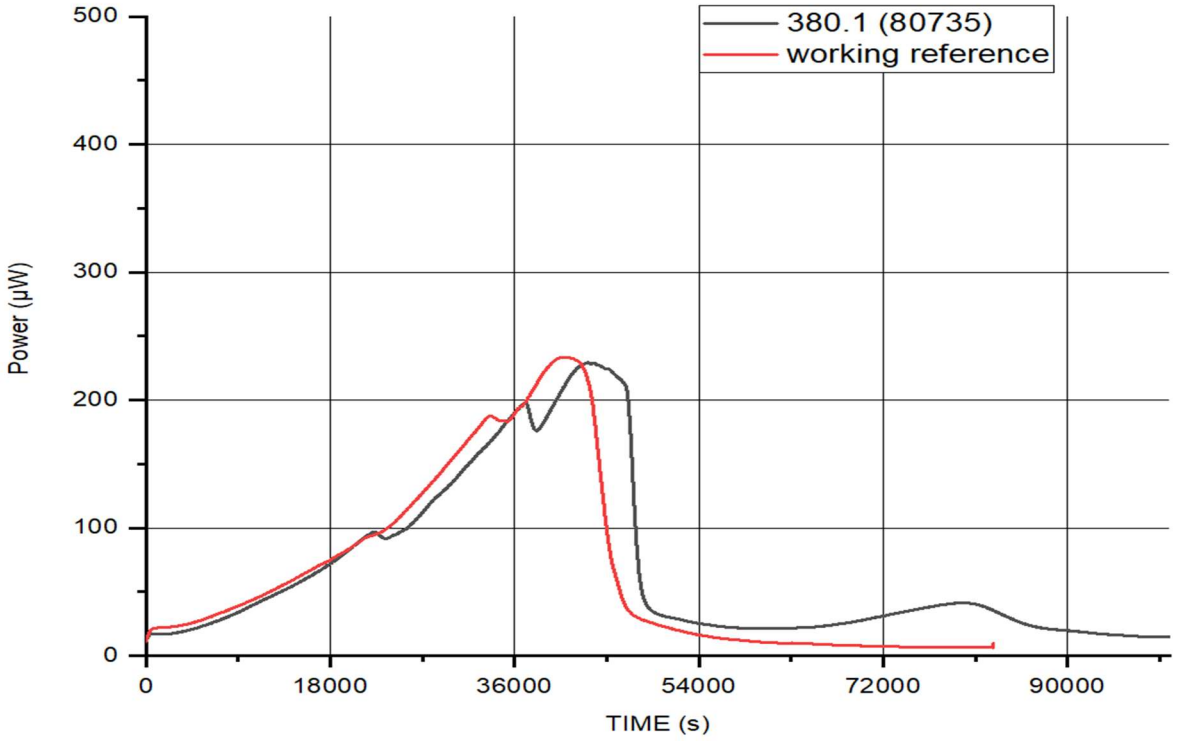
380.1 (80735)
working reference
Power (µW)
TIME (s)
0
100
200
300
400
500
0
18000
36000
54000
72000
90000

c)

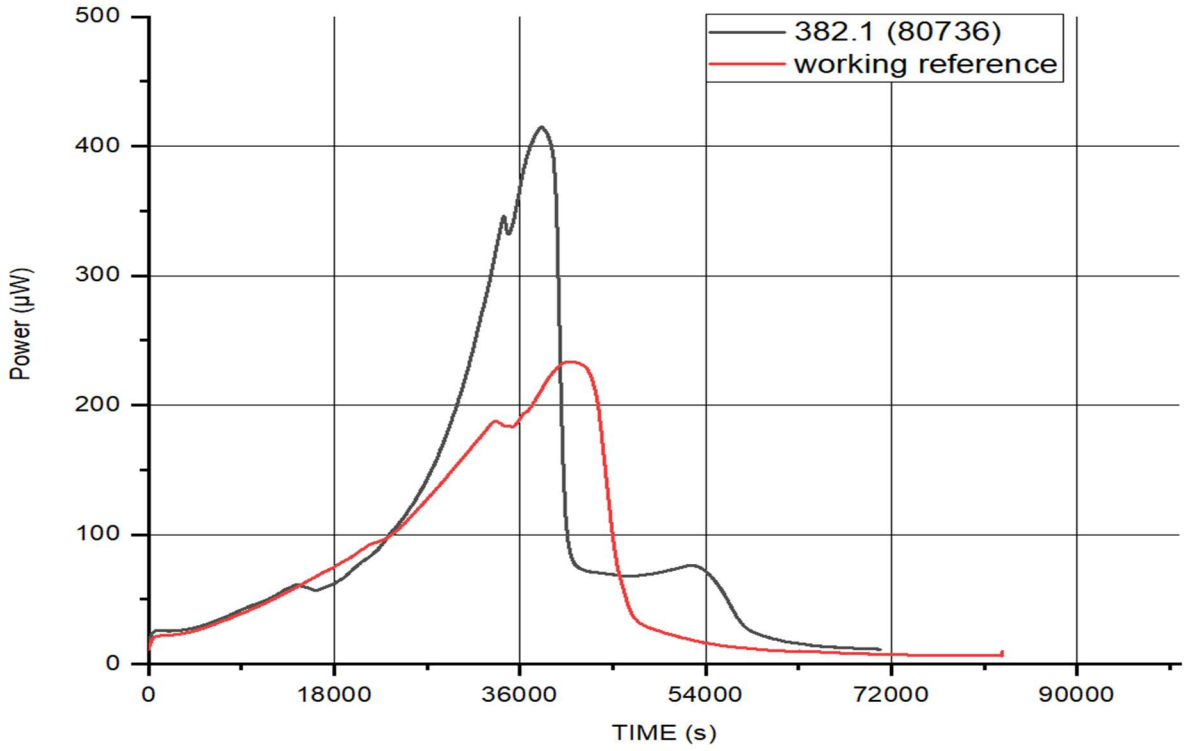
382.1 (80736)
working reference
Power (µW)
TIME (s)
0
100
200
300
400
500
0
18000
36000
54000
72000
90000

d)

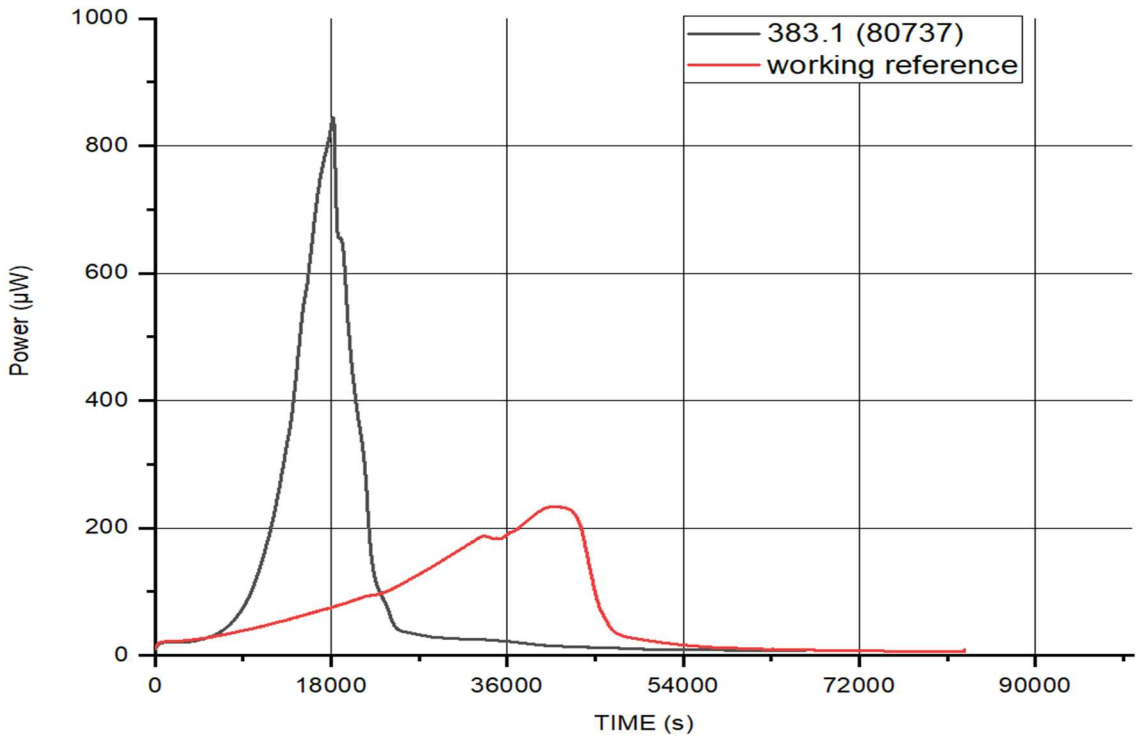
383.1 (80737)
working reference
Power (µW)
TIME (s)
0
200
400
600
800
1000
0
18000
36000
54000
72000
90000

e)

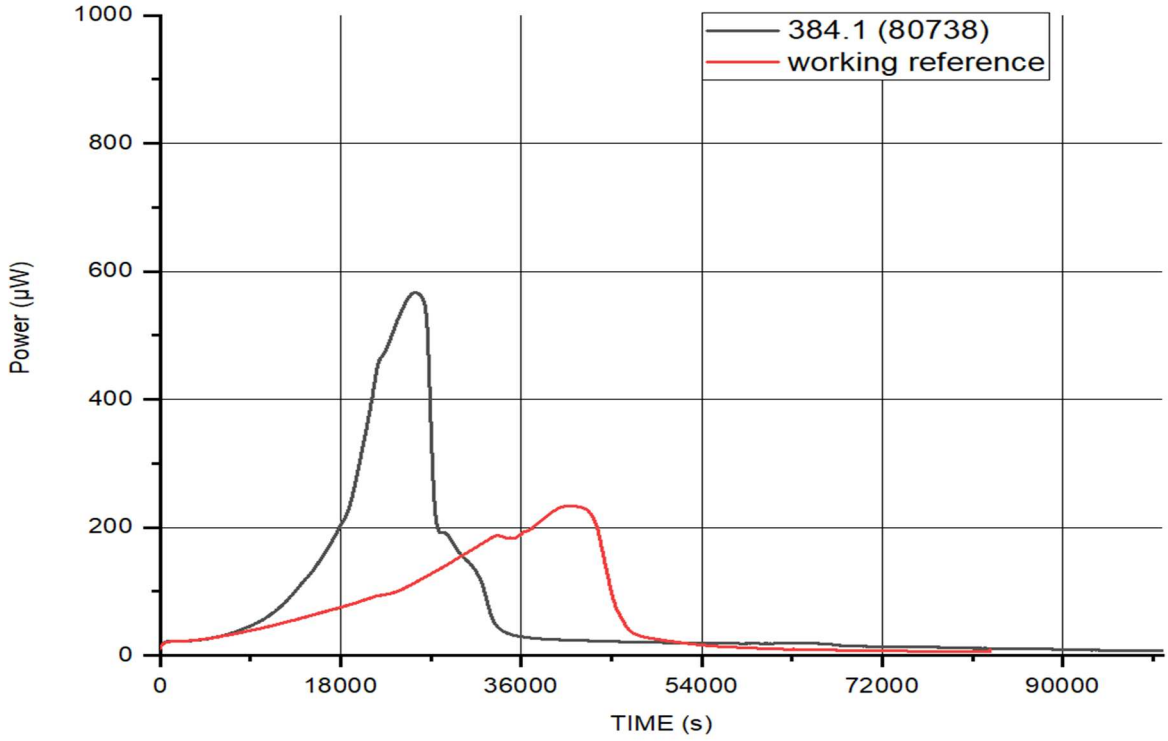
384.1 (80738)
working reference
Power (µW)
TIME (s)
0
200
400
600
800
1000
0
18000
36000
54000
72000
90000

f)

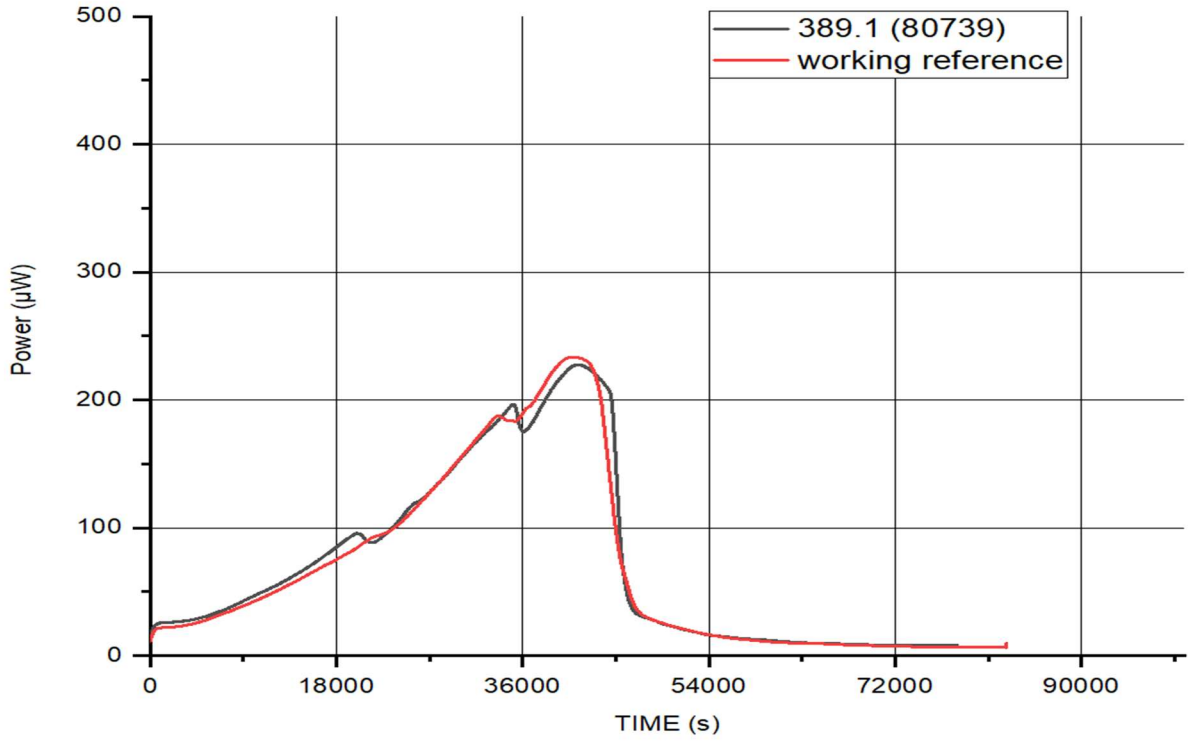
389.1 (80739)
working reference
Power (µW)
TIME (s)
0
100
200
300
400
500
0
18000
36000
54000
72000
90000

g)

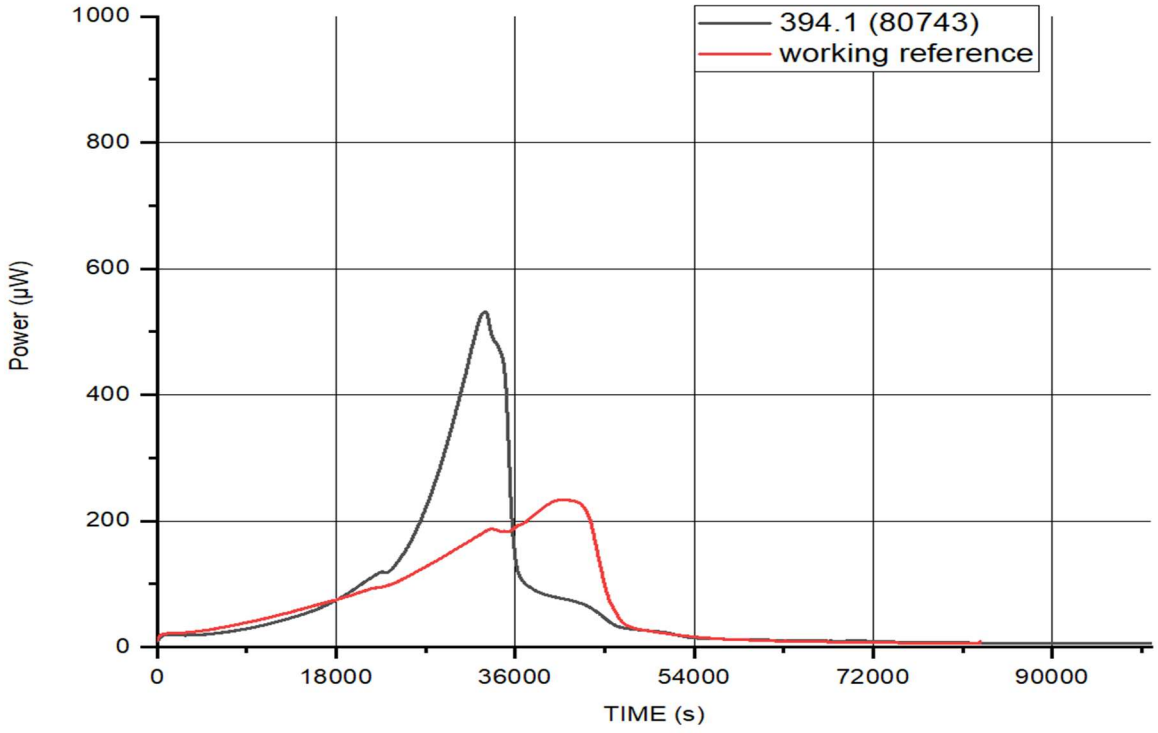
394.1 (80743)
working reference
Power (µW)
TIME (s)
0
200
400
600
800
1000
0
18000
36000
54000
72000
90000

h)

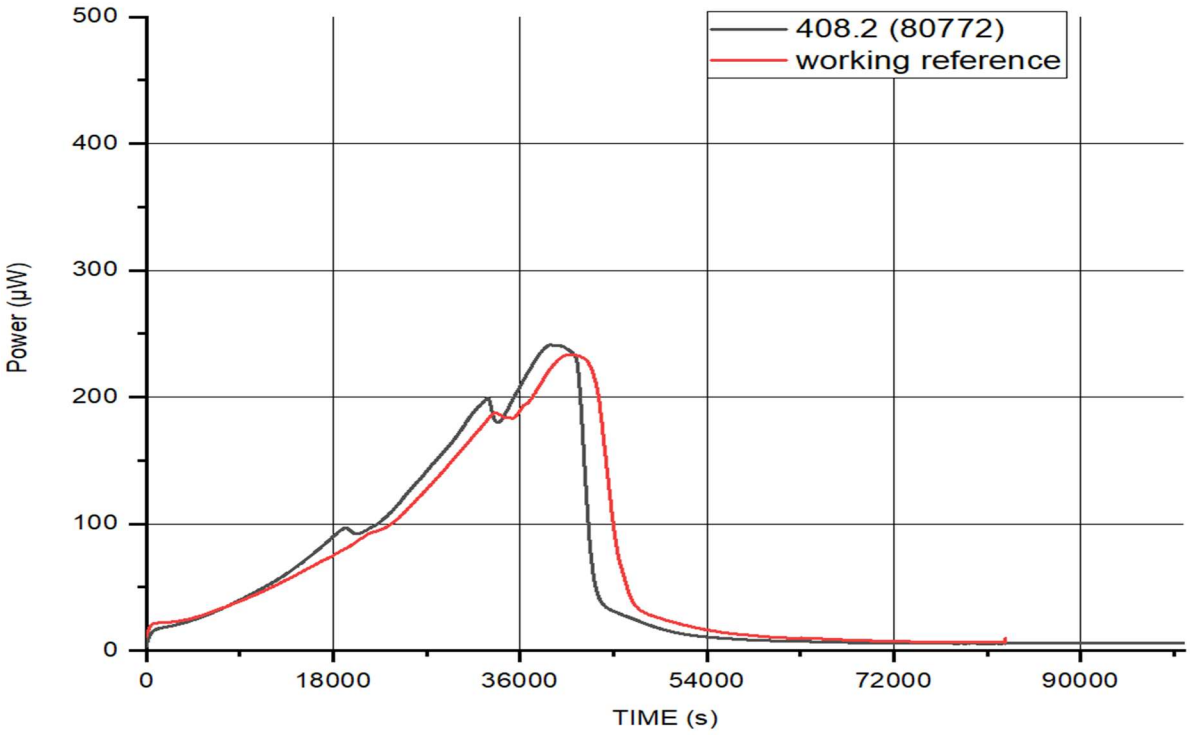

i)

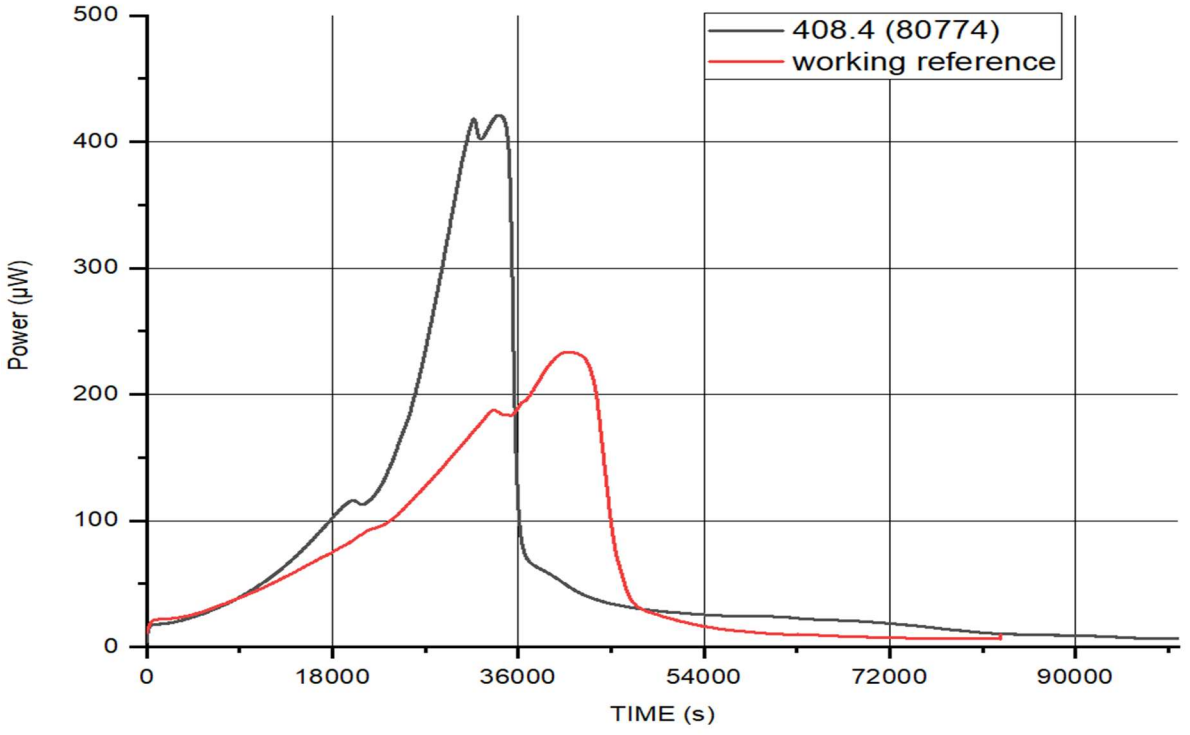

j)

Figure 2.5a-j Detail of individual comparisons of 8 batches with conflicting lab results (a, b, c, d, e, f, h and j) and 2 batches with agreeing lab results (g and i) against the mean working reference batch (red line in all figures a-j).

It took on average 15 hours (54000 seconds) to determine out of specification (OOS) results via IMC. **Table 2.5** summarises all tests that were done to determine what was the cause of the problem in the batches. Identification of a contaminant (ID) was done by MALDI-TOF

analysis. Lab 2 performed additional testing for detection of *Staphylococcus spp.* which were all negative (this is indicated in **Table 2.5** as Staph/0).

This section offered several practical examples, where IMC measurements indicated unexpected results (anomalous p-t curve shapes) of FV1-real batches when compared with the working reference curve. There were no indications other than the IMC results outside of ± 2x SD of the working reference curve, which hinted a problem of a not obvious nature (no smell, taste or fizziness issues and pH in a specified range). The challenge was that the standard Lab 1 test results did not indicate any issues with these same batches. Given these circumstances Symprove co. decided to investigate this further and contracted a second independent laboratory (Lab 2) to test the same batches in parallel. The results of these parallel tests are summarised in **Table 2.5**.

Comparison of IMC, Lab 1 and Lab 2 test results										
IMC ref no	**Batch**	**IMC OOS**	**Lab 1 (standard test)**	**Lab 1 extra test**	**Lab 1 ID**	**Lab 1 turnaround time (days)**	**Lab 2 (standard test) CFU/mL**	**Lab 2 extra test**	**Lab 2 ID**	**Lab 2 turnaround time (days)**
Exp 378.1	80733	yes	no	yes (Staph plate)	*E. faecalis*	8/8*	1.57 x10^2	-	*E. faecalis*	6/34 *
Exp 379.1	80734	yes	no	yes (Staph plate)	*E. faecium*	7/7*	6.70 x10^2	Staph/0	*E. faecium*	5/33 *
Exp 380.1	80735	yes	no	no		11	5.40 x10^2	Staph/0	No ID performed	6
Exp 382.1	80736	yes	no	yes (Staph plate)	*E. faecalis*	15/15*	2.27 x10^2	Staph/0		6
Exp 383.1	80737	yes	no			7	1.00 x10^2	Staph/0		5
Exp 384.1	80738	yes	no			6	7.70 x10^2	Staph/0		4
Exp 389.1	80739	no	no			6	no	Staph/0		4
Exp 394.1	80743	yes	no			7	7.50 x10^8	Staph/0	*E. faecium*	3/16 *
Exp 408.2	80772	no	no			10	no			3
Exp 408.4	80774	yes	no			8	1.96 x10^4			7

Table 2.5 Summary of comparisons of IMC, and two microbiological labs (Lab 1 and Lab 2) test results. Green highlights represent agreement between IMC and the Labs.

2.6.2.2 Discussion

Lab 2 performed better overall in comparison with the Lab 1 in detection of low-level contaminants in FV1 samples. IMC was able to detect contamination in all studied samples considerably faster than both laboratories despite the fact that the medium used for testing (TSB) was non-specific. Further improvements could be made if other growth media were used, for example, specific contaminant media or chemically defined media. Faster contaminant detection could be potentially achieved if a variety of media were tested for this purpose. This would require establishing a good growth reference curve in each of the potential medium.

IMC performed again successfully and reliably and became a routine screening tool for batch integrity. Any anomalous p-t curves thereafter did trigger additional testing as and when required. The following section **2.6.3** will demonstrate another practical example where IMC succeeded in discovering and solving the most elusive problem to date in the industrial setting of Symprove.

One condition in which the product could go astray was if the inoculum itself was bad (*e.g.*, contaminated or not viable). This was fundamentally important and is presented in the next section **2.6.3**. Given that the above system of looking at organisms in a medium (*i.e.*, FV1) was organised on a good statistical basis (working reference) to define a good product, it became possible to examine not only the final product but also the individual components of the product, such as the inoculum. When there was control over the system (FV1 and product) there was a capacity to look at the possibility, for example, what role did the 5 $x10^4$ specification for inoculum purity have (see **1.4.2.1** for more detail on lower purity of the production inocula as per supplier's specification). Additionally, it also offered an opportunity to investigate other means of contamination getting into the system, because there was a control over what the outcome (p-t curve) of a good product should look like.

2.6.3 Strain quality and purity maintenance at Symprove co.

Historically, Symprove relied on a single supplier of bacteria (Supplier 1) whose specification permitted ≤ 5 $x10^4$ CFUs per gram of aerobic contaminants (see **1.4.2.1**) in an expected 1 $x10^9$ – 1 $x10^{10}$ CFUs per gram concentration of the target bacterial strain, excluding pathogenic species. This meant that the purity of a target strain may be affected/cross-

contaminated by a different strain or species of non-pathogenic bacteria in their industrial process. It also introduced a wide range of variability between individual batches (as seen in **Figure 2.6a**). This clearly indicated that exploration of the inocula quality should be attempted using IMC. The contract laboratories or the Supplier 1 did not have the IMC method available to them therefore could not offer this test to Symprove. It was also questionable whether their testing would detect all potential pathogenic bacteria. While this might be acceptable in the agricultural sector, it could have a detrimental effect in the food or pharmaceutical industries. Several of their batches were previously rejected by Symprove as the supplier's own internal specifications were not met. As this was the sole supplier at the time, and Symprove required higher purity bacteria, Supplier 1 suggested that they could produce a laboratory scale batches away from their main production line which should be of higher purity than their industrial scale batches. Symprove did identify an alternative supplier (Supplier 2) at a later stage as an emergency back-up, however, Supplier 1 remained the main supplier.

The quality of the final product of Symprove depended, crucially, on the quality and purity of the individual ingredients, especially bacteria, providing the production process itself was not compromised in any way. Most importantly, quality and safety maintenance in terms of viability and purity of the individual bacterial strains was fundamental.

All batches of *L. acidophilus* used in Symprove production came from the same master batch which was held in the NCIMB safe deposit facility. When a new batch was required, NCIMB sent a vial of pure strain (aliquot of the master batch), on request from Symprove co. to Supplier 1 or other prospective manufacturer. When the manufacturer produced a new batch of bacteria and it complied with their internal quality specification, the batch was then despatched to Symprove co. A sample of each new batch was then sent to an external independent laboratory for quality and safety testing. These new batches of bacteria were used in the main production after all the test results were completed and shown to be within specification.

Initially, some FV1 batches were contaminated, and some were not (according to Lab 1). The contaminations were identified as *E. faecium* by MALDI-TOF. It was concluded that the most likely source was cross-contamination during the production process as *E. faecium* was used in FV2 and the same pumps and transfer hoses were used (with standard cleaning procedure between swapping the equipment from FV1 to FV2). To resolve the problem, extra deep cleaning procedures were introduced; however, the issue persisted with some

batches of FV1 contaminated and some free of contamination (as per Lab 1 tests). An exhaustive internal investigation was concluded, and nothing was discovered as out of specification, however the problem of FV1 being contaminated on and off by *E. faecium* persisted. Going further up the supply chain all individual ingredients were tested with no root cause determined.

Consequently, IMC was used to test individual bacteria comprising FV1. Finally, it was determined that the on/off contaminations detected by Lab 1 were caused by their tests not being sensitive enough to pick up all the positive results. New batches of *L. acidophilus* were tested primarily by Lab 1 as they were the main testing laboratory at the time. Arguably, Lab 1 might have provided many more false negative results (no contamination in FV1s) than was previously suspected. Note here that Lab 1, as demonstrated in **2.6.2**, was giving false negative results as compared with Lab 2 and IMC results.

2.6.3.1 Results

IMC test results concerning *L. acidophilus* are presented below. Initial experiments using new batches of *L. acidophilus* from Supplier 1 and Supplier 2, without their prior fermentation are shown in **Figure 2.6a and 2.6b,** respectively. These initial experiments helped to establish suppliers batch consistency. Detailed analysis of the results is offered in **2.6.3.2**.

There were significant differences in the p-t curves between all 3 batches from Supplier 1, **Figure 2.6a**. Differences in p-t curves between suppliers could be attributed to some variations in their production processes. However, significant differences in the p-t curves between different batches of the same bacteria from one supplier, suggested there might be some problems with the batches themselves or the supplier's manufacturing method. **Figure 2.6b** illustrates the consistency between 3 batches of *L. acidophilus* made by Supplier 2 and shows that all 3 batches produce very similar p-t curves in TSB. Consistency between different batches from one supplier suggests consistency in their production process.

A second round of experiments to simulate real production conditions (*e.g.*, growing the bacteria in wort), then testing these in TSB are shown in **Figure 2.6c** (master batch NCIMB) and **Figure 2.6d** (Supplier 1 batch). *L. acidophilus* grown in wort shows much faster growth in TSB when compared with unfermented *L. acidophilus*. Unfermented means that the *L. acidophilus* used in the experiments was taken directly from a defrosted vial as supplied by

the manufacturer without any treatment such as enrichment or incubation. Note: **Figure 2.6c** and **Figure 2.6d** should show similar p-t curves (and they do not, in fact they are substantially different) because *L. acidophilus* in both cases came from the same master batch (held at NCIMB) and in both cases was grown in wort.

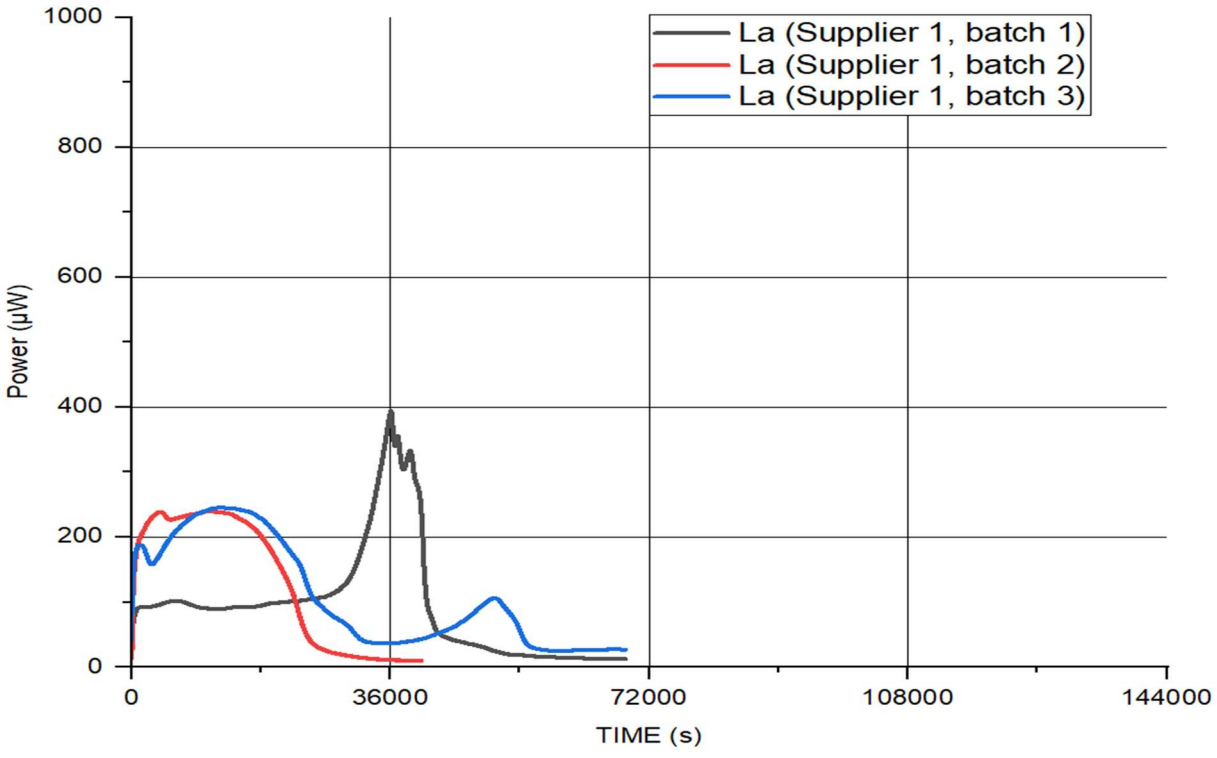

a)

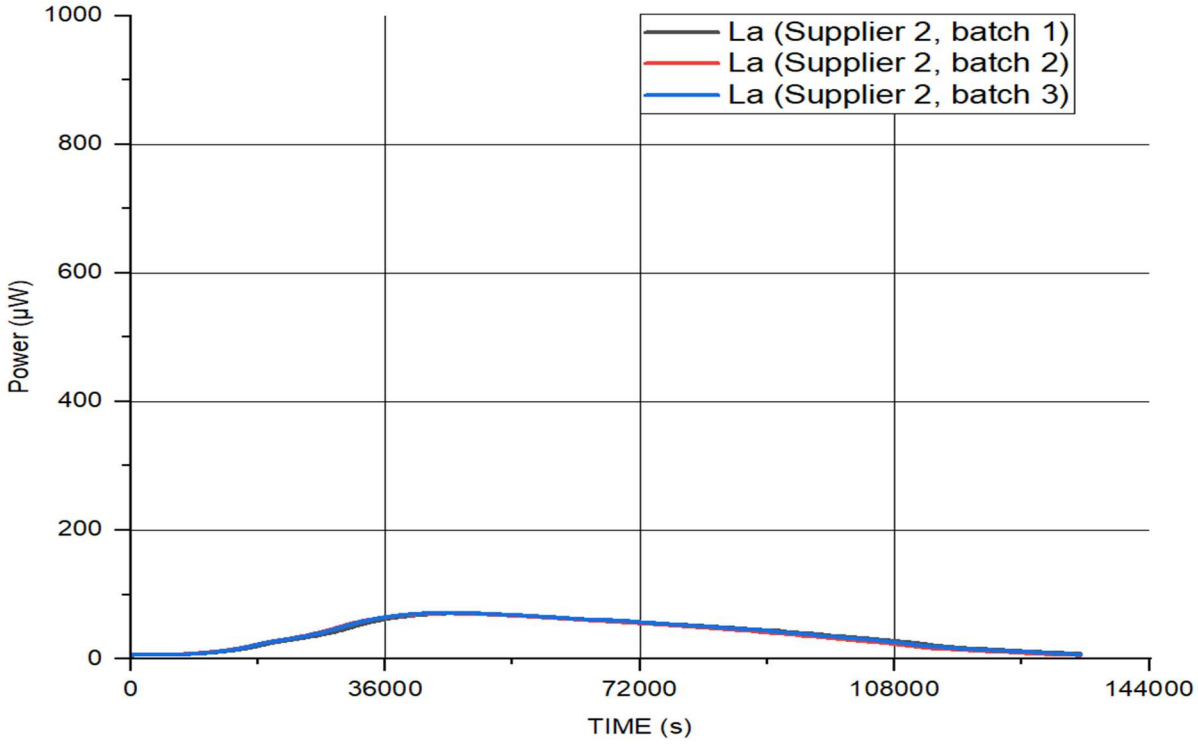

b)

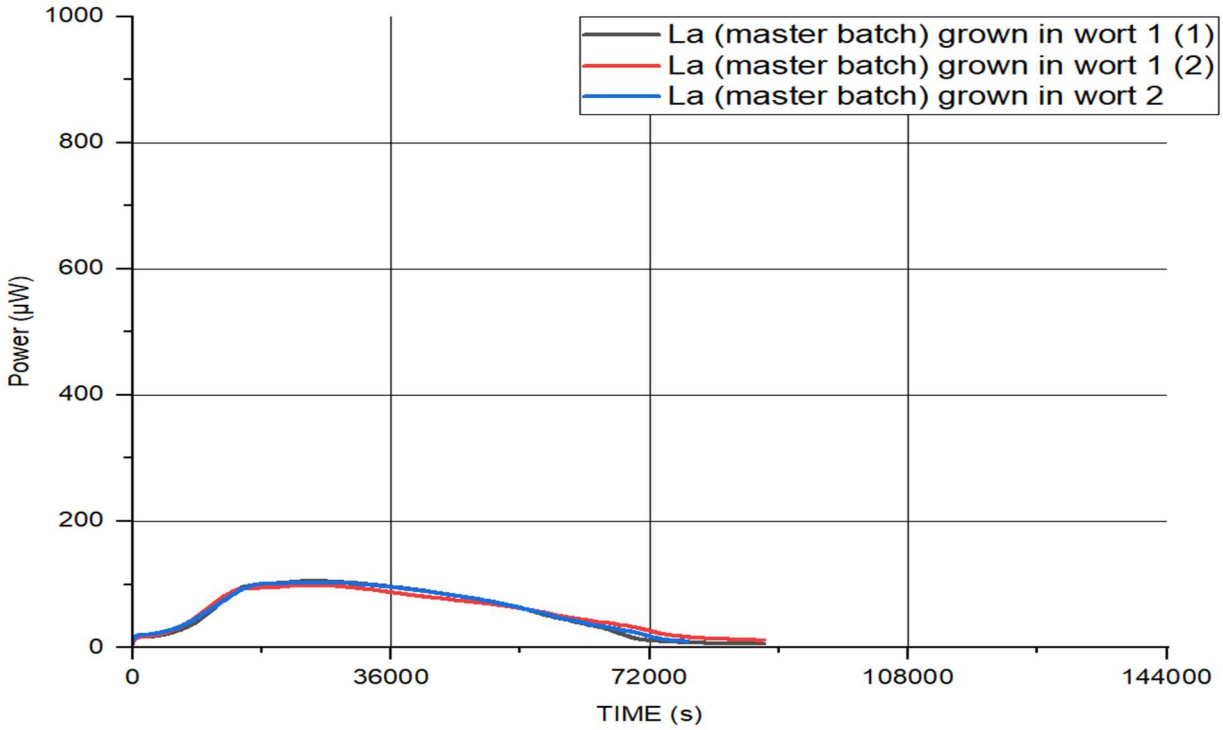

c)

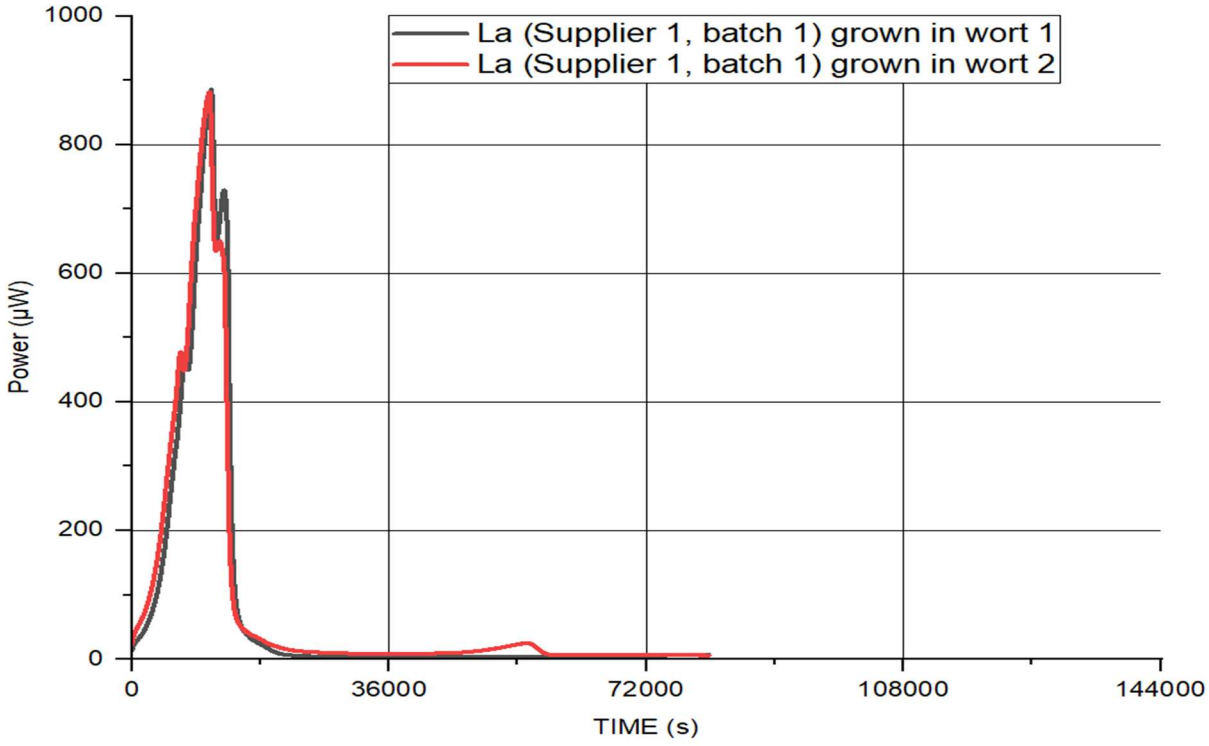

d)

Figure 2.6 Comparison of 2 different suppliers of *L. acidophilus.* 3 batches from Supplier 1 a); 3 batches from Supplier 2 b); *L. acidophilus* master batch (NCIMB stock) grown in 2 batches of wort (red curve is a duplicate of black) prior IMC testing c); *L. acidophilus* (Supplier 1) grown in 2 batches of wort prior IMC testing d). IMC testing medium was TSB in all experiments. (The same scale was maintained in all four figures for easy comparison.)

An organism's history (medium used to produce the organism, storage conditions, *etc.*) will affect the metabolism and the growth of the organism as can be seen in **Figure 2.7b and Figure 2.7d**. Evidently, *L. acidophilus* seems to grow better and faster in TSB when previously grown in wort than *L. acidophilus* pure (from frozen storage), see **Figure 2.7b**.

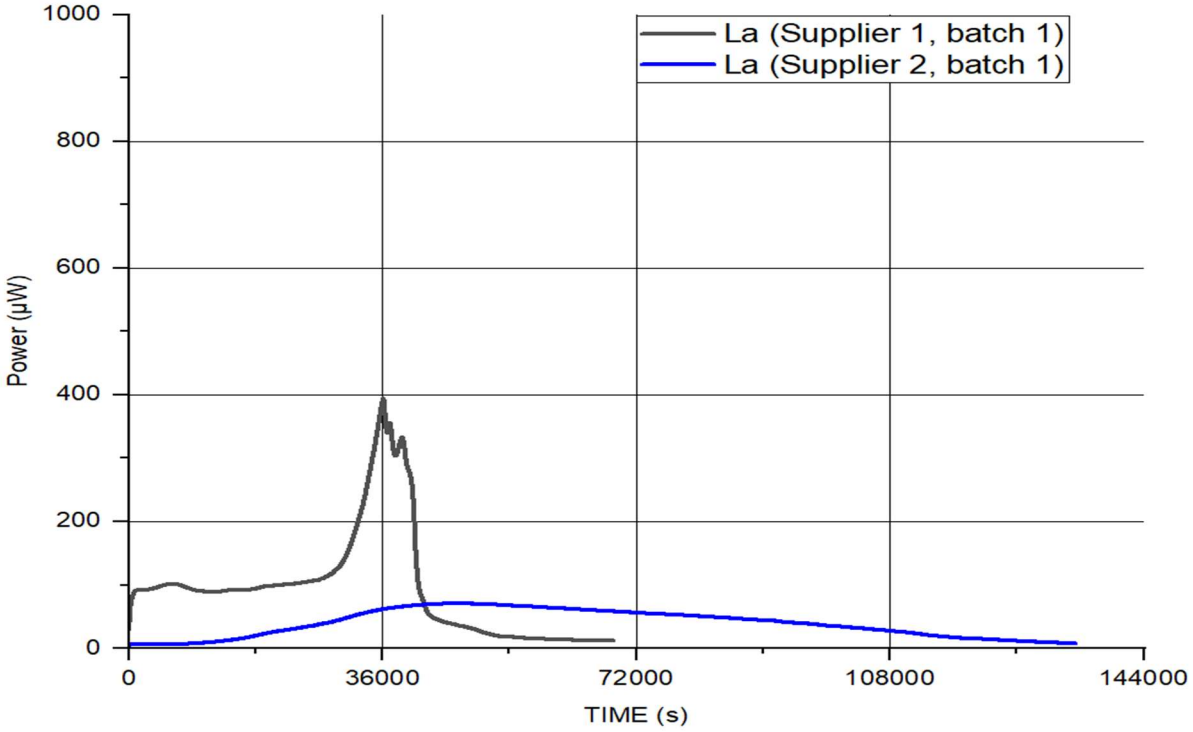

a)

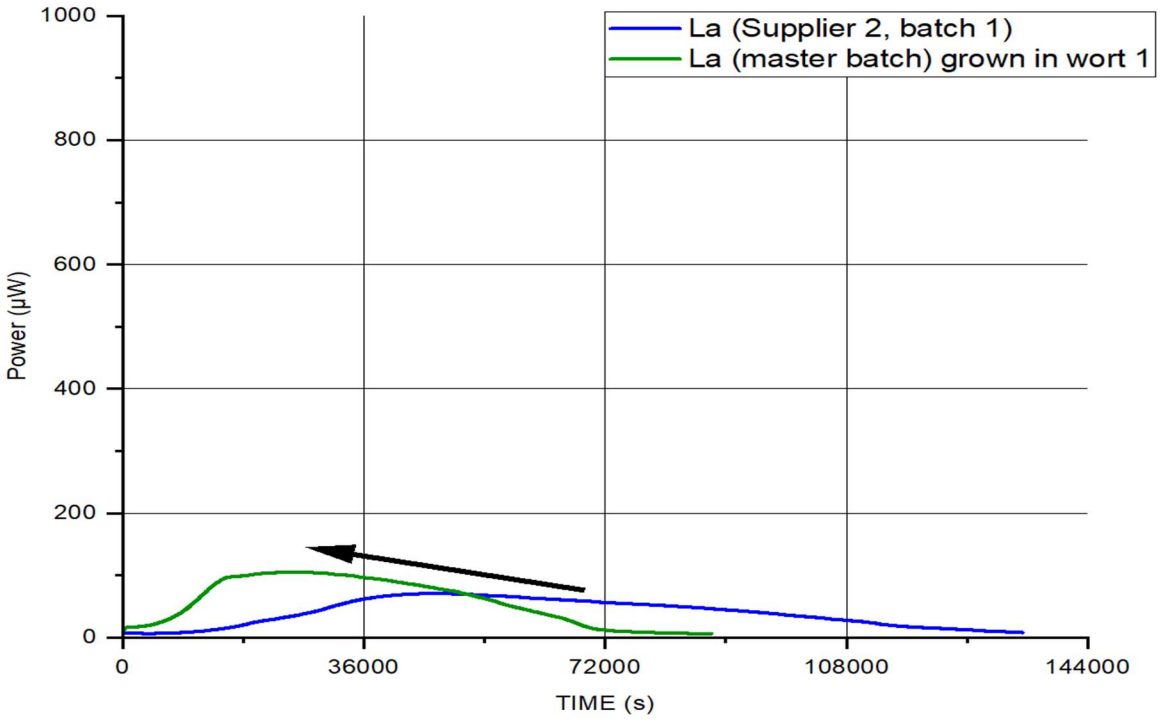

b)

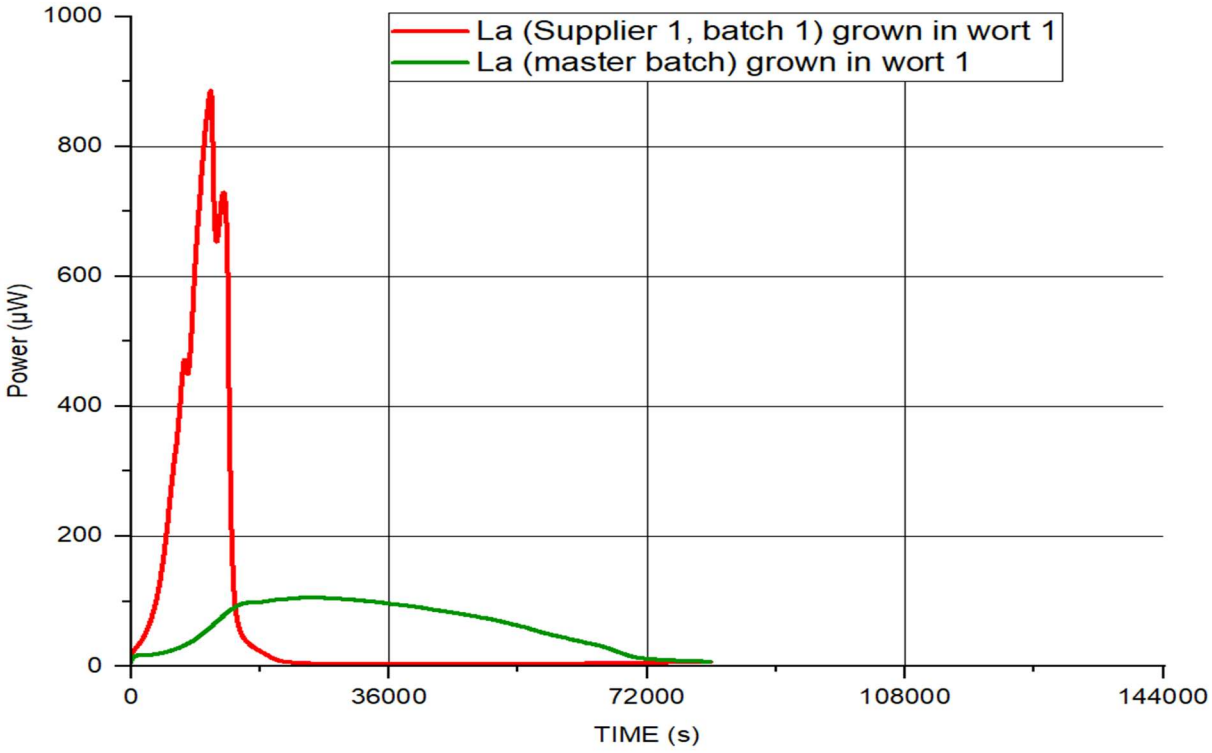

c)

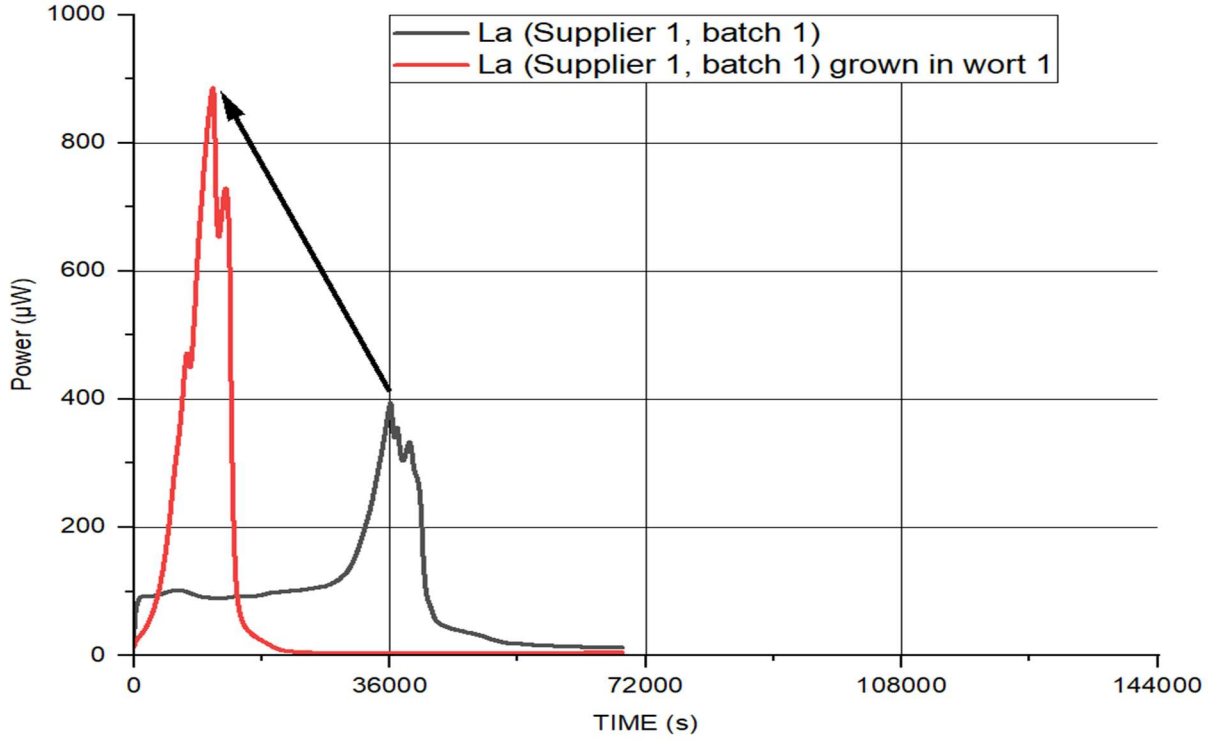

d)

Figure 2.7 Differences between expected curve (blue) and Supplier 1 curve (black) a); effect of the organism history b); same organism history *i.e.*, both grown in wort, master batch (green) and Supplier 1 batch (red) c); effect of the organism history (Supplier 1) d). (The same scale was maintained in all four figures for easy comparison.)

The results in **Figure 2.8** show how growing in wort affected the response of *L. acidophilus* when subsequently tested in a calorimeter. *L. acidophilus* (blue curve), pure culture without

any contaminants from Supplier 2, had a long, almost 5 hours lag time when tested in TSB. Blue arrow indicates a shift between *L. acidophilus* (Supplier 2) before fermentation (blue curve) and *L. acidophilus* master batch after fermentation (green curve). The blue curve was the expected p-t curve for *L. acidophilus* (NCIMB 30175) tested in TSB and the green curve was the expected p-t curve for pure *L. acidophilus* grown in wort and subsequently tested in TSB. In contrast, the black arrow shows a shift between *L. acidophilus* (Supplier 1) before fermentation (black curve) and after fermentation (red curve). It was anticipated, in the standard production process, that inoculation of large numbers of *L. acidophilus* into wort would, itself, contribute to eliminating any contaminating organisms potentially present in the fermenting vessel. This assumption would not be true if the contaminating organisms grew much faster than the *L. acidophilus* (which was the case of *E. faecium*). There was a significant shift to the left on the time axis when the same strain of *L. acidophilus* from Supplier 2 was grown in wort (24 hours at 37ºC to simulate the real fermentation process) indicated by the blue arrow compared with the position of the *L. acidophilus* pure strain (blue). This shift on the time axis shows that lag time of *L. acidophilus* is much shorter when previously grown in wort. There is also a noticeable rise in peak power between the two from about 70 µW (blue) to about 100 µW (green). This shift could be attributed to some advantages of the wort grown organisms over the pure culture. One reason for the longer lag time observed in the pure culture might be the need of the pure culture to accommodate to its new environment, having been previously stored at -80ºC (with addition of the cryoprotectant glycerol) as bacterial metabolism possibly changes in a different environment with the availability of different nutrients. It is likely that wort enhances the growth properties of *L. acidophilus* when subsequently tested in TSB. Screening new batches of inocula with IMC offers an early detection of a problem and this was demonstrated in **Figure 2.8**.

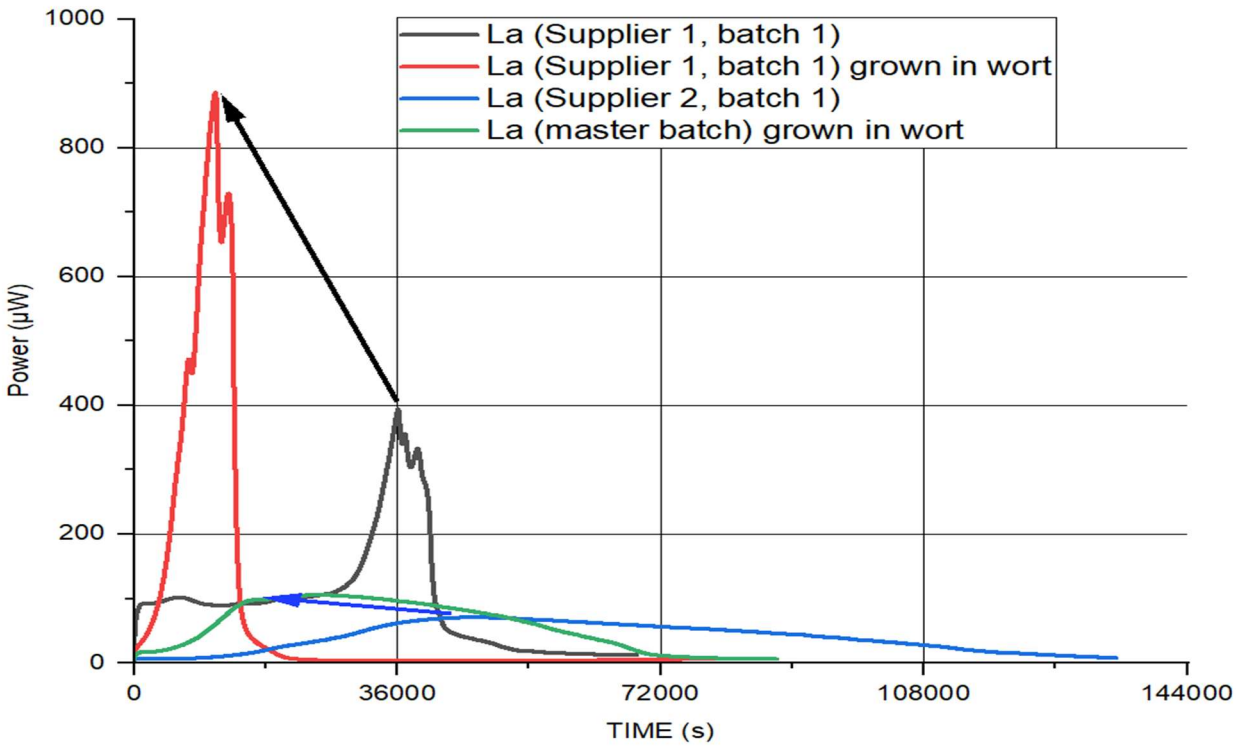

Figure 2.8 Effects of growing (fermenting) *L. acidophilus* in wort. .

2.6.3.2 Discussion

Barley, the main material to produce wort, is naturally variable in its nutritional composition. Different batches of wort will have some variations in their nutritional compositions even with the production process being the same. This will marginally affect the p-t curves as seen in **Figure 2.2a** and **Figure 2.6c**. Wort is a complex growth medium in which a wide variety of microorganisms can grow. It is reasonable, however, to assume that, if a single strain organism (such as pure *L. acidophilus*) was grown in wort, and then tested for instance in TSB, the resulting p-t curves would be reproducible as demonstrated in **Figure 2.6c**. These minimal variations in the p-t curves could be attributed to different batches of wort (variations in micronutrients are expected) in which the *L. acidophilus* was grown as well as cell density variations resulting from nutrient availability. Despite these variations, the power did not rise above approximately 100 µW and the shapes of the p-t curves were similar as in **Figure 2.7b**.

When the organism's history is not exactly known as in **Figure 2.6a** it is questionable how this could affect the organism's response in the calorimetric experiment using the same testing medium (*e.g.*, TSB). However, if different batches of the same organism (from the same master batch) from the same supplier, were grown in the same medium (such as wort),

prior to the calorimetric experiment, it was expected that the resulting p-t curve should be similar when compared with the master batch organism which was grown in the same medium (such as wort) prior to the IMC testing. This was not the case as observed in **Figure 2.7c**, where the expected p-t curve shown in green (which was the *L. acidophilus* master batch grown in wort and then tested in TSB). In the same figure, in red, is shown what a Supplier 1 made batch of *L. acidophilus,* (from the same master batch, then grown in wort and subsequently tested in TSB) looked like. What was observed in this particular case was very different from that expected (in green).

Analysis of the calorimetric results presented in **Figure 2.7** prompted further testing of the new *L. acidophilus* (Supplier 1). IMC results were considered as a reliable trigger to investigate batches in question in greater detail. Incidentally, the batches of *L. acidophilus* used in all contaminated (as well as in all FV1 batches in between the contaminated and non-contaminated batches as per Lab 1 test results) were from Supplier 1. Samples of *L. acidophilus* (Supplier 1) together with samples of contaminating organisms isolated from FV1s were sent to NCIMB for a detailed analysis. This included microbiological plating of these samples undiluted as well as in different dilutions and on TSA, MRS, and Nutrient agar, both aerobic and anaerobic conditions as well as a wide range of incubation temperatures and durations (up to 72 hours).

L. acidophilus batches from Supplier 2 were cultivated in parallel with NCIMB master batch, then checked against each other for purity as per NCIMB work instructions MALDI-TOF analysis was performed at the same time by Lab 1 confirming the identity and purity of the isolates as *L. acidophilus.* This step was taken to make sure Supplier 2 provided a pure strain of *L. acidophilus*. Note here that Supplier 1 permitted ≤ 5 x10^4 CFUs per gram of aerobic contaminants.

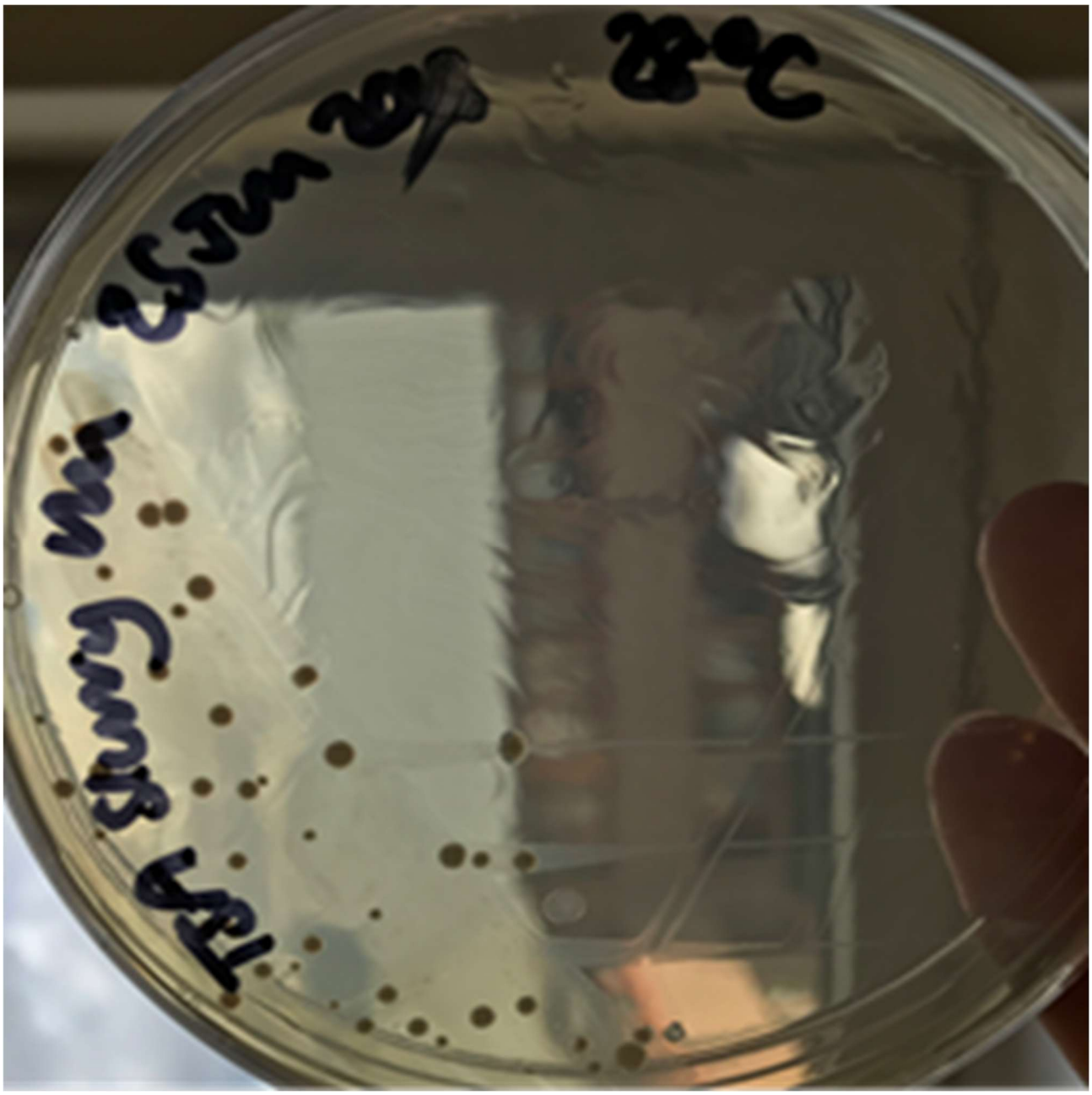

Figure 2.9 *L. acidophilus* (Supplier 1) —sample previously unopened, direct from the manufacturer. Undiluted on TSA plate, incubated at 28°C for 48 hours. The presence of two distinctive organisms is visible. Courtesy of NCIMB.

The sample in **Figure 2.9** came from Supplier 1 (previously unopened vial).. It was expected that only one organism would grow on the plate, however there were two different organisms present. Further testing was undertaken to identify the two distinctive organisms. One was identified by 16s rDNA sequencing as *L. acidophilus* (small, translucent colonies, **Figure 2.9**), and no further testing was done as this was the expected organism. The other organism from the plate was identified, by the same method, as *E. faecium* probable CNCM I-1721 strain (much larger opaque colonies, **Figure 2.9**). This was an unexpected and confusing

result. The confusion was caused by the fact that Symprove used *E. faecium* in their product. However, it was not possible that Supplier 1 would contaminate *L. acidophilus* with Symprove's strain of *E. faecium* during the manufacture as they did not produce *E. faecium* for Symprove previously. Further identification of the contaminating *E. faecium* using multi-locus sequence typing (MLST) revealed that this *E. faecium* was a different strain from the one Symprove used in their product.

During this time, any contaminants found in FV1s were identified to species level by MALDI-TOF. Slopes of the isolates were prepared and stored, should they be needed for future analysis as the problem was not yet resolved. This proved to be very useful as the contaminating organism from FV1s (where the contaminated *L. acidophilus* from Supplier 1 was used) was a match with the *E. faecium* isolated from the previously unopened *L. acidophilus* (Supplier 1) sample (shown in **Figure 2.9)**. Importantly, *E. faecium* isolated from the unopened *L. acidophilus* (Supplier 1) vial, was not a match with the Symprove's own *E. faecium.*

Finally, it was also confirmed by Supplier 1 that they had previously produced the *E. faecium* (probable CNCM I-1721 strain) for another customer. This was the root cause of *E. faecium* contaminating their facility, consequently contaminating several batches of *L. acidophilus* manufactured for Symprove company.

Multiple routine microbiology tests done by Lab 1 on several *L. acidophilus* batches from Supplier 1 were unable to detect the contaminating organism, whilst IMC was showing clear differences between the expected p-t curve and the measured one in both pure and fermented cultures as demonstrated in **Figure 2.8**.

The major time saving objective was to develop a method which allowed Symprove to shorten, if possible, the analysis required to assess whether a good product was made. It was essential that effort was made to extract all the information that could be extracted from this study provided there was sufficient time. However, the major objective was satisfied at this point, *i.e.*, it was possible in less than 24 hrs to determine whether a new batch of product was fit to be bottled instead of waiting for 7-15 days.

In practical terms, Symprove wanted to have a routinised procedure; one which took a sample of the final product as was (no dilution, no sample preparation), tested it in a given medium (MRS, TSB) and said, yes, the product was good, or not. It would not be commercially viable to use one laboratory for testing (*e.g.*, Lab 1) and if IMC would give

contrary results to go to another laboratory (*e.g.*, Lab 2) to confirm whether a batch was good or not. Additionally, if there was no IMC testing, a batch would be bottled and sold as per initial laboratory test results.

The examples given in **Chapter 2**, raised the distinct possibility to understand how contaminants could be detected through anomalous IMC outcomes when the test medium (TSB) was controlled. However, this kind of analysis also raised the distinct possibility of exploring alternative new media for production purposes (such as industrially produced wort, rather than currently onsite produced barley wort, or other natural or synthetic growth media). Examples of this are given in **4.3.2**, where one such medium Dohler wort was investigated. Dohler wort is barley wort which was produced industrially by a specialised company with high standards and quality control procedures. Their batch to batch variations should be significantly lower compared with much lower scale wort batches produced by Symprove without rigorous production parameters control.

The challenge of finding the root cause of FV1 being contaminated by *E. faecium* was a particularly difficult one. Many factors contributed to the complexity of the problem.

Firstly, Symprove relied on and was confident in Lab 1 (GMP, GLP, FDA certified laboratory) with a long-standing relationship and so it was not obvious at the beginning to doubt their testing procedures and results or sensitivity of their standard tests to detect low levels contamination.

Secondly, the only manufacturer of bacteria at the time was a professional large-scale producer and despite some failed batches in the past they were confident in their laboratory scale batches being of high purity, which was confirmed by Lab 1.

Thirdly, Symprove uses *E. faecium* in their own product manufacture and as they did not operate GMP facility, the primarily focus of the investigation was therefore the possibility of cross-contamination by their own bacteria (*E. faecium*).

The above factors created a problem as the bacteria used in the compromised and clear FV1 batches were from the same manufacturer (and the same batch). Lab 1 testing confirmed the contaminant was *E. faecium,* however, not analysed to a strain level. It was not obvious that the contaminating *E. faecium* could possibly be a different strain, as *E. faecium* was a component of the final product.

2.7 Chapter conclusion

What has been described so far in this thesis was the result of some 500 experiments. These were done in order to refine the protocol in order to arrive at much more standardised performance and to establish reproducibility of p-t curves of a good product. However, it was not yet sufficiently well-established so as to yield a simple analysis of data because essentially it relied on shape analysis of p-t curves. Further work was needed to make identification of a good growth much more secure. This involved determination of quantitative parameters including the growth rate and the intercept. Since the analysis relied on the shape of the p-t curve only, the whole IMC experiment until the signal returned back to the baseline needed to be recorded. However, if more parameters could be measured quantitatively it may be possible to significantly reduce the time demand of the IMC experiment and so significantly shorten the time to report the results for decision making.

Calorimetry appeared to have excellent sensitivity and reproducibility and could show abnormalities (see **Figure 2.5a-j)**. It was shown that IMC could identify the difference between good and bad products. Whilst basic analysis of p-t curve shapes offered some limited information about peak power, peak time and AUCs the analysis largely relied on parameters related to shape analysis as noted earlier in **2.5.** This meant, there was not meaningful and significant quantitative data attached to these simple growth studies reported in this chapter. P-t curves contain much more information that has been extracted from the data so far. Such data would, if available, significantly improve the prospect of developing the black box of data processing and contribute markedly to the diagnosis of a good product.

Considering the future black-box analysis, it was considered desirable to increase and improve the information content derived from the IMC data. In other words, the potential information yield from these p-t curves should be maximised as an aid to a judgement based on multiple quantitative parameters, about whether the product was good or not.

Shape analysis, *i. e.*, comparing the shapes of the p-t curves visually, was important, and its utility was demonstrated in this chapter. However, the definition of the baseline in order to calculate AUC depends crucially on defining the start time and end time of the signal (this way of defining a baseline is subject to individual operator's judgement, especially when manual shape analysis is performed). Experience from work during the exploratory phase

as well as work involved in shape analysis (data not provided), hinted that some simpler time dependent analysis (such as automatic data analysis) would be more appropriate.

The pragmatic outcome could be applied to the Symprove product because, from a practical point of view, each time a p-t curve was produced within specified parameters, it could be indicative of a good product (at least metabolically). Therefore, the pragmatic outcome was sufficient for Symprove and no further detailed analysis was required. However, it would be a wasted opportunity to get more theoretical insights if the whole information contained within the p-t curve was not extracted and analysed. It was plausible that by pursuing further developments past the pragmatic outcome, by analysing the information contained within the p-t curve, this would contribute towards developing the theory behind this method. The theoretical analysis of information such as growth metabolism, and organismal behaviour would enable expansion of the knowledge on how to disentangle the information contained within a simple p-t curve.

Fermentation for ca. 15 hours was the main stage in the production process described in **1.4.1**. However, no monitoring was implemented throughout this time that would reveal any problems during this critical production stage. Mimicking the fermentation was possible by IMC with a potential to be implemented as an on-line monitoring method after the above presented successful exploratory studies. As such IMC could produce data which contain kinetic and energetic information about the fermentation, including all metabolic processes covering the whole fermentation duration (Sardaro *et al*., 2013). These data could then be analysed and potential problems could be assessed. IMC has been used previously to monitor or control fermentation processes involving lactic acid bacteria and yeasts amongst other microorganisms. For instance, investigations of alcoholic fermentation (Türker, 2004; Morozova *et al*., 2017; Morozova *et al*., 2020), production of dairy products (Schäffer, Szakaly, and Lorinczy, 2004; Schäffer and Lorinczy, 2005), bread production (panification) (Mihhalevski *et al*., 2011), yeast growth (Beezer, 1977; Beezer *et al*., 1979). and bacteria (Okada *et al*., 1998; Braissant *et al*., 2010b; Fredua-Agyeman *et al*., 2018) showed that IMC was an immensely adaptable technique.

Some of the challenges described in **1.4.2** could be elucidated by using IMC. Namely, IMC offered shortening the waiting times for results significantly (a matter of hours rather than days as with traditional microbiology). The reproducibility of the IMC method was better than the currently used microbiological culture methods. Additionally, this method could be implemented on-line recording the process and progress of bacterial growth and its

metabolic activities. The capacity of IMC to deal with the system under investigation “as is” meaning no sample manipulation (such as dilution, drying or purification) as well as the capacity for automation if implemented on-line directly in a fermenting vessel offers additional advantages.

The utility of IMC as an early, fast, and reliable warning system was demonstrated. IMC proved to be sensitive enough to detect a contaminating organism in a high density concentrated bacterial culture (*L. acidophilus*) where the conventional microbiology testing was unable to do so. As a result, the testing procedure for new batches of bacteria was changed such as each new batch of bacteria was routinely tested via IMC as well as by both laboratories.

It was demonstrated that IMC could be used to determine the quality and integrity of the inocula, much faster and with higher sensitivity than traditional microbiological tests.

A new manufacturer of bacteria was contracted with upgraded specifications for new batches of inocula (no other contaminants allowed at any level).

It was desirable to be able to obtain and process quantitative data for a number of reasons. Quantitative data could be utilised by Symprove but was not fundamental for their QA shape analysis. However, it could be expected that theoretical interpretation of the p-t curves, some fundamental data (such as information about growth rates, growth substrate limits and shifts in metabolism from simple to more complex carbon sources) contained within these curves could be extracted offering an enhanced analysis of otherwise simple shape analysis. This was important as until now the project only dealt with the industrial outcome without any theoretical basis. Simply put, a deviation from a defined shape suggested there was a problem, but there was no theoretical basis to place that on. Developing basis for a better BB outcome necessarily meant that data obtained would have theoretical implications. Any theoretical development that would allow to have a better BB outcome all in itself incorporates a theoretical outcome as well.

The information yield in the experiments presented was greater than offered by the shape analysis. An approach to extract significant quantitative data from a basic p-t curve is attempted in **Chapter 3** which deals with equations describing exponential growth of microorganisms and their calorimetric applications to express further theoretical insights and their practical applications (**Chapter 4**).

Chapter 3 Developing the theory

3.1 Introduction

In the previous chapters of this thesis a case for the use of IMC in industrial settings was made. It was discussed why it was chosen as a research tool for this project and how it fitted into Symprove's company testing protocol. The results in **Chapter 2** showed that IMC had a high degree of reproducibility (within 3%) and was accurate, fast and accurate in detecting abnormalities. Thus, IMC is a promising tool for the quality assurance that can help shorten the time for product release. Despite these advantages, IMC has not become a more widely used testing method in the area of microbiological testing in industry. On the one hand, thermodynamics is an area of knowledge that has not been appropriately developed among microbiologists, who are more comfortable with their own traditional methods. On the other hand, since the data IMC provides is complex, containing all processes happening simultaneously, it is difficult to interpret the data, requiring a specialist in thermodynamics rather than a technician for that. While redressing these issues was beyond the scope of this thesis, some steps could be taken towards ensuring easier, shorter, and more accurate ways of applying IMC to industry, and in particular, the food industry.

Although the results presented in the previous chapter were very encouraging, it was not sufficient to rely only on the shape of the plots as an accurate and objective method. What was needed for this purpose was a quantitative analysis of the data provided by the TAM. If rate constants could be quantified here (as has been done in the chemical field for example complex chemical reactions (Beezer, 2001; Beezer *et al*., 2001; Almeida e Sousa *et al*., 2012) additional information could be extracted from the same p-t curves, which were previously only assessed visually (**Chapter 2**, shape analysis examples). Quantitative analysis so established would further strengthen how great any differences (in the exponential growth phase) were, which were only revealed visually in the shape analysis. With this purpose in mind, this chapter is largely theoretical, with focus on the development of models and tools for interpreting the IMC testing method and its data interpretation for industrial applications. The first step in this direction consisted in developing calorimetric equations concerning exponential bacterial growth.

Whilst basic analysis of p-t curve shapes offered some limited information about peak power, peak time and AUCs, the analysis largely relied, therefore, on parameters related to shape analysis as noted earlier in **2.3** and **2.7.** If additional quantitative information was available,

this would significantly improve the black-box objective and contributed markedly to the diagnosis of a good product.

In principle, calorimetry can be used to study all chemical and physical processes that have detectable changes in enthalpy or heat content of a studied process or reaction. Consequently, calorimetric data contain both thermodynamic as well as kinetic data about the reaction itself, such as the rate of the reaction, mechanism of the reaction and other kinetic parameters of the processes involved (Willson *et al*., 1995). By using a calorimeter to study these reactions thermodynamically, the possibility/opportunity to extract information about the individual thermodynamic and kinetic parameters from data collected by the calorimeter is presented. Knowledge about the system under investigation so gathered can help to understand these parameters. The understanding of the rate of the reaction (in the case reported in this thesis —fermentation) and the mechanism of the reaction can help to control these parameters, hence control the system itself. This knowledge is a valuable tool in industrial process control as trends and patterns can be determined and a facility to optimise specific compounds or metabolites can be unlocked (O'Neill *et al*., 2004).

The main goal of this chapter was to develop an equation that simply describes the exponential growth phase. If it was possible to get reliable quantitative data earlier in the process, getting the analysis down from 24-48 hours (the whole of the p-t curve shape) to 5-15 hours (the average exponential growth phase of Symprove bacteria), it would prove very useful, not only for Symprove but also, and importantly, for the food and other biotech industry in general (the exponential growth phases might differ in different biotech processes).

If it was possible to ascertain that the controlled experiment, an illustration of this highly complex system, provided an acceptable (yet to be satisfactorily defined) degree of reproducibility, the method under discussion would be better placed than standard time-consuming microbiological methods to deal with real-world batches. Hence, the equation development was a step towards achieving a method that provided theoretical and empirical confidence. If the procedure in the product manufacture was constant and adequately controlled, there ought to be a constant outcome within acceptable limits, same or better than the current gold standards (Foddai and Grant, 2020). This confidence was the basis for the consideration of the black-box approach being proposed. It was therefore essential to develop the mathematical models that permitted unfolding some biological parameters

from the p-t curve provided by the TAM so they could suit the purpose and lay the basis for the study of other similar systems.

3.2 Background

3.2.1 Phases of bacterial growths

In a batch system, bacterial growth constituted the main part of the production process described in **1.4**. As described by Monod (1949), bacterial growth consists of four main phases (**Figure 3.1)**: lag (1), exponential or log (3), stationary (5) and decline (6). In addition to this, two intermediary phases also take place: acceleration, which occurs between the lag and exponential growth (2), and retardation, which is a transition from exponential to stationary (4)**.** The lag phase starts right after inoculation into a sterile growth medium and is characterised by the need of the bacterial culture to adjust to this new environment. The growth is essentially zero during this phase. The acceleration phase starts as soon as the bacterial cells are ready to synthesise cellular constituents and available nutrients, resulting in division leading to identical new cells. When all the cells reach the acceleration phase, the growth proceeds exponentially thereafter. The growth rate eventually starts to decrease, which indicates the start of the retardation phase. This is because of some batch system limiting factors (*e.g.*, exhaustion of a nutrient, metabolite build up). The subsequent stationary phase is characterised by zero growth rate and is followed by a decline in the overall cell numbers as a result of cell death. The above mentioned phases constitute a bacterial growth curve that can be analysed, for example, to get a growth rate of the bacterial culture.

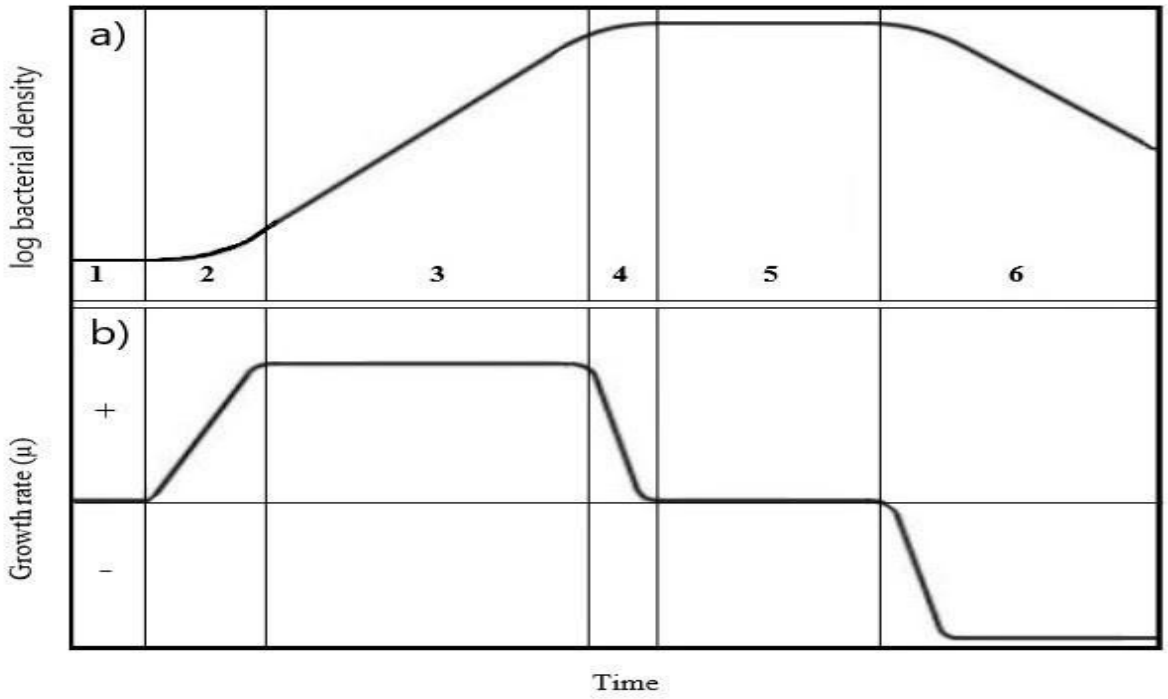

Figure 3.1 Phases of bacterial growth in a batch culture. 1-lag, 2-acceleration, 3-exponential or log, 4-retardation, 5-stationary, 6-decline a); bacterial density contrasted with variations of growth rate b). (Adapted from Monod, 1949.)

3.2.1.1 Kinetics of bacterial growth

Chemical kinetics is concerned with describing and quantifying the rates at which interactions between chemical compounds occur. The study of chemical kinetics offers a guide towards a mechanism controlling the reaction (Carr, 2007). It can therefore provide information about the chemical reaction, *e.g.*, speed, yield and duration. These can be then used in the development of models which formalise mathematical descriptions of the system (such as a chemical reaction) through quantitative terms.

Chemical kinetics lays the basis for the kinetics of bacterial growth. It measures and interprets the rates of chemical reactions and is well established (Mortimer and Taylor, 2002). It helps with understanding the complexity of reaction mechanisms including calculating specific rate constants and determining reaction orders to understand individual mechanistic steps that take place whilst the reaction progresses from reactant towards product (Klippenstein *et al*., 2014). The rate of chemical reaction is the main kinetic parameter and is correlated to the reactant concentration, governing the order of the reaction (zero, first, second) (Ramesh, 2019).

Calorimetry has been successfully used to resolve a lot of the complexity of chemical reactions quantitatively (Freeman and Carroll, 1958; Ozawa, 1970; Carroll and Manche, 1972; Beezer *et al*., 1974a; Willson *et al*., 1995; Beezer, *et al*., 1999; Gaisford *et al*., 1999; Sarge *et al*., 2014). This means that reaction mechanisms were described through quantitative terms such as rate of the reaction, reaction order, following reactants transformed into products using calorimetry and using chemical analysis to analyse the intermediates. Purely chemical kinetics are relatively easier to resolve quantitatively compared for example with enzyme kinetics as enzymes are often highly complex, undergo fast structural changes and serve as scaffolds for chemical reactions (Klippenstein *et al*., 2014; Ramesh, 2019). However, enzyme kinetics are also well established (Cornish-Bowden, 2012) and calorimetry has been applied to resolve problems in enzyme chemistry kinetics (Beezer and Tyrrell, 1972; Todd and Gomez, 2001; Wang *et al.*, 2020; Siddiqui *et al.*, 2022).

Biological systems represent an even greater degree of complexity from a kinetic point of view. Here, calorimetry has offered its utility to resolve some of this complexity quantitatively since it was first used. Efforts to study complex biological systems calorimetrically — biocalorimetry— dates back to the 18th century (Wadsö, 1979). For instance, in Lavoisier's ice calorimeter guinea pig experiment, it was implicit that something about the metabolism of the guinea pig could be concluded quantitatively through kinetic analysis. However, he did not specify anything about the kinetics of the metabolism of the guinea pig despite the possibility of extracting kinetic information at the time. If Lavoisier measured the amount of water that resulted from the melting of the ice by the guinea pig in regular time intervals, he would generate time dependent data for establishing the kinetics of the metabolism of the guinea pig. It is plausible he did not realise that he could have extracted this quantitative information from the experiment that was available to him at the time. The point of this example is emphasising complexity in order to elaborate on the kinetics whilst suggesting IMC has this remarkable capacity to investigate really complex systems and obtain valuable information about the mechanisms of studied reactions.

Much later, the basic principle of calorimetry remains the same: power vs. time. However, it was not until highly sensitive instruments, capable of measuring processes on a micro scale, became available (Monk and Wadsö, 1968) that the potential of calorimetry found its utility for studying microbiological systems (Beezer, 1977; Barisas and Gill, 1978). Wider applications of calorimetry to more specific biological problems intensified with instruments design development for example in the study of yeast (Beezer *et al*., 1976; Nunomura and

Fujita, 1981; Marison and Stockar, 1988; Perry *et al*., 1990; Battley *et al*., 1997; Saboury *et al*., 1999; Morozova *et al*., 2020) and bacteria (Spink and Wadsö, 1976; Fujita *et al*., 1978; Gram and Søgaard, 1985; Schiraldi, 1995; von Stockar *et al*., 2006; Braissant *et al*., 2010b; Wadsö *et al*., 2011; Fessas and Schiraldi, 2017; Corvec *et al*., 2020).

3.2.2 Studying bacterial growth using microcalorimetry

The bacterial growth curve described (**Figure 3.1**) provides a schematic basis to understand the process under consideration. In fact, as will be discussed further, the focus of this project has been established in reference to the exponential growth phase in this curve. It is worth bearing in mind that although the calorimetric p-t curve obtained with the TAM of the same batch experiment shows certain similarity with the bacterial growth curve, one should be careful not to equate them. Equivalent to the phases of the bacterial growth curve, the p-t curve representing microbial growth also follows a rise and decline **(Figure 3.2**, top plot**)**. Yet, this resemblance between the two curves does not mean that the same processes are taking place. For instance, a decrease in power does not necessarily indicate a decline in cell numbers (Braissant *et al*., 2013); the key finding in this study was that a correct model is used for a corresponding portion of the data. There is correspondence, however, between the exponential growth section of the p-t curve and its counterpart in the bacterial growth curve.

When bacterial growth is studied using microcalorimetry, IMC generated data contains kinetic information about the process and progress of metabolism of the studied bacterial system and other physical/chemical processes happening at the same time. As previously said, the interest here resided in extracting quantitative parameters from the IMC data. In a similar fashion, work leading to describe the kinetics of bacterial growth and derive quantifiable outcomes has proved successful (Beezer and Tyrrell, 1972; Schaarschmidt *et al*., 1976; Itoh and Takahashi, 1984; Xiufang *et al*., 1997; Maskow and Harms, 2006; Wernli *et al*., 2013; Cabadaj *et al*., 2021). An advantage derived from the p-t curve is continuous data capture, and this provides a way to give biological interpretation to the information encoded in it. For this to be done, the appropriate theoretical framework, that is to say, mathematical models and algorithms, needs to be in place (Braissant *et al*., 2015a).

At the most basic level, the p-t curve reveals the cumulative heat by integration (a proxy to bacterial growth curve), which is also indicative of the total number of cells produced during

an experiment, and by converting the power signal logarithmically then linear sections can be identified (Braissant *et al*., 2013), which may be indicative of first-order reactions such as exponential growth, as exemplified in **Figure 3.2**. From such a linear section it is possible to obtain the growth rate constant (the slope of the curve) and the beginning of the log phase (the intercept). However, to obtain these two parameters, it was necessary to obtain the equation of that curve, otherwise they were subject to interpretation by the operator of a data analysis software such as OriginPro (OriginLab Corporation) that performs nonlinear curve fitting and parameter calculation as described by, for example, Cabadaj *et al*. (2021). Hence the need for the development of appropriate equations is offered in this chapter. It was also plausible that on transforming the whole calorimetric output dq/dt vs. time logarithmically, it may be revealed there were multiple linear periods. However, only the first major linear period related to exponential growth (see **Chapter 3**) was to be analysed in detail in this project. Any others that may arise may indicate a first-order process not investigated in this project. There were several reasons for this focus, for example, the ease of modelling of this phase, and exploring the shortest, reasonable, reproducible and meaningful duration of testing.

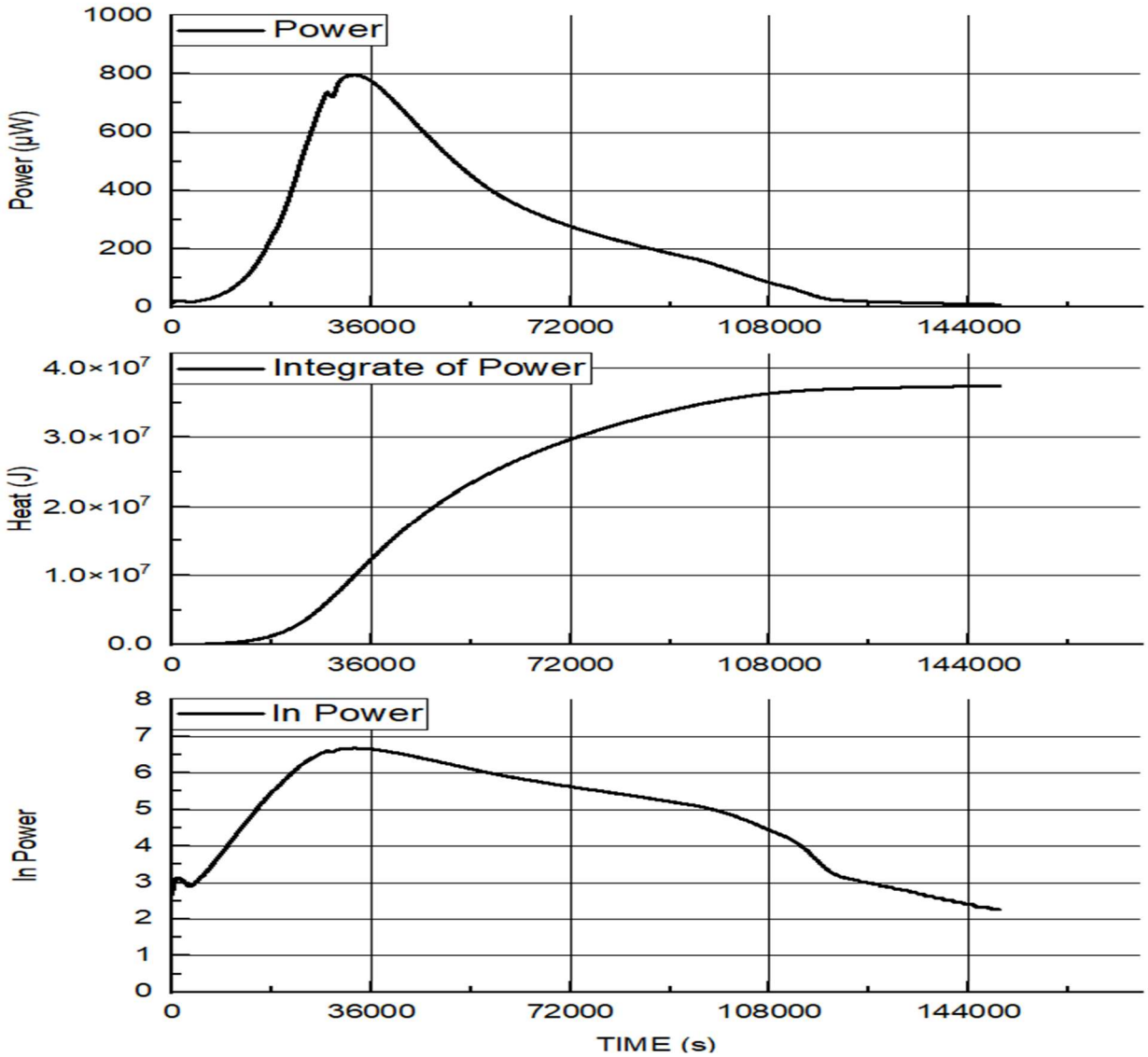

Figure 3.2 Mathematical transformation of p-t curve. Raw data (top), integration of the raw data (middle) and logarithm of the raw data (bottom). 503.1 sample.

3.2.3 Modelling bacterial growth

Bacterial growth has been modelled through mathematical means starting with simple, single substrate models of Blackman, Monod, and exponential kinetic models (Bader, 1978). Further development of the theory was done as interest in the field increased (Hinshelwood, 1946; Monod, 1949; Contois, 1959; Pirt, 1965; Law et. al., 1975; Droop, 1983; Zwietering et. al., 1990; Jannasch and Egli, 1993; Kovárová-Kovar and Egli, 1998; Egli, 2009). Model development is a way of formalising a system, in this case a highly complex biological one, in mathematical terms. A simple kinetic model could be difficult to construct because of the unpredictable interactions of even a single type of microorganism in a medium of varied composition such as barley wort. As with any mathematical model that aimed to provide a

description of an empirical process or system, it was an application of theoretical, and often ideal, conditions that had to be contrasted through experiments. This check offered the degree of accuracy and extent to which it was capturing in quantitative terms the peculiarities of that process or system.

The exponential phase is characterised by organisms doubling in numbers at regular intervals. Mathematical expression of this exponential bacterial growth is based on the premise of doubling of cell numbers (N) at a constant rate (*k*) and constant generation time (*g*). This can be represented by the geometric series $2^0 \rightarrow 2^1 \rightarrow 2^2 \rightarrow 2^3 \rightarrow 2^n$. It means when one bacterial cell divides into two, it can be expressed as $2^0 \rightarrow 2^1$, these two cells divide again, $2^1 \rightarrow 2^2$, then again, all new cells divide, $2^2 \rightarrow 2^3$ and so on. The generation time can be determined from the number of generations (*n*) that happened during the exponential growth phase time (*t*) as expressed by **Eq. 3.1** below (Madigan *et al*., 2015);

$$n = k.t = \frac{t}{g} \qquad \textbf{(3.1)}$$

where *n* is the number of generations, *k* is a rate constant and *g* is the generation time or doubling time.

3.2.4 Equation development

This section is concerned with the identification and development of equations, related to the exponential growth phase, that could be used to extract useful kinetic parameters from IMC data in order to determine whether the growth of microorganisms in a batch culture proceeded as expected. The ambition was to determine these kinetic parameters through suitable approaches based on the available information. In this sense, the scope of this chapter went beyond Symprove.co's setup. Thus, the aim here was to show a way in which growth based on the initial cell numbers, growth based on biomass or cumulative heat of the growing culture could be investigated through a model based upon the heat output ($\Delta_N H$) per cell. Applications subsequently developed contribute to the existing theory by enabling fast, reliable and precise parameter extractions from basic p-t curves. Past work done by, for example, Braissant *et al*. (2013) and Fricke *et al*. (2020), provide a theoretical approach that relates several variables that depend on the equilibrium of a system, such as the one being studied(FV1), making it then possible to extract these parameters.

Mathematical models based on empirical observations of specific cultures have been recently developed to unfold information about microbial systems from the calorimetric p-t curve (Miyake *et al*., 2016). As another example, when analysing the growth of *E. coli*, Ying *et al*. (2017) have proposed a simple exponential model:

$$P_t = P_0 e^{kt} \quad \textbf{(3.2)}$$

Where P_0 is the power output from a sample at time $t = 0$; P_t is the power output at any other time during the experiment; and k is a thermokinetic parameter (growth rate constant). The p-t curve for *E.coli* has two exponential growth phases and the model they developed allowed them to determine the growth rate constant (k), the heat output (Q) for each of them, and subsequently for the overall curve.

Bonkat *et al*. (2012) also used a simple exponential model developed for four different bacterial pathogens; *Staphylococcus aureus, Enterococcus faecalis, Proteus mirabilis and Escherichia coli*. They calculated the growth rate constant from the integration of the p-t curve which represents the heat produced by the cells during the exponential growth phase in this case;

$$Q_t = Q_0 e^{\mu t} \quad \textbf{(3.3)}$$

Where Q_0 represents heat at time = 0; Q_t represents the heat at any other time t, (*i.e.*, the integral of the p-t curve over the exponential part of the curve); and μ is the growth rate (h^{-1}).

Once they calculated μ, they were also able to determine generation time (t_g) from a simple relationship;

$$t_g = ln\ 2\mu \quad \textbf{(3.4)}$$

Another example is provided by Garcia *et al*. (2017) where they established a correlation between the initial viable cell numbers of *Lactobacillus reuteri* and the time it took to produce a certain amount of heat generated by growth;

$$t = -\frac{1}{0.434\mu} log\ X_{v0} + \frac{1}{0.434\mu} log\left(\frac{\mu Q}{k_c V}\right) \quad \textbf{(3.5)}$$

Where μ is a specific growth rate, X_{v0} is the cell concentration (CFU/mL) at time 0, Qv is the heat produced by the cells in volume V of medium and k_c is the heat production rate per cell.

They noticed a linear correlation between the logarithm of viable cell numbers and the time it took to reach a certain power. This outcome was used by Nykyri *et al*. (2019), who developed it further in their detection time equations for the relationships between initial microbial cell densities and detection time for *Pseudomonas brassicacearum, Bacillus amyloliquefaciens subsp. plantarum and Clonostachys rosea.*

Further developments in getting an important kinetic growth parameter from empirical data (*e.g.*, integrated p-t curve) have been achieved for example in detection of *Legionella pneumophila* (Fricke *et al*., 2020). Their simple exponential model takes cell numbers (*N*) instead of power as in **Eq. 3.2** or heat as in **Eq. 3.3** using more sophisticated models such as the Gompertz equation (Gompertz, 1825), **Eq. 3.6** below;

$$Q(t) = Q_{max} \times exp\,(-exp(-\mu_{max} \times (t - \gamma))) \qquad \textbf{(3.6)}$$

Q_{max} represents the total heat evolved during the growth, μ_{max} is the maximum growth rate during the exponential phase and γ (in hrs.) is the lag time. Their equations depend upon taking the heat output (enthalpy) rate of a cell (J/cell/s), whereas the proposition in this work was to take the heat (enthalpy) of metabolism (J/cell).

The above mathematical models have fruitfully enabled kinetic analysis of data produced by a calorimeter and therefore are an important starting point for this project. They have also paid particular attention to the exponential growth phase. However, although these models have arrived at first degree linear equations and analysed their slope, the significance of the intercept has been largely neglected as a meaningful parameter of evaluation for the establishment, by precise quantitative means, of the time zero (t_0) of that phase.

As Braissant *et al*. (2015b) have pointed out, the beginning of the exponential growth of the studied bacterial sample can be estimated by establishing from zero, to the intercept of a line tangent to the maximum growth rate point in the heat-time curve (integrated p-t curve). While this development points in the right direction, it is based on estimation of the best fit of the heat-time curve with statistical software R as proposed by Kahm *et al*. (2010). That is to say, the intercept is not obtained directly from an equation and therefore cannot be used for the purpose of the black-box analysis. Additionally, this project aimed at getting the value of the intercept. This was key for establishing when exponential growth started in a very simple, accurate and reproducible fashion for a semi-closed system (as described in **1.4.1**). This was expected to be achieved through the development of an empirically based equation that decoded the value of the intercept from the p-t curve.

3.2.4.1 Growth based on cell number

Suppose there is an initial sample with N_0 cells and after a certain interval of time $\Delta t = t - t_0$ there is N number of cells. Then, empirically, the total number of cells $\Delta N = N - N_0$ divided by the interval of time Δt is approximately $\frac{\Delta N}{\Delta t} = kN$ where k is a rate constant. Then;

$$\frac{dN}{dt} = kN \qquad \textbf{(3.7)}$$

This equation tells how the number of cells is changing over time as $N = N(t)$. The solution for **Eq. 3.7** is below:

$$N(t) = N_0 e^{kt} \qquad \textbf{(3.8)}$$

Let us now define a useful quantity which is the heat produced by the cells;

$$q_N = \Delta_N H N \qquad \textbf{(3.9)}$$

where $\Delta_N H$ is the enthalpy of growth per cell (in J/cell). Now, since N depends on time and there were N_0 cells initially, to express q_N for the entire process we will need to consider $\Delta N = N(t) - N_0$ instead of just N in the above equation. By doing that and by replacing **(3.8)** in **(3.9)** one arrives at;

$$q_N = \Delta_N H(N(t) - N_0) = N_0 \Delta_N H(e^{kt} - 1) \qquad \textbf{(3.10)}$$

Similarly, as before, let us now think that instead of considering one entire cell with q_N at a certain time t, we consider infinitesimal (very small) differences of them that are denoted by dq_N and dt. Now we are interested in measuring how dq_N changes over time dt. To do this in a simple way, we can divide the above equation by Δt and then take infinitesimal quantities, it can be found that;

$$\frac{dq_N}{dt} = N_0 \Delta_N H \, k \, e^{kt} \qquad \textbf{(3.11)}$$

Applying logarithm to (11) yields;

$$\boldsymbol{ln\left[\frac{dq_N}{dt}\right] = lnP(t) = ln[N_0 \Delta_N H \, k] + kt} \qquad \textbf{(3.12)}$$

Eq. 3.12 is the central equation of this project.

Exploring different ways of getting *k* is demonstrated below in **Eq. 3.13** where taking another derivative with respect to time in **(3.11)** yields;

$$\frac{d}{dt}\left(\frac{dq_N}{dt}\right) \equiv \frac{d^2q_N}{dt^2} = N_0\Delta_N H k^2 e^{kt} \qquad \textbf{(3.13)}$$

Furthermore, it can be noticed that by diving the above equation by **(3.11)**, *k* can be obtained directly;

$$\frac{\frac{d^2q_N}{dt^2}}{\frac{dq_N}{dt}} = \frac{N_0\Delta_N H\, k^2 e^{kt}}{N_0\Delta_N H\, k e^{kt}} = k \qquad \textbf{(3.14)}$$

Fricke *et al*. (2020) suggest using the second differential of the power vs. time to define the time period for data analysis. Their work suggests the potential to eliminate shifts in baseline and enables to distinguish the physical from the metabolic effect.

This means that plots may not be required —only that the differential of the power is required at any time *t* and this, with the power itself at that time allows determination of *k*. Hence many values of *k* can be determined throughout the exponential period and an average of those through the constant (*e.g.*, exponential) period can be calculated.

3.2.4.2 Growth based on biomass

Egli (2009) has outlined the central considerations and approaches to the interpretation of kinetic data for microbial growth under a range of conditions. As noted in **3.2.2** there is a long history of the study of microbial systems through experimental microcalorimetry. Presented here is the approach taken for quantifying microcalorimetric data for kinetic analysis based on biomass.

The computation is an extension to the above development. First, postulate a formula (by hand-empirical);

$$\frac{dM}{dt} = \mu M \qquad \text{(Belaich, 1980)} \qquad \textbf{(3.15)}$$

where *M* = *M(t)* is the increase of the biomass of growing culture and *μ* is a parameter that is called the growth rate. Following the same as in **3.2.4.1** (since the differential equation is the same), one can find that;

$$ln\frac{dq_M}{dt} = ln(M_0\Delta_M H\mu) + \mu t \quad \textbf{(3.16)}$$

Thus, a plot of $ln(dq_M/dt)$ vs. time (this can be a direct application of the experimental data *i.e.*, power vs. time) will be linear with a slope of *μ* and an intercept of $ln(\mu\Delta_M H M_0)$. If the number of bacteria present at *t* = 0 is M_0 (in terms of biomass rather than cell numbers) and the number of Joules evolved per cell during the logarithmic phase is $\Delta_M H$ then q_M can be set equal to $\Delta_M H M_0$ and the intercept now becomes $ln\mu q_M$.

3.2.4.3 The link between cell number and biomass

The equations in **3.2.4.1** and **3.2.4.2**, describe an exponential growth phase, with the possibility to be applied later in the p-t curve, should another first order process occur an exponential growth phase for a given calorimetric data set can be expressed in terms of either cell numbers **Eq. 3.12** or biomass **Eq. 3.16**. Thus, the values of *k* and *μ* for a given data set (experiment) will be the same. This in turn requires, for the models to apply, that the cells forming the biomass and the total cell number during the exponential growth to be identical (dividing cells, no respiring cells).

3.2.4.4 Analysis based on cumulative heat determination over the exponential growth phase

Eq. 3.10, can be rearranged for e^{kt};

$$N_0\Delta_N H(e^{kt} - 1) = q_N \quad \textbf{(3.10)}$$

$$e^{kt} = \frac{q_N}{N_0\Delta_N H} + 1 \quad \textbf{(3.17)}$$

Now, if e^{kt} is replaced in **Eq. 3.11** for **Eq. 3.17;**

$$\frac{dq_N}{dt} = kq_N + N_0\Delta_N Hk \quad \textbf{(3.18)}$$

Eq. 3.18 indicates that a plot of dq_N/dt (power) versus time (the value of q at time when dq/dt is registered) q_N (not *ln*), will yield a line of slope k.

3.2.4.5 Time from inoculation to signal detection

Let N_s be the number of organisms required (in the sample volume placed into the IMC) to give a specified signal – this will be the same for all similar samples independent of the initial inoculum density. For a reference set of number N_r with an inoculation time t_r such that one achieves a specific signal for N_s, it can be written;

$$N_s = N_r e^{kt_r} \quad \textbf{(3.19)}$$

At some other cell number with time t_{exp} and N_{exp} we have again that;

$$N_s = N_{exp} e^{kt_{exp}} \quad \textbf{(3.20)}$$

since all the samples should have the same N_s. Then, we can equate the **Eq. 3.19** and **Eq. 3.20**, yielding;

$$N_r e^{kt_r} = N_{exp} e^{kt_{exp}} \quad \textbf{(3.21)}$$

By applying logarithm and re-arrangement of **Eq. 3.21**;

$$ln(N_r) = ln(N_{exp}) + k(t_{exp} - t_r) \quad \textbf{(3.22)}$$

As a result, the relative cell numbers could be established. Alternatively, if the cell numbers were known in the reference sample, the cell numbers in the experimental sample could be established.

3.2.4.6 Generation (or doubling) time

If we start with N_0 number of cells, they will double to $2N_0$ cells over a time period t_d–doubling time during which a new generation of microorganisms is produced. Both terms were used interchangeably in this thesis because the focus of the work was on the exponential growth phase with the assumption noted in **3.2.4.3**. The same applies for $q_n \rightarrow 2q_n$.

Then it follows by using **Eq. 3.8** and by denoting the time t_d as the doubling time;

$$N(t) = 2N_0 = N_0\, e^{kt_d} \quad \textbf{(3.23)}$$

$$\Rightarrow e^{kt_d} = 2 \quad \textbf{(3.24)}$$

$$kt_d = ln\,(2) \quad \textbf{(3.25)}$$

$$t_d \approx \frac{0.693}{k} = 0.693g \quad \textbf{(3.26)}$$

where *k* = 1*/g* with *g* being the generation time. Then, if **Eq. 3.23** is used, the number of cells after doubling the process *n* times will be;

$$N(t) = N_0\, 2^n \quad \textbf{(3.27)}$$

Now use **Eq. 3.10** to find;

$$\frac{q_N}{\Delta_N H} = N(t) - N_0 = N_0\, 2^n - N_0 = N_0\,(2^n - 1) \quad \textbf{(3.28)}$$

where **Eq. 3.27** was used. Finally, the above equation follows;

$$\frac{q_N}{\Delta_N H} = N_0\,(2^n - 1) \quad \textbf{(3.29)}$$

$$\frac{q_N}{N_0\,\Delta_N H} = 2^n - 1 \quad \textbf{(3.30)}$$

Eq. 3.30 could be used to calculate the number of generations *n* evolved during the exponential growth phase.

3.2.4.7 Degree of reaction

One further application having determined cumulative heat (see **Figure 3.2**) could be calculating the degree of reaction which should be proportional to the number of cells as demonstrated by Fessas and Schiraldi (2017) and validated by traditional microbiological methods (Gardikis *et al*., 2017).

Degree of reaction completion α can be given by;

$$\alpha = \frac{q_t}{Q} \quad \textbf{(3.31)}$$

where q_t, is the cumulative heat at time *t* and *Q* is the total heat evolved. Then it can be found that;

$$\frac{d\alpha}{dt} = \frac{\frac{dq_t}{dt}}{Q} = \left(\frac{\alpha k e^{kt}}{1-\alpha}\right) \quad \textbf{(3.32)}$$

By applying logarithm to **Eq. 3.32** it can be found;

$$ln\left(\frac{d\alpha}{dt}\right) = ln\left(\frac{\alpha k}{1-\alpha}\right) + ln\,(e^{kt}) \quad \textbf{(3.33)}$$

Finally, after rearrangement;

$$ln\left(\frac{d\alpha}{dt}\right) = ln\left(\frac{\frac{q_t}{Q}}{1-\frac{q_t}{Q}}k\right) + kt \quad \textbf{(3.34)}$$

Eq. 3.34 offers yet another way of getting the growth rate *k*.

3.2.4.8 Relative cell numbers

Furthermore, relative cell numbers could be determined from inoculum volume experiments by modifying **Eq. 3.12** by setting *t = 0*;

$$ln\frac{dq}{dt} = lnk\Delta_N HN_0 \Rightarrow \frac{dq}{dt} = k\Delta_N HN_0 \quad \textbf{(3.35)}$$

Inoculum volume meant in the context of this project either predetermined increments or decrements of the inoculum volume, for example, if the standard inoculum volume is 30µL, inoculum volume experiments could be in 2µL decrements. These experiments, in principle, reflect decrease in inoculum densities and may help in studying the effect of cell numbers on the response time when tested in the calorimeter. Decreasing or indeed increasing cell densities in the inoculum offers an opportunity to study the effect of this on the growth curve. It was plausible that at different cell densities the cell might behave differently, such as forming a biofilm instead of being in a purely planktonic state.

3.3 Discussion

3.3.1 Central equation

The central equation *i.e.*, **Eq. 3.12** relates to the logarithm (log) of power to time through a line of slope *k* and the intercept $ln[N_0\Delta_N H\ k]$; the value of the intercept is the value of the power when mathematically *t* is 0. The central equation was couched entirely in terms of accounting for the exponential phase of microbial growth. It is a special case of first order process, where the plot of logarithm power vs. time is a straight line with a slope, which is equal to the rate constant of the described reaction (exponential microbial growth). In other words, the generalised case was that the logarithm of power vs. time described the first order process, and the special case was the exponential growth of microorganisms.

When the logarithm of (*dq/dt*) was plotted against *t*, **Eq. 3.12** was explicitly turned upon the exponential growth; that is to say, the equation was expressed entirely in terms of microbiological growth and mathematically accounted for exponential growth only for the purpose of this thesis. Additionally, plotting the log of power against time is a way of identifying a first order process (Willson *et al*., 1995; Beezer *et al*., 2001) and the slope of that line is the rate constant. This suggested that the rate constant would be both a function of the organism and the medium in which the organism was grown assuming that the temperature and other important experimental parameters were kept constant. Therefore, medium investigation as well as organism investigation was possible. If the medium was kept constant, the changes observed could be attributed to organism variations and vice versa. Indeed, if it was true that these investigations were possible, then it raised the prospect of using the equations to explore the history of the organisms (the effects of the original growth medium in which the organism was prepared and the storage conditions on the growth performance of the organism in the subsequent tests) as well. This could aid in determining the ideal conditions under which the organism would be used in the real production process.

Yet, more could be done with the central equation. For example, manipulations based on the **Eq. 3.12**, where *t = 0* (an equation of a straight line results) a plot of *dq/dt* vs. *Q* would offer a rather trivial way of getting *k* from the TAM output. This is practical, as just adding up dq/dt (because there are the same time intervals constituting the area) and plotting these against each other gives *k*.

The development of an empirically based central equation, **Eq. 3.12**, established on the basis of the exponential growth of bacteria, has largely focused on establishing a simple and fairly accurate way of identifying the exponential growth phase and thus setting a working definition of what was to be considered as t_0. The significance of defining t_0 as the moment when the exponential phase started had implications both for the pragmatic and the theoretical outcomes of this project. At a pragmatic level, having t_0 as a parameter could be significant for production monitoring. The moment in which the exponential growth started in a given batch of the Symprove product (or, in fact, of any process of fermentation) could be a good indicator of the behaviour of the bacteria involved. For instance, if the exponential growth started too late with respect to a reference, this might signal a low concentration of organisms in the inoculum or some alteration in the inoculum's history, such as contamination or different metabolic pathway reaction. If the exponential growth started too early compared with the reference, this might indicate that there was an excess number of organisms in the inoculum, or there might be contaminants that grew faster than the bacteria of interest expected to be there (see **Chapter 4** on contaminants). Hence, having an easy and reproducible way to compare this parameter would be an important tool for production control and monitoring.

At a theoretical level, a value of t_0 could be defined in several ways. Firstly, as the time when the ampoule was inoculated. Secondly, when the TAM signal started, and thirdly when exponential growth started. Defining t_0 becomes all the more important given that the equations referred to N_0, which had to be congruent with the definition of t_0 – be it the inoculum density at the beginning of the experiment or the number of organisms present at initiation of exponential growth, for example. Whilst it was possible to know the value of the inoculum, any subsequent cell number throughout the growth was unknown in the absence of a highly equipped lab, as was the case at Symprove. Setting t_0 was therefore important for making the model applicable to real world data.

By defining t_0 as the moment in which the exponential growth phase strictly started, this research avoided conflating measurable experimental landmarks, such as ampoule inoculation or TAM recording, with the much more difficult empirically established beginning of the exponential growth. Avoiding this conflation provided an opportunity to contribute towards having future parameters within the matrix of results and conformed with the acknowledgement that the p-t curve, despite its differences, was in line with the bacterial growth curve in which the different phases were clearly defined. Yet, the difficulty of establishing with precision the moment in which the exponential growth started had

sometimes led to the assumption that it coincided with the moment in which the TAM began recording power (Cabadaj *et al*., 2021).

Attention to the distinction of the bacterial growth phases in the p-t curve to construct a mathematical model has been scarce. While Chang-li *et al*. (1988) recognised the importance of defining t_0 as the beginning of the log phase for the calculation of the growth rate during that phase, they did not provide a method for establishing it mathematically from their equations. This meant that the only way of getting the value of the moment in which the exponential growth began was via finding the best linear fit of a line on the experimental data with some software. Although the concern of Braissant *et al*. (2015b) was neither the definition of t_0 with reference to the exponential growth (they defined it as the TAM power recording start) nor the establishment of the beginning of the exponential growth phase, they tried at differentiating the growth phases in the p-t curve. Closely following the idea of Zwietering *et al*. (1990), they suggested a method for establishing the lag phase by getting the x-intercept (with the x-axis representing t) of the tangent of the maximum growth rate (maximum slope) in the heat over time curve. As Zwietering *et al*. (1990) had done before using the bacterial growth curve instead of the heat-time curve, they estimated that the lag phase duration was between t_0 and that intercept. This approach did not really suit the purpose of this research because the end of the lag phase did not strictly coincide with the beginning of the exponential phase (there is an acceleration phase in between, see **Figure 3.1**), hence it was not possible to use their method to establish t_0 as defined here (*i.e.*, the beginning of the exponential phase). Similar principles have been used by Astasov-Frauenhoffer *et al*. (2011) for identifying the length of lag phase as a function of the initial bacterial concentration to determine, for example, viable but nonculturable bacteria in the sample. Fessas and Schiraldi (2017) defined the duration of the lag phase by the intercept of the tangent at the flex point with the baseline.

3.3.2 Rate constant (*k*)

As stated above, the equation $N(t) = N_0e^{kt}$ (*i.e.*, **Eq. 3.8**) described bacterial growth over time based on cell number. As the equation signalled, bacterial growth had a segment that was exponential and therefore could appear as a straight line when expressed in logarithmic terms. The calorimetric derivation of the rate constants is well established (Willson *et al*., 1995; Gaisford *et al*., 1999; Willson *et al*., 1996; Hills, 2011) and this helped in quantifying and assigning more theory to these rate constants in the cases at stake in this project.

Although it was apparent from looking at the shapes in the examples given in **Chapter 2** that the values of *k* changed from one case to another, no quantification of that change was made. It should be noted that getting the slope *k* of this line is equivalent to what microbiologists have been doing for years; that is, plotting the logarithm of cell numbers against time as a straight line and getting the rate and generation time. By analogy, a similar principle applies to the p-t curve because calorimetry, as used in this project, is mirroring the cell growth over time.

The rate constant *k*, the main parameter of growth, was relatively easy to obtain from the transformation of the p-t curve (see **3.2.2**). This was in line with Braissant *et al*. (2015a) where they pointed out that some growth parameters (*e.g.*, growth rate and doubling time) could easily be obtained from both the p-t curve as well as the integrated p-t curve. The logarithm of power as a function of time seemed like the simplest approach for obtaining the rate constant. This was because a first order reaction gave a straight line representing exponential growth (the first segment of the curve), and this region was easy to visually determine in the plot. Although the rate constant could be obtained in a number of other ways, as for example, $(dq/dt)/Q = k$; or $(d^2q/dt^2)/(dq/dt) = k$; or $ln(d^2q/dt^2)/(t) = k$, these approaches involved further data manipulation, making them more time consuming without an obvious advantage. Furthermore, when the automatisation of data analysis takes place, the coding of the simplest procedure is preferable.

The manipulation of the central equation allows the development of other conclusions based on it. For example, if the growth rate is dependent on the medium, the *k* value ought to reflect changes of growth rate conditioned by changes in the growth medium. This is important for a production process such as fermenting bacteria in a specific growth medium. Consideration of alternative growth media, as for example, moving from small scale batches of wort to commercially produced wort could be assessed by having some quantitative views about how the same types but differently produced worts compared when subjected to the same growth conditions of the same bacteria. Further exploration of *k* is presented in **Chapter 4**.

3.3.3 Intercept

The y-intercept derived from the plot of the logarithm (*ln*) of the power signal against time was a calorimetric intercept that incorporated the rate constant *k*, the Joules per cell $\Delta_N H$,

and the inoculum N_0. The identification of the intercept was the mathematical outcome of writing **Eq. 3.12** describing explicitly the straight line associated with the exponential bacterial growth. Furthermore, the extrapolation of this straight line all the way down to the x-axis (y = 0) would theoretically, define the time at which the exponential growth described by **Eq. 3.12** had begun. This suggested that the approach taken here to exploit the intercept consisted of at least two aspects.

First, the challenge to find the value of t_0 that was implicit in the equation above and could be addressed if t_0 was set as t = 0, meaning a mathematical start that corresponded with the start of the regression analysis (which was the equivalent of the theoretical start of the exponential growth).

Second, the intercept should reflect the relative cell numbers (CFUs) at inoculation. If this was true, there should be an easy way to test this hypothesis. For example, adding variations of 3, 10, 30, 300 µL of inoculum volume were (assuming 10^6 CFU/ml in 30 µL for the purpose of this project) into a sterile medium that supports well the growth of the given inoculum. From the equations, the regression analysis should yield the values of k. Assuming the enthalpy was also constant, the ratios of the intercepts *i.e.*, using 3 µL as a reference, should be 3.33, 10, and 100 for 10, 30 and 300 µL inoculum, respectively. This should be seen as a shift on the x-axis either to the left with increased inoculum volume (30 µL and 300 µL, taking 3 µL as a reference) or to the right with decreased inoculum volume (0.3 µL and 0.03 µL, again, taking 3 µL as a reference).

The initial lag time duration could be determined as the interval between zero and the x-axis intercept (from the regression analysis).

When enumerated, the intercept would yield values that could contribute to a set of calculated growth parameters (for example intercept / k ratio) to confirm a good growth occurred. The intercept value could be another parameter to say whether the growth observed compared to the standard reference growth and how closely it compared with the standard. This is practically explored in **Chapter 4**.

3.3.4 Enthalpy per cell $\Delta_N H$

The power that was measured at any time during a calorimetric experiment was attributed to the sum of the power that was produced by living and actively dividing bacteria (assuming

that all exponentially growing bacteria produced the same amount of heat) at that particular time point. Therefore, determining enthalpy from the p-t curve required additional information such as microbiological plate counts (or optical density measurements, possibly cytometry) of the same culture as the one tested in the calorimeter. A change of enthalpy, in principle, would move the data (p-t curve) up or down with respect to the x-axis. Enthalpy could be calculated from the p-t curve data and the plate counts of the same culture. This is done by setting up a sufficient number of equivalent ampoules, some of which will be tested in the calorimeter, and some placed in an incubator (of the same temperature setting as the calorimeter). Whilst the calorimetric experiments will produce continuous data, the ampoules from the incubator will need to be opened and plated in several time intervals (*e.g.*, every hour, for at least as long as the p-t curve reaches the first peak, past the exponential growth) to provide an insight into the growth and get the actual bacterial counts at each particular time step. Getting the value of enthalpy for the exponential phase could then be calculated from the actual power value that was recorded on the particular hour when the associated plate counts were taken and (other methods such as automatic plate reader or flow cytometry could also be used), dividing it by the number of cells that were obtained by plate counting at that point.

If enthalpy was to be exploited as a useful parameter of growth, one needs to have the capacity of performing plate counts alongside the calorimetric experiments, or other suitable method that enables the enthalpy to be calculated. As mentioned previously in **1.4.4.1**, no calculations of enthalpy were offered herein because of limited laboratory provisions at Symprove co.

3.4 Conclusion

The equations presented are simple, satisfactory and if they are reproducible, their simplicity is a great advantage in comparison with more complex models such as Gompertz or Richards models (Zwietering *et al*., 1990). They have not yet been previously written in the explicit form as demonstrated above. Whilst many attempts to simplify calorimetric data analysis have adopted the logarithmic form of the p-t curve, there has not been much attention paid to the significance of the intercept, therefore, to that extent, the exploitation of the intercept was an important extension of the analysis.

The central equation **3.12** offered several practical applications, some of which are demonstrated in **Chapter 4** (it is not, however, an exhaustive demonstration of all applications). The simplicity of getting the main growth parameter, rate constant, *k* made the analysis of complex calorimetric data easier. . It is explored, in **Chapter 4**, how the rate constant (and the intercept) changed when the bacteria were grown in one medium (MRS, TSB), then tested in MRS or grown in another medium (wort, Dohler wort) then tested in the same MRS.

A clear definition of what the intercept was has been proposed above and this made it a good addition to other easily extractable parameters including growth rate (*i.e.*, slope), peak power, time to peak power and area under curve. In other words, these equations represent something which was quantifiable in both its slope and its intercept, and their reproducibility could be tested.

The application of these equations offered a functional, practical system that could be used for Symprove production monitoring and control, however, was not limited to Symprove production. It was obvious that the values of *k* and intercept were in essence just numbers for Symprove to determine whether the growth of their bacteria was good or not, however, an extension of applicability of the equations to more fundamental aspects are concerned with the availability of easily extractable parameters and their analysis. For example, examining the performance (*e.g.*, how good are the values of *k* and intercept) of the equations could be done by looking at their reproducibility in a controlled experiment (reference). The evaluation of the slopes and the intercepts that came from the logarithm plots was immediate and the calculation of t_0 was possible using the equations. Further analysis using the equations could examine how cell numbers or relative cell numbers could be determined.

The main guiding principle behind the practicality of these equations was that if a real system followed them satisfactorily, and if some meaning (*e.g.*, what dis the changing values of slopes and intercept represent) could be associated to that, something could be written about conventional biological counting systems, their accuracy, and whether it could be improved using IMC.

The work described in this chapter could also aid in further analysis of subsequent (followed after the first exponential growth) first order processes observed in the p-t curves, graphically illustrated in **Figure 4.10** (**Chapter 4**) and analysed in **Table 4.4** (**Chapter 4**). Each time

there is a change in the p-t curve, there is an opportunity to study this change as the basic information such as start time and duration of the change is known. The changes observed in the p-t curve capture changes in the metabolism and behaviour of the studied organism, for example, a nutrient being exhausted and organism switching to a different nutrient or energy source, metabolite build or switching from fermentation mode to respiration. IMC captures, very precisely, both time scales as well as energetic extents of these events. Furthermore, the aim of kinetic analysis was to provide a mathematical model that explained the behaviour observed and whether the model fitted the data and how well. Kinetic analysis of the observed behaviour was only a mathematical description of it. To discover what the actual process was (such as the first exponential growth), other auxiliary experiments need to be done in parallel and these were outside the scope of the project.

The nature of the discussion in this section was purely theoretical; contrasting the theory against the empirical results is the task of Chapter 4, where, through already established reference-standards, was possible to measure the reproducibility of the experiments and to assess the empirical applicability of these equations.

Chapter 4 Industrial application of the theory

4.1 Introduction

The previous chapter developed theoretical equations related to the exponential phase only. It was noted (**3.2.2**) that the p-t curve revealed the cumulative heat by integration, which was also indicative of the total number of cells produced during an experiment. The cumulative heat (represented by the area under curve) enabled the exploration of how good the repeatability of IMC experiments was, in recording cell growth, assuming the same starting inoculum numbers and $\Delta_N H$ (heat/cell) values. A logarithmic transformation of the power recorded by a calorimeter plotted against time helped in identification of first order reactions represented by linear portions in the logarithmic plot (Beezer and Tyrrell, 1972; O'Neill *et al*., 2003; Willson and Beezer, 2003; O'Neill *et al*., 2004). The first major linear portion in the logarithmic plot was expected to be directly related to the exponential growth phase. Once the linear portion was identified, parameters such as growth rate (Braissant *et al*., 2013; Cabadaj *et al*., 2021), and the beginning of the exponential phase (the intercept of the linear portion with the time axis) could be determined. The logarithmic plot also necessarily revealed generalised first order processes (such as microbial inactivation) other than just the first exponential growth.

This chapter addressed the industrial concerns of this thesis *i.e.*, could the time cost (from the end of fermentation to bottling) of the product testing to Symprove be improved through use of IMC. "FV1-real", in the context of this thesis, meant a full production scale (*i.e.*, 1000L) batch of FV1, according to Symprove's standard operating procedure (as detailed in **1.4.1** or its later variations). Previous chapters have explored whether a good product showed up in IMC tests as a consistent outcome (**Chapter 2**) and the theoretical developments (**Chapter 3**) needed for the mathematical interpretation (**Chapter 4**) of the p-t curves derived from calorimetric experiments. This was done through IMC's capacity to study complex systems without significant sample treatment prior to evaluation –and that its data was available in real time. In other words, a template for the evaluation of IMC as a tool to assist industrial process performance was developed. In order to do this, it was first imperative to establish a set of standard references, as they did not exist for IMC reactions in relation to the Symprove product. It was desirable that the standard references be simple to perform, with high repeatability without the need for advanced laboratory provisions. After the references were established, the repeatability of the system could be determined, and coding developed. The latter was done to enable an automatic and operator independent

procedure to streamline data processing and QA decision making. Importantly, should IMC be used as a standalone method, determining its performance for detecting a good growth (good fermentation) in an industrial setting, a comparator of conformity with classical microbiological methods (plate counts (PC) and optical density (OD)) was done in section **4.3.1.1.1**). Additionally, IMC reference systems could be used to ensure instrument performance over time.

An attempt to establish standard references to analyse the role and importance of the equations previously developed is presented in the first part of the chapter. Here, for the sake of practicality and simplicity, a model organism, *L. rhamnosus*, was selected from amongst those in Symprove and tested in a controlled medium, MRS (previously discussed in **Chapter 2.2.2**). *L. rhamnosus* was studied exhaustively to make sure that the objective to discover and implement this procedure to the real product (FV1-real was a subject of the thesis; FV2-real and Mix-real form a scope of future work) could be achieved. It was simpler and more productive to take one organism first, as a case study (see **4.3.1**), instead of the full product, so, the prerequisites of repeatability (and hence estimates of uncertainty and the performance of the method could be determined), medium issues could be established with better accuracy and then proceed by stages to the complexity of the product (*i.e.*, FV1-real).

Once the references were successfully established for *L. rhamnosus*, *L. acidophilus* and FV1-artificial, the repeatability of the system could be determined. Quality controlled product procedure required that all aspects of the procedure were as closely controlled as practically possible. For example, the experiments were tightly controlled (timings were the same, temperatures were the same, growth medium was controlled, the procedure was simple to perform and the instrument's performance was verified) and all these should enable repeatability over time, which should ensure confidence in the procedure/testing itself. It was desirable that the repeatability of the experiments should be better than the repeatability of traditional microbiological plating methods (Corry *et al.*, 2007) used by the Symprove company for QA at the time.

Taking the best-case scenario of pure *L. rhamnosus* in a controlled MRS medium to test the repeatability of the experiments seemed logical as variations arising from medium composition and bacterial strain impurity would be minimised. MRS medium was selected after a significant investigation was carried out to find a suitable growth medium (see also **4.2.3**). MRS was recommended for Lactobacilli and it also showed less complexity in

resulting p-t curves when compared with TSB. Upon conclusion that this best case scenario offered satisfactory confidence in the method, the method was applied to the second constituent of FV1, *L. acidophilus*, and then to FV1-artificial (equal mix of *L. rhamnosus* and *L. acidophilus*, to simulate, at a laboratory scale, FV1-real. Using **Eq. 3.12** offered the opportunity to demonstrate that the values of chosen parameters, once established, fell within a specified range. It was expected that the ranges determined for a real scenario (*e.g.*, FV1) would be wider than the ranges for a precisely controlled experiment (*e.g.*, the best-case scenario).

The strategy employed consisted, first, in doing manual analysis of data using OriginPro software (OriginLab Corporation) to then implement the coding and automation of the data processing. Developing operator independent and streamlined data processing only made sense after it was established that it was worthwhile doing so. A proof of concept was successfully demonstrated by Cabadaj *et al*. (2021).

The range of data that was accessible from the calorimeter meant that the simple analysis (p-t curve derived parameters and their reproducibility, see later in **4.3.1.2**) was possible as well as the analytical outcome from the application of the equations (parameters derived from the logarithmically transformed p-t curve *i.e.*, slope which is the rate constant, intercept value and AUC) was obtainable.

These data when quantified allowed a clear quantitative comparison of the performance of *L. rhamnosus* in the calorimeter, with, for example, *L. acidophilus*. The same approach was used to understand whether the FV1-artificial behaved in any way similar to FV1-real. This offered the opportunity to study the performance of an alternative wort (Dohler wort) with respect to barley wort produced on site. It was also possible to distinguish whether there was a contaminant present (sections **4.5.1.3**, **4.6.1.3** and **4.7.1.3**.

This chapter explored whether calorimetry could substitute for traditional microbiology, and whether there was a greater insight to be gained from the exploitation of the equations developed in **Chapter 3**. This chapter also described comparative studies of *L. rhamnosus*, *L. acidophilus*, FV1-artificial, FV1-real, and some contaminants isolated from real production samples of FV1.

The main aims of this chapter were:

1. To develop reference standards for *L. rhamnosus*, *L. acidophilus* and FV1
2. To establish basic shape analysis parameters as well as quantitative analysis parameters (rate constant, intercept)
3. To develop comparison matrices of both shape parameters and quantitative analysis parameters
4. To demonstrate practical applications of IMC through contaminant detection experiments

4.2 Materials and methods

4.2.1 Testing protocol

The general experimental protocol consisted of filling sterile glass ampoules (3 mL) with pre-warmed (37 ºC) sterile growth medium (2.97 mL) and inoculated with 30 µL of *L. rhamnosus* (an aliquot of frozen organism was thawed in a water bath at 40 ºC for 3 min, then vortexed for 1 min before inoculation). The ampoules were immediately sealed under aseptic conditions then inserted into the thermal equilibration position of the Thermal Activity Monitor (TAM) 2277 (TA Instruments Ltd., UK) for 30 min before lowering them into measuring position and data capture began. TAM collected data using a software package Digitam 4.1. The software collected data at 4 Hz for 24-48 hours or until the signal came back to the baseline; here, once 40 data points were collected, the average value was recorded, giving a final data set comprised of 1 data point every 10 seconds (this method had the effect of smoothing the power data). Any differences from this protocol were noted as appropriate. Electrical calibration was performed in accordance with the Instruction manual (Thermometric, 1996). Optical density readings were performed using Thermo Scientific Spectronic 200 Spectrophotometer at 600 nm. Plate counts were obtained using *L. rhamnosus*, sterile PBS and sterile vials; dilutions of 1:10 (-1) through to 1:100 000 000 (-8) were performed. These dilutions were done for 8 time points (each time point corresponding to 1 hour). Colonies were counted 24 hours later to give CPU counts.

Manually derivable parameters from both the p-t curve and its logarithmic transformation were obtained by using OriginPro software (OriginLab Corporation). This was done by

uploading raw data, analysing peak power, time to peak power, calculating areas under curve, logarithmic transformation of the raw data, after which the best straight line from the beginning of the data up to peak power was identified and the parameters of slope, intercept and the best coefficient of determination obtained.

4.2.2 Microorganisms

Strains of *L. acidophilus* NCIMB 30175 and *L. rhamnosus* NCIMB 30174 manufactured by Supplier 1 were of lower purity (allowing ≤ 5 x 10^4 CFU/g of total aerobic contaminants) even though these were made from pure controlled stocks held at NCIMB. The exact procedure for their manufacture was not available because of the proprietary nature of the process. However, it was not possible for them to provide pure strains because of their large-scale operation.

Pure strains of *L. rhamnosus* NCIMB 30174 (Supplier 2 provided three different batches LrJ2, LrJ3 and LrC3) and *L. acidophilus* NCIMB 30175 were manufactured by Supplier 2, also from the controlled stocks held at NCIMB. *L. rhamnosus* culture was tested using traditional microbiological methods *e.g.*, optical density (OD) measurements and plate counts in hourly intervals up to the peak power observed in the p-t curve (cell counts and OD measurements performed at a contract laboratory for the purpose of this thesis only and could not become routine at Symprove because of their limited laboratory provisions). Note that batch LrJ2, (**Figure 4.6**, red line) had a total loss of viability during storage as determined by IMC and later confirmed by an external independent laboratory. De Man, Rogosa and Sharpe (MRS) agar, from Sigma-Aldrich, was prepared according to the manufacturer's recipe. Phosphate buffered saline (PBS, pH 7) tablets and glycerol were purchased from Sigma-Aldrich, UK. Both strains were grown separately overnight in MRS broth for 16 h at 37 ºC. Cells were then centrifuged, washed in PBS, resuspended in 15% (v/v) glycerol at an organism density of 1 x10^8 CFU/mL and frozen in aliquots (1 mL) at -80 ºC (see Said, 2014 for more detail on preparing pure inocula). By "pure" (related to bacteria) in the context of this thesis, was meant that the inocula did not contain any contaminating organisms and were manufactured according to the protocol of Supplier 2 just described in this paragraph and were not subcultured for the IMC experiment (unless noted otherwise).

For inoculum volume experiments, 10-fold dilutions of *L. rhamnosus* were prepared using sterile PBS, pH 7.

4.2.3 Media selection

Around 400 calorimetric experiments were carried out in order to arrive at an informed decision to select a suitable growth medium. For reasons of brevity, only the more successful results were displayed and discussed here. However, the following media were considered and tested to lesser or greater extent: various barley worts and extracts produced on site or bought in (these included: regular wort –meaning wort produced by Symprove on site according to their standard operating procedure (see **Chapter 1.4**); organic lager malt wort (Warminster Maltings, UK) and premium pilsner malt wort (Neale's brewing suppliers, UK) produced experimentally on site at Symprove; Dohler wort (DLW) –barley malt wort produced off site by Doehler GmbH Germany, cooked meat medium (Thermo Fisher Scientific, UK), brain hear infusion (Thermo Fisher Scientific, UK), tryptone soya broth (TSB) Thermo Fisher Scientific, UK), a selection of chemically defined media (CDM) (Sigma-Aldrich, UK) and De Man, Rogosa and Sharpe (MRS) broth (Sigma-Aldrich, UK).

In order to select the best testing medium for establishing the references and have an insight into the sensitivity to growth media *L. rhamnosus* was defrosted and 30 µL dropped aseptically, straight from a cryovial into 2970 µL of a sterile growth medium including barley worts, CDM, TSB, and MRS (in the case of wort media, these were not strictly sterile but rather boiled at 100ºC for 1 hour) –results in **section 4.2.3**.

Additionally, *L. rhamnosus* was subcultured in a variety of growth media (including regular as well as industrially produced barley worts mentioned earlier, TSB and MRS). Then each of these cultures was in turn tested in the calorimeter using a variety of fresh testing media. These preliminary studies showed that some combinations of the growth and testing media supported the consistency and growth of *L. rhamnosus* better than others (results in **4.3.2** and **4.3.3).**

Furthermore, all the experiments carried out provided the ground for choosing MRS both as the growth medium and as the testing medium for establishing the references. Exploring these media also allowed investigations of the sensitivity of the equation analysis of the growth rate and the intercept to the background of the *L. rhamnosus* (history of the organism). The basic principle was to grow *L. rhamnosus* in a variety of media and test it in order to see the consequence of growing organisms in one medium and testing in other medium.

Figures 4.1–4.6 below are presented for an overview of detailed analysis of growth media tested. This work, started right at the beginning of IMC experimentation phase. It was a process of unravelling the effects of lower purity inocula (Supplier 1), variable composition of growth media, their interplay and resulting varied consistency of the final products. Starting from the point of highest complexity (variable composition of growth medium, wort produced on site and using variable quality of organisms produced by Supplier 1) was a natural consequence of the initial experimental and laboratory provisions at Symprove rather than an informed and thought through process. Efforts were made, however, to try to limit any controllable variable by for example selecting just one organism and a wort medium that was produces in a standard production process described in **1.4**. Even though barley wort was produced in a semi-controlled way –times and temperatures of the actual cooking process were exact, other variations impacting the final composition of the medium arising from differences for example in germination rates, different varieties of barley or ambient temperature were experienced. These variations affected the rate of germination, sugar, mineral and vitamin levels resulting in different nutritional composition of the final wort. Examples of these are seen in **Figure 4.1**, where significant difference, both in the time scale as well as in the actual shapes of the p-t curves were observed.

The term “uncontrolled” was used either for bacteria or media and meant there were variations either in purity and cell density of the bacteria or nutritional composition of the medium. In contrast the term “controlled” is used to describe pure strain bacteria of known cell density, chemically defined media or media produced industrially through controlled production process for laboratory, analytical or industrial purposes.

After understanding the problems with more general contaminations in the product (see also section **2.6**) and more specific contaminations present in the inocula (demonstrated in **2.6.3**), it was decided that only pure inocula would be used. It was not yet clear to what extent medium variation would impact the resulting p-t curves, when pure organisms would be used. However, some differences were expected. These are presented in **Figure 4.2**, where the controlled organism *L. rhamnosus* pure was tested in 5 different batches of barley wort. Black curve in **Figure 4.2** represents a batch of DLW that was expired, however, still supported the growth of *L. rhamnosus* to some extent. This suggested that the shelf life of the medium could be investigated via IMC. It was clear from these experiments, that controlling the quality and purity of the organism did influence times to reach peak power as these were now more grouped together, however, the shapes of the p-t curves were significantly different, even for Dohler wort (DLW) of which 2 different batches were tested.

The two different batches of the wort from this supplier were of different expiry dates and it was hoped that testing these could show aging of the medium over shelf life. It turned out to be true and there was a noticeable difference between peak powers and areas under curve of these two worts suggesting that the wort with expired shelf life (black curve) did not support the growth of the same organism to the same extent as the fresh batch of the wort (purple curve).

The next step in investigating medium and organism suitability for establishing calorimetric references was to test the same controlled organism (*L. rhamnosus*) in a properly controlled medium. For this purpose, chemically defined medium RPMI 1640 (Sigma-Aldrich, UK) was selected as it was ready to use and easily obtainable. This medium did not show encouraging results –presented in **Figure 4.3**, where virtually no growth was observed. To confirm that the medium did or did not support growth of any of the four Symprove bacteria, pure strains of these were tested in it, **Figure 4.4**. Best growth was observed for *E. faecium*; less favourable conditions for *L. plantarum,* however, no growth was detected for *L. acidophilus* and yet again no growth for *L. rhamnosus*. Therefore, this medium was deemed unsuitable (without additional modification) for this work.

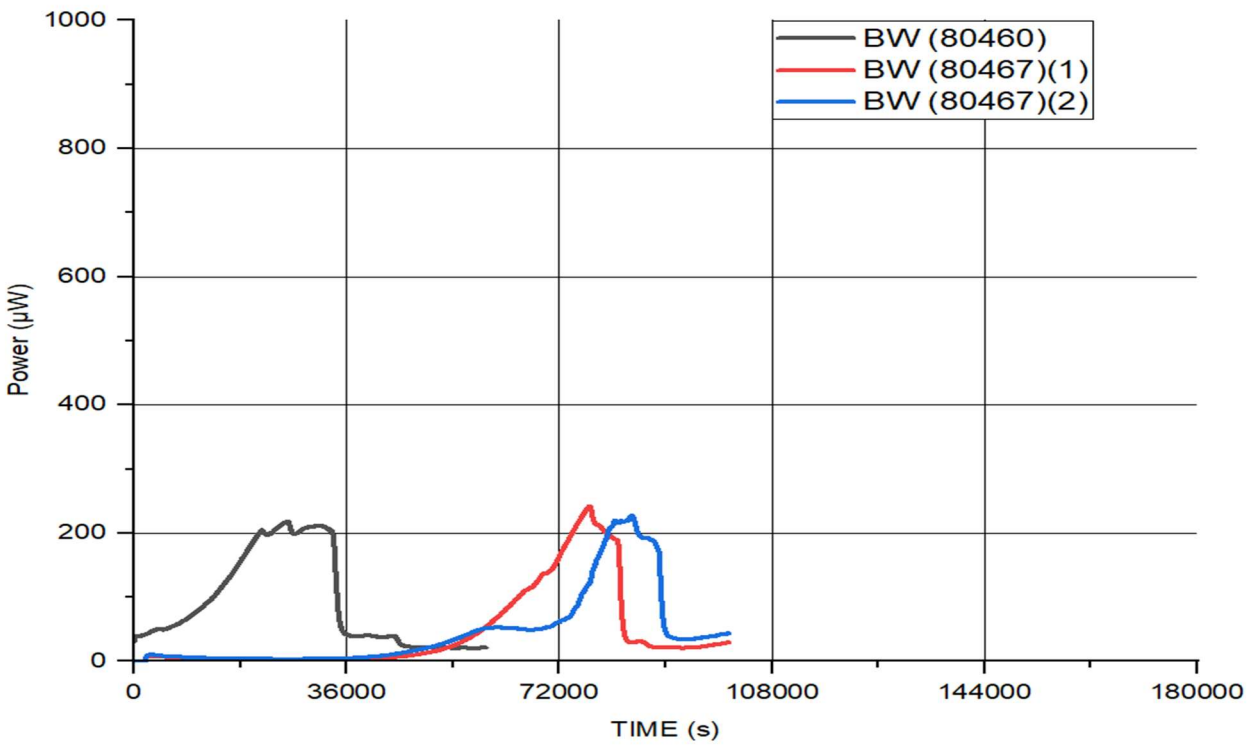

Figure 4.1 Uncontrolled organism (*L. rhamnosus*, Supplier 1) and uncontrolled medium (on site produced batches of barley wort). Note that red and blue curves represent the same batch of testing medium (wort) inoculated with one batch of *L. rhamnosus*.

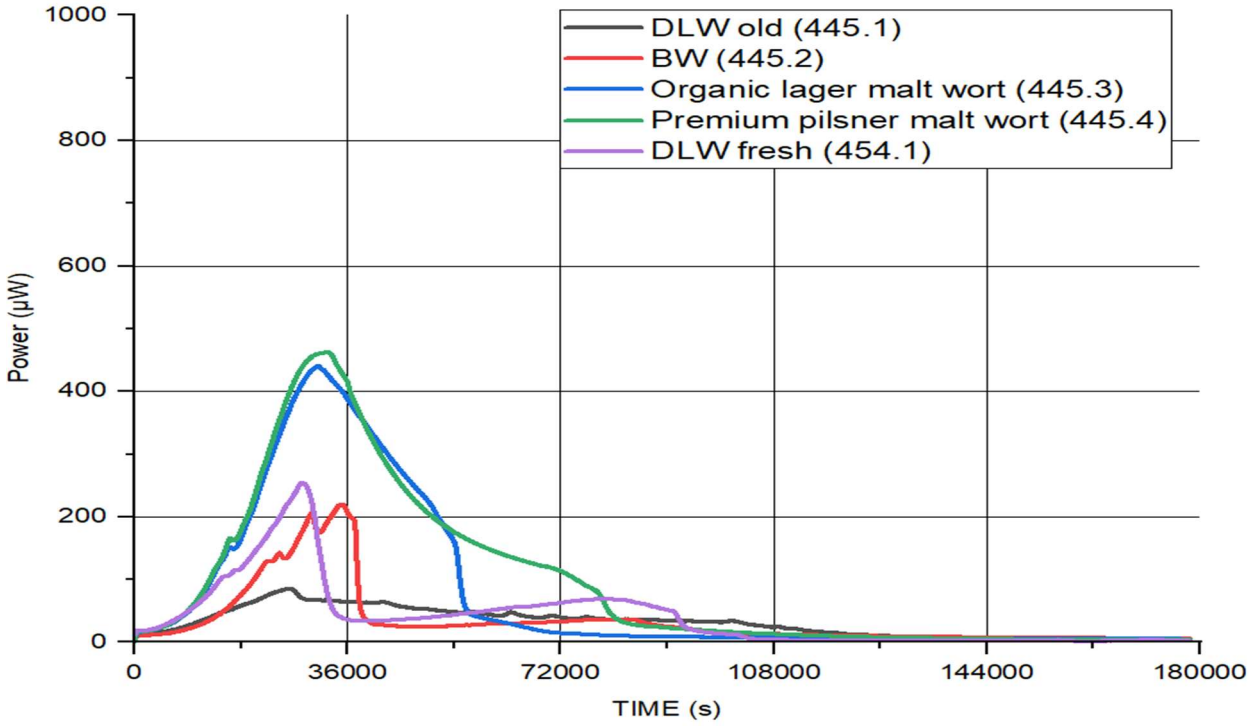

Figure 4.2 Controlled organism (*L. rhamnosus* pure) tested in various barley worts. Dohler wort (DLW) produced externally by a specialist company, the other 3 worts, red, blue and green curves, produced on site). Black curve represents a batch of DLW that was expired.

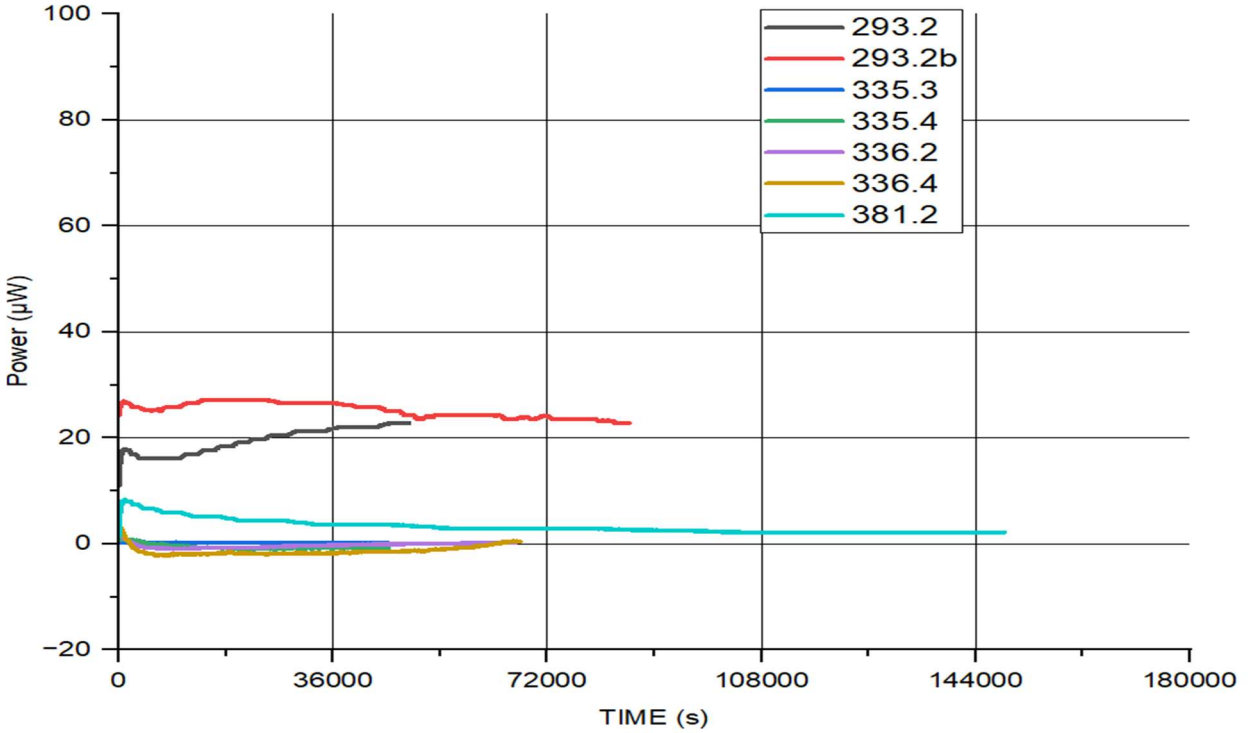

Figure 4.3 Controlled organism (*L. rhamnosus* pure) tested in controlled medium (chemically defined medium RPMI 1640). Note the power scale detail is 10 x increased in comparison to the previous figures to distinguish the resulting p-t curves from zero.

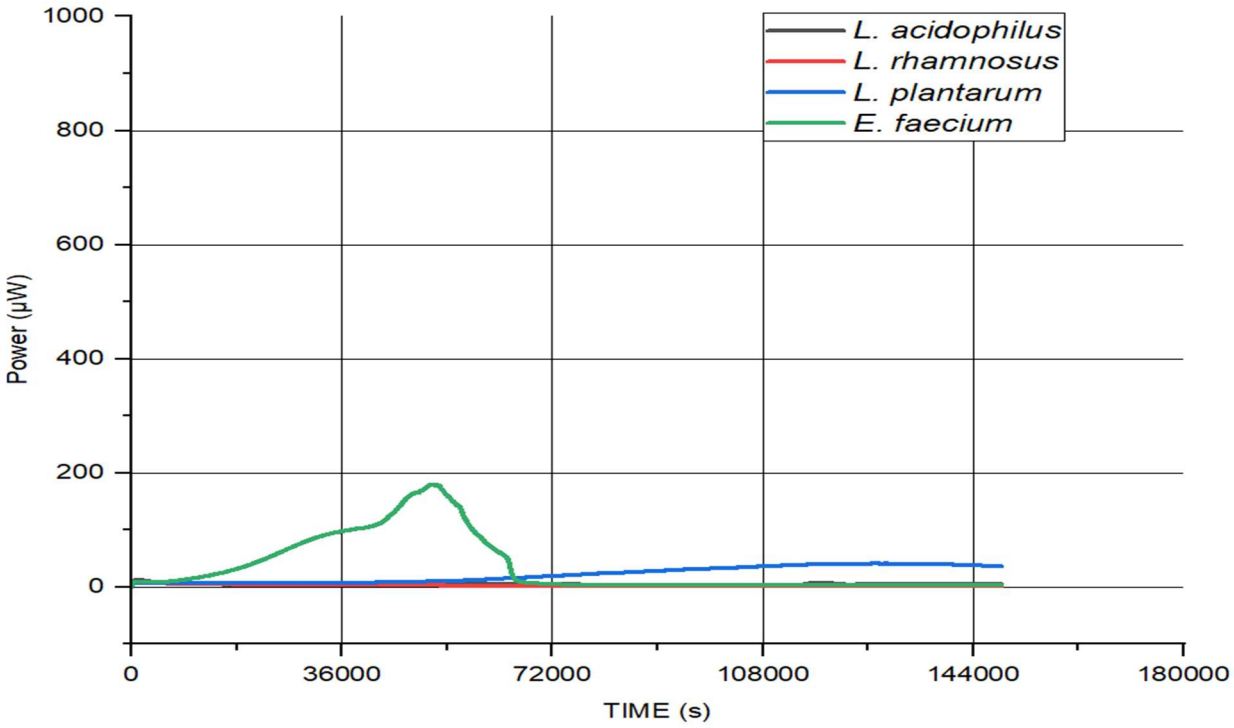

Figure 4.4 All four pure strains of Symprove product tested in chemically defined medium (RPMI 1640, Sigma Aldrich, UK.). (381 series.)

Another medium considered for standard reference establishment was Tryptone Soya Broth (TSB) from Thermo-Fisher Scientific, UK. It was included because this medium was recommended for testing purposes by a contract laboratory used for QA at the time. *L. rhamnosus* pure was tested in several different batches of TSB. One litre batch of sterile TSB (W) was provided by a contract laboratory (this was sufficient for all work presented here) to avoid batch to batch variations. Results in **Figure 4.5** showed that there was a decent consistency in the shapes of the p-t curves, except for the experiments 386.2 (orange curve) and 348.1 (red curve). It was concluded that most likely the age of the medium (whilst still in date) played a role in 386.2 as it was the last experiment of the set. It was also discovered that while the general shape of 348.1 was similar to the rest of the experiments in **Figure 4.5**, the peak power was approximately 1/3 lower. This was caused by the particular TAM channel being out of calibration .The out of calibration channel was detected, only as a result of keeping the medium and the organism constant, hence the 1/3 difference in peak power compared with the other 3 experiments in the same 348 series had to be the influence of the instrument).

For comparison purposes, two batches of *L. rhamnosus* pure (LrJ2 and LrJ3) were tested in TSB (see **Figure 4.6**). They were expected to show good reproducibility. However, it was

discovered firstly, with calorimetry, that there was no detectable signal for LrJ2 batch (red curve), assuming no viable organisms present. This was later confirmed by traditional microbiological plating methods that the LrJ2 batch of *L. rhamnosus* pure produced by Supplier 2 had a total loss of viability on storage. The second batch of *L. rhamnosus*, LrJ3, produced p-t curves as expected. The reason for the loss of viability was not immediately discovered. There were no immediate observations other than a few temporary power cuts. The freezers were not monitored at that point. Storing and freezing facilities at Symprove at -80ºC did not provide a uniformed temperature profile across the whole batch (*e.g.*, 500 vials). Most likely the occasional power cuts caused the bacteria to thaw slowly in the freezer as the temperature in the freezer rose above the freezing point of the prepared inocula suspended in 15 % (v/v) glycerol. These repeated thaw and freeze cycles most likely damaged the stock to the point of no viability.

There needed to be a stock of controlled organisms (master batch, used to produce a standard reference p-t curve) to have two kinds of control. One, to see whether the instrument was working correctly. The other one was to do with the notion that the same number of organisms (not random number) was added into the production vessel every time. Finally, at the end of the standard reference batch and when another supply was taken, it would be assessed against the standard reference batch and make that a new standard reference batch. It is plausible that the reference standards for the master batch would be shifting slightly, given that this was a complex system.

The above was an excellent example of how IMC can contribute to a rapid industrially implementable, and cheap QC procedure. Another batch of *L. rhamnosus* pure (batch designation: LrC3) produced by Supplier 2 showed a good growth and good reproducibility (**Figure 4.6**; experiments 545.3 and 545.4).

The curves in **Figure 4.5** showed good reproducibility as discussed above, however these also showed more complexity compared with the curves in **Figure 4.6**. Therefore, I decided to investigate another medium *i.e.*, MRS (see **4.3.1**)to find out whether less complexity could be achieved in the resulting p-t curve.

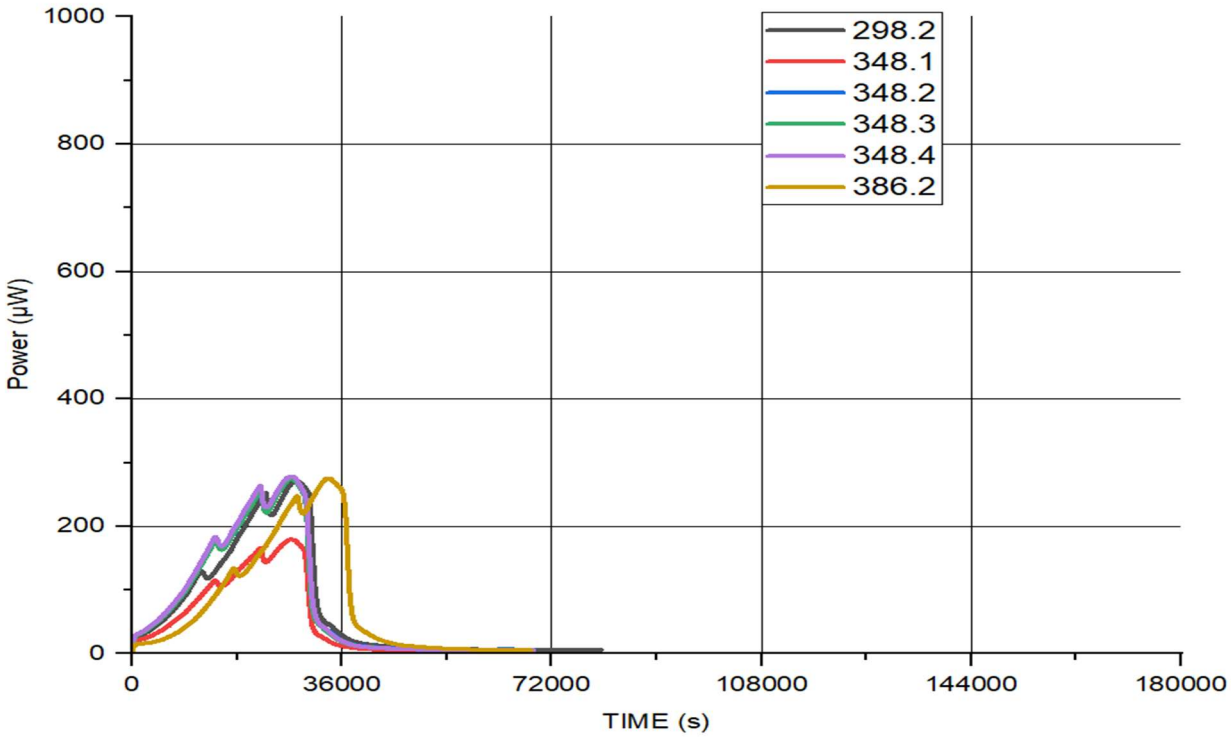

Figure 4.5 *L. rhamnosus* pure tested in one batch of TSB(W), (W –designated batch marking).

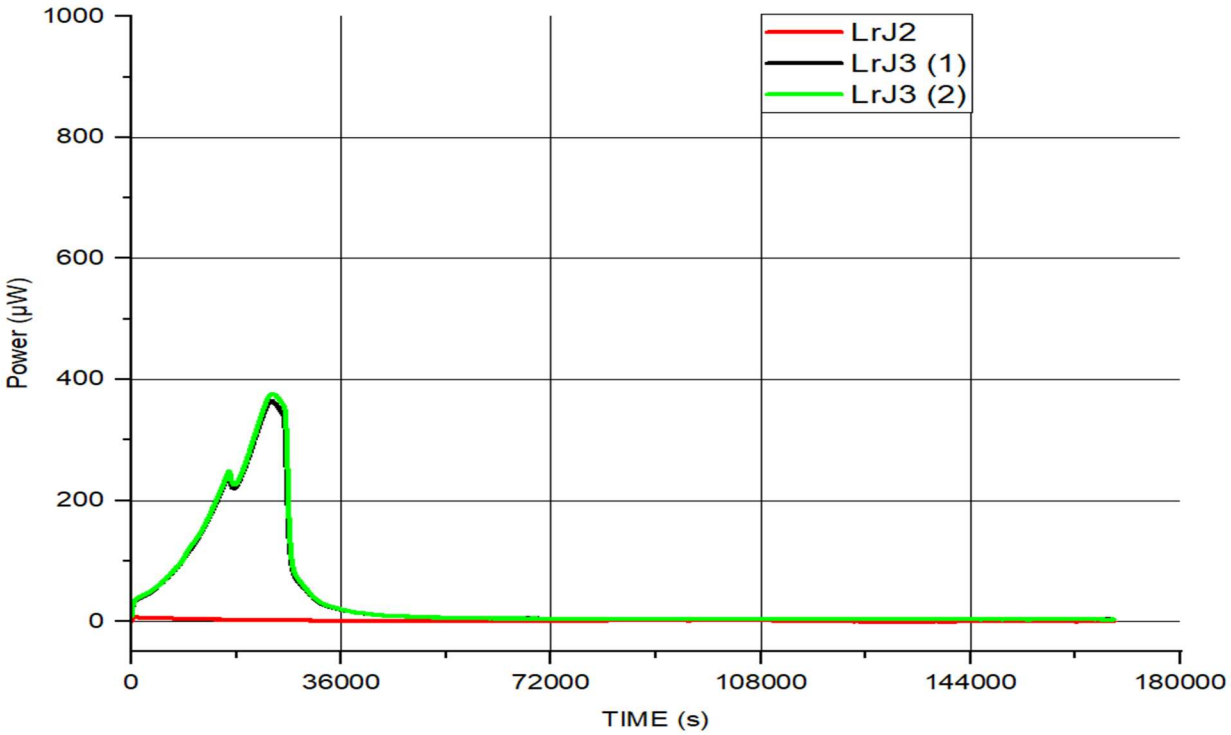

Figure 4.6 Comparison of 2 different batches of *L. rhamnosus* pure tested in TSB.

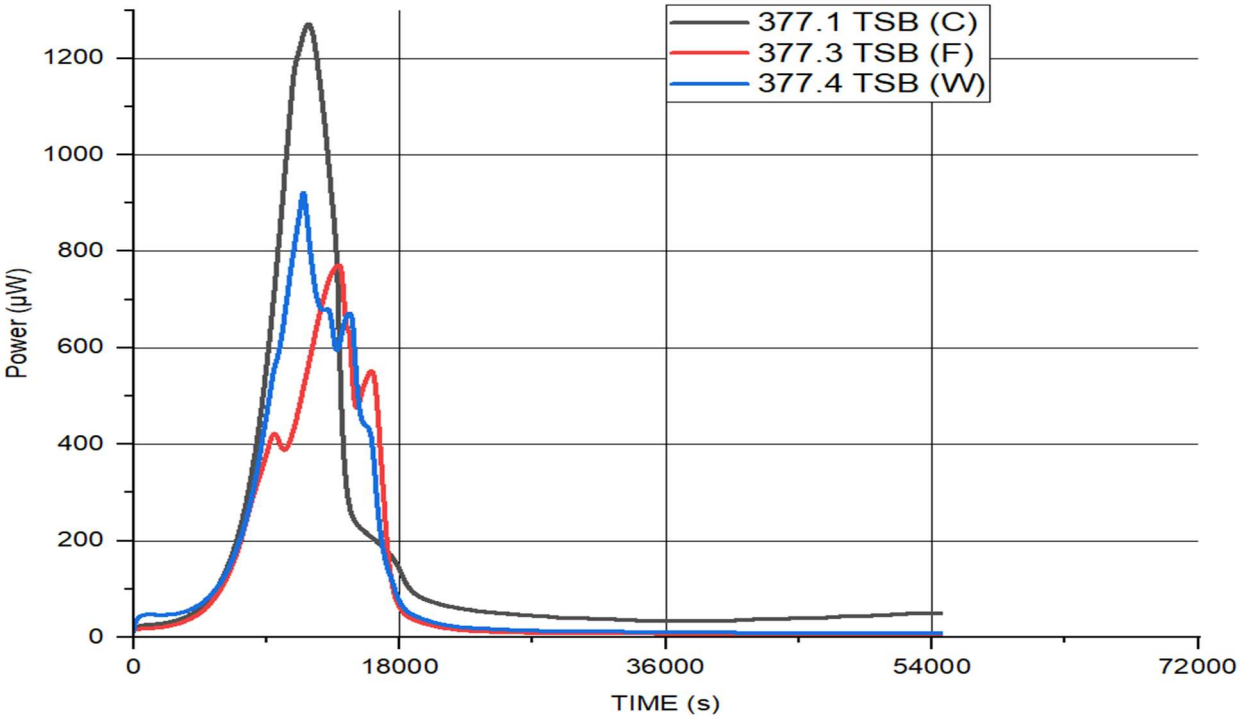

Figure 4.7 Comparison of 3 different suppliers of TSB. 1 batch of full Symprove product was tested in 3 batches of TSB. TSB(C) was TSB from Corning Mediatech, Inc, USA; TSB(F) was TSB from Fisher Scientific, UK; TSB(W) was TSB supplied by Wickham labs, UK.

The differences in supporting the growth (of the same batch of product *i.e.*, mix 2 80728) between different suppliers of TSB can be seen in **Figure 4.7**. It was discovered, from additional work on *E. faecium* tested individually in TSB, that the high power outputs were caused mainly by *E. faecium* .This means TSB was unsuitable for reference work as it was a highly variable medium. Consequently, a consideration of the possibility of medium selection, using IMC opened up. TSB was less than satisfactory. It was good at sustaining rapid growth, but TSB from different suppliers yielded different p-t curves, and that meant in the search for a test medium and a reference medium, TSB did not fulfil the criteria established earlier on, unless TSB from one supplier only, would be used. However, it was also discovered that TSB itself was a highly variable medium and produces rather complex p-t curves.

Whilst TSB was very good, all the TSBs examined, were good at supporting growth (**Figure 4.7**), they nonetheless produced different p-t curves, and this disqualified TSB from consideration as a reference medium but thus pointed to the sensitivity of IMC in detecting medium difference. Therefore, IMC studies herein offered a significant contribution to fundamental microbiology. It was possible to study subtle differences in metabolism of a

pure organism, and in this case the subtle differences were generated by different suppliers (and composition of their media) and not by the organism. One advantage of TSB in comparison with the previously discussed media was that the whole experiment (significant changes in the p-t curves) finished in under 10 hours.

The investigations of the medium suitability were done on the basis that the organism, *L. rhamnosus*, as well as the testing conditions were kept constant, therefore any variations in the p-t curves would be caused by the medium (be it the same medium from different suppliers of different media all together). Conversely, if the medium and the testing conditions were kept constant, the variations in the organism (*e.g.*, different batches of the same organism, the same organism produced by different manufacturers, two or more different organisms) could be investigated (see later sections **4.5, 4.6, 4.7**). Similarly, history of the organism can be investigated, for example if the testing medium was kept constant and the organism was sub-cultured in different media, the effect of the sub-culturing medium on the organism could be determined (see **4.3.2** and **4.3.3**). All of the above and the fact that MRS broth was specially designed for the isolation and cultivation of *Lactobacillus* species from a variety of sources (Sigma-Aldrich, 2013), while inhibiting the growth of some other competing microorganisms provided the ground for choosing MRS broth as the growth and testing medium for establishing the references.

There were some added benefits discovered whilst carrying out the work above, commissioned primarily to investigate medium suitability for bacterial references establishment. These benefits were: the possibility to assess quality and viability of new and existing stocks of bacteria (see **Figure 4.6**) and the possibility of assuring the performance of the instrument used for this work (see **Figure 4.5**). By extension this observation, whilst extreme, underlined the need for a reference reaction that could be used, say, annually to confirm the performance characteristics of the IMC. One of the requirements for a reference reaction was the confirmation on a regular (*e.g.*, annual, 6 monthly) basis, that the machine (*e.g.*, TAM) was functioning consistently over time (see the extreme case illustrated in **Figure 4.5** –red curve). If, however, there was a detectable change over time the reason for it needs to be investigated.

In conclusion the various worts tested showed large variations even between worts of the same batch as the organisms were not controlled (bulk powder of a low purity as discussed in **Chapter 2**). In addition, RPMI 1640 did not support growth of *L. rhamnosus* despite initial experiments involving 6 different RPMI variations used to test FV1-real sample (not

presented here) showed some growth. TSB which supported growth of *L. rhamnosus*, yielded rather lower PPs and more complex curves in the exponential growth phase compared with barley worts and MRS, additionally, results differed from those found for different suppliers of the seemingly same growth medium (TSB). Consequently, MRS from one supplier only was selected for the reference work.

4.3 Results and discussions

The best way to test the practical applicability of the equation **3.12** to the industrial setting of Symprove was to start with *L. rhamnosus* which, out of all the four strains contained in the product, was the most likely to cause issues because it was heterofermentative and relatively slow growing, compared to the other strains. This meant that it would be the most demanding of the 4 organisms for example, if there was contamination, there was a better chance of its establishment. Starting with this strain seemed like a reasonable choice as if successful, the rest would be easier to complete

The main focus of this study was the exponential growth phase to determine, as fast as possible using IMC, that the growth proceeded as expected. From the graph discussed in the previous chapter (**Figure 3.2**), it was clear, considering that the integrated heat flow gave information about the growth of cell numbers, that the exponential phase continued to the peak of the p-t curve, and although thereafter the cell numbers remained constant, the power declined. This is also illustrated in **Figure 4.8**, where additional logarithmic transformation of the integrated p-t curve is displayed (**Figure 4.8** (blue curve)) and this could be indicative of no further exponential growth past the peak power at around 10 hours. Hence, the exponential growth phase was the most important to investigate.

Figure 4.8 shows a characteristic p-t curve observed when *L. rhamnosus* pure was tested in MRS. It is clear that up to the peak of the curve, there is a phase of exponential growth. The same exponential growth phase can also be observed in **Figure 4.9**. Thereafter, other metabolic features, not related to the exponential growth were recorded. It was not obvious from the p-t curve or its integration (cumulative heat evolved during the experiment) that there was no further growth after the peak as there was more heat evolved after the peak power, which was not related to exponential growth. There might be additional bacterial growth, however, this would be insignificant in comparison to the first exponential growth phase. The maximum cell density of 8.57 $x10^8$ CFU/mL was reached at around 28000

seconds which corresponds with peak power time in the p-t curve (see below **Figure 4.9**). The maximum bacterial counts from real production samples were between 1 x10^8 – 1 x10^9 CFU/mL. Note that there was a delay of approximately 30 minutes in the measured maximum plate count when compared with the peak power in the p-t curve. This delay was caused by the time needed to equilibrate the temperature of the ampoule with the instrument's internal temperature.

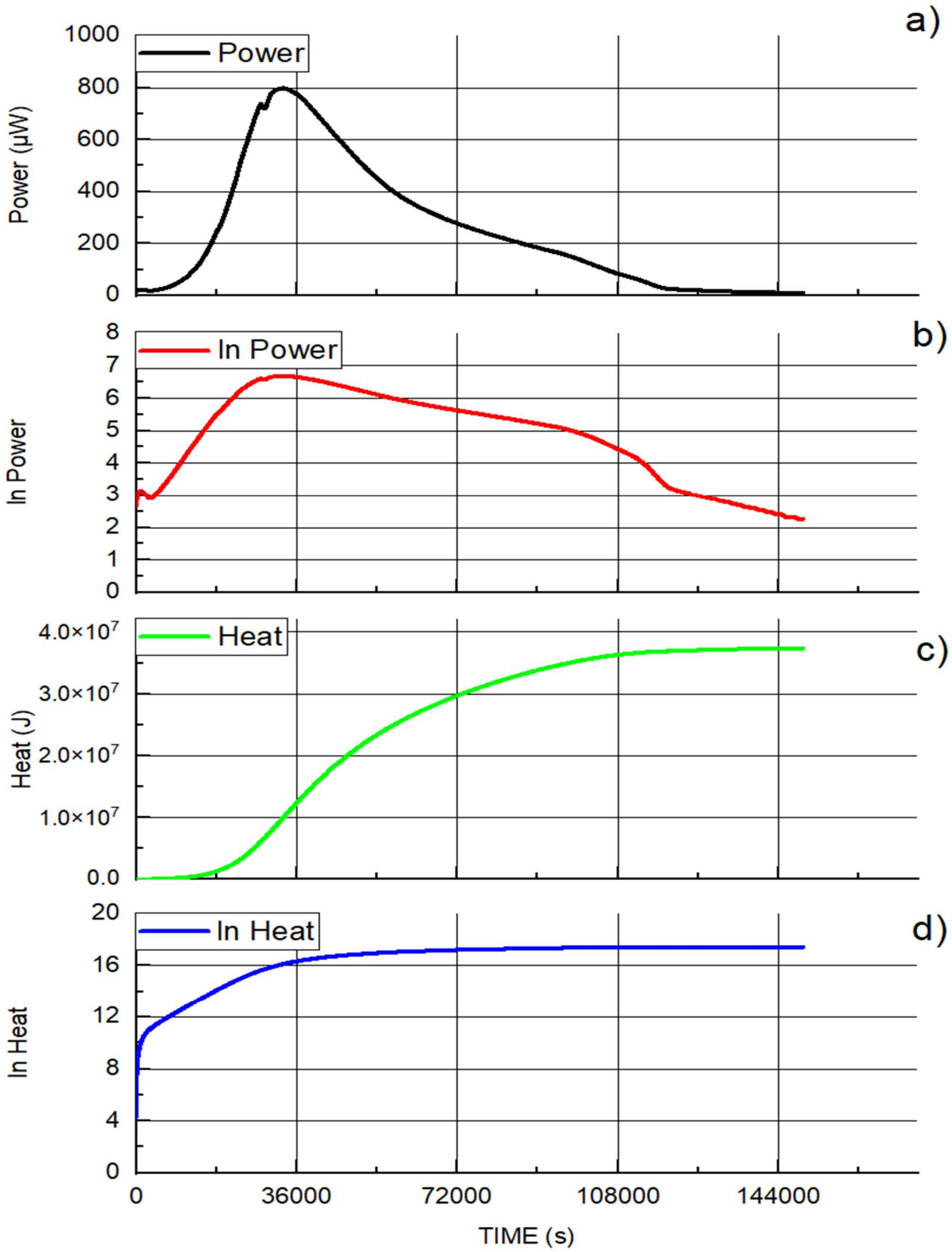

Figure 4.8 Mathematical transformation of p-t curve. Raw data a) (black curve), logarithmic transformation of the raw data b) (red curve), integration of the raw data reveals total heat produced c) (green curve) and logarithmic transformation of total heat curve d) (blue curve).

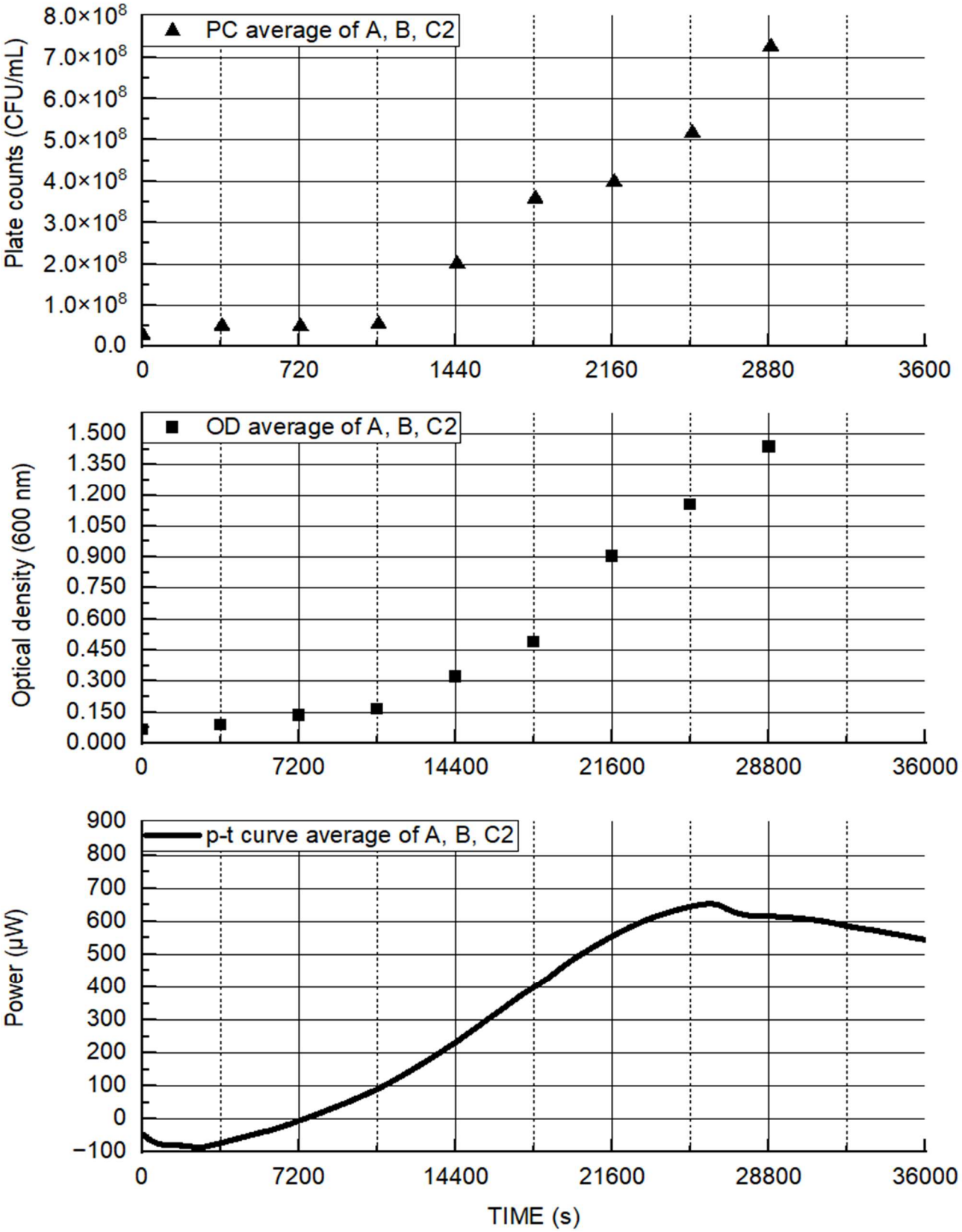

Figure 4.9 *L. rhamnosus* pure tested in MRS, plate counts (PC) (top), corresponding optical density readings (OD) in hourly intervals (middle), and p-t curve of the same culture (bottom). Each experiment performed in triplicate *i.e.*, A, B, C2. (Data from **4.3.1.1.1**.)

Since, for the purpose of this case study, the whole event from inoculation through peak power and back to the baseline at the end of the experiment was calorimetrically recorded, it was intriguing to analyse the entire curve of those components, which conform to first order processes. Bringing this down to the case study, the *L. rhamnosus* plot and its manual logarithmic transformation using OriginPro software showed that there were several linear periods observable, see **Figure 4.10**. Yet, only the first was the one that the equations explicitly applied to; all the other linear periods were first order processes which would have negative rate constants in the decline phase of power, therefore not related to growth. Now, it is worth noting that the curve was showing that something was declining, be it a substrate, an enzyme in the decline phase, but it was not cell growth. Further details presented in **4.3.1.3**. On the one hand, was it clear that this was important for other kinetic processes in theoretical microbiology, because it gave insights into the process and progress of metabolism, but not growth, in real time. On the other hand, it provided information about periods where, for example, substrate may be in decline, marking the precise moment at which one should look for the identification of a limiting factor such as substrate, if one was interested in metabolism. This would be done by chemical analysis and the exact time at which this analysis should commence was possible to determine from the p-t curve.

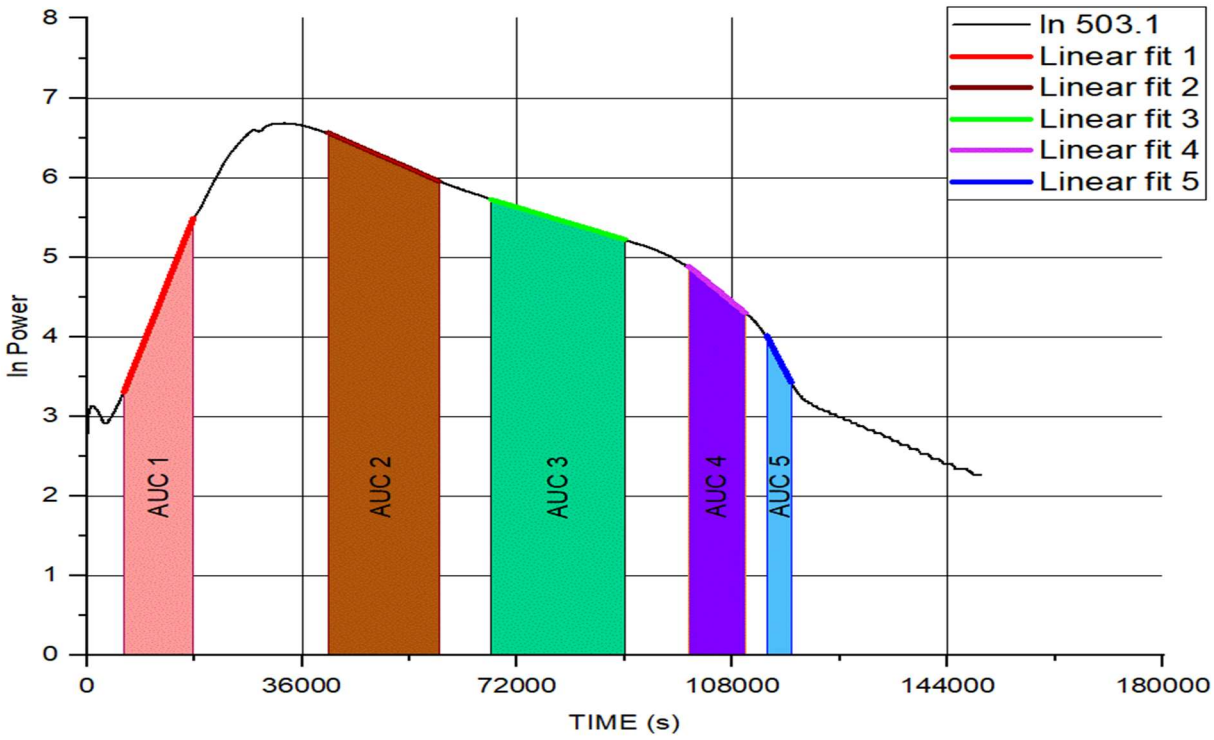

Figure 4.10 Manual fitting of visually observable linear portions (503.1). Red line above AUC 1 represents the exponential growth period, pink area represents AUC 1 during the studied period (6200 - 17800 seconds in this case).

The parameters that could be derived and reproduced in **Eq. 3.12**. were growth rate, start of the exponential growth (intercept) and AUC. It was therefore possible to get the rate constant *k* and therefore derive the generation time, and the intercept value. The question remained whether these parameters could be used to establish the quality of the product. If that was possible, it would be a signal achievement for reducing the timescale from 15 days to less than 15 hours.. To answer that question, one organism *L. rhamnosus* was taken while controlling everything that was within my capacity, inoculum purity and the medium. That was considered as the best possible outcome for establishing whether the approach proposed, analysing the first linear portion of the curve, had a degree of reproducibility that was acceptable for my purposes..

Therefore, if this was to be considered as an industrially appropriate procedure, then it was necessary to establish that the method proposed was a proper and reliable way to go forward before getting to the coding or automating stage. There was no other way than doing this manually on a limited set of data. For this purpose, the 503 series was analysed in detail. It was important to ask whether the procedure would be simple enough for a good technician to perform, as opposed to a highly qualified scientist. It was also important that the resulting data could be analysed without the need of a specialist and could be put into coding. One of the ambitions of this project was to demonstrate reproducibility, simplicity for experimentation and acceptability of outputs.

4.3.1 *L. rhamnosus* pure tested in MRS

L. rhamnosus pure (Supplier 2) and MRS (Sigma-Aldrich, UK) were chosen, in order to explore what the best possible and practical outcome (best case scenario) for reference establishment could be. These experiments also formed the basis for the study published by Cabadaj *et al*. (2021) and followed the protocol listed earlier (**4.2.1**).

The most important point in this part was to determine the reproducibility, firstly by visual p-t curve shape analysis and its simple, manually derivable parameters (**4.3.1.2**), and secondly proceed with derivation of the logarithmically transformed p-t curve (*e.g.*, rate constant and others in **4.3.1.3**) of this best case scenario. It was conceivable however, there could be greater uncertainty when FV1-real was tested later on, because of the background, against which the real production took place (such as variable wort and less control over exact volumes).

The work presented here started with the most basic experiment of one pure organism in one controlled medium. The subsequent data analysis proceeded from the most basic visual shape analysis, through deriving its parameters to more elaborate p-t curve analysis in **4.3.1.3**.

4.3.1.1 Establishing reference standards

Six independent experiments performed on *L. rhamnosus* presented in **Figure 4.11** appeared visually in a very good alignment hence it suggested a high degree of repeatability. Considering that no previous experiments or data had been created for the purpose of reference development, it was encouraging that references in a complex standard medium such as MRS appeared to be possible. In addition to that, the fact that this was the simplest case for testing Symprove, paved the way for introducing more complexity by adding the other strain and their combination (see later in sections **4.3.5, 4.3.6** and **4.3.7**). The maximum number of experiments in each series was 4 as the calorimeter used was a 4-channel instrument.

Note that in **Figure 4.11** (inset) there was a little shoulder just below 200μW, perhaps it may represent a change in metabolism, however, there was not enough discrimination (detail) available to be able to separate the two functions, it was observable but not analysable (within the project) as a separate function. Hence this part of the p-t curve was treated as one continuous row of information. (See also **Table 4.3** where parameters of these curves were analysed in detail.)

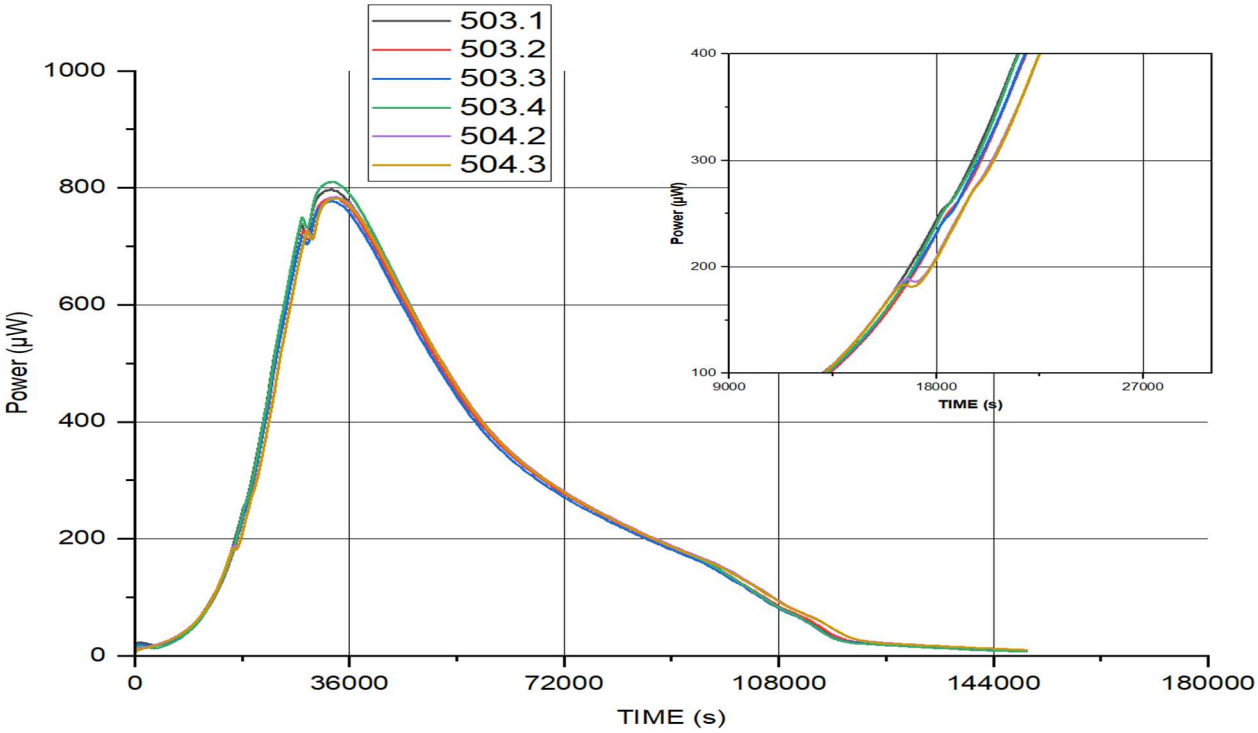

Figure 4.11 P-t curves of 503 and 504 series (30 μL of *L. rhamnosus* pure, directly inoculated into 2970 μL of sterile MRS).

4.3.1.1.1 Growth curves and OD measurements

Traditionally, microbiological plate counts (Handbook of Microbiological Criteria for Foods, 2020) and optical density (OD) methods are used to estimate cell density in a sample. Plate counts (PC) were also used by Symprove for their QA. As mentioned in **4.1,** IMC measurements were compared with classical microbiological methods, PC (growth curves derived from aforementioned PC) and OD in this section. This was done to illustrate the reliability of IMC in the absence of either PC or OD as was the case in most of IMC experiments (lack of sufficient laboratory provisions at Symprove at the start of this project).

Table 4.1 summarises OD, PC and calorimetric power readings of A, B and C2 representing triplicate testing of LrC3 in MRS which were compared with the reference experiment 503.1. OD were data not available for 503.1. Note that LrJ1 used in 503.1 experiment and LrC3 used in A, B and C2 were two different batches of the same organism –*L. rhamnosus*.

Figure 4.12 compares OD readings with power readings at hourly intervals in a semi-logarithmic plot. Note that logarithm of power (A), red dotted curve had negative values of power for 0-3 hours as a result of the sample not equilibrated enough (see **Table 4.1**), hence

the first 3 hours showed zero values in this plot. A, B and C2 represent triplicate testing of LrC3 in MRS. OD and PC are compared in **Figure 4.13**.

	LrC3 in MRS(M23)																		LrJ1 in MRS		
Time [hrs]	A						B						C2						503.1		
	OD (600nm)	ln OD (A)	Power [µW]	ln Power (A)	Plate counts (cfu/ml)	ln Plate counts (A)	OD (600nm)	ln OD (B)	Power [µW]	ln Power (B)	Plate counts (cfu/ml)	ln Plate counts (B)	OD (600nm)	ln OD (C2)	Power [µW]	ln Power (C2)	Plate counts (cfu/ml)	ln Plate counts (C2)		Power [µW]	ln Power (503.1
0	0.066	-2.72	-200	-	3.20E+07	17.28	0.067	-2.70	37	3.61	2.40E+07	16.99	0.06	-2.81	19	2.94	2.80E+07	17.15		15	2.71
1	0.084	-2.48	-316	-	7.73E+07	18.16	0.085	-2.47	46	3.83	4.00E+07	17.50	0.093	-2.38	53	3.97	3.40E+07	17.34		19	2.94
2	0.122	-2.10	-186	-	4.00E+07	17.50	0.131	-2.03	81	4.39	5.80E+07	17.88	0.149	-1.90	91	4.51	4.90E+07	17.71		32	3.47
3	0.166	-1.80	-36	-	3.20E+07	17.28	0.166	-1.80	147	4.99	5.30E+07	17.79	0.156	-1.86	161	5.08	7.70E+07	18.16		65	4.17
4	0.299	-1.21	162	5.09	1.58E+08	18.88	0.301	-1.20	254	5.54	1.48E+08	18.81	0.364	-1.01	280	5.63	2.95E+08	19.50		127	4.84
5	0.482	-0.73	366	5.90	1.59E+08	18.89	0.529	-0.64	396	5.98	4.52E+08	19.93	0.451	-0.80	435	6.08	4.65E+08	19.96		244	5.50
6	0.803	-0.22	538	6.29	2.17E+08	19.20	0.908	-0.10	536	6.28	3.36E+08	19.63	1.001	0.00	590	6.38	6.43E+08	20.28		403	6.00
7	1.099	0.09	635	6.45	5.58E+08	20.14	1.186	0.17	619	6.43	4.21E+08	19.86	1.177	0.16	678	6.52	5.71E+08	20.16		607	6.41
8	1.315	0.27	608	6.41	6.31E+08	20.26	1.467	0.38	590	6.38	8.57E+08	20.57	1.526	0.42	644	6.47	6.90E+08	20.35		721	6.58
	Time to reach PP [hrs]		Peak Power [µW]				Time to reach PP [hrs]		Peak Power [µW]				Time to reach PP [hrs]		Peak Power [µW]				Time to reach PP [hrs]	Peak Power [µW]	
	7.3		649				7.3		629				7.2		685				9.2	798	

Table 4.1 Optical density (OD) readings with corresponding plate counts (and their logarithmic values) and power readings (and their logarithmic values) at corresponding time steps. LrJ1 in MRS (last 3 columns, 503.1) for comparison.

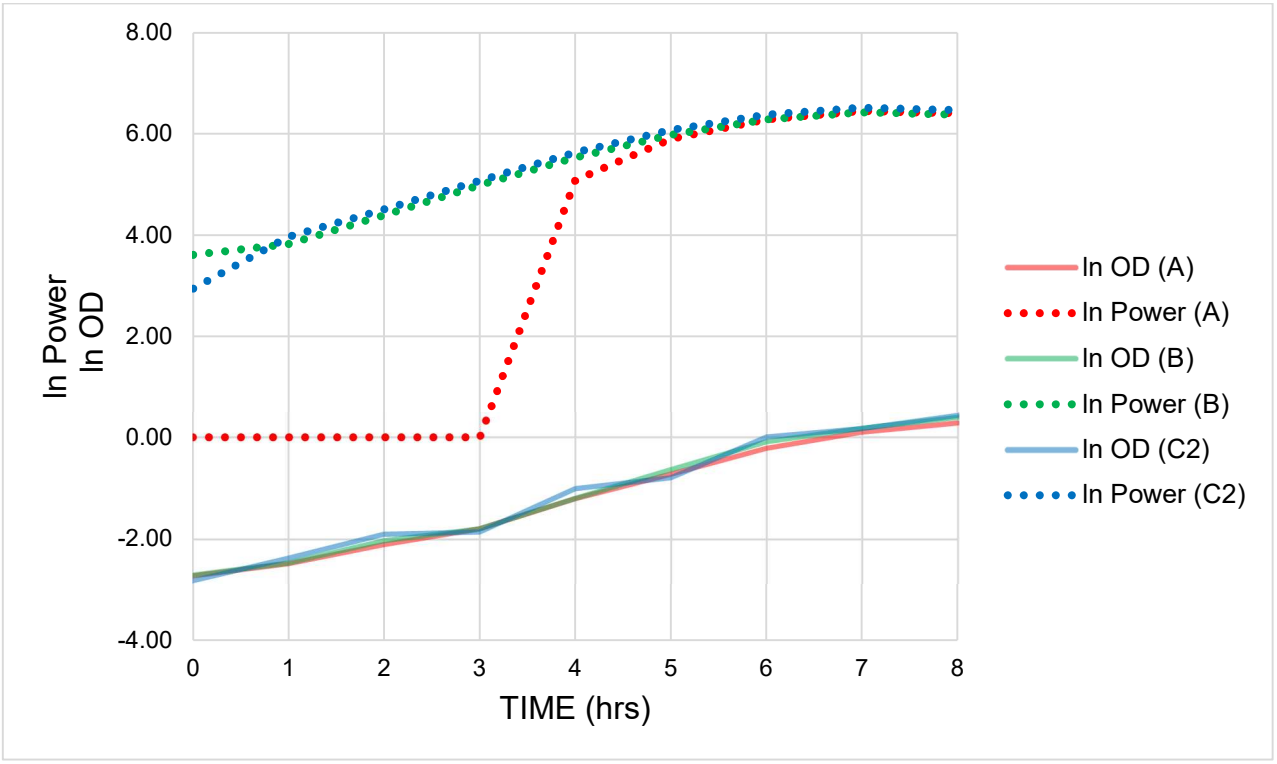

Figure 4.12 Semi-logarithmic plots of OD readings against time in comparison with semi-logarithmic plots of the corresponding power-time curves against time.

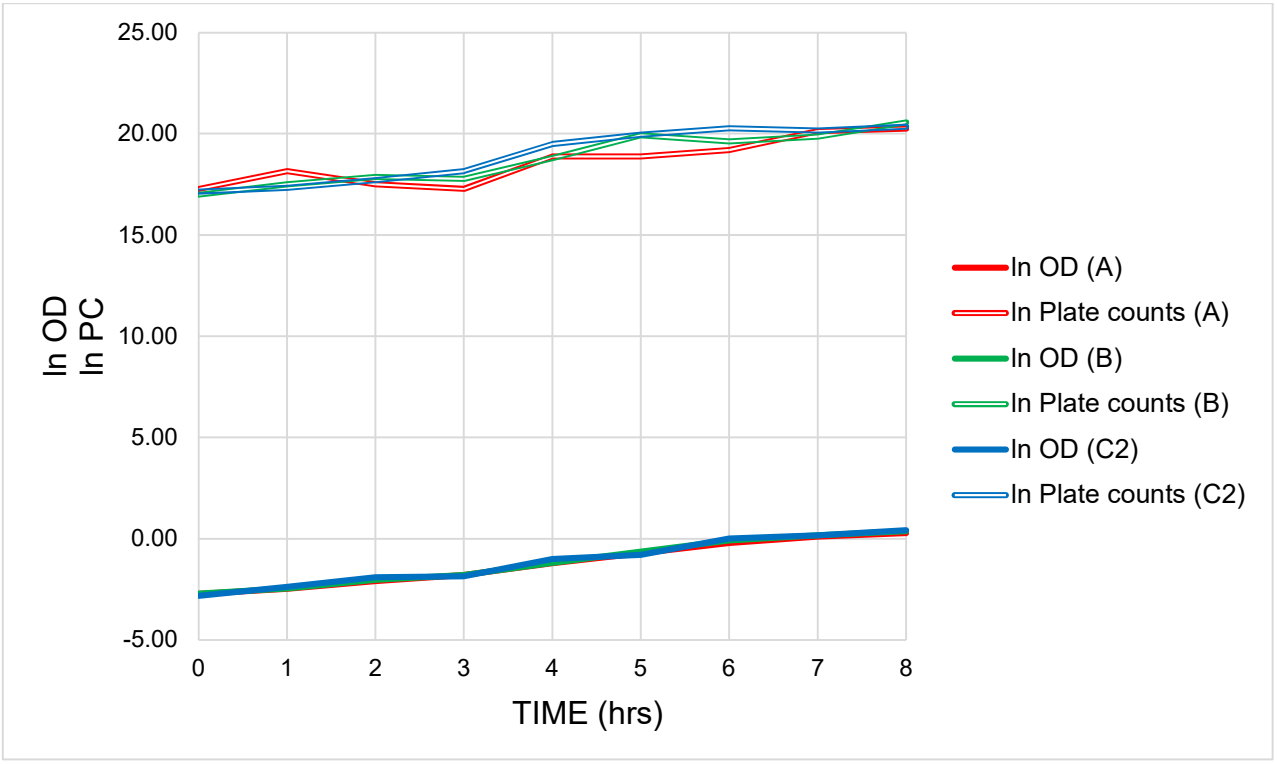

Figure 4.13 Semi-logarithmic plots of OD readings compared with the corresponding semi-logarithmic plots of plate counts (PC) against time. LrC3 in MRS in triplicate (A, B, C2).

It is obvious that the heat was generated faster by B and C2 than by 503.1 (discarding A as it had an initial endothermic reaction lasting approximately 3 hours: red dashed heat curve **Figure 4.15**, as well as red dotted power-time curve in **Figure 4.14**). The heat evolved was calculated by integration of the p-t curves and was compared with PC in **Figure 4.15**.The potential reason for the delay in heat generated by LrJ1 and LrC3 might be the age of the inoculum. LrJ1 batch was made much earlier that LrC3 batch. Yet, another difference between the 2 batches was the protocol for their manufacture and this could explain the difference in attained peak powers (see **Table 4.1**). The time difference to reach peak powers between the two batches of *L. rhamnosus* was 2 hours with the fresher batch (LrC3) reaching PP faster, however, its PP value was significantly lower compared with the older batch (LrJ1).

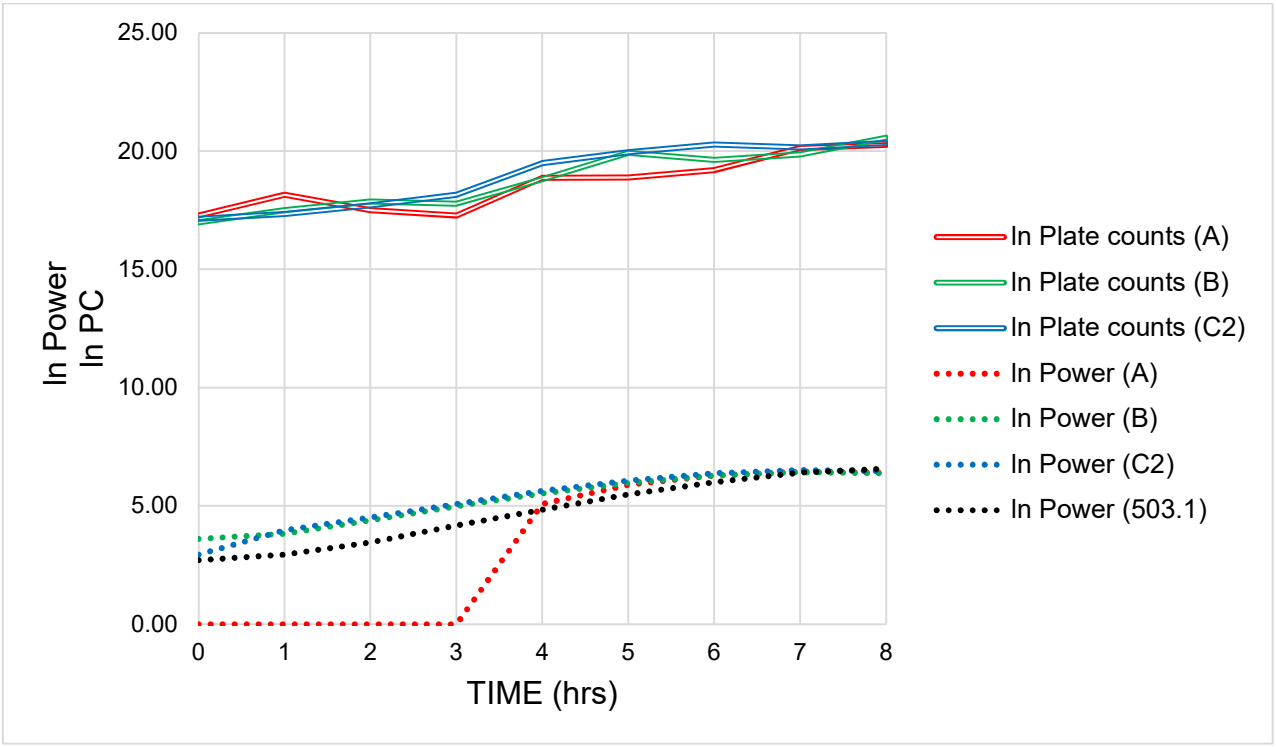

Figure 4.14 Semi-logarithmic plots of partial power-time curves (reading taken hourly to reflect time steps of the plate counts) compared with corresponding microbiological plate counts, in triplicate. (503.1 is the reference p-t curve.)

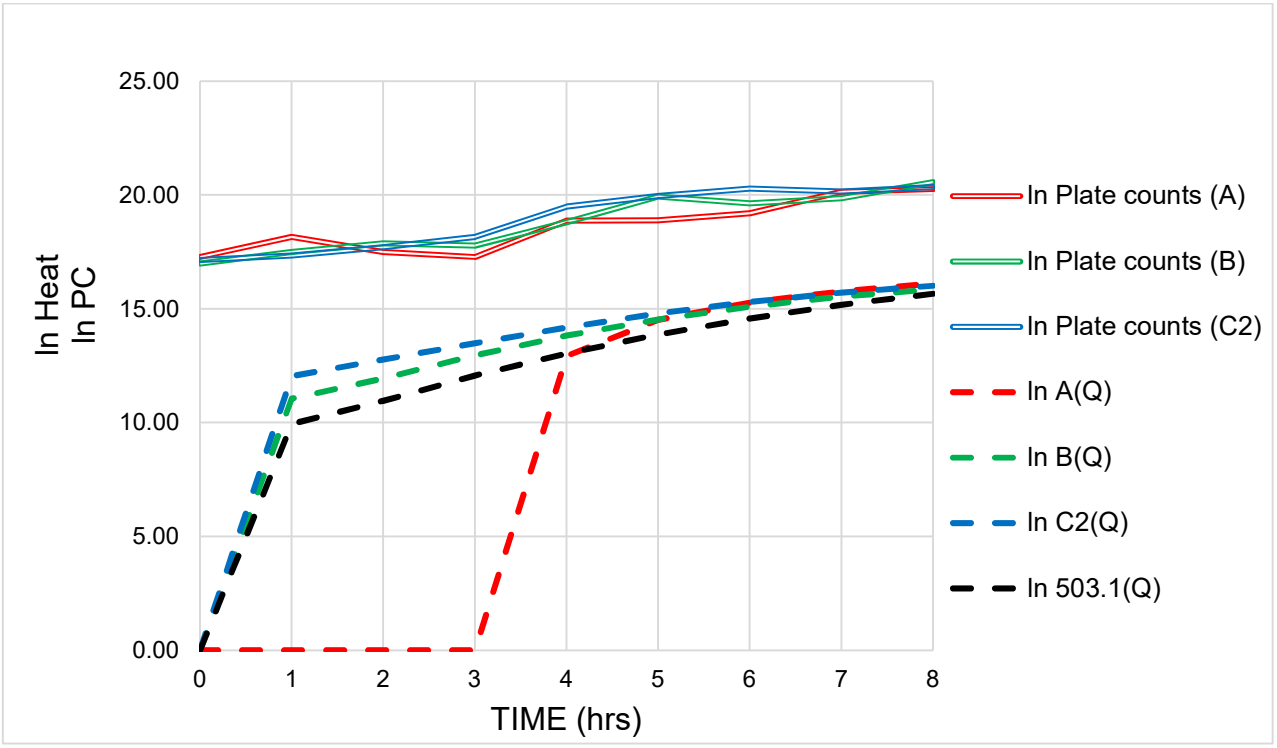

Figure 4.15 Semi-logarithmic plots of heat (Q) evolved during the IMC experiments compared with the semi-logarithmic plots of PC (in triplicate).

	Heat Q(μJ)			
time (hrs)	**A (Q)**	**B (Q)**	**C2 (Q)**	**503.1 (Q)**
0	0.00	0.00	0.00	0.00
1	-5.50 x10^5	6.36 x10^4	1.71 x10^5	2.09 x10^4
2	-7.62 x10^5	1.55 x10^5	3.54 x10^5	5.74 x10^4
3	-4.77 x10^5	4.24 x10^5	7.29 x10^5	1.74 x10^5
4	4.11 x10^5	1.01 x10^6	1.44 x10^6	4.59 x10^5
5	2.03 x10^6	2.05 x10^6	2.67 x10^6	1.06 x10^6
6	4.31 x10^6	3.62 x10^6	4.47 x10^6	2.14 x10^6
7	7.07 x10^6	5.60 x10^6	6.71 x10^6	3.92 x10^6
8	9.94 x10^6	7.69 x10^6	9.04 x10^6	6.36 x10^6
	ln A(Q)	**ln B(Q)**	**ln C2(Q)**	**ln 503.1(Q)**
0	-	-	-	-
1	-	11.06	12.05	9.95
2	-	11.95	12.78	10.96
3	-	12.96	13.50	12.07
4	12.93	13.82	14.18	13.04
5	14.52	14.54	14.80	13.87
6	15.28	15.10	15.31	14.58
7	15.77	15.54	15.72	15.18
8	16.11	15.85	16.02	15.67

Table 4.2 Data related to **Figure 4.15** (for information only).

There was a good concordance between OD and PC methods and calorimetric p-t curves in expressing the increase in: the amount of light absorbed, number of bacterial colonies and the power generated by the same culture as seen in **Figures 4.12 - 4.18**.

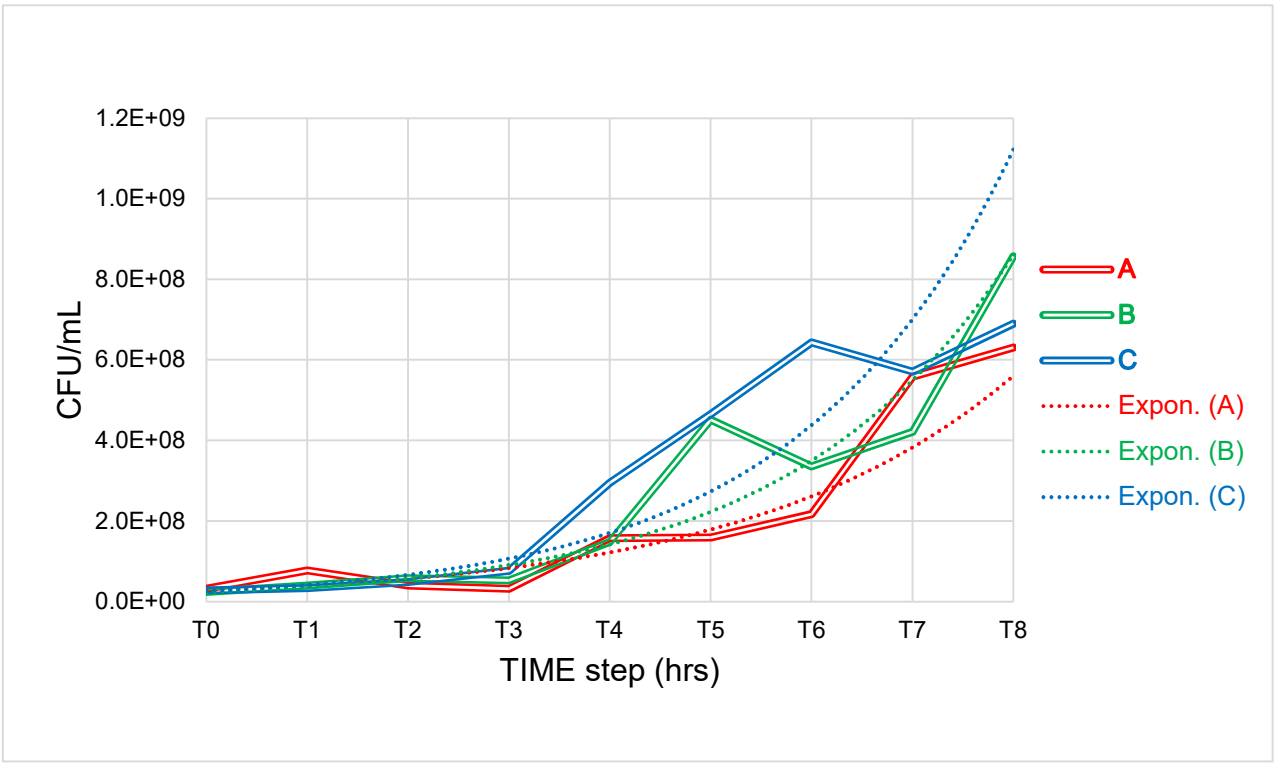

Figure 4.16 Fitting exponential trend lines into individual growth curves using Excel. *L. rhamnosus* growth curves, three independent repeats.

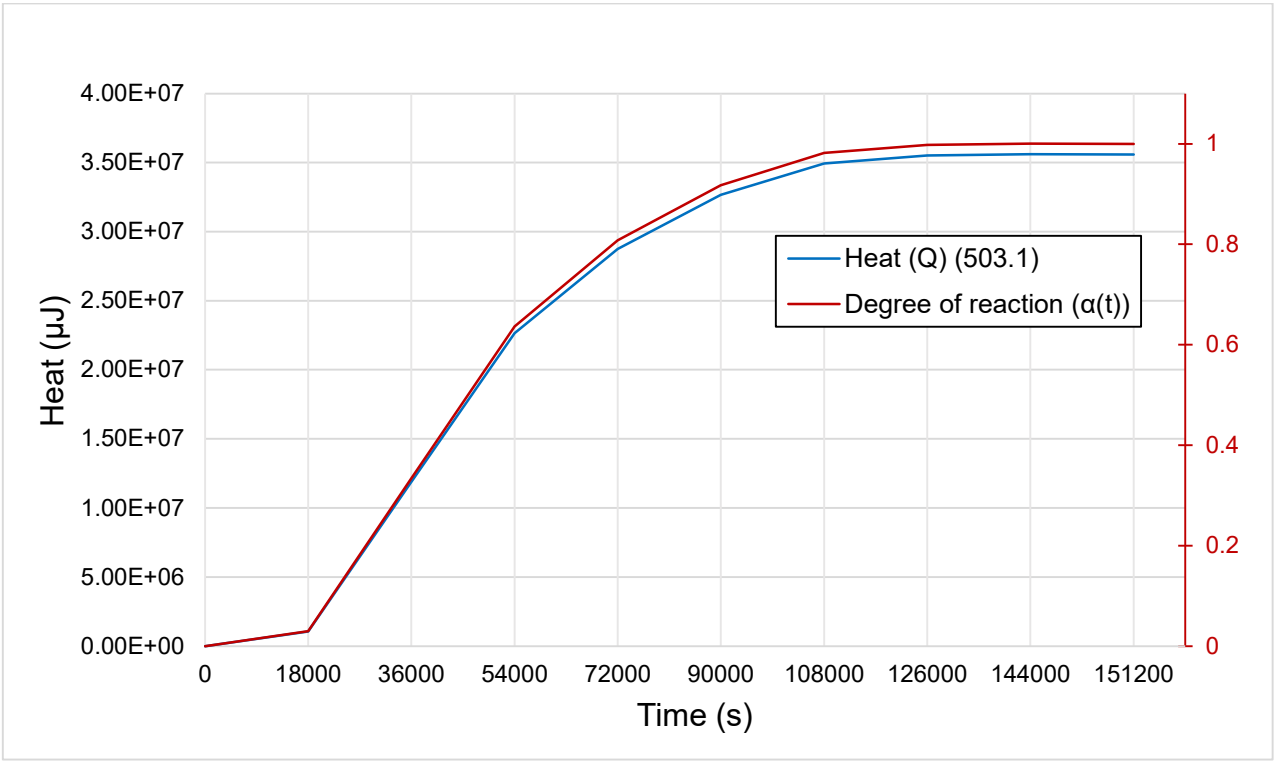

Figure 4.17 Degree of reaction completion (secondary axis) as a function of time compared with heat-time curve of the same experiment. (For information only). $\alpha = \frac{q_t}{Q}$, where q_t, is the cumulative heat at time *t* and *Q* is the total heat evolved. (*L. rhamnosus* 503.1.)

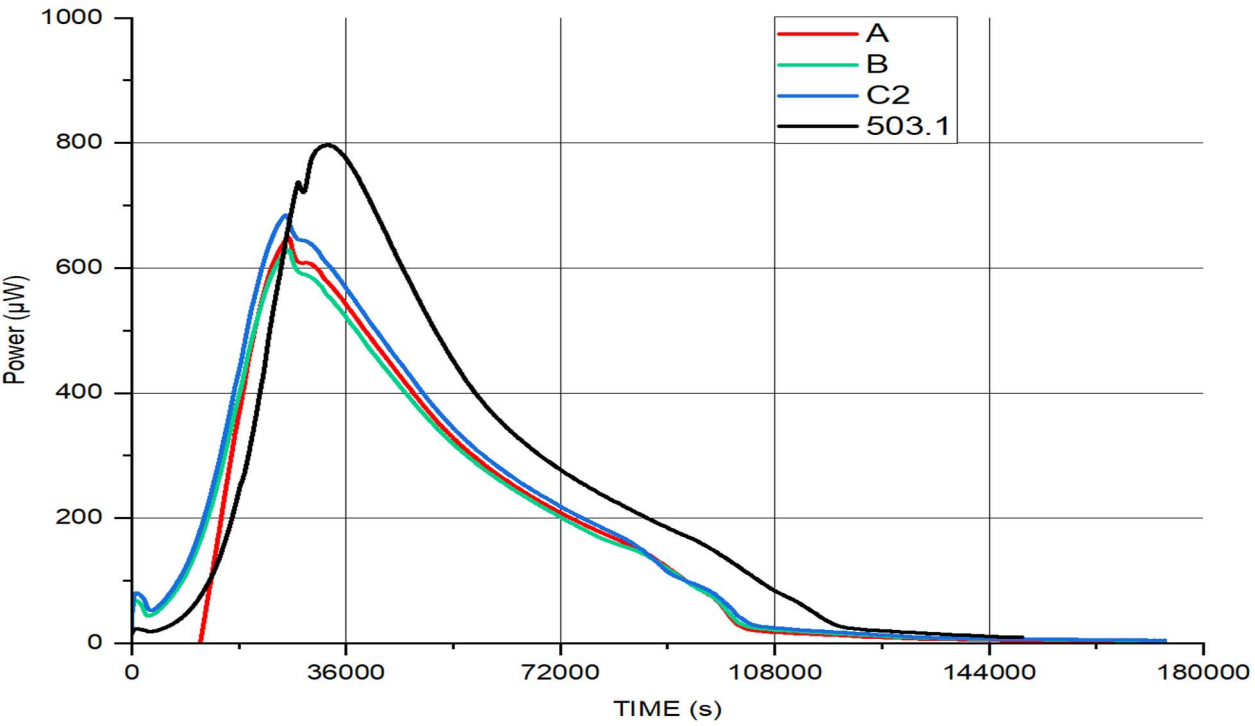

Figure 4.18 P-t curves of the cultures used for growth curves and optical density measurements described above (A, B, C2), compared with 503.1.

Having established a good visual concordance and to demonstrated this further, calculations of slope representing the growth rate of these cultures is offered below. These calculations were done for all three methods OD, PC and Q (heat obtained from the calorimetric experiments).

Slope calculation using OD (data from **Table 4.1**);

Formula: slope = $\{\ln(OD_8) - \ln(OD_0)\} / t_{\text{duration of experiment}}$

Slope A = $\{\ln(OD_8) - \ln(OD_0)\} / 28800$

= $\{0.27 - (-2.72)\} / 28800$

= $3.08 / 28800$

= $\underline{\underline{1.04 \times 10^{-4}}}$

Slope B = $\{0.38 - (-2.70)\} / 28800$

= $3.08 / 28800$

= $\underline{\underline{1.07 \times 10^{-4}}}$

Slope C2 = $\{0.42 - (-2.81)\} / 28800$

= $3.23 / 28800$

= $\underline{\underline{1.12 \times 10^{-4}}}$

Slope calculation using PC (data from **Table 4.1**);

Formula: slope = $\{\ln(PC_8) - \ln(PC_0)\} / t_{\text{duration of experiment}}$

Slope A = $\{(\ln PC_8\} - \ln(PC_0)\} / 28800$

= $(20.26 - 17.28) / 28800$

= $2.98 / 28800$

= $\underline{\underline{1.03 \times 10^{-4}}}$

Slope B = $(20.57 - 16.99) / 28800$

= $3.58 / 28800$

= $\underline{\underline{1.24 \times 10^{-4}}}$

Slope C2 = (20.35 – 17.15) / 28800

= (3.20) / 28800

= 1.11×10^{-4}

Slope calculation using heat (Q) (data from **Table 4.2**);

Formula: slope = $\{\ln(Q_8) - \ln(Q_1)\} / t_{\text{duration of experiment}}$

Q_1 was taken as the first point for simplicity instead of Q_0 (at time = 0) which would yield an error input. Alternatively, the first reading at 5 seconds recorded by TAM could be taken as time zero. In that case logarithmic values for B, C2 and 503.1 were 0.68, 1.92, and -2.16, respectively.

Slope A = $\{\ln(Q_8) - \ln(Q_4)\} / t$; Q4 taken as the previous time steps were negative.

= (16.11 – 12.93) / 28800

= 3.18 / 28800

= 1.10×10^{-4}

Slope B = (15.85 – 11.06) / 28800

= 4.79 / 28800

= 1.66×10^{-4}

Slope C2 = (16.02 – 12.05) / 28800

= 3.97 / 28800

= 1.38×10^{-4}

Slope 503.1 = (15.67 – 9.95) / 28800

= 5.72 / 28800

= 1.99×10^{-4}

The growth rate is the main quantitative parameter. All three methods of calculating the growth rate just presented offered a simple way to obtain it. Even though these calculations were done on a very limited number of experiments, there was a good agreement between all three methods.

4.3.1.2 Basic shape analysis parameters

Although the visual analysis of the curves (**Figure 4.11**) was encouraging, further assessment was required to meet the objectivity and automating prospects that this project set out to achieve. The first step was to determine, manually, using OriginPro software (OriginPro 2020b, OriginLab Corp.), parameters of shape analysis, as was demonstrated in **Chapter 2 (**section **2.3, Table 2.1 and Table 2.2)**. Parameters such as peak power (PP), time from the beginning of the experiment to reach PP, and area under curve (AUC) are presented below in **Table 4.3**. AUC to PP is reflective of cell numbers. This was a better indicator of reproducibility when considering exponential growth as described by the equations in **Chapter 3**. It was still expected that there would be some other processes, alongside exponential growth, because there were observable periods, from the start of the signal recording to PP, where the p-t curve was not strictly exponential. Additionally, AUC of the whole p-t curve is reflective of the energy associated with exponential growth and subsequent non-growth metabolism. The whole p-t curve does not represent growth only. It represents growth + metabolism + other processes.

Experiment number	**503.1**	**503.2**	**503.3**	**503.4**	**504.2**	**504.3**
p-t curve parameters						
PP [μW]	798	784	777	811	785	782
Mean	790					
SD (reproducibility)	12 (1.52%)					
Time to PP [s]	32940	33010	33020	33030	33830	33440
Mean [s]	33208					
SD (reproducibility) [s]	317 (0.95%)					
AUC to PP	9.97×10^6	9.67×10^6	9.68×10^6	9.99×10^6	1.00×10^7	9.66×10^6
Mean	9.83×10^6					
SD (reproducibility)	1.61×10^5 (1.64%)					
AUC (whole p-t curve)	3.74×10^7	3.70×10^7	3.65×10^7	3.77×10^7	3.75×10^7	3.73×10^7
Mean	3.72×10^7					
SD (reproducibility)	4.03×10^5 (1.08%)					

Table 4.3 Basic shape analysis parameters for 503 and 504 series.

Table 4.3 demonstrated the reproducibility of the experiments. The total AUC (providing the organism and the medium are controlled) was highly reproducible (the range of reproducibility is 97.92 – 101.20% from total mean AUC), which was reflective of growth and metabolism, post growth. The AUC up to the peak was reflective of the growth and that again was highly reproducible (the range of reproducibility is 98.28 - 101.84 % determined from the mean AUC to PP). Both AUC for the whole p-t curve as well as the AUC to PP showed very good reproducibility, much better than the microbiological plating methods used by Symprove and it was well within 3% which was previously demonstrated by Beezer (1977).

However, the precise values of the parameters were subjective as these were determined by the operator. In order to eliminate subjective judgements of the operator, it was necessary to try to get as much quantitative data as possible from the p-t curve using an automated procedure. The above-mentioned parameters (PP, time to PP, AUC) were indeed operator independent, however their extraction did require an operator decision since the data processing was not automated. Furthermore, it was desirable, given that there was a lot of information contained in the p-t curve (Beezer, 1980; James, 1987), that additional effort was made to extract other parameters (*e.g.*, rate constant) which would enable quantitative interpretation of microbial kinetics involved in these experiments. Stimulated by the good reproducibility of the p-t curves, I decided to proceed further to try to extract quantitative parameters of these curves. This is presented in the next **section 4.3.1.3.**

4.3.1.3 Logarithmic transformation of the p-t curve

Considering that there are many processes occurring simultaneously during microbial growth (Hu, 2018.) IMC experiments shown here yielded rather simple p-t curves. These curves could be analysed further to attempt extraction of characteristic quantitative growth parameters which would offer some information about growth rates, generation doubling time, growth substrate limits and shifts in metabolism. This is explored in the next section.

It was postulated that other first order processes observed via logarithmic transformation reflected metabolic processes which were substrate limited or metabolic waste related. These were not the subject of this thesis which was not strictly concerned with the detail of the metabolism of the microorganisms. However, the analysis of these kinds of data may

contribute to production management decision strategies in an industrial setting as well as offering the possibility to explore, in real time mechanisms of metabolic activities.

As noted earlier in **Chapter 3, section 3.2.2**, at the most basic level, the p-t curve revealed the cumulative heat by integration which was also indicative of the total number of cells produced during an experiment. It was only the heat up to the peak power, represented by AUC to peak power, which should reflect the cell numbers. The area under the whole p-t curve did not reflect only the cell numbers because at the peak the exponential growth ceased. Further metabolism and processes not related to exponential growth continued past peak power, assuming the same starting inoculum numbers and $\Delta_N H$ (heat/cell) values. Additionally, when the p-t curves presented in **Figure 4.11** were transformed logarithmically, see **Figure 4.19** (visually a very good alignment of all 4 runs in the studied exponential period)., this linearised portions of the p-t curves, (first order processes), and enabled direct extraction of quantitative parameters from these linear portions. Such parameters were the growth rate constant (the slope of the first exponential portion of the curve had a positive rate constant, all others had negative rate constants, see **Table 4.4**) and the time of the beginning of the logarithmic phase (the intercept). These parameters are of great industrial as well as theoretical interest because they can be used to optimise for example the fermentation process itself.

The whole duration of the experiments was logarithmically transformed to explore all first order processes. This transformation revealed all first order processes (**Figure 4.10**). Exponential growth, being a first order process, was expected (from the manual analysis done earlier) to appear between 0 and 36000 seconds. The ambition, however, was that when it came to managing Symprove production samples, the analysis should end up with just looking up to PP, and if possible, less than that. Anything in this example after about 36000 seconds was not exponential growth as PP was reached by that time.

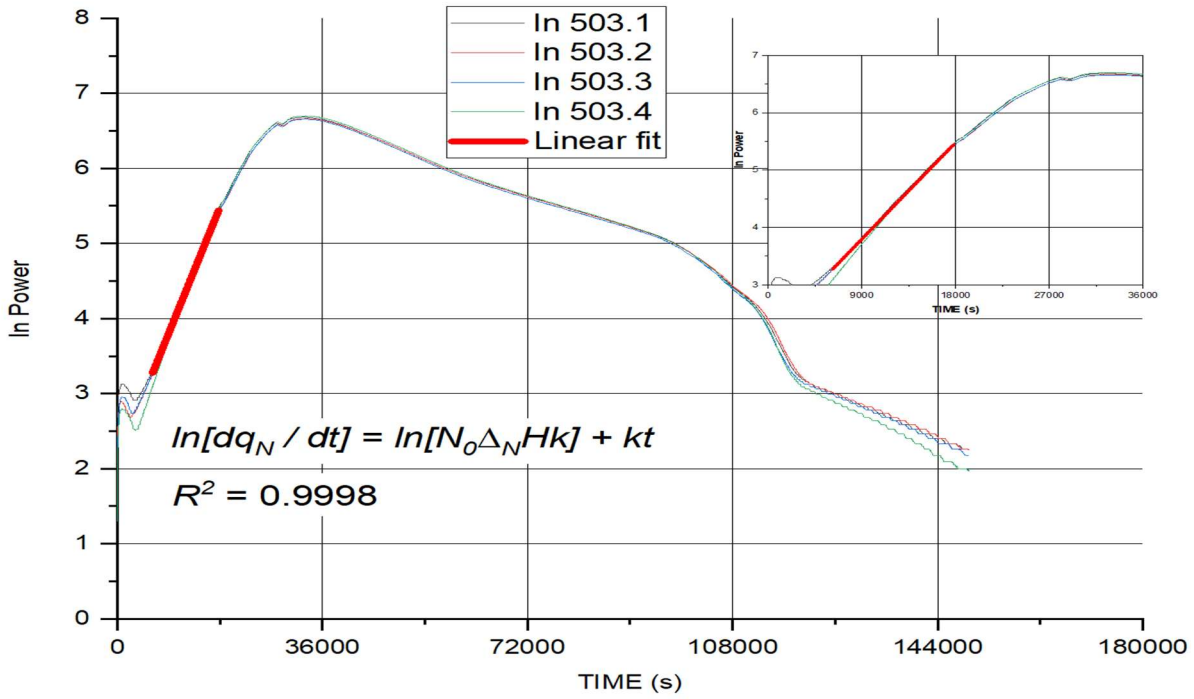

Figure 4.19 Logarithmic transformation of 503 series. Detail of the linear fits in the inset.

By observation of **Figure 4.10** five linear periods were identified. The first linear period was wholly expected –exponential growth phase. There was no exponential growth, in principle, after PP was reached. The equations from **Chapter 3** strictly apply only to this first linear period. However, because a logarithmic plot allowed observation of first order processes, the other 4 linear periods might be related to first order processes which would not be related to exponential cell growth. Rather these four arose in periods when there were other processes involved in shaping the p-t curve and are highlighted in brown, green, purple and blue (area 2, 3, 4 and 5 respectively). These periods which were identified visually were acceptably reproducible (see **Figure 4.19**, a good alignment between these 4 curves suggested that the same linear portions would be identified visually in all 4 curves) and were contributions to fundamental interpretation of calorimetric data, descriptive of detailed organismal metabolic activity (such as metabolite build up, nutrient exhaustion, switching from fermentation to respiration or changing a metabolic pathway).

There was lots of information in the p-t curves, which were closely reproducible. The p-t curves were indicative of the organism's behaviour with respect to some components in the medium, limiting factor or critical parameter, and thereby presented a unique opportunity to

gain insight into the process and progress of metabolism. It was not known yet whether deriving parameters just from the exponential phase of the curves would be sufficient to make a judgement about a good growth (successful fermentation) or whether it would be necessary to go further and identify not only the initial first order growth rate but also, the other four rate constants in order to get a matrix of results to make a decision to go ahead and bottle the product. All the information within the p-t curve could contribute to confirming reproducibility and defining outcomes for Symprove, who were not concerned with detailed metabolic information at this stage, rather yes/no information (*i.e.*, bottle or not). However, the project ambition to reduce time as much as possible aimed to concentrate, in the first stage of the detailed analysis, on the exponential phase only (up to PP, approximately the first 10 hours of growth, or less if possible).

Analysis of the individual linear portions is presented in **Table 4.4**. The first linear fit is the exponential growth region. AUCs were determined for the exact area from the beginning to the end of the individual linear fits and calculated from logarithmically transformed p-t curve. All these could be used for studying the organism's fundamental metabolism, behaviour and its relationship with its environment from a production perspective as well as basic microbiological perspective. This opened up the possibility to identify with precision, the exact point when one should analyse chemically a substrate diminution, medium modification or critical environmental conditions related to the organism's metabolism.

The possibilities of enhancing further growth through for example, addition of extra substrate or buffer modification of the current product (see **Chapter 1.4**) could be explored. This could also mean controlling the acidity through slowing the rate of acidification and could be done using data contained in a simple p-t curve. This would also mean that the final products could be tailored for example to provide higher concentrations of particular metabolites which were beneficial (*e.g.*, lactate which was shown to boost the fermentation process, resulting in a cascade of cross-feeding reactions, thus reducing pro-inflammatory protein (*e.g.*, cytokines) levels (Marzorati *et al*., 2020)) to the host, hence the need to understand the gut environment in general as noted in **1.2.1**.

Experiment number	Linear portion number				
503.1	1	2	3	4	5
In curve parameters	Manual Analysis (OriginPro derived)				
Slope	1.89×10^{-4}	-3.28×10^{-5}	-2.25×10^{-5}	-6.19×10^{-5}	-1.43×10^{-4}
Intercept	2.13	7.89	7.25	11.11	20.25
AUC	50996	115777	122127	43482	15259
R^2	0.9998	0.9997	0.9998	0.9987	0.9985
Data range [s]	11600	18501	22310	9471	4100

Table 4.4 Quantitative growth parameters of 503.1 with other non-growth parameters of the second, third, fourth and fifth observed linear portions determined manually using OriginPro. Linear portions from **Figure 4.10**.

4.3.1.3.1 Growth rate constant

The slope *k* (as described in **3.3.1,** derivable from the central equation 12), of the first linear portion (**Figure 4.10**) is the growth rate constant. It was constant over a long period *i.e.*, 11600 seconds (**Table 4.4**). This meant that the cell division remained constant for the same length of time. It demonstrated that the growth rate constant *k* was obtainable, therefore the generation time could be determined (see later in **4.3.1.3.4**). All the other four rate constants calculated from second, third, fourth, and fifth linear portions (**Table 4.4**) represent first order processes which occurred in the decline phase of power, therefore had negative rate constants hence not related to cell growth and not discussed here.

The question whether this parameter *k* as well as parameters described later (intercept, generation time, AUC) could be used to establish the quality of the product remained to be answered. If it was possible, it would be a remarkable achievement to reduce testing time from 1 - 2 weeks down to 10 - 15 hours.

Experiment number	503.1	503.2	503.3	503.4	504.2	504.3
In curve parameters						
k	1.89×10^{-4}	1.87×10^{-4}	1.87×10^{-4}	1.87×10^{-4}	1.84×10^{-4}	1.87×10^{-4}
Mean	1.87×10^{-4}					
SD (reproducibility)	1.46×10^{-6} (0.78%)					
Intercept (ln value)	2.13	2.11	2.12	2.12	2.20	2.15
Mean intercept	2.14					
SD (reproducibility)	0.030 (1.40%)					

Intercept (antiln value)	8.41	8.25	8.33	8.33	9.03	8.58
Mean intercept	8.49					
SD (reproducibility)	0.26 (3.06%)					
AUC to PP	1.65×10^5	1.63×10^5	1.64×10^5	1.63×10^5	1.69×10^5	1.65×10^5
Mean	1.65×10^5					
SD (reproducibility)	1.90×10^3 (1.15%)					
R^2	0.9998	0.9999	0.9998	0.9993	0.9995	0.9996
Mean R^2	0.9997					
SD (reproducibility)	0.00021 (0.02%)					

Table 4.5 Manually determined parameters for the first linear portion of 503 and 504 series. *L. rhamnosus* pure tested in MRS.

The data reported in **Table 4.5** show excellent reproducibility for all parameters, including the growth rate constant. These parameters were derived from the application of the equations *i.e.*, analysis of the logarithmically transformed p-t curves. Additionally, antilogarithm values of the intercept were presented as these gave the actual value of $k\Delta_N HN_0$.This gave confidence, in the case where there was no contamination, a pure organism and a controlled medium, so that a highly reproducible account of this microbiological system was observed. This was an encouraging outcome as it was then plausible to apply IMC to develop an assay for Symprove which identified a good growth in real production conditions.

Whether the same success could be achieved for the other organism present in FV1 (*L. acidophilus*) and indeed for both organisms (*L. rhamnosus* and *L. acidophilus*) together formulating FV1-artificial was explored later in part **4.3.5** and **4.3.6.** Artificial in this context meant that the FV1 was made up of equal parts of pure *L. rhamnosus* and pure *L. acidophilus* inoculated into MRS (more detail in **4.3.6**).

The experiments 503 and 504 series (see **Figure 4.11**) were very carefully controlled. Such experiments would be less controlled in real world conditions of an industrial production. The reproducibility achieved for *k* was 0.78%, as calculated in **Table 4.5**. The reproducibility in a real sample could be potentially somewhat different as the real conditions of an industrial scale production could not be as tightly controlled as in a laboratory setup. However, this was explored and is discussed later in **4.3.7**.

Further analysis and discussion of *k* is explored later (see **4.3.5, 4.3.6, 4.3.7**) as it offered an opportunity to examine the medium (when the organism was controlled), relationships between two or more organisms (did they produce additive rate constants for example or was there antagonism between them). All these possibilities and perhaps many more were a result of the utility of highly reproducible growth rate constant. The other component (intercept) of the central equation is discussed separately next.

Consistent IMC results (slope values in **Table 4.5**) were essentially the same as slope values (all slope values were between 1 $x10^{-4}$ and 2 $x10^{-4}$) calculated from OD and PC see **4.3.1.1.1**. (Sadly, PC and OD were not easily done at Symprove, therefore PC and OD was a very limited study). IMC is a convenient, real time, continuous, much easier method to perform, with all its advantages over traditional microbiological culture methods. It was just established here that IMC worked splendidly with high repeatability (hence much lower variability in results obtained compared with traditional microbiological methods). This also confirmed that IMC was good for the purpose of this project as outlined earlier. Additionally, not having PC or OD measurements presented no concern (*e.g.*, Symprove not doing PC or OD) as IMC did not need that. The IMC method was adequately set up to keep going.

4.3.1.3.2 Intercept

Detailed description of the intercept (as $\ln k\Delta_N HN_0$) obtained from the central **Eq. 3.12** was given in **Chapter 3**. This intercept (y-axis intercept, obtained from **Eq. 3.12**) appeared to be rather challenging to interpret in terms of what (if any) real biological meaning could be assigned to it. Given that **Eq. 3.12** was entirely couched on the exponential growth phase of a microbiological system (*L. rhamnosus* pure tested in MRS; however, in later sections the analysis will be extended to *L. acidophilus*, FV1-artificial and eventually FV1-real), it was not expected that either x-axis intercept or indeed y-axis intercept would be described in real terms (their biological meanings). Their mathematical values, which were easily extractable, however could be used (as previously mentioned in **Chapter 3**) as additional parameters (without any assigned meaning) to confirm a good growth occurred (see **Table 4.6**).

Another use of the intercept was in estimating the duration of the lag phase. This could be done by using the integrated p-t curve as demonstrated by Braissant *et al*., (2015a). However, somewhat different approach was taken here. Assuming that the medium was consistent, the inoculum density was the same, and the physiological state of the organism

inoculated into the medium was the same, and the same experimental procedure was followed, it was a reasonable expectation that the same rate constant and the same intercept value would be obtained. Therefore, the same lag time should be obtained as a result. One more point needed consideration *i.e.*, the inoculum density (1 x10^6 CFU/mL) should generate sufficient heat to be detectable by the TAM (considering 30µL was inoculated into 2970µL of medium) (Cabadaj *et al*., 2021). In other words, as soon as the lag phase together with the acceleration phase were finished, the exponential growth should be detected. Therefore, the duration of the lag phase could be calculated from the moment of inoculation into the medium until the exponential growth appeared. In the case of *L. rhamnosus* tested in MRS (and in fact in all the other experiments reported in this thesis, unless stated otherwise) it was calculated that: ampoule preparation took on average 5 minutes; equilibrating time was 30 minutes; lowering the ampoules into the measuring position and initiating data capture was 3 minutes, resulting in 38 minutes (2280 seconds) of inoculum being in the medium for which the data were not being captured. From the first linear fit, the beginning of the exponential phase t_0 was detected at 6200 seconds from the beginning of the data capture. This added up to 8480 seconds in which the actual duration of the lag phase was contained. This was important because if the same inoculum was used in the same growth medium the same lag phase should be observed. Enumeration of the intercept yielded values that could contribute to a set of calculated growth parameters, for example, intercept / k ratio as shown in **Table 4.6**. These could be added to a final parameter comparison matrix to aid precision in determining a good growth assuming $\Delta_N H$ was constant.

Experiment number	**503.1**	**503.2**	**503.3**	**503.4**	**504.2**	**504.3**
Intercept/k	1.13 x10^4	1.13 x10^4	1.13 x10^4	1.13 x10^4	1.20 x10^4	1.15 x10^4
Mean	1.15 x10^4					
SD (reproducibility)	2.57 x10^2 (2.24%)					

Table 4.6 Intercept */ k ratio* (data from **Table 4.5**).

There were two perspectives taken here to look at the values of the intercept. One was that from Symprove perspective, what mattered was that the same intercept value (and the same rate constant) for doing the same experiment was obtained, meaning the same process of fermentation took place (no contamination, no different metabolism, approximately the same

number of cells present at the end of the exponential phase). The other one was perhaps to try to interpret what the real meaning of the intercept might be, and if it could be used for cell number determination for example (see the next section **4.3.1.3.3**), which would involve the notion what N_0 was; some of this was explored in later sections about different inoculum densities – inoculum volume experiments (**4.3.1.3.4**). The intercept values reported in the above table were within 3 % of their mean value, showing again an excellent repeatability of the experiments.

It was encouraging that the values of the intercept were of high reproducibility for a consistent experiment. As manual analysis was operator dependent and could be highly subjective (see later in **Figure 4.25**), it was considered worthwhile to develop coding to analyse the data of the experiments. This approach took out all subjectivity as well as the need for a trained expert oversight. To make sure the coding and automation of data processing ass in line with the manual analysis, a comparison between the two was done (see later in **4.3.4** or for detailed description in Cabadaj *et al*., (2021)). The majority of results were from manual analysis; however, it was demonstrated that these were very close to the outcomes of coding.

The consistency in the intercept values (see **Table 4.6**) gave confidence (in addition to consistent slope values) that IMC could be useful in determining a good growth in a carefully controlled experiment. Whether this was also true in the real production process conditions (statistically reliable values of the intercept and slope were what was needed) was explored in **4.3.7**.

4.3.1.3.3 Cell numbers

As previously suggested the other part of the central equation, the intercept could be in theory utilised for counting the organisms. Some exploratory data (inoculum volume experiments, see **4.3.1.3.4**) was done on the possibility of counting the organisms. Additional work was done by my laboratory colleague Dr. Shazia Bashir (unpublished data) on the effects of simulated gastric acid exposure on the survival of *L. rhamnosus* culture.

There were limitations in cell numbers determination from the intercept, as it was problematic to interpret the significance (*e.g.*, what did this mean in the whole recorded metabolism of the organism) of t_0 from the equation of the straight line. The linear portion in

the logarithm of power vs. time plot was selected visually by me and was not based on the theoretical evaluation of when the exponential period started. For this reason, the cell numbers the intercept value reported assumed that in getting these cell numbers, the cells had the same division time from the moment of inoculation. There was however some time when there ass not visibly any significant movement from the baseline. The cells were in the lag phase learning to adapt to their environment and they enter into acceleration phase during this time. Eventually, they entered true exponential growth seen visually, assuming the enthalpy stayed constant and the division time (because the rate constant was constant over a long time and that was the division time) remained constant.

4.3.1.3.4 Inoculum volume experiments

Rationale for 30µL inoculum volume was that the initial cell density should be 10^6 per mL, in order for the calorimeter to pick up the heat from the cells (detection limit). Later it was postulated, the inoculum volume be varied to investigate whether changes in metabolism appeared with different densities or indeed the metabolism stayed unchanged with changing inoculum density. Alternation in inoculum volume (**Figure 4.20**), and consequently cell densities of the same inoculum, was a good way to investigate for example, the inoculum relationship with the medium (providing the medium was the same). This approach was taken here, to understand in more depth the behaviour of *L. rhamnosus* pure in MRS.

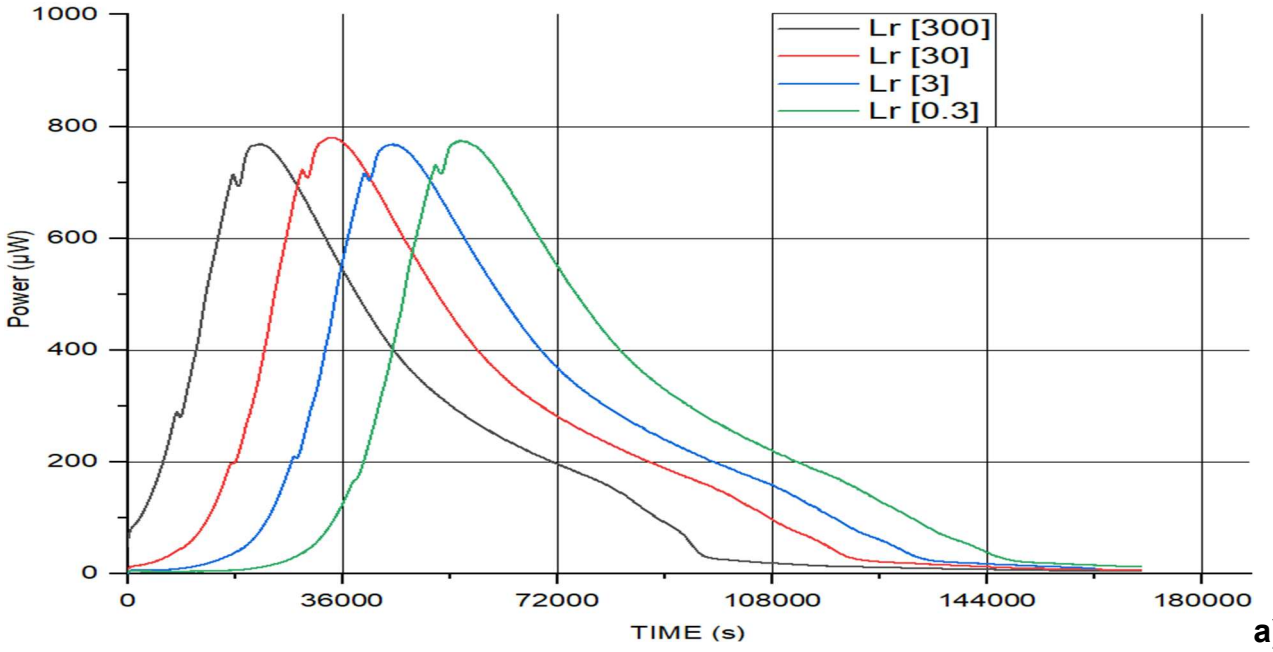

a)

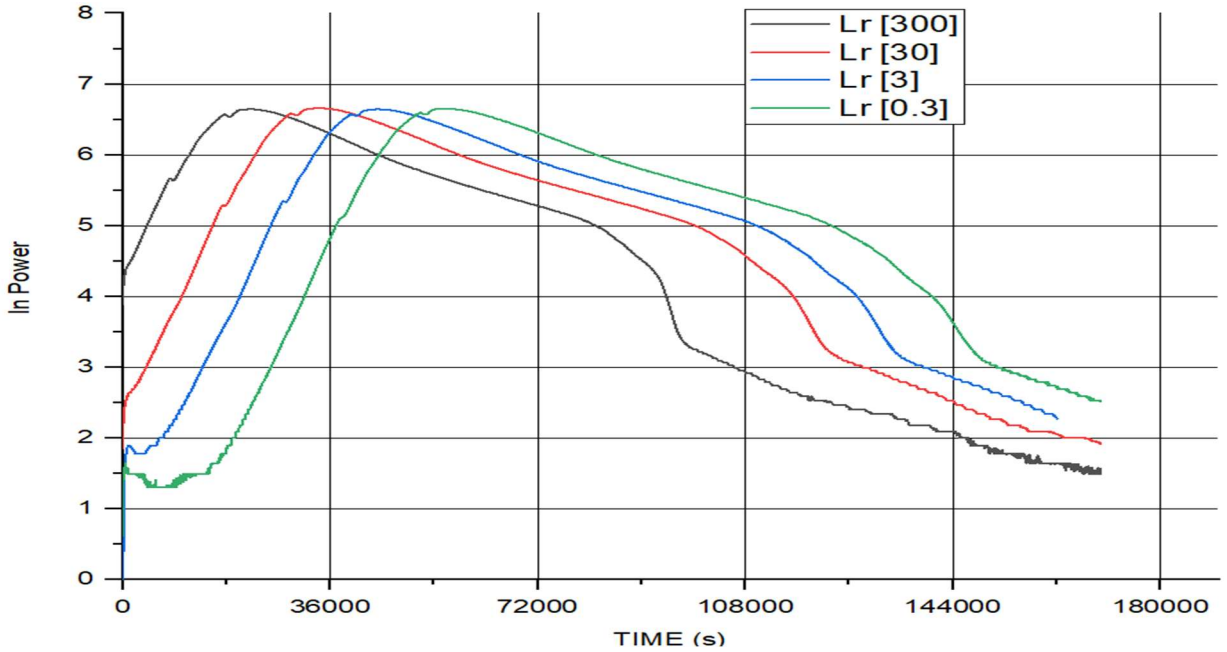

Figure 4.20 *L. rhamnosus* pure tested in MRS, 10-fold inoculum volume variations. P-t curves a), and their logarithmic transformation b). 508 series.

Summary of all parameters calculated for inoculum volume variations is in **Table 4.7**. Slope *k* was the same for all volume variations with a high R^2. Whilst the number of generations varied during the linear, this was attributed to the variation of the duration ($t_{lin\ fit}$) of the linear fits. AUCs for the whole curve as well as AUCs up to PP showed minimal differences between the individual inoculum variations. PPs were very similar in all four inoculum variations. Whilst times to reach PP were different in all four inoculum variations, these differences were regular, reflecting the 10-fold difference in the inoculum volumes. In other words, the times between peaks from 300 µL to 0.3 µL were 11510, 10551 and 11210 respectively, reflecting approximately 3 generations given that the generation time (t_d) was 4125 seconds.

Exp. no (inoc. Vol.) [µL]	ln Intercept	Intercept value	Slope (*k*)	R^2	t_d = ln2/*k*	$t_{lin\ fit}$	No. of gen*	ratios	AUC (total)	AUC to PP	PP [µW]	Time to PP (from x=0)	t_{ref} to $t_{other\ dilution}$ [s]	No of gen to PP**	$t_{inoc.\ to}$ $t_{exp\ growth}$ [s]
508.1 (300)	4.3	73.7	1.68×10^{-4}	0.999	4125	4840	1.2	7.39	3.41×10^{7}	9.40×10^{6}	769	22442	-11510	5.4	-22786
508.2 (30)	2.3	9.97	1.68×10^{-4}	0.999	4125	10250	2.5	1	3.74×10^{7}	9.77×10^{6}	780	33952	0	8.2	-12170
508.3 (3)	0.64	1.9	1.68×10^{-4}	0.998	4125	15661	3.8	0.19	3.74×10^{7}	1.01×10^{7}	768	44503	10551	10.8	-1845
508.4 (0.3)	-1.29	0.28	1.68×10^{-4}	0.999	4125	15430	3.7	0.028	3.88×10^{7}	1.00×10^{7}	775	55713	11210	13.5	8953

Table 4.7 Comparison of growth and other parameters of 10-fold inoculum volume variations. *L. rhamnosus* pure in MRS. Reference volume 30µL corresponds to 1 $\times 10^6$

CFU/mL. * = number of generations during the linear fit; ** = number of generations from inoculation to PP.

The duration of the linear fit in **508.1** was much shorter than the other 3 experiments. This was most likely because dq/dt for this growth was so great that at the data capture initiation a large value of power was recorded. This also meant that there was already metabolic reaction in progress before data capture begun. This would be true for all inoculum volumes, however without detectable power output increase (the metabolism did not yield a detectable power for 30 µL, 3 µL, and 0.3 µL at the same time as it did for 300 µL). When 30 µL was compared with 300 µL, it took 9621 seconds, approximately 3 generations, to reach the same power value, as was the first data point for the 300 µL. Despite this, and the fact that measuring very small inoculum volumes was difficult, it seemed the ratios were in a good approximation of the inoculum volumes 300 : 30 : 3 : 0.3, *i.e.*, 7.69 : 1 : 0.15 : 0.023.

The exponential growth was observed after approximately 1 generation from the start of data recording, *i.e.*, 4041 seconds (67 minutes) using 30 µL volume, see **Figure 4.21**.

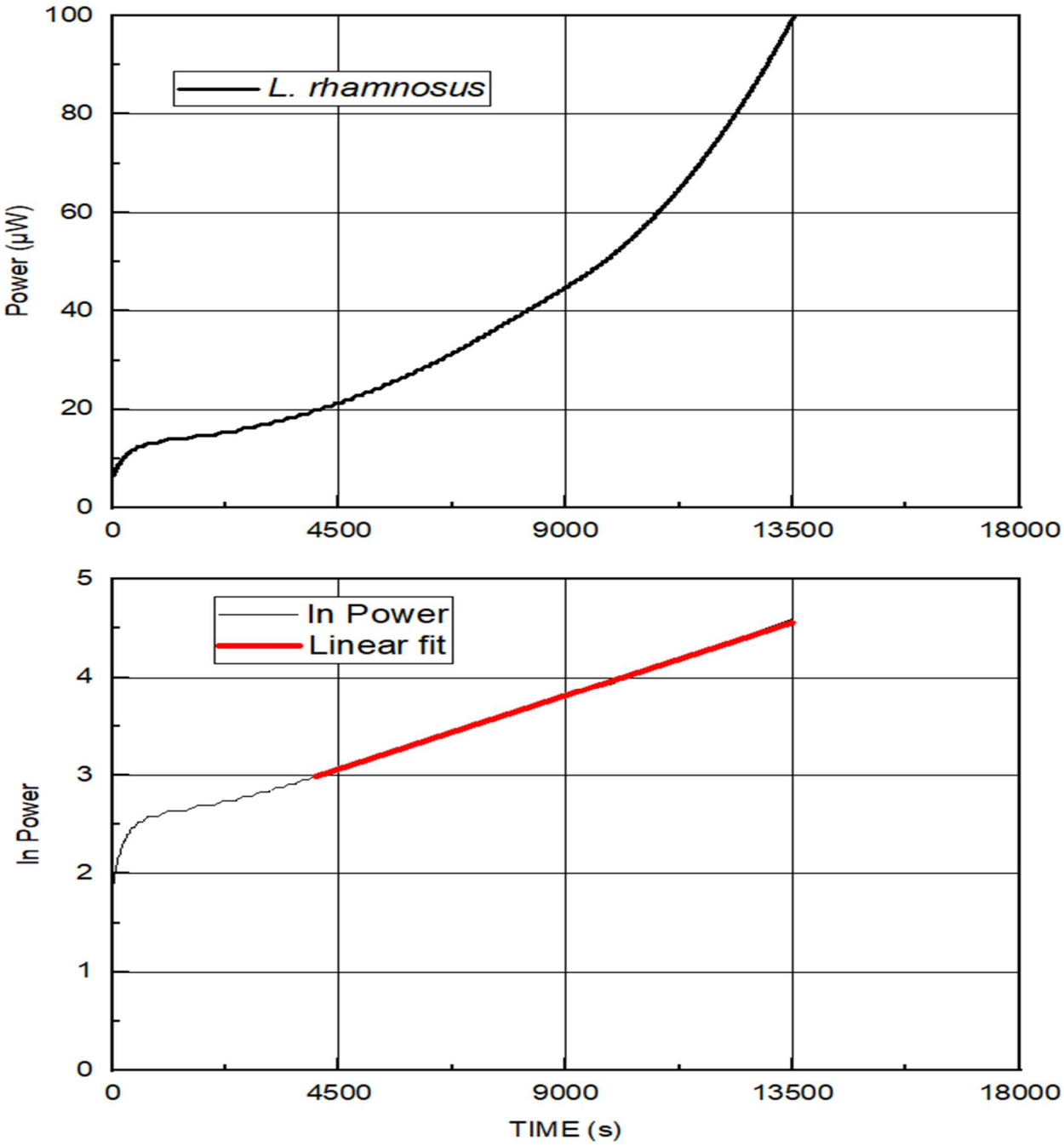

Figure 4.21 The first 100 μW, (508.2, 30 μL inoculum of *L. rhamnosus*, 10^6/mL density)..

There was a time for a signal recognition to become established because the errors associated with recording the signal were greatest when the signal was very small; as the signal increased, the errors in determining the value of the signal reduced. The time before the signal was well established lasted approximately 67 mins from the start of the signal recording before it went exponentially –as illustrated in **Figure 4.21**.

Taking 30 μL as the reference volume, and 300 μL as its 10-fold increase, it was possible to estimate the most likely duration of the lag phase. It was assumed that there was no

change in relation of the medium to the cells when inoculating different densities, *e.g.*, no crowding effect when more inoculum was used or no overwhelming effect of medium when less inoculum was used. The metabolism was observed to be the same for 0.3 µL all the way through to 300 µL (There was no detectable change in the slope values, hence t_d remained constant, AUC constant, PP constant). The size of the inoculum (of up to 10-fold increase from the reference volume 30 µL, as no higher volumes were investigated) made no difference to metabolic activities of the cells (essentially the same p-t curves were observed for all 4 volume variations with just a shift on the time axis as seen in **Figure 4.20a**).

It was plausible to assert that the organisms' metabolism started at the same time regardless of the inoculum volume (limited to the range of volumes investigated) because the same bacteria were tested in the same medium. The only difference was the inoculum volume. It meant that the instrument was not sensitive enough to detect their metabolism immediately when the data capture started (see **Figure 4.20a**, black curve).

The question when exactly the exponential phase started was more difficult to answer. One approach how the start of the observable exponential phase could be determined using logarithmic transformation of the p-t curve is illustrated in **Figure 4.21**. It was also probable that the exponential growth (using 3 and 0.3 µL inoculum volume), was already happening during the time when there was not obviously exponential signal being recorded, in other words the signal recorded did not reflect exponential growth as the cell division reaction did not produce enough energy detectable by TAM. The exponential deviation from the baseline was not observed until there were enough cells producing sufficient heat to be recognised as exponential by the instrument.

The reason why it was probable that exponential growth was occurring at low power, unobserved power, and some analyses were based on this assumption, was because when the results were assessed, the PPs were separated by approximately 3 generations (see **Table 4.7**), and when that was true, all that it did to the p-t curves was shifting along the time axis, but all were growing at a standardised rate. However, the results could only be seen when they got to about 10^6 cells/mL –which was reflective of 30 µL inoculum volume. Therefore, the detection limit of a calorimeter was an issue. Perhaps with more experiments designed to explore the metabolism of the organisms it would be possible to gain some insights into that unobserved period.

Assuming that all cells were dividing and at the same rate and there was no cell death the time to reach for example 100 µW for 30 µL compare with 300 µL should be in a precise ratio. This was found to be true from the data analysis as the same rate constant (k = 1.68 x10^{-4}) was obtained for all volumes.

Table 4.8 shows times to reach set power values. This could be indicative of the culture growing as expected. P_{50} was the first recorded power value for the 300 µL. Thereafter 100 µW intervals were taken and this was indicated by the subscript numbers. Despite the differences in the inoculum volume, they all reached the same point where the power started to be recorded and the power profiles (p-t curves) were essentially the same, independent of their starting inoculum volume (**Table 4.8** and **Table 4.9**).

Volume [µL]	P_{50}	P_{100}	P_{200}	P_{300}	P_{400}	P_{500}	P_{600}	P_{700}	PP
300	0	2101	5961	9451	11521	13151	15161	17271	22442
30	9621	13541	18061	20852	22952	24642	26562	28622	33952
3	19752	23582	27472	30902	33132	34932	36893	39143	44503
0.3	30952	34752	39543	42093	44403	46343	48313	50633	55713

Table 4.8 Times in seconds to reach set power values for individual volumes.

	To catch up with the next 10-fold [s] to reach 100µW	To catch up with the next 10-fold [s] to reach 200µW	To catch up with the next 10-fold [s] to reach 300µW	To catch up with the next 10-fold [s] to reach 400µW	To catch up with the next 10-fold [s] to reach 500µW	To catch up with the next 10-fold [s] to reach 600µW	To catch up with the next 10-fold [s] to reach 700µW	To catch up with the next 10-fold [s] to reach PP
0.3 - 3	11170	12071	11191	11271	11411	11420	11520	11210
3 - 30	10041	9411	10050	10180	10290	10331	10521	10551
30 - 300	11440	12100	11401	11431	11491	11401	11351	11510

Table 4.9 An overview of times required for the individual inoculum volumes to reach a certain power value in 100 µW intervals up to peak power (PP).

30µL										
Power [µW]	6	10	15	20	25	30	35	40	45	50
Time to reach [s]	0	221	2071	4141	5391	6481	7381	8231	9071	9741

Table 4.10 5 µW power increments to determine times required for their increase.

It took 9741 seconds for the 30µL inoculum volume to reach power value 50 µW (see **Table 4.10**). By the time, data recording started, the first power value recorded for 300 µL inoculum volume was already 50 µW. It was assumed that the lag phase was the same for all inoculum volumes, starting at the point of inoculation. If a straight line was drawn as illustrated in **Figure 4.22** with a starting point x-y coordinate for 30 µL inoculum volume *i.e.*, [0 seconds, 6 µW] and the other point was [9741 seconds, 50 µW], it was then possible to make a parallel line with 300 µL through 50 µW, and then the coordinates of the point crossing through x-axis should indicate a more precise start of the exponential phase for the 300 µL (pink lines). The same was done for 100 µW (blue lines), 200 µW (green lines), as illustrated in **Figure 4.22**, and by extension to the other inoculum volumes. The question remained why the point of crossing indicated by the black arrow in **Figure 4.22** was at approximately minus 12000 seconds. One explanation for this was that this manual method of estimating the beginning of the exponential growth of the 300 µL volume was rather simple, however, reflecting rather precisely 3 generations difference (3 x t_d = 3 x 4125 seconds (value from **Table 4.7**) = 12375 seconds) between the 10-fold inoculum volume increase. This also demonstrated that these highly reproducible curves could be used to compensate for missing data as the beginning of the 300 µL curve was at approximately 50 µW, hence the power profile from 0 to 50 µW was missing).

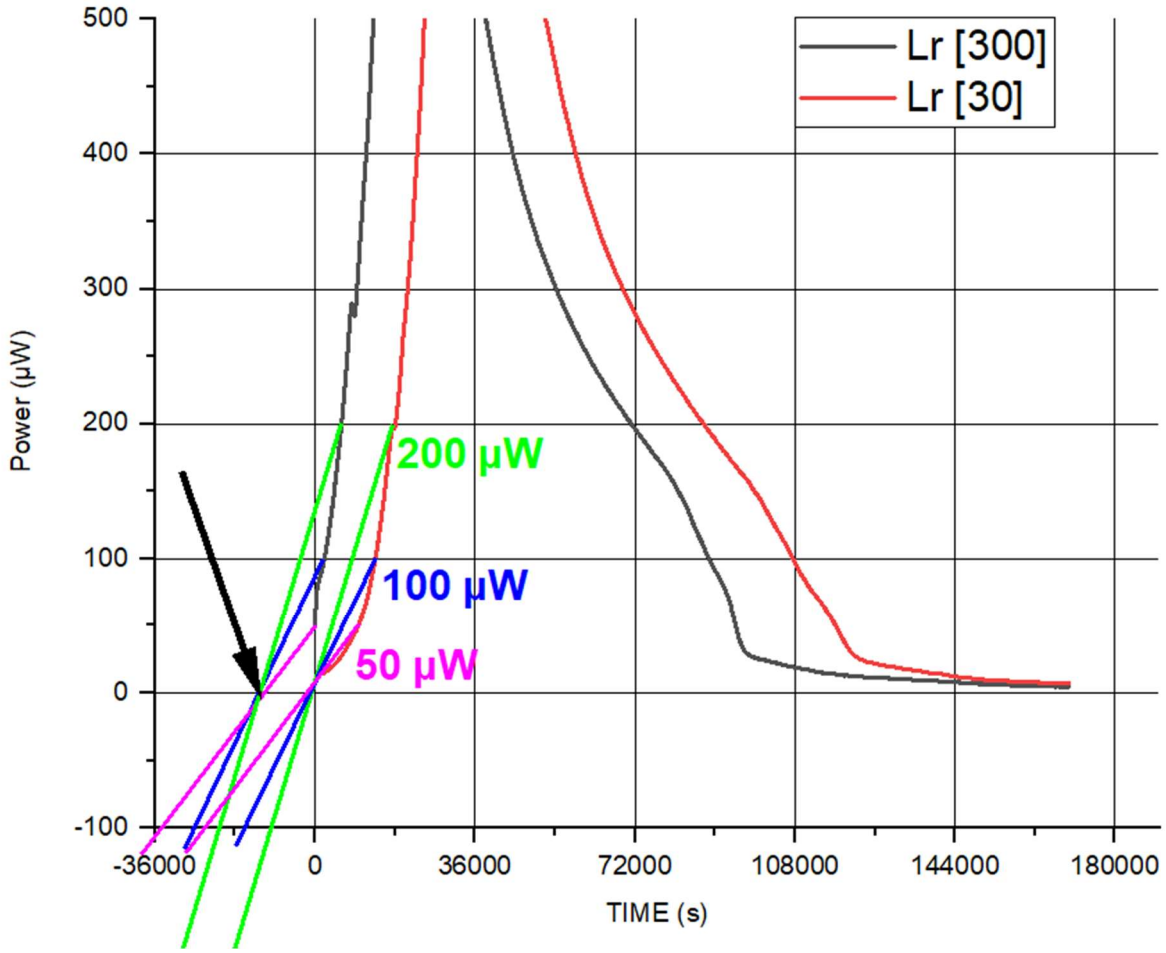

Figure 4.22 Estimating the start of the exponential growth for 300 µL using the next lower inoculum volume 30 µL.

It was possible to use a t_{lag} elimination method described below to overcome the difficulty for estimating t_{lag};

$$t_{peak} = t_{lag} + nt_g \qquad (\mathbf{4.1})$$

where t_{peak} is the time from inoculation to peak power, n is the number of generations throughout the growth period to the peak power. t_{lag} is constant, assuming it took the same time for the cells to start growing independent of the inoculum density. t_g is constant as the same organisms were grown in the same medium for all volume titrations (*i.e.*, 0.3, 3, 30 and 300µL). This method yielded ratios between the individual inoculum volumes, which in principle should be the same (*i.e.*, the number of generations required to catch up with the next 10-fold increase in the inoculum volume). Detail of the calculation is in **Appendix 4**.

Assuming that it took the same number of cells to reach PP, the difference between inoculation volume 0.3 µL and 3 µL, to reach PP, was the number of cells required to produce the same heat from starting with 0.3 µL inoculum volume as it took to do the same with 10 times more cells *i.e.*, 3 µL inoculum volume.

A different way of finding cell number ratios between different inoculum volumes could be calculated using the below intercept over slope relation:

$$\frac{intercept}{slope} = \frac{k\Delta_N HN_0}{k} = \Delta_N HN_0 \qquad (\mathbf{4.2})$$

Then, 3 µL vs. 0.3 µL ration follows;

$$\frac{\frac{k\Delta_N HN_{0(3)}}{k}}{\frac{k\Delta_N HN_{0(0.3)}}{k}} = \frac{\Delta_N HN_{0(3)}}{\Delta_N HN_{0(0.3)}} = \frac{N_{0(3)}}{N_{0(0.3)}} = \frac{10^5}{10^4} = \mathbf{10}$$

Repeat for 30 µL and 300 µL;

$$\frac{\frac{k\Delta_N HN_{0(30)}}{k}}{\frac{k\Delta_N HN_{0(3)}}{k}} = \frac{\Delta_N HN_{0(30)}}{\Delta_N HN_{0(3)}} = \frac{N_{0(30)}}{N_{0(3)}} = \frac{10^6}{10^5} = \mathbf{10}$$

$$\frac{\frac{k\Delta_N HN_{0(300)}}{k}}{\frac{k\Delta_N HN_{0(30)}}{k}} = \frac{\Delta_N HN_{0(300)}}{\Delta_N HN_{0(30)}} = \frac{N_{0(300)}}{N_{0(30)}} = \frac{10^7}{10^6} = \mathbf{10}$$

As expected, the ratios between the 10-fold increases in the inoculation volumes were 10.

A	B	C	D	E	F	G	H	I
Inoculum volume [µL]	**Bacterial density [cells/mL]**	**Bacterial density [cells/L]**	**Intercept**	**Intercept value**	**Linear fit duration [seconds]**		***dq/dt* [W]**	
					Start	End	Start	End
300	10^7	10^{10}	-9.52	7.3 x10^{-5}	3351	8191	1.26 x10^{-4}	2.89 x10^{-4}
30	10^6	10^9	-11.51	1.0 x10^{-5}	4041	14291	1.99 x10^{-5}	1.16 x10^{-4}
3	10^5	10^8	-13.18	1.9 x10^{-6}	10221	25882	1.10 x10^{-5}	1.54 x10^{-4}
0.3	10^4	10^7	-15.11	2.7 x10^{-7}	20052	35482	8.10 x10^{-6}	1.14 x10^{-4}

	J	K	L	M	N	O	P	Q
		N_0	***k***	***h****	**ln(*k*)**	**ln(*h*)**	**ln(*dq/dt*)**	
300		4.2 x10^{11}	1.68 x10^{-4}	10^{-12}	-8.69	-27.63	-8.98	-8.15
30		5.8 x10^{10}	1.68 x10^{-4}	10^{-12}	-8.69	-27.63	-10.82	-9.06
3		1.1 x10^{10}	1.68 x10^{-4}	10^{-12}	-8.69	-27.63	-11.42	-8.78
0.3		1.5 x10^9	1.68 x10^{-4}	10^{-12}	-8.69	-27.63	-11.72	-9.08

Table 4.11 Data and calculated parameters of 508.1-4 series.

* Value of enthalpy from James (1987).

Then it was possible to calculate N_0 (the initial cell numbers at the beginning of the linear fit) using **Eq. 3.12**. Set t = 0, this point referred to the point when, logarithm of power = the intercept, because at that point, t = 0, the straight line cut through the y-axis, at the time t = 0. However, the time t = 0 was related to the logarithm of power and nothing else. It was a theoretical time zero for the exponential portion of the p-t curve that was linearised. Then;

$$ln\left[\frac{dq_N}{dt}\right] = ln[N_0 \Delta_N H\, k] \qquad (\mathbf{4.3})$$

substitute $ln\left[\frac{dq_N}{dt}\right]$ on the left-hand side of the equation with the intercept number from the column D (**Table 4.11**). The results are presented in **Table 4.12**.

The calculated N_0 was from 4.2 x10^{11} through to 1.5 x10^9 for 300 through to 0.3 µL, respectively. If the units of volume played a role (*e.g.*, units would be in cells per litre), it would mean that the resulting N_0 values would need to be modified by 10^{-3} going from litres to millilitres. This appeared to be true and the results are presented in **Table 4.13.**

If the above was right, then it was plausible that at the beginning of the exponential phase for 300 µL, (where t = 0, this point corresponded with 3351 seconds from the beginning of

signal recording (see column F in **Table 4.11**)), the calculated N_0 could be in the region of 4.2 x10^8.

Consequently, considering the t_g = 69 minutes (4125 seconds) the number of cells should increase by a factor of 1.17, because the duration of the studied linear portion was 4840 seconds (column G minus column F). This was demonstrated by the increase in the power from 1.26 x10^{-4} to 2.89 x10^{-4} Watts. This observed, recorded by TAM, increase in power for the given time interval (4840 seconds) agreed well with calculated power increase based on the generation time.

Column H, **Table 4.11** (300 inoculum volume) the power 1.26 x10^{-4} doubled in 4125 seconds to 2.52 x10^{-4}. The remaining 715 seconds (4840 - 4125 = 715) represented 0.17 of the next generation, therefore, in this time the power 2.52 x10^{-4} would increase to 2.95 x10^{-4}. The power recorded by the TAM at the end of the linear period was 2.89 x10^{-4} W.

Inoc. volume	Step 1	Step 2	Results
300 µL	-9.52 = ln(kh) + ln N_0	26.77 = ln $N_0 \Rightarrow N_0$	$N_0 = e^{26.77} = 4.2 \times 10^{11}$
30 µL	-11.51 = ln(kh) + ln N_0	24.78 = ln $N_0 \Rightarrow N_0$	$N_0 = e^{24.78} = 5.8 \times 10^{10}$
3 µL	-13.18 = ln(kh) + ln N_0	23.11 = ln $N_0 \Rightarrow N_0$	$N_0 = e^{23.11} = 1.1 \times 10^{10}$
0.3 µL	-15.11 = ln(kh) + ln N_0	21.18 = ln $N_0 \Rightarrow N_0$	$N_0 = e^{21.18} = 1.5 \times 10^{9}$

Table 4.12 N_0 (number of cells at the start of the first linear portion) calculations using the central equation.

	Inoculum density [CFU/ml]	Inoculum volume [µL]	Medium volume [µL]	Cells/mL in 3mL ampoule	Equivalent of cells/litre	cells/litre at t_{exp} = 0	cells/3mL ampoule at t_{exp} = 0	Cells/1mL at t_{exp} = 0
1	10^8	300	2700	10^7	3.3 x10^9	4.2 x10^{11}	1.26 x10^9	4.20 x10^8
2	10^8	30	2970	10^6	3.3 x10^8	5.8 x10^{10}	1.74 x10^8	5.80 x10^7
3	10^8	3	2997	10^5	3.3 x10^7	1.1 x10^{10}	3.3 x10^7	1.10 x10^7
4	10^8	0.3	2999.7	10^4	3.3 x10^6	1.7 x10^9	5.1 x10^6	1.70 x10^6

Table 4.13 Details of cell density calculations needed to achieve particular final cell densities in a 3mL calorimetric ampoule at inoculation compared with the cell numbers at the beginning of a linear fit for each inoculum volume.

The units of the power were modified by 10^{-6} prior to the manual analysis to work with Watts instead of the raw data which were recorded by Digitam software in µW. An illustration of the difference in units is in **Figure 4.23** where a unit's difference resulted in a large difference between the intercept values, potentially interfering with the interpretation of the meaning of the intercept.

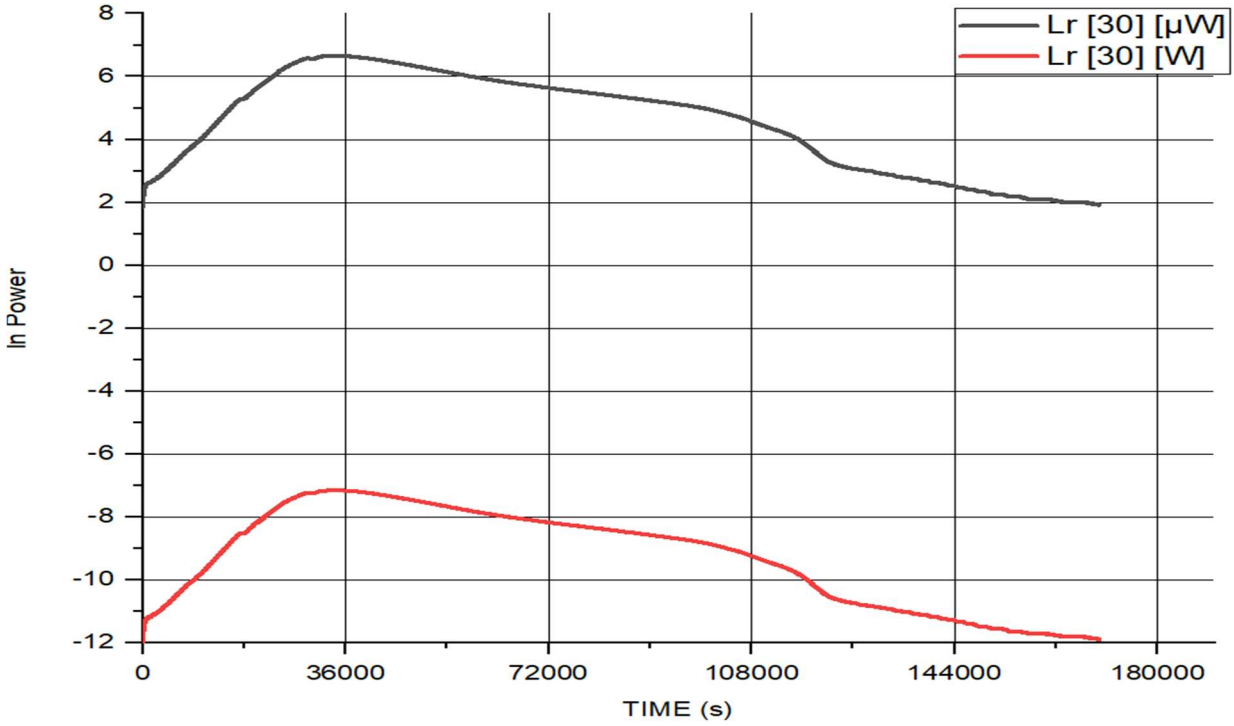

Figure 4.23 An illustration of units' difference W vs. µW.

4.3.1.3.5 Generation numbers

As discussed in Cabadaj *et al*. (2021), "if $\log_2$ of power was used, the y-axis would represent the number of generations". The estimation in this case was that the number of generations produced during the studied part of the exponential phase (**Figure 4.24**, green linear fit) was 7.88 - 4.77 = 3.11 generations.

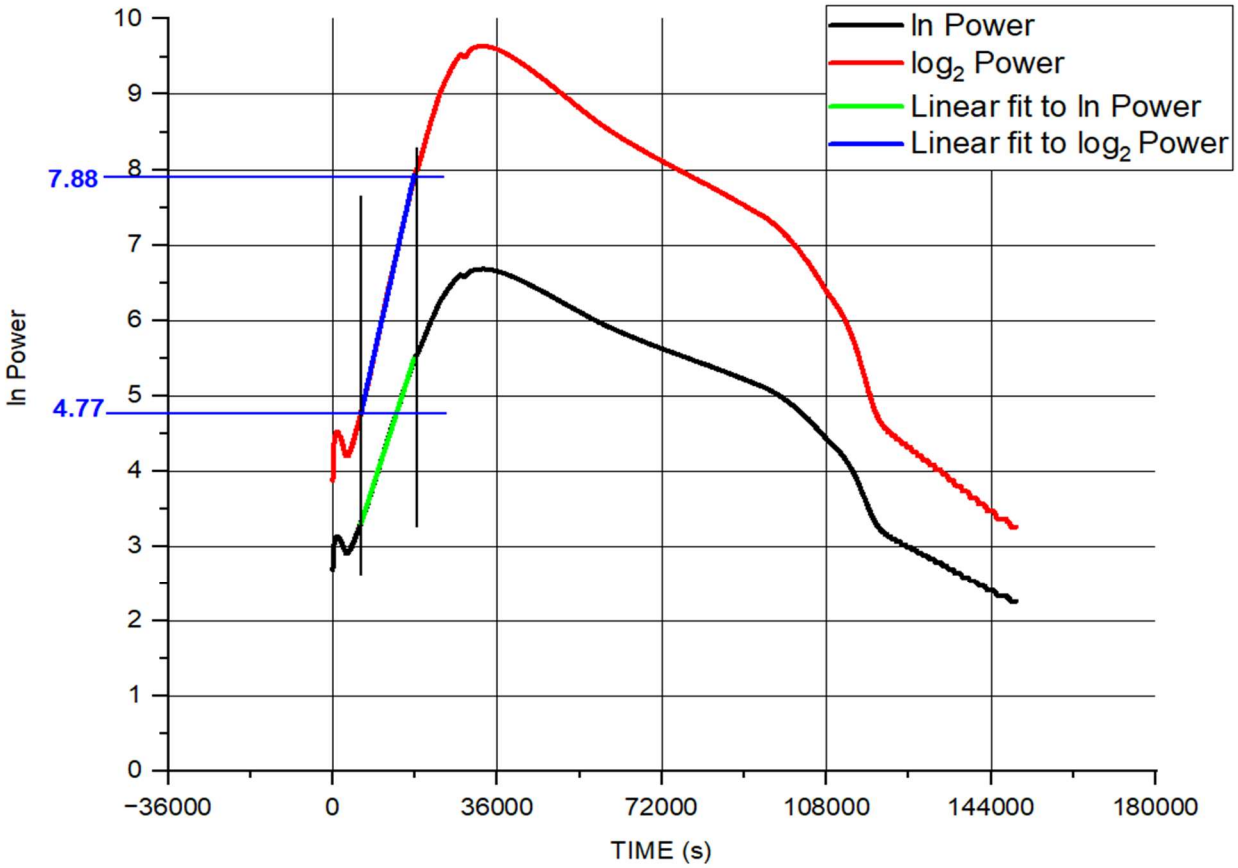

Figure 4.24 Determining the number of generations using $\log_2$ of power (logarithm with base 2).

4.3.1.3.6 Area under curve

Area under curve (AUC) was yet another parameter, which was easily extractable from the basic data set (p-t curve) and could be added to a set of comparators to determine a successful growth. It was however just the AUC up to peak power (PP) that would be used for cell numbers determination, because anything after PP was reached was not related to exponential growth. It would still be just a rough estimation of the cell numbers as the lag time (*e.g.*, 8480 seconds in this case) was not fully reflected in the AUC. The AUC up to PP was another way of representing cell numbers. It was not the number of cells, but it represented them.

Different transformations of the p-t curve were attempted to determine the best reproducibility (see **Table 4.14**). These attempts were made to find out what would give the highest percentual representation of the AUC related to the first linear portion (which lasted from 6200 - 17800 seconds and was denoted below as AUC_{exact}) to the AUC from the start of the signal recording to PP, denoted below as AUC_{PP}. It was found that the best percentage

representation of the studied (linear portion) versus portion of the curve from the beginning of the data capture to PP were the AUC calculated from the logarithmic transformation of the integrated p-t curve at 33.57% followed by the AUC calculated from the logarithmically transformed p-t curve at 30.88%..Details of the calculations are available in **Appendix 4**.

It seemed that the best option for comparing AUCs was the logarithmic transformation of the integrated p-t curve as AUC_{exact} of the linear portion represents 33.57% of the AUC to PP. Logarithmic transformation of the p-t curve, which yielded 30.88% containment within AUC_{PP} meant less data transformation (not having to integrate the raw data and then take the logarithm) and still a very good representation.

Parameter	**503.1**	**503.2**	**503.3**	**503.4**	**Mean**
Analysis	Manual				
Intercept	2.13 ± 1.03 x10^{-3}	2.11 ± 7.44 x10^{-4}	2.12 ± 1.05 x10^{-3}	1.88 ± 2.89 x10^{-3}	2.06±1.43 x10^{-3}
Slope	1.89 x10^{-4} ± 8.26 x10^{-8}	1.87 x10^{-4} ± 5.97 x10^{-8}	1.87 x10^{-4} ± 8.42 x10^{-8}	2.03 x10^{-4} ± 2.31 x10^{-7}	1.92 x10^{-4} ± 5.72 x 10^{-8}
AUC_{exact} (ln transformed p-t curve)	5.10 x10^{4} 0.96%	5.04 x10^{4} 0.23%	5.06 x10^{4} 0.12%	5.01 x10^{4} 0.87%	5.05 x10^{4} 0%
AUC to PP (ln transformed p-t curve)	1.65 x10^{5}	1.63 x10^{5}	1.64 x10^{5}	1.63 x10^{5}	1.64 x10^{5}
AUC_{exact} (p-t curve)	1.14 x10^{6} 3.63%	1.08 x10^{6} 1.89%	1.09 x10^{6} 0.32%	1.08 x10^{6} 1.62%	1.10 x10^{6} 0%
AUC to PP (p-t curve)	9.97 x10^{6}	9.67 x10^{6}	9.68 x10^{6}	9.99 x10^{6}	9.83 x10^{6}
R^2	0.9998	0.9999	0.9998	0.9985	0.9995
Data range	11600 seconds	11600 seconds	11600 seconds	11600 seconds	11600 seconds

Table 4.14 Comparison of quantitative growth parameters of 503 series. “exact” means that the AUC was calculated for the duration of the linear fit only *e.g.*, 11600 seconds.

In red: difference from mean = reproducibility when calculated from ln transformed data.
In green: difference from mean = reproducibility when calculated from raw data.

Manual data processing was time consuming and subjective to an operator's error or interpretation to determine the best straight line, AUC and other parameters. The subjectivity of an operator processed data is illustrated in **Figure 4.25a,** where the best linear fit based on the coefficient of determination (R^2) was manually selected. Manual selection of the best straight line was done based on a visual assessment of the logarithmically transformed p-t curve using OriginPro software. However, for the consistency of comparison of the 503 series, this linear fit 503.4 was adjusted, see **Figure 4.25b**, to reflect the same length of data as in the previous 3 runs of this series (*i.e.*, 11600 seconds). Clearly having an automated procedure would make this kind of adjustments unnecessary and the data processing would be more consistent when processed without the involvement of an operator. The differences between the two approaches are compared in **Table 4.15**.

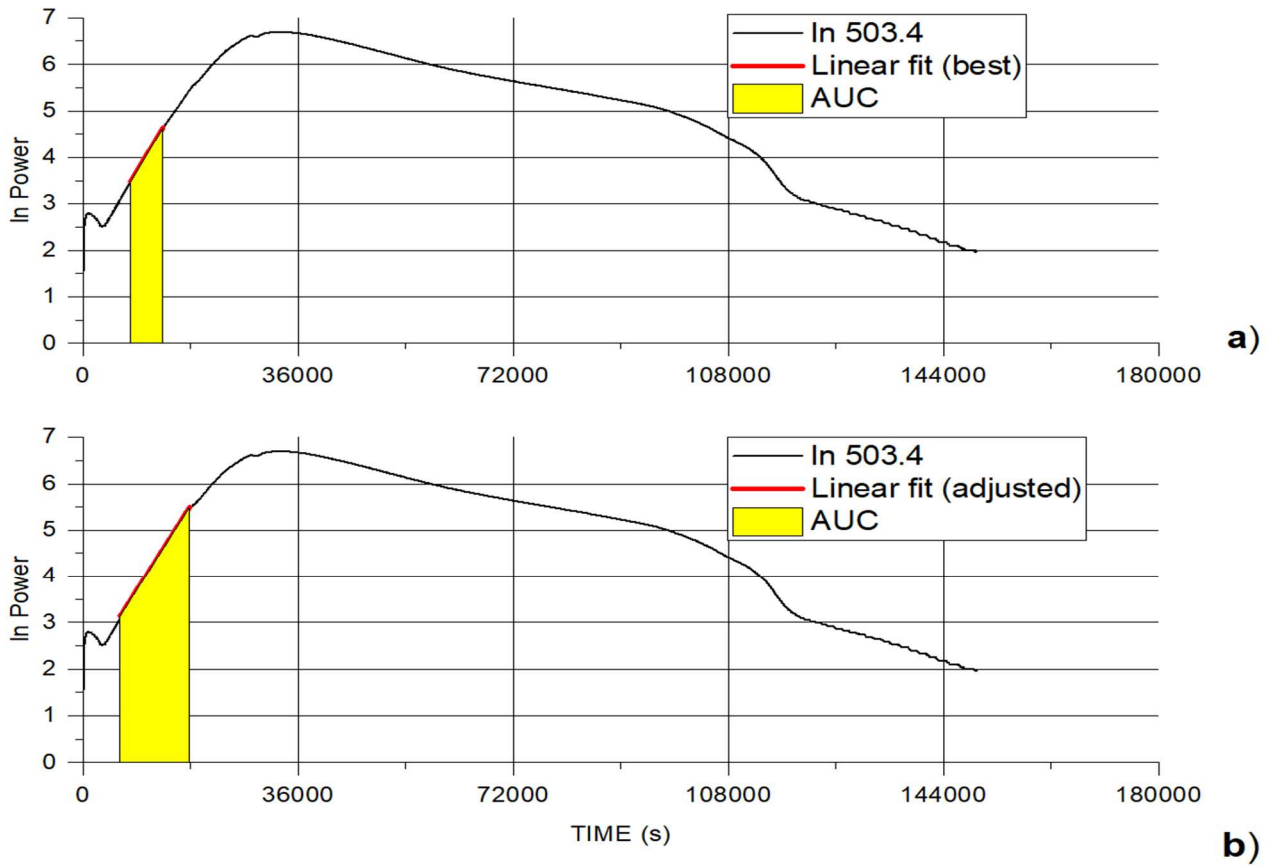

Figure 4.25 Potential subjectivity of an operator when analysing data.

The logarithm of AUC ought to be equivalent to the logarithm of the cell numbers. If the logarithm of the AUC to PP was plotted as a function of time that should be equivalent to cell numbers, because all the values of the area would be transformed through constant

enthalpy, $\Delta_N H$, into cell numbers. Therefore, the rate of change of that area ought to be the same as the rate of change of cell numbers.

503.4	Best fit	Adjusted fit
Intercept	$1.79 \pm 9.71 \times 10^{-4}$	$1.88 \pm 2.89 \times 10^{-3}$
Slope	$2.13 \times 10^{-4} \pm 9.03 \times 10^{-8}$	$2.03 \times 10^{-4} \pm 2.31 \times 10^{-7}$
AUC	2.20×10^{4}	5.01×10^{4}
R^2	0.9999	0.9985
Data range	5420 seconds	11600 seconds

Table 4.15 Quantitative growth parameters of 503.4.

4.3.1.4 Discussion

It was known what a desirable outcome of the above reference building experiments should be: deriving growth rate constant, intercept, AUC with a good R2 capturing as much exponential growth as possible. However, it was not known what the parameters' values should be, as none were established before these experiments (503 and 504 series) were done. The ambition with the experiments was to establish the parameters that conform to a good growth. It was also not known whether analysing the first linear portion (i.e., first 10 - 15 hours of the p-t curve) would be sufficient to determine good growth. However, the project's ambition was to reduce testing time as much as possible and to concentrate in this first stage of the detailed analysis on the exponential phase only. The basic and minimum requirement before setting up the experiments was to find out whether they are reproducible otherwise it was not worth going forward. Hence establishing the range of parameters values conforming to a good growth with repeatable and satisfactory outcome was desirable.

It was clear however that a good reproducibility range for a precisely controlled reference standard reaction might need to be widened for a real product. What the acceptable range would be for the real products needed to be determined because a precisely controlled experiment of an experimental sample did not describe a real situation, but an ideal one - the best. So, it was plausible that a wider range could appear, meaning lower reproducibility with a real product sample.

The p-t curves were highly reproducible, and these were therefore very useful for Symprove for their pragmatic requirements of determining a good growth.

The curves were also indicative of the constancy of the metabolism of the tested organism – *L. rhamnosus* in the testing medium (MRS) independent, within the investigated range, of experimental runs (503, 504) as well as the inoculum densities (300, 30, 3 and 0.3 µL). The system was robust across a wide range of conditions.

The analysis of the logarithmic transformations of the p-t curves yielded consistent *k* values (1.68×10^{-4}, which was also in close agreement with PC and OD derived slope values). The consistency was also demonstrated by analysing of the p-t curves data for 50 -100 µW, 100 - 200 µW *etc.* (**Table 4.8**). All the inoculum volume experiments as well as the standard reference curves (503 and 504 series) showed that the data are not randomly dispersed, there were not large errors or variations associated with them.

4.3.2 *L. rhamnosus* grown in two barley worts, tested in MRS

During the course of this project, I realised that producing barley wort manually onsite with limited process control was not sustainable in the long run, especially when producing increased volumes of the final product. Therefore, I undertook a selection process of a suitable industrial scale manufacturer of ready to use barley wort. The selected product, wort produced by Dohler company, was tested against the regular barley wort produced onsite.

The experiments presented in this section were conducted to explores the extent to which calorimetry can offer insights into a growth medium selection and whether there was something that could be established to have the best control possible over the medium (wort). The effects, of the regular barley wort produced onsite (wort, **Figure 4.26**) and wort commercially produced by Dohler company (DLW, **Figure 4.27**) on the growth of *L. rhamnosus* were investigated. The TAM testing medium –MRS as well as *L. rhamnosus* used in these experiments were each from one batch only (including the reference experiments)– therefore any changes observed between the reference (503.1) and *L. rhamnosus* grown in the two worts (24 hours at 37ºC) prior to testing in MRS could be attributed to the effects of the worts on *L. rhamnosus* whilst being grown in them.

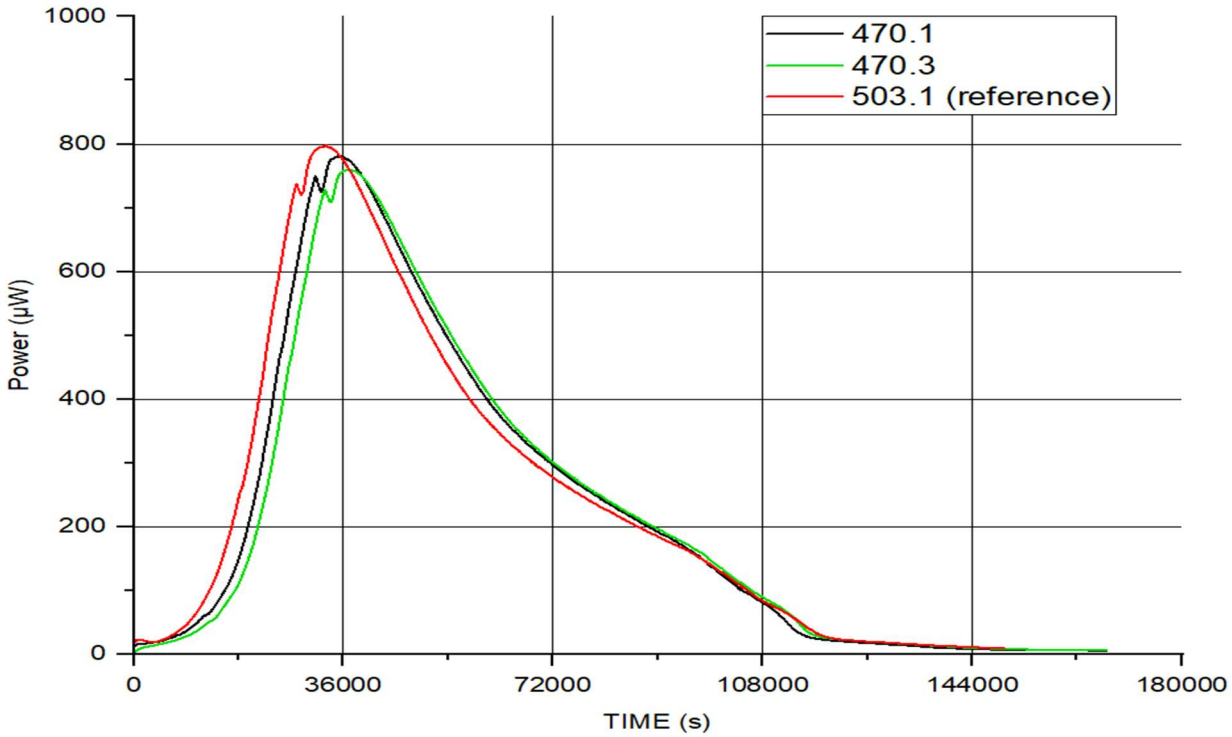

Figure 4.26 *L. rhamnosus* grown in a regular barley wort produced onsite, tested in MRS (in duplicate, black and green curves) and its relationship with 503.1 (red curve) –the reference of *L. rhamnosus* pure tested in MRS.

Exp.	PP [µW]	Time to PP [s]	AUC to PP (p-t plot)	AUC to PP (ln plot)	Slope	Intercept	R^2
470.1	781	35351	9.83×10^6	1.72×10^5	1.70×10^{-4}	1.94	0.9995
470.3	760	36612	9.32×10^6	1.71×10^5	1.70×10^{-4}	1.67	0.9995
503.1	798	32940	9.96×10^6	1.65×10^5	1.89×10^{-4}	2.13	0.9998

Table 4.16 Basic shape analysis parameters (PP, time to PP, AUC) and logarithmic transformation parameters (slope, intercept) of *L. rhamnosus* grown in wort (470 series), tested in MRS. 503.1 reference set values for comparison.

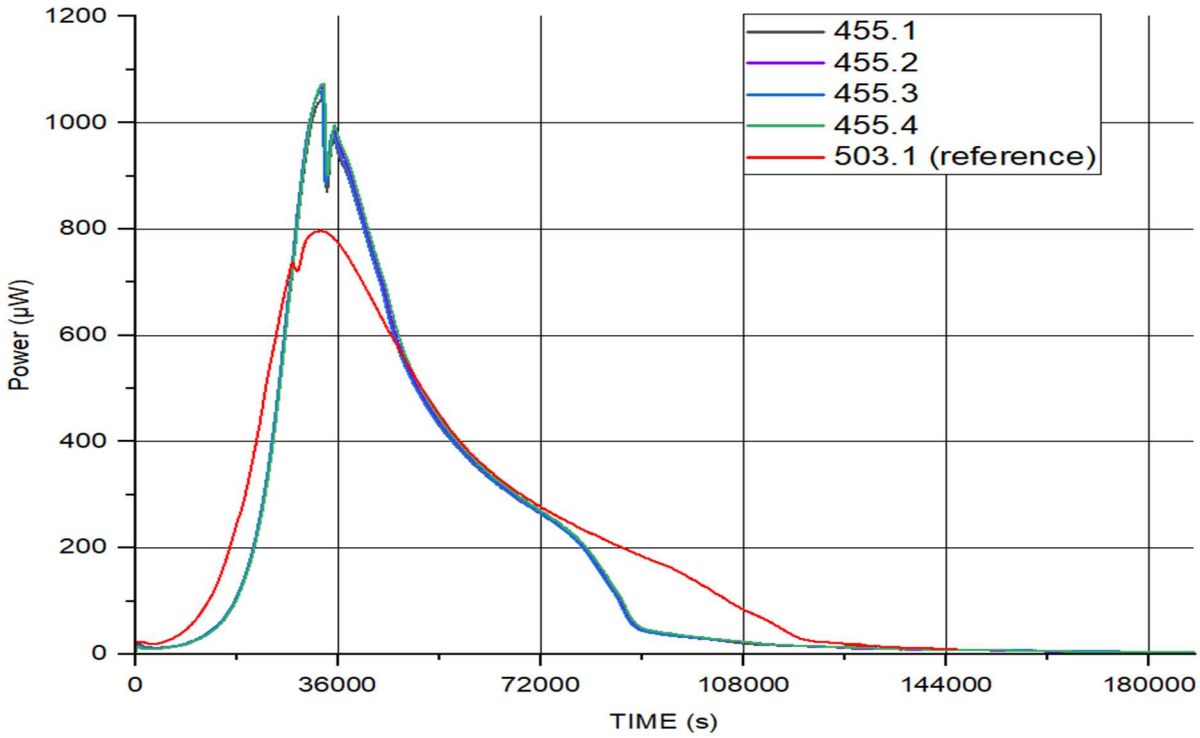

Figure 4.27 *L. rhamnosus* grown in DLW, tested in MRS (in quadruplicate) and its relationship with 503.1 –the reference of *L. rhamnosus* pure (red curve) tested in MRS.

Exp.	PP [µW]	Time to PP [s]	AUC to PP (p-t plot)	AUC to PP (ln plot)	Slope	Intercept	R^2
455.1	1047	33301	8.86×10^6	1.50×10^5	2.09×10^{-4}	0.87	0.9998
455.2	1069	33251	8.94×10^6	1.50×10^5	2.06×10^{-4}	0.94	0.9997
455.3	1059	32831	8.66×10^6	1.48×10^5	2.06×10^{-4}	0.99	0.9996
455.4	1073	33271	8.86×10^6	1.48×10^5	2.07×10^{-4}	0.91	0.9998
503.1	798	32940	9.96×10^6	1.65×10^5	1.89×10^{-4}	2.13	0.9998

Table 4.17 Basic shape analysis parameters (PP, time to PP, AUC) and logarithmic transformation parameters (slope, intercept) of *L. rhamnosus* grown in DLW (455 series), tested in MRS. 503.1 reference set values for approximate comparison.

Exp.	PP [µW]	Time to PP [s]	AUC to PP (ln plot)	Slope	Intercept	R^2
455.1_{DLW}	1047	33301	1.50×10^5	2.09×10^{-4}	0.87	0.9998
470.1_{wort}	781	35351	1.72×10^5	1.70×10^{-4}	1.95	0.9995
503.1_{ref}	798	32940	1.65×10^5	1.89×10^{-4}	2.13	0.9998

Table 4.18 The relationship of *L. rhamnosus* grown in wort and DLW with *L. rhamnosus* pure - the reference 503.1. 503.1 reference set values for comparison.

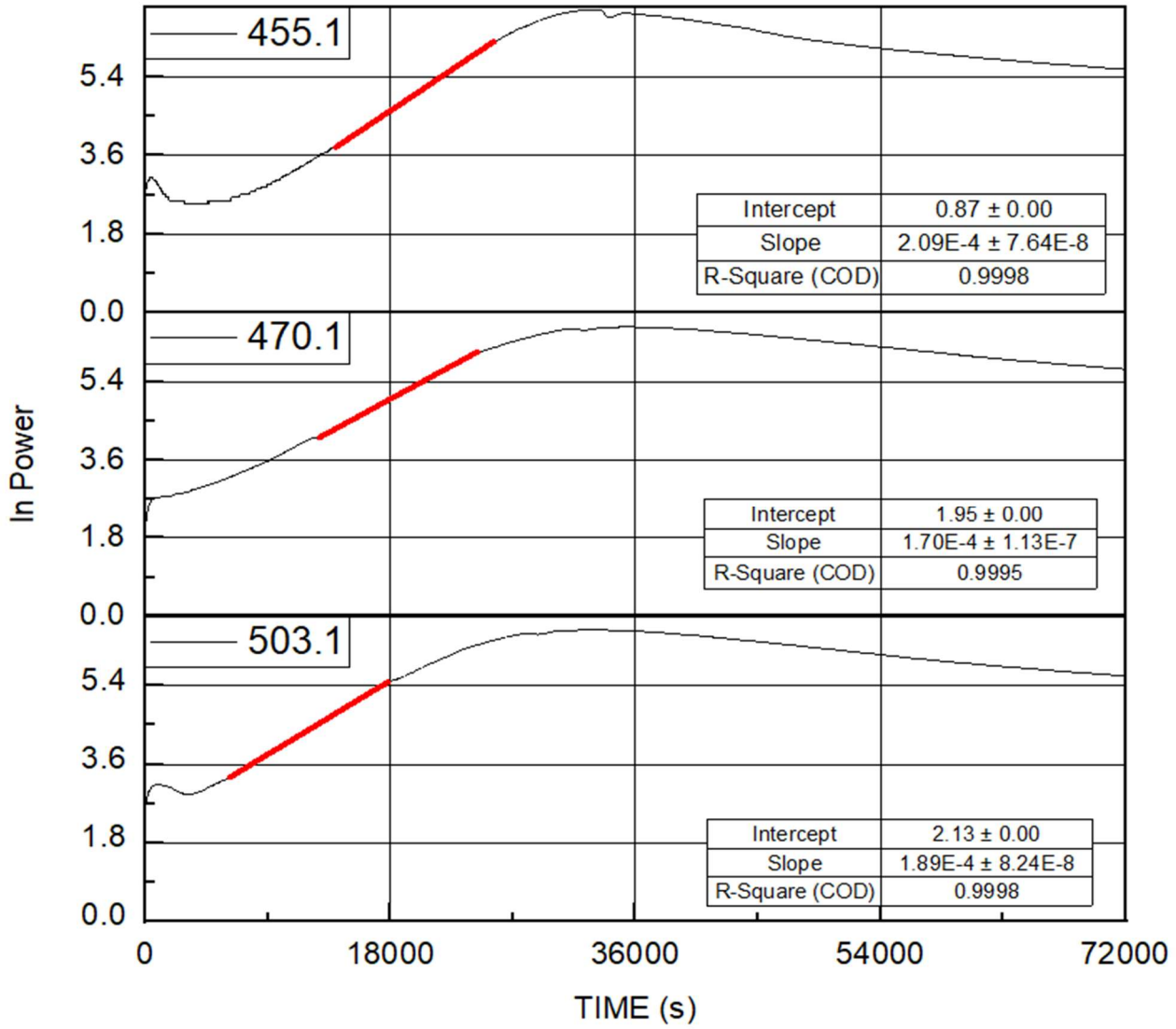

Figure 4.28 Logarithmic transformation of p-t curves (455.1(DLW), 470.1(wort) and 503.1). Red portions indicated in each curve represent linear fits.

4.3.2.1 Discussion

The metabolism of *L. rhamnosus* pure did not appear to change significantly when this organism was grown in wort compared with the reference 503.1, see **Figure 4.26**. *L. rhamnosus* was grown in the laboratory, on its own in wort, to simulate its FV1 fermentation process (assuming only *L. rhamnosus* would be grown in FV1. However, these experiments were limited and the effects of co-culturing *L. rhamnosus* and *L. acidophilus* were explored in later sections **4.3.6** and **4.3.7**). There was not an obvious advantage (*e.g.*, increased rate of fermentation, increased number of organisms) observed between using just defrosted inocula (*L. rhamnosus* pure) and growing the same inocula in wort prior to IMC testing. The parameters of 470.1 (PP, time to PP, AUC slope and the intercept) were approximately in

agreement with the same parameters of the reference reaction (503.1), see T**able 4.18** (if everything was consistent, then the linear period of 503.1 ought to be the same linear period of 470 series).

By contrast, *L. rhamnosus* pure grown in wort produced by Dohler company (DLW), prior to IMC testing in MRS, showed a different behaviour when compared with the same *L. rhamnosus* pure (the reference 503.1), see **Figure 4.27**. It was also clear upon examining basic shape parameters and logarithmic transformation parameters (**Table 4.18**) that the metabolism of *L. rhamnosus* pure changed (as indicated by the p-t curves and their parameters) after it was grown in DLW. These findings suggested that there was an observable, therefore investigable difference in the composition of the two worts. DLW seemed to support the growth to a greater extent.

The values of slope could be indicative of similar or indeed different processes taking place at a particular time. It can be seen in **Table 4.18** that basic shape analysis parameters (*e.g.*, PP and AUC to PP) were complementing other parameters (especially slope) in determining whether similar or different processes were happening over the same time period. For example, the slope value of the reference reaction (503.1) was very similar to the slope value of DLW grown *L. rhamnosus*, however, their PPs were very different, whilst their times to reach PP were very similar; at the same time their AUCs to PP as well as their intercepts (**Figure 4.28**) were rather different. Based on these easily extractable parameters a more informed decision about bottling or quarantining a particular batch of product could be taken.

It was reasonable to assume that changing intercept values (increase/decrease) reflected the initial inoculum density (see **4.3.1.3.4**) –the higher the value of the intercept the higher the initial inoculum density (and vice versa). Note that the just mentioned experiments would not reveal what growth extent to expect in different growth media (such as wort and DLW). It was clear however, that the nutrient distributions differed in wort and DLW. This nutrient distribution effect could be seen visually (**Figure 4.27**) as well as when the growth parameters were compared (**Table 4.18**).

If the constituents in wort sustained growth in a similar way to MRS, and there was an indication of that (**Figure 4.26**), it was reasonable to say that the same extent of growth occurred in both media (it was also reasonable to assume this given that the AUC was related to cell numbers; $AUC_{470.1}$ was within 4.4% of $AUC_{503.1}$). However, the situation was different with DLW, and one would need to explore further whether the same extents of

growth occurred in DLW (for example a facility to perform plate counts would need to be available, as noted before in **Chapter 3**); $AUC_{455.1}$ was within 8.8% of $AUC_{503.1}$.

L. rhamnosus reference (503 series) was used to determine if the calorimeter was capable of yielding highly repeatable data (this kind of experiment can also confirm that a batch of *L. rhamnosus* used for establishing the reference reaction had not degraded over time –*i.e.*, its shelf life) and it was also used to show that the calorimeter performed well over time. The reference reaction could also be used as a control reaction to check the precision of a technician in setting up the experiments. It also hinted about the capacity of wort and the capacity of DLW to sustain growth, because one was faster than the other and it peaked higher and their AUCs were different.

The references demonstrated that it was rational to go ahead with this investigation because the calorimeter was capable, in these complex systems, of giving highly reproducible data and indicating when there was something wrong with the instrument (see **4.2.3**). It was demonstrated that it was possible to have, if consistent inocula were obtainable (in this case *L. rhamnosus* pure), highly reproducible p-t curves (within 3%).

The reproducibility that could be achieved from data on real systems (FV1, FV2 or the mix of these) and the practical outcome of having an authority to release a batch of product for bottling and sale would be determined by the repeatability of those experiments (discussed in later sections **4.3.6** and **4.3.7**).

Whilst the reference 503.1 was determined on different criteria (repeatability and TAM performance over time) it was fortunate that the comparison made between 503.1 and 470.1 yielded very similar curves. However, when the same organisms were pre-grown in another medium for example DLW, it was discovered that the outcome was not the same. This revelation demonstrated that calorimetry was telling, absolutely, about medium constituents and influence of their effects on the metabolism of *L. rhamnosus*.

4.3.3 *L. rhamnosus* grown in MRS, tested in MRS

The purpose of the experiments presented in this section was in part to explore whether calorimetry could be useful for examining Symprove production protocol, and the potential for shelf life testing. Fermenting time of up to 24 hours was required for FV1 to reach desirable levels of microorganisms (Symprove, 2021). Therefore *L. rhamnosus* was grown

in a medium (MRS), for the length of time that might be used in the real production, *i.e.*, 24 hours. Once produced and bottled Symprove was stored and shelf life was determined by a contract laboratory, on repeated sampling for viability. To discover what was the consequence of storing Symprove after it was bottled, a limited simulated test for shelf life (calorimetric viability test) was performed; *i.e.*, 48 hours fermentation in MRS. Certainly, this kind of test could be extended to cover as long period as necessary (weeks, months or even years in length with regular sampling). This way of testing is in essence testing of the viability of microorganisms in a closed system of spent growth medium (*e.g.*, a bottle of Symprove product). This was not the same as taking a fresh *L. rhamnosus* pure sample out of a freezer and put it into the same (MRS) because *L. rhamnosus* would have been potentially 24 hours in the fermenting vessel, by the time it was sampled. Therefore 24 hours could be seen as the state of *L. rhamnosus* at the end of fermentation, and the 48 hours could be at the point after it was freshly bottled.

x When *L. rhamnosus* was grown (pre-cultured) in MRS for 24 hours at 37ºC, it grew faster in the subsequent IMC test than *L. rhamnosus* pure (see **Figure 4.29**). MRS media used in **4.3.3** for growing as well as calorimetric testing of *L. rhamnosus* pure were from the same batch. *L. rhamnosus* pure was from one batch only in all experiments reported in **4.3.3**. PPs of the pre-cultured *L. rhamnosus* reached significantly lower levels compared with *L. rhamnosus* pure whilst times to reach PP were much shorter for pre-cultured *L. rhamnosus* as noted in **Table 4.19**. There was also a large difference between AUCs, with *L. rhamnosus* pure giving much greater AUC to PP. **Table 4.19** shows a clear difference in the rates of growth between the two cultures where the growth rate of *L. rhamnosus* pure was significantly greater compared with the pre-cultured *L. rhamnosus*. The intercepts of the pre-cultured *L. rhamnosus* indicate that there was a much greater initial number of organisms when compared with *L. rhamnosus* pure.

When *L. rhamnosus* was grown (pre-cultured) in MRS for 48 hours at 37ºC, it grew slower in the subsequent IMC test than *L. rhamnosus* pure (**Figure 4.30**). Times to reach PP doubled (**Table 4.20**) for *L. rhamnosus* pre-cultured for 48 hours compared with 24 hour pre-culturing. There was not a significant difference between AUCs of the reference 503.1 and 48 hour grown *L. rhamnosus*.

Comparison of the basic shape analysis parameters and logarithmic transformation parameters of *L. rhamnosus* pure (503.1 reference set) with *L. rhamnosus* grown in MRS at 37ºC for either 24 hours or 48 hours is presented in **Table 4.21**. **Figure 4.31**.

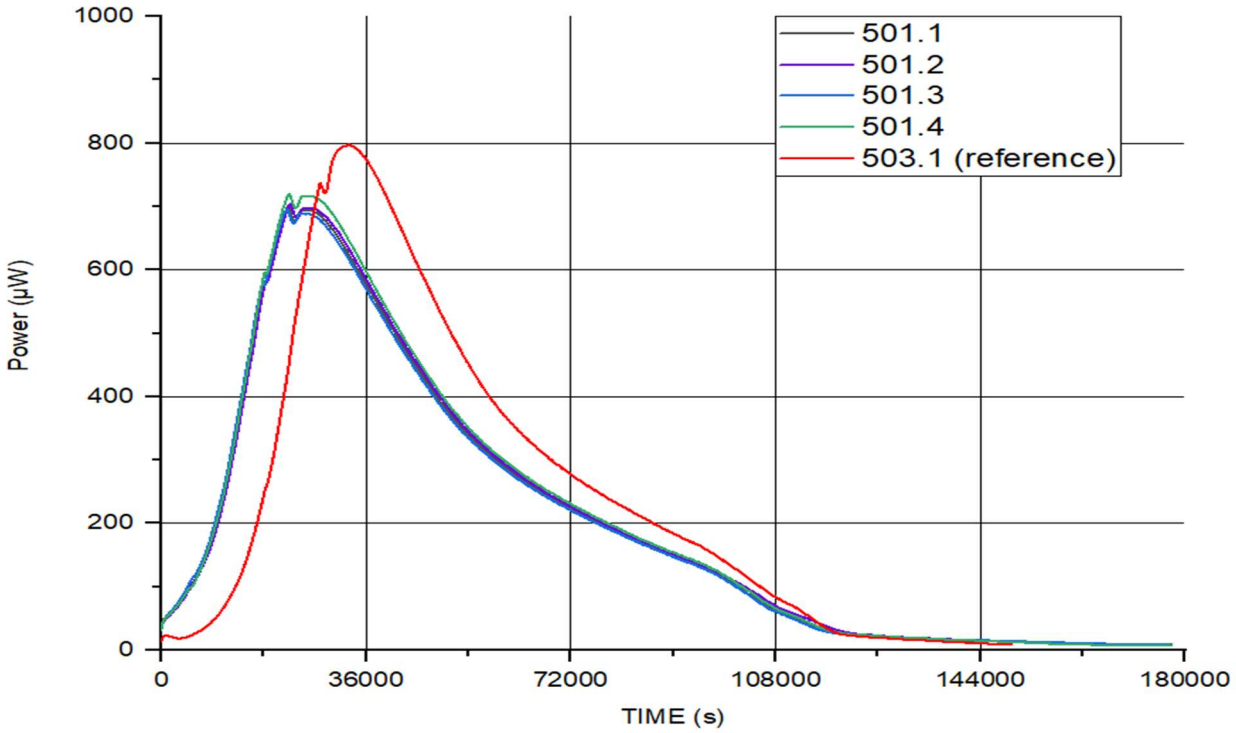

Figure 4.29 *L. rhamnosus* pure grown in MRS for 24 hours at 37ºC, tested in MRS (in quadruplicate). For comparison, 503.1 (red reference curve) is *L. rhamnosus* pure tested in MRS.

Experiment	501.1	501.2	501.3	501.4	503.1
p-t curve parameter					
PP [µW]	701	704	696	720	798
Time to PP[s]	22351	22721	22111	22451	32940
AUC to PP	6.95×10^{6}	7.05×10^{6}	6.93×10^{6}	7.09×10^{6}	9.97×10^{6}
ln curve parameters					
Slope	1.52×10^{-4}	1.51×10^{-4}	1.50×10^{-4}	1.56×10^{-4}	1.89×10^{-4}
Intercept	3.83	3.80	3.89	3.77	2.13
R^2	0.999	0.999	0.999	0.999	0.999

Table 4.19 Basic shape analysis parameters and logarithmic transformation parameters of *L. rhamnosus* grown in MRS for 24 hours at 37ºC (501 series), tested in MRS. 503.1 reference values for comparison.

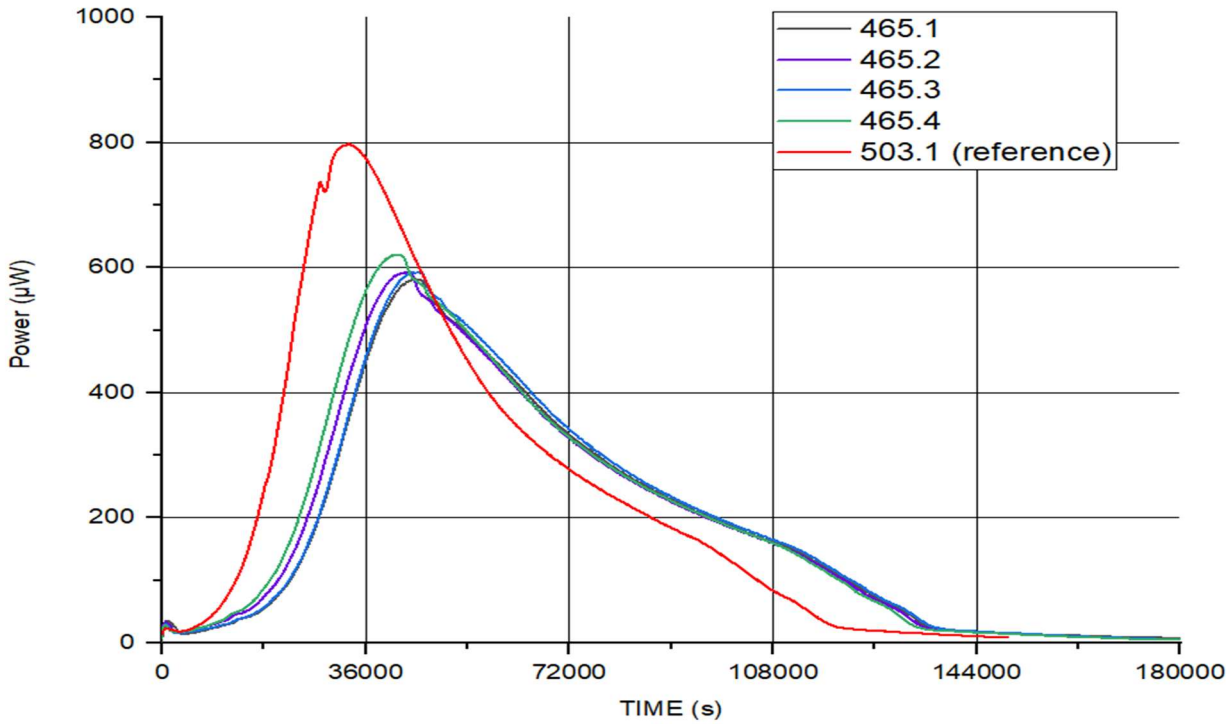

Figure 4.30 *L. rhamnosus* grown in MRS for 48 hours at 37ºC, tested in MRS (in quadruplicate). For comparison, 503.1 (red reference curve) is *L. rhamnosus* pure tested in MRS.

Experiment	465.1	465.2	465.3	465.4	503.1
p-t curve parameter					
PP [µW]	581	592	592	621	798
Time to PP[s]	44612	42902	45652	41472	32940
AUC to PP	8.89×10^{6}	9.14×10^{6}	9.67×10^{6}	9.37×10^{6}	9.97×10^{6}
ln curve parameters					
Slope	1.33×10^{-4}	1.30×10^{-4}	1.30×10^{-4}	1.32×10^{-4}	1.89×10^{-4}
Intercept	1.61	1.97	1.73	2.09	2.13
R^2	0.999	0.999	0.999	0.999	0.999

Table 4.20 Basic shape analysis parameters and logarithmic transformation parameters of *L. rhamnosus* grown in MRS for 48 hours at 37ºC (465 series), tested in MRS. 503.1 reference values for comparison

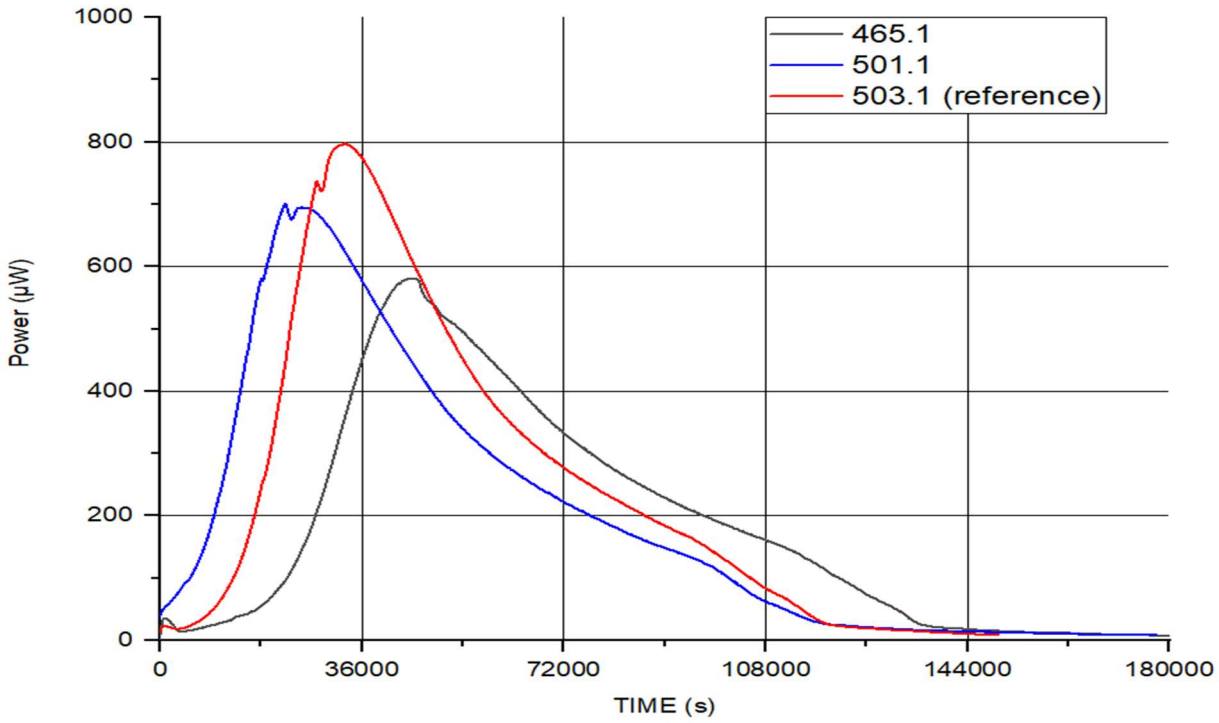

Figure 4.31 Visual (shape analysis) assessment of p-t curves of *L. rhamnosus* pure and the same *L. rhamnosus* pure pre-cultured for 24 and 48 hours in MRS.

Experiment	**465_{48}**	**501_{24}**	**503.1**
p-t curve parameter			
PP [µW]	597	705	798
Time to PP[s]	43660	22409	32940
ln curve parameters			
Slope	1.31×10^{-4}	1.53×10^{-4}	1.89×10^{-4}
Intercept	1.85	3.82	2.13
R^2	0.999	0.999	0.999

Table 4.21 Comparison of *L. rhamnosus* pure (503.1) with *L. rhamnosus* grown in MRS at 37ºC for either 24 hours or 48 hours. ().

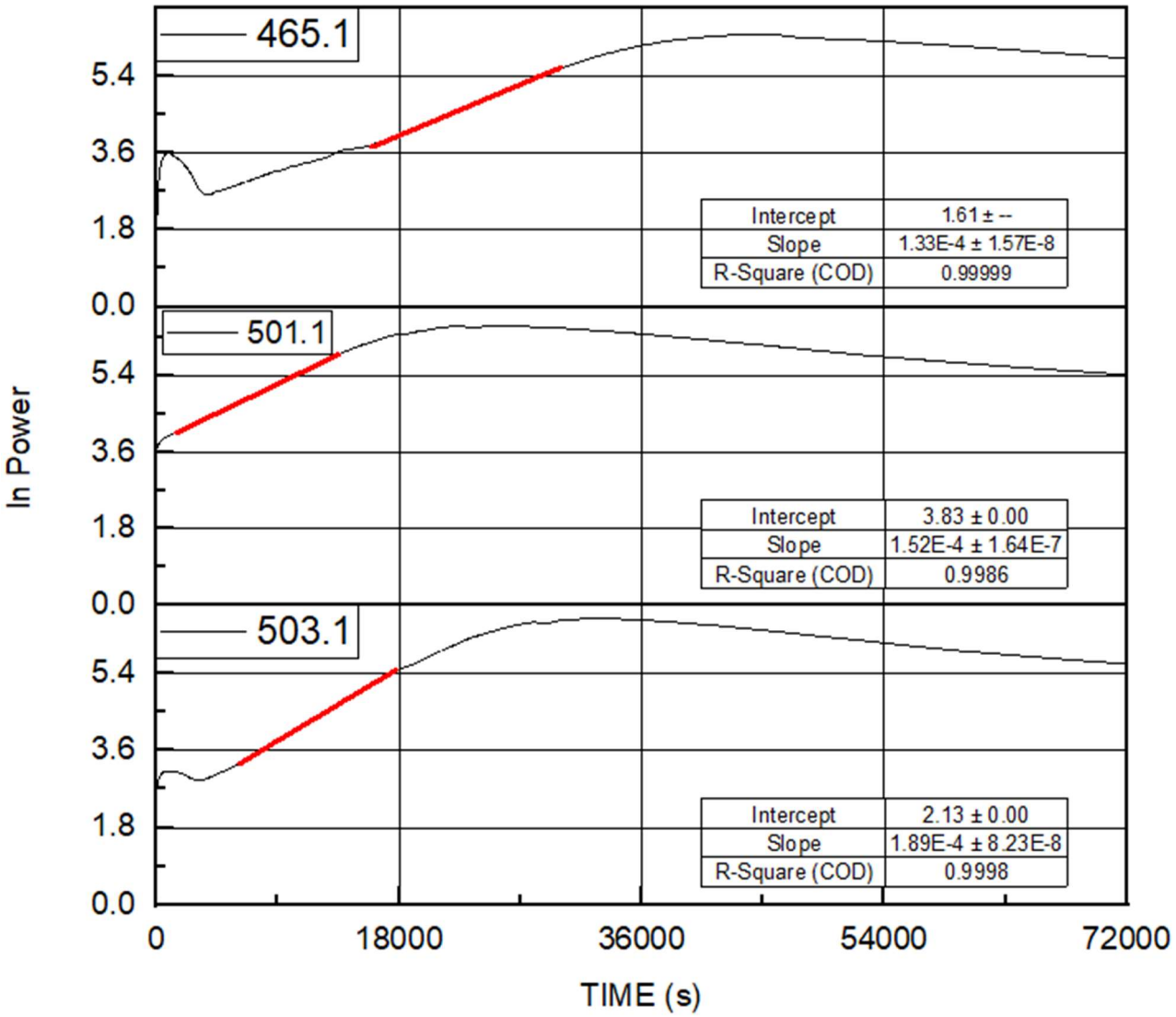

Figure 4.32 Logarithmic transformation of p-t curves (465.1, 501.1 and 503.1) and applying a linear regression model. Red portions indicated in each curve represent linear fits determined visually to get the best R^2.

4.3.3.1 Discussion

The method of pre-culturing *L. rhamnosus* pure seemed to be advantageous if there was a need to shorten the lag time. It was plausible that when *L. rhamnosus* pure was pre-conditioned –grown in one medium (*e.g.*, grown in MRS prior to testing in MRS, or potentially in any other medium such as wort)– this would give it better properties for subsequent faster growth in the same medium (as the one that was used for pre-conditioning).

However, an optimal pre-conditioning time would need to be experimentally determined, because if the same *L. rhamnosus* pure was grown in MRS for 48 hours at 37ºC (see **Figure 4.30**) this had an opposite effect. The reason behind this might be the effects of metabolic

build up during the extra 24 hours of growth when compared to the *L. rhamnosus* pure grown in MRS for 24 hours only. The metabolism of *L. rhamnosus* pure showed some change according to all parameters after it was grown in MRS either for 24 or 48 hours (see **Table 4.21**) when compared with the reference values (503.1).

A closer examination comparing 24 hours and 48 hours data showed that AUC_{48} was bigger than AUC_{24}; the slope k_{48} was 1.3 x10^{-4} which was different from k_{24} of 1.5 x10^{-4}; time to PP was extended in 48 hours growth to almost double of 24 hours growth; and the PP was higher in 24 hour growth than that in 48 hours growth. Even though both growths (24 and 48 hours) were done in the same MRS they were still reacting differently with longer lag time for 48 hours growth. There was a significant difference in the rates of growth between these two cultures. Whilst the differences in the intercept values between the two cultures could be attributed to differences in cell numbers, the different *k* values were not well understood (there could be some change in metabolic processes related to cell age, or the effects of a build-up of metabolites).

Unfortunately, because of an incapacity to determine cell numbers, there was no more in-depth analysis of these different rates of growth or indeed the cells themselves. However, even in the absence of cell counts, (something that some would regard as critical information), an outcome which in principle, appeared to offer a significant advantage to Symprove was obtainable and analysable.

If Symprove company adopted this approach, the presented data revealed that the fermentation would have to be controlled much more carefully, and would have to stop at a precise time, not a random or a wide range of time, but exact time because the cells change and will have different properties in accordance with the time and temperature they spend in the growth medium. Therefore, what these experiments were also doing were directing towards a prescription for control of Symprove production process and a simple protocol for stability and viability testing (shelf life of the product).

It was established that a useful and practical reference system (*L. rhamnosus* pure in MRS) could be developed. The reproducibility of the experiments was better than the traditional microbiology. Easily extractable parameters from the p-t curve (PP, time to PP, AUC to PP) and its logarithmic transformation (growth rate constant, intercept) could be used to determine a good growth with high accuracy and high reproducibility. It was considered

worthwhile at this point to go further and explore the possibilities of automation of data processing (**4.3.4**) and to establish the same reference systems for *L. acidophilus* (**4.3.5**), the combination of the two –FV1-artificial (**4.3.6**) as well as investigating FV1-real (**4.3.7**).

It was demonstrated in this chapter so far that:

- the prerequisites of repeatability of the system of interest (testing procedure for *L. rhamnosus*, which was the most challenging one in Symprove product) were met;
- the equations (**Chapter 3**) and interesting parameters (growth rates, intercepts, AUCs) were reinforced by the presented data, which showed the conformity between data derived from PC and OD with IMC data; in other words, a sound relationship between classical microbiological methods and IMC was established;
- IMC was capable of yielding useful data for a real utility of IMC towards industry in general and specifically Symprove. An excellent reproducibility for standardised experiments was achieved and this led towards a possibility to establish a reference reaction which showed not only that the performance of the calorimeter could be checked but also allowed to have a view about the best-case scenario and a confidence that the IMC data were better, in principle, that those of the classical microbiology. The accuracy and reproducibility in the above detailed controlled experiments was very good, therefore, it was reasonable to expect that in the real world of an industrial scale production a good reproducibility and accuracy could be achieved. The potential for the utility of IMC here was great, it related well to classical microbiology, but it did better in many aspects mentioned (accuracy, repeatability, dealing easily with complex samples and speed of testing);
- IMC was capable of investigating differences in medium composition affecting the growth kinetics of a microbiological system (exemplified by *L. rhamnosus* grown in different growth media (**4.3.2** and **4.3.3**) before being tested in the calorimeter). This also contributed to extending the possibilities of investigating the history of a given microorganism.

The following sections investigated, in the same manner, the second component of FV1 –*L. acidophilus* (section **4.3.5**) and the combination of the two microorganisms *i.e.*, FV1-artificial (section **4.3.6**) before proceeding to the full complexity of FV1-real (section **4.3.7**) because it was absolutely clear that IMC had the capacity to investigate Symprove's or any other such system.

4.3.4 Coding and automation

The previous section **4.3.1** laid ground for the manual analysis required to obtain quantitative parameters from a simple p-t curve. In order to take the manual analysis of data forward, it would be good to have an automated approach (data processing algorithm) which could do a simple modelling of *k* (growth rate constant) based on a logarithmic plot. Other desirable parameters such as peak power, time to peak power, the value of the peak power, the intercept and the coefficient of determination would also form a part of a parameter comparison automated output (compared with expected values, *i.e.*, reference values) which would not require a specialist to determine whether the growth was good or not; essentially provide a BB to data analysis. The procedure was previously demonstrated (see Cabadaj *et al*., 2021), where it was established that the concordance between the manual and coding analysis was good, however coding could make sure that as much time as possible was saved in analysis. Enabling an easy industrial application of the automated data analysis would require a BB with raw data as an input and pass/fail answer as an output. Black box is briefly discussed in the second part of this section.

The automatic data processing was only applied to *L. rhamnosus* pure set as a proof of concept. There was no further automatic analysis presented. The reason for not continuing the automatic data processing was the death of David Haskins (to whom I am ever thankful), the code developer, during this project and related difficulties (the program was not accessible thereafter which meant that the cost and time required to resolve those issues was not feasible within the time frame of this project) in enabling the code to run on a different platform.

4.3.4.1 Coding development

The raw data coming from the growth of bacteria were recorded by the TAM every 10 seconds in power-time format. Consequently, there was an enormous data yield available for analysis and that meant if coding could be written (using the knowledge of the equations developed in **Chapter 3**) the whole analysis could be automated. The role of such an automated quantitative data analysis would be to determine, much faster than a manual analysis and operator independent, whether the investigated p-t curves were pass or fail when compared with a reference.

The logarithmic transformation of the original data set meant that any first order reaction (*e.g.*, exponential bacterial growth, but also any other first order processes) would be visible as a linear portion of the given data set. The coding required to find the best straight line up to the peak power (because there was no exponential growth after peak power, concerning *L. rhamnosus* growth in MRS and the same was observed in later sections in *L. acidophilus* as well as FV1, and this thesis treats only the exponential growth period). Therefore, this basic analysis of plotting logarithm of power against time would yield, in principle, the first order process *i.e.*, exponential bacterial growth (the interpretation of the first linear phase is the exponential growth). The advantage of the logarithmic transformation approach application into bacterial growth, by definition, (see **Chapter 3**) was that the slope of the straight line obtained, from the region of exponential growth, was the rate constant of the exponential bacterial growth. This linear portion could be extrapolated back where y=0, and this would indicate the theoretical time point at which the bacteria started to double exponentially. To make sure that the coding approach was in line with the manual analysis, both approaches were done simultaneously and compared (these are presented in **Table 4.22** and more detail in Cabadaj *et al*. (2021)).

Some of the advantages of the automatic approach to data processing included:

- technician or scientist independent interpretation of complex data;
- fast and consistent data processing (no subjectivity in selecting predefined parameters and getting the results in the matter of seconds);
- prospect of a rapid enquiry into performance both bacterial performance in the calorimeter (*e.g.*, FV1-real, in principle, the full product, too) as well as the performance of the calorimeter over time (using a control reaction *e.g.*, *L. rhamnosus* pure in MRS).

Coding with its obvious advantages (fast data processing and always selecting predefined parameters) also had the deficiency that no scientist/expert would look at once it became a routinised procedure for a technician. The control over the black-box system would be given to coding therefore any anomaly from an expected, pre-defined parameters would automatically mean a failed result.

Analysis (*L. rhamnosus* pure)	Slope (s^{-1})	Intercept
Manual	1.88 ± 0.06 $x10^{-4}$	2.12 ± 0.07
Coding	1.34 ± 0.06 $x10^{-4}$	3.00 ± 0.10

Table 4.22 Mean values for the slope and intercept calculated for the first linear region of the logarithmically transformed p-t curves derived by manual analysis and with the coding analysis. *L. rhamnosus* pure in MRS (mean of 4 experiments, series 503).

Despite the ambition set forth at the beginning of the project to have completely scientist independent analysis of data *i.e.*, black box, most of the data were analysed manually, because of the loss of access to the coding program as described in **4.3.4**. However, the close relationship between the coding outcomes and manual calculations were already demonstrated (**Table 4.22**; Cabadaj *et al*., 2021) and the unfortunate death of the code developer did not at all invalidate the notion that coding was employable directly and if developed and introduced by Symprove would provide a technician manageable situation.

4.3.5 *L. acidophilus* pure tested in MRS

Quantitative analysis of IMC data and its practical applications was demonstrated in **4.3.1**, using *L. rhamnosus* as a model organism. This study formed a basis for the analysis of *L. acidophilus* –the second bacterial component of FV1 in the same way. This section establishes reference standards of *L. acidophilus* pure tested in MRS (the same protocol was followed as previously described for *L. rhamnosus* pure in **4.2.1**). The results are presented in **Figure 4.33**, **Table 4.23** and **Table 4.24**.These results formed a basis for a quantitative parameter comparison for the performances of the two microorganisms in a calorimeter. Whether it was possible to distinguish between the two microorganisms (*e.g.*, did they behave differently in the same medium?), based on the parameters studied was elucidated here and in more detail in **4.3.7** (**Table 4.36** and **Table 4.37**). In all subsequent studies the same testing protocol as in **4.2.1** was followed (unless stated otherwise).

Whilst IMC got quantitative data faster and more accurately than the traditional plate count methods (**Chapter 2**) it also offered a characteristic performance of, for example *L. rhamnosus* in the standard experiment (described as being a reference experiment in **4.3.1**). Therefore, if *L. acidophilus* was subjected to the same testing procedure, it would yield data

which could be used to determine how different, if at all, the performances of these two microorganisms were. In other words, they would be different if their p-t curves were different (*i.e.*, where comparisons of derived data were presented, for example studies with *L. rhamnosus*, *L. acidophilus*, FV1-artificial or FV1-real then differences were declared if the respective means ±2SD did not overlap).

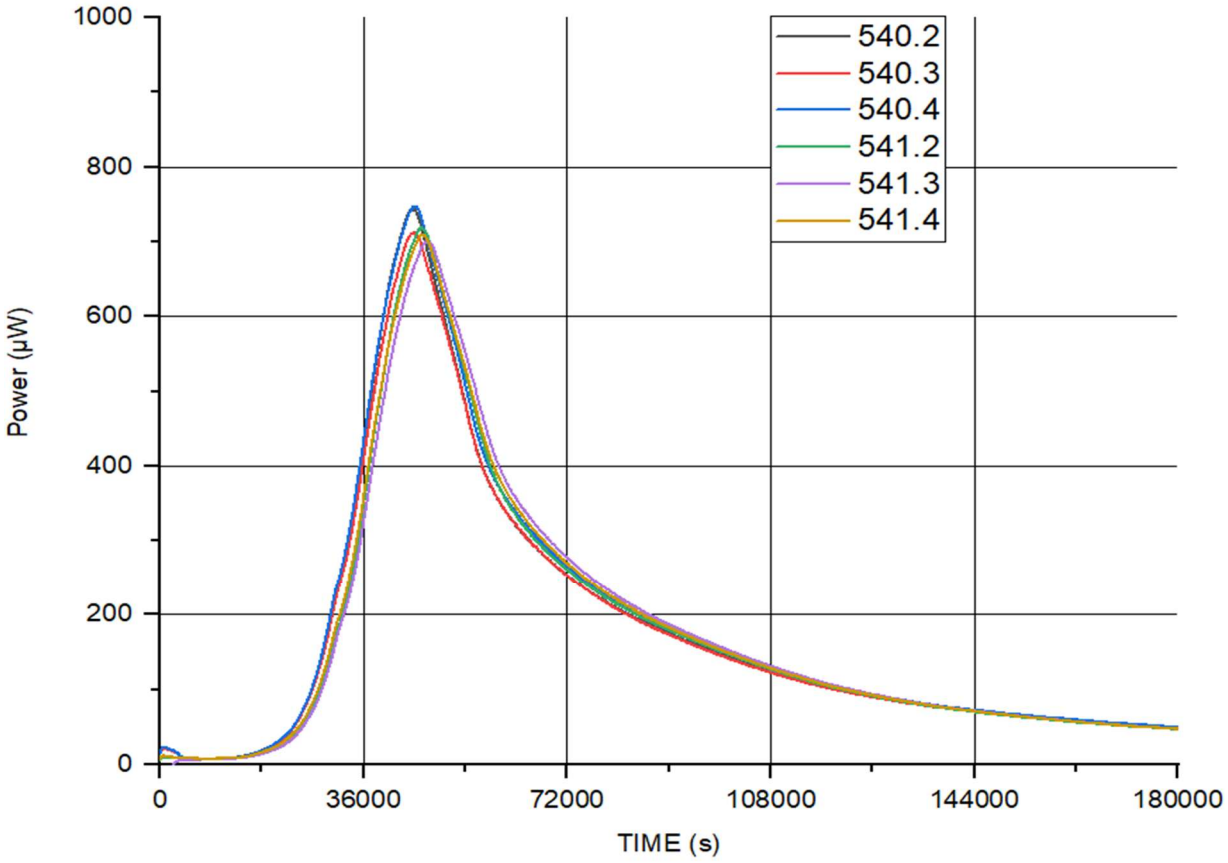

Figure 4.33 P-t curves of *L. acidophilus* pure tested in MRS.

Experiment number	540.2	540.3	540.4	541.2	541.3	541.4
p-t curve parameters						
PP [µW]	746	713	748	719	701	710
Mean PP	723					
SD (reproducibility)	18 (2.49%)					
Time to PP [s]	44722	45072	44972	46132	47252	46372
Mean time to PP [s]	45754					
SD (reproducibility) [s]	905 (1.98%)					
AUC to PP	8.25×10^6	8.11×10^6	8.48×10^6	8.00×10^6	8.13×10^6	8.24×10^6
Mean AUC to PP	8.20×10^6					
SD (reproducibility)	1.50×10^5 (1.83%)					

Table 4.23 Basic shape analysis parameters of *L. acidophilus* pure tested in MRS. 540 series time distant from 541 series.

Experiment number	540.2	540.3	540.4	541.2	541.3	541.4
ln curve parameters						
k	2.05×10^{-4}	2.06×10^{-4}	2.08×10^{-4}	1.99×10^{-4}	2.02×10^{-4}	1.99×10^{-4}
Mean *k*	2.03×10^{-4}					
SD *k* (reproducibility)	3.44×10^{-6} (1.69%)					
Intercept (ln value)	-0.90	-0.95	-0.97	-0.99	-1.18	-0.96
Mean intercept	-0.99					
SD (reproducibility)	0.09 (9.09%)					
Intercept (antiln value)	0.41	0.39	0.38	0.37	0.31	0.38
Mean intercept	0.37					
SD (reproducibility)	0.03 (8.11%)					
AUC to PP	1.82×10^5	1.83×10^5	1.84×10^5	1.83×10^5	1.79×10^5	1.86×10^5
Mean AUC to PP	1.83×10^5					
SD (reproducibility)	2.11×10^3 (1.15%)					
R^2	0.9999	0.9998	0.9999	0.9997	0.9999	0.9999
Mean R^2	0.9999					
SD (reproducibility)	7.64×10^{-5} (0.008%)					

Table 4.24 Parameters derived from the logarithmically transformed p-t curves. *L. acidophilus* pure tested in MRS.

Basic shape analysis of the p-t curves (**Table 4.23**) showed a high degree of reproducibility in these experiments. PPs' reproducibility was within 2.49% (providing the organism and the medium were controlled). The AUCs to PP were reflective of the exponential growth and these again were highly reproducible (1.83%) whilst times to reach PPs were also highly consistent (1.98%). This was encouraging as it was possible to establish, with a high degree of confidence, that calorimetry could yield highly consistent results for both microorganisms (*L. rhamnosus* and *L. acidophilus*).

4.3.5.1 Growth rate constant

The growth rate constant (slope *k*) was obtained in the same way as the slope derived in **4.3.1.3.1**. The significance of the difference between the slopes of the two microorganisms as well as the FV1-artificial and FV1-real is discussed at the end of this chapter. However, it was clear from the data (**Table 4.24** and **Table 4.5**) that a distinction between the slopes of *L. acidophilus* (mean 2.03 $x10^{-4}$) and *L. rhamnosus* (mean 1.87 $x10^{-4}$) could be determined (the means ± 2xSD did not overlap).

4.3.5.2 Intercept

Table 4.24 shows that the reproducibility of the intercept values was lower than the one obtained for *L. rhamnosus*. The calorimetric method used was highly sensitive to small variations or errors (medium preparation, testing procedure precision, inoculum volume) therefore a rather dramatic response of the intercept (or some other parameter) could be seen as a result. Yet, the reproducibility achieved was more in line with the traditional plating methods for this parameter, therefore acceptable.

4.3.5.3 Contaminant detection

One frequent problem encountered in the production process of Symprove was FV1-real cross-contaminated by *E. faecium* (Symprove strain) and in addition to that some batches of FV1-real were contaminated with another strain of *E. faecium* (as detailed in **2.6.3**). These contaminations were the reasons for exploring the capacity of IMC to detect *E. faecium* in co-culture of *L. acidophilus*. The results are presented in **Figure 4.34** and **Table 4.25**. There

were no mean values or SD values available as these were single experiments (no repeats), data were obtained from *L. acidophilus* spiked with *E. faecium* contaminant.

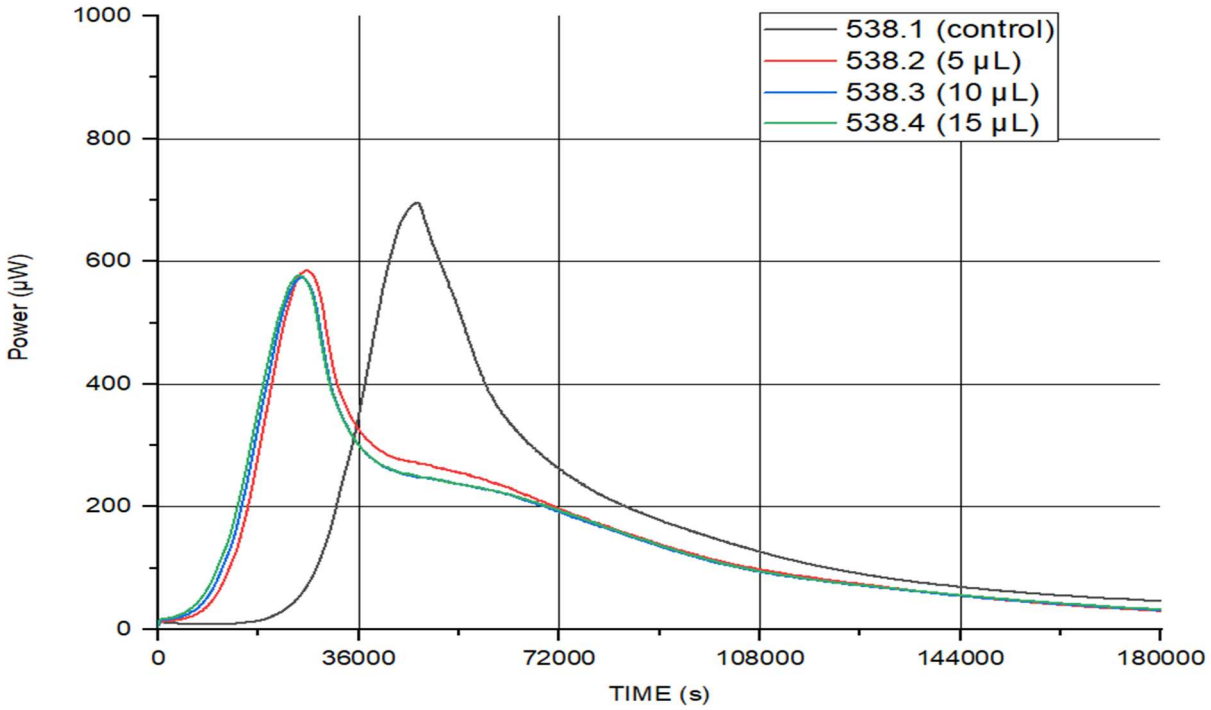

Figure 4.34 P-t curves of *L. acidophilus* pure (black curve) and the same *L. acidophilus* pure spiked with 3 different concentrations of *E. faecium*; tested in MRS.

Experiment number	**538.1**	**538.2**	**538.3**	**538.4**
E. faecium inoculum volume (µL/ampoule)	0	5	10	15
p-t curve parameters				
Time to PP [s]	46712	26592	25742	25442
PP [µW]	696	585	574	577
AUC to PP	8.4×10^{6}	5.41×10^{6}	5.47×10^{6}	5.69×10^{6}
ln curve parameters				
k	1.97×10^{-4}	2.45×10^{-4}	2.37×10^{-4}	2.29×10^{-4}
Intercept (ln value)	-0.98	1.48	1.88	2.17
Intercept (antiln value)	0.38	4.39	6.55	8.76
R^2	0.9999	0.9996	0.9997	0.9998

Table 4.25 Basic shape analysis parameters and parameters derived from logarithmically transformed p-t curves.

4.3.5.4 Discussion

It was discovered that the performance of *L. acidophilus* in the calorimeter was different from that of *L. rhamnosus*. All the basic shape analysis parameters of *L. acidophilus* (mean PP = 727 μW, mean AUC = 8.20 $x10^6$ and mean time to reach PP = 45754 seconds) were significantly different from those of *L. rhamnosus* (mean PP = 790 μW, mean AUC of 9.83 $x10^6$ and mean time to reach PP 33208 seconds).

Looking at the parameters derived from the logarithmic transformation of the p-t curves, it was also clear that the growth rate of *L. acidophilus* (2.03 $x10^{-4}$) and the growth rate of *L. rhamnosus* (1.87 $x10^{-4}$) were different. Additionally, all the parameters (except the *L. acidophilus* intercept values) were of high reproducibility of less than 3%.

The analysis of *L. acidophilus* contaminated with 3 different concentrations of *E. faecium* showed that there were significant differences between *L. acidophilus* pure and *L. acidophilus* spiked with *E. faecium* (see **Table 4.25**). The higher the concentration of *E. faecium* the shallower the slopes. AUCs to PP were significantly smaller when *E. faecium* was present compared with the AUC reference value of *L. acidophilus* pure. It was possible that the two microorganisms affected each other, for example, influences of their metabolites, resulting in different growth rates. It was also probable that enthalpies per cell of the two microorganisms were marginally different. Furthermore, the highest concentration of *E. faecium* (15 μL) generated the largest AUC (when comparing *E. faecium* containing experiments only). Finally, the higher the concentration of *E. faecium* the faster the time to reach PP.

It was established that, by using calorimetry alone, it was possible to distinguish between the performance of *L. acidophilus* and *L. rhamnosus* based on the selected parameters. It was therefore rational to proceed further and test these two microorganisms together – formulating FV1-artificial. This step was essential in determining whether the same analysis was viable to investigate FV1-real.

4.3.6 FV1-artificial tested in MRS

“Artificial” in the context of this section means that *L. acidophilus* and *L. rhamnosus* were in 1:1 ratio and their individual inoculum cell densities were the same when inoculated into MRS. The main purpose was to determine what was the behaviour (performance in a

calorimeter) of FV-artificial with respect to *L. rhamnosus* and *L. acidophilus*, separately (How did FV1 relate to the growth of *L. rhamnosus* and *L. acidophilus*?). For example, was FV1-artificial a mixture of the two microorganisms, was one dominant over the other? Furthermore, contaminants were a natural but irregular occurrence in the production process, and to this end the sensitivity of IMC to detect a selected contaminant –*E. faecium* was investigated.

The same testing protocol was followed for FV1-artificial as for *L. rhamnosus* and *L. acidophilus*, except that the inoculum was made up of 50:50 % mixture of the two organisms so that the same number of organisms were added. The results are in **Figure 4.35**, **Table 4.26** and **Table 4.27**. There were two time-distant series of experiments performed *i.e.*, 527 series and 535 series, and for each series a fresh batch of MRS was used, the consequences of which is discussed below.

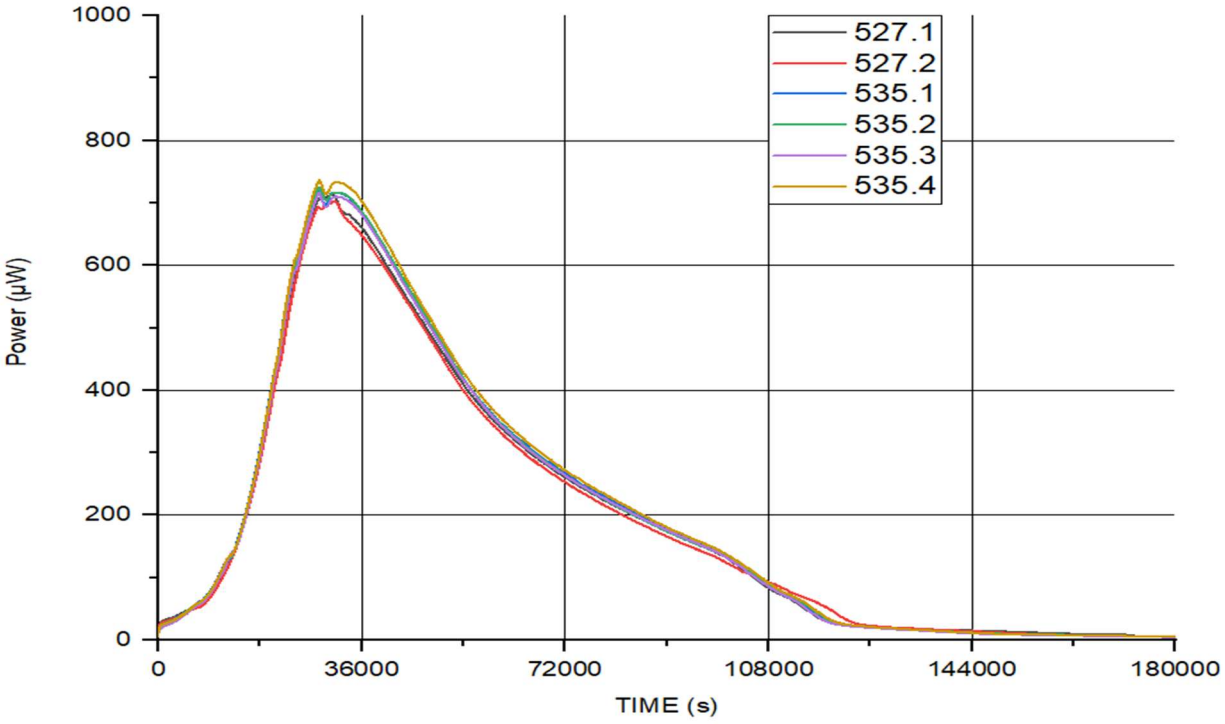

Figure 4.35 P-t curves of FV1-artificial tested in MRS.

Experiment no	527.1	527.2	535.1	535.2	535.3	535.4
p-t curve parameters						
PP [µW]	714	702	723	725	716	736
Mean PP	719					
SD (reproducibility)	11 (1.53%)					
Time to PP [s]	30932	31192	28372	28472	28422	28452
Mean time to PP [s]	29307					
SD (reproducibility) [s]	1244 (4.24%)					
AUC to PP	9.01×10^6	9.05×10^6	7.49×10^6	7.52×10^6	7.33×10^6	7.56×10^6
Mean AUC to PP	7.99×10^6					
SD (reproducibility)	7.37×10^5 (9.21%)					

Table 4.26 Basic shape analysis parameters of FV1-artificial tested in MRS.

Experiment no	527.1	527.2	535.1	535.2	535.3	535.4
ln curve parameters						
k	1.61×10^{-4}	1.60×10^{-4}	1.63×10^{-4}	1.62×10^{-4}	1.62×10^{-4}	1.63×10^{-4}
Mean *k*	1.62×10^{-4}					
SD *k*	1.07×10^{-6} (0.66%)					
Intercept (log value)	2.79	2.78	2.79	2.79	2.77	2.78
Mean intercept	2.78					
SD (reproducibility)	0.007 (0.25%)					
Intercept (antilog value)	16.28	16.12	16.28	16.28	15.96	16.12
Mean intercept	16.17					
SD (reproducibility)	0.12 (0.74%)					
AUC to PP	1.60×10^5	1.61×10^5	1.44×10^5	1.44×10^5	1.43×10^5	1.44×10^5
Mean AUC to PP	1.49×10^5					
SD (reproducibility)	7.91×10^3 (5.30%)					
R^2	0.9995	0.9997	0.9994	0.9994	0.9992	0.9993
Mean R^2	0.9994					
SD (reproducibility)	0.0002 (0.02%)					

Table 4.27 Parameters derived from the logarithmically transformed p-t curves of FV1-artificial tested in MRS.

4.3.6.1 Growth rate constant

Data presented in **Table 4.27** showed excellent reproducibility (0.66%) in the growth rate constant. Whilst the rates of growth were very consistent in the two series (527 and 535), it was clear that the times to reach PP were less so (**Table 4.26**). This was perhaps caused by the effects of the medium and its capacity to support growth of the same bacteria to the same extent (2 distinct batches of MRS were used), and as discussed in the previous part (**4.3.5.2**) even a small variation in medium preparation (*e.g.*, uniformity of powder, water composition *etc.*) could have a significant impact on some parameters given the high sensitivity of IMC.

4.3.6.2 Intercept

The reproducibility of the intercept values was better than those obtained for *L. rhamnosus,* and this might be caused in part by the subjectivity of the manual analysis of data. The best straight line was selected based on the best R^2 and that fixed the exact duration of the linear fit. This meant the intercept values varied and if better consistency in selecting the individual linear fits was required (*e.g.*, time exact linear portions would be selected) this would affect R^2. It seemed rational to base the analysis on the best R^2 as the linear portion with the highest R^2 would best represent the exponential growth under investigation.

4.3.6.3 Contaminant detection

The microorganism chosen for this study, *Enterococcus faecium* NCIMB 30176, was the component of the second fermenting vessel (FV2) and the finished product, Symprove, however, it was also detected in FV1-real because of a cross-contamination issue in the production process. Whilst this contamination would not pose a serious health risk, it had the potential to disturb the bacterial balance of the finished product, hence it was important to have a tool to be able to detect it. The purpose of this study was to determine, whether it was possible to detect *E. faecium* in co-culture with FV1-artificial by using IMC. Four samples of the same FV1-artificial were used; one without any *E. faecium* - the control and three samples with different volumes of *E. faecium* (*i.e.*, 5, 10 and 15 µL; these were selected to see the sensitivity of IMC to detect low levels of the contaminant) were directly added to 30 µL of the remaining three FV1-artificial samples –**Figure 4.36**.

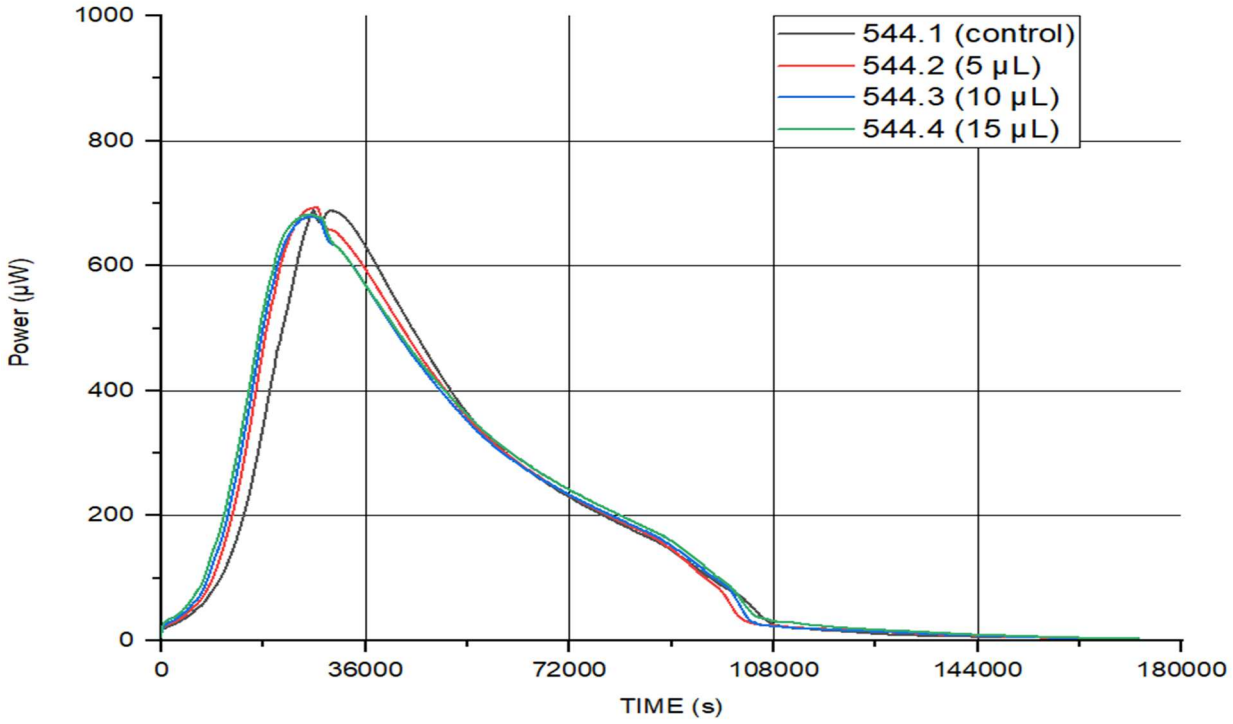

Figure 4.36 P-t curves of uncontaminated FV1-artificial (black curve) and the same FV1-artificial batch spiked with 3 different concentrations of *E. faecium*; tested in MRS.

Experiment number	**544.1**	**544.2**	**544.3**	**544.4**
E. faecium inoculum volume (µL/ampoule)	0	5	10	15
p-t curve parameters				
Time to PP [s]	26872	27372	26502	25572
PP [µW]	689	693	679	682
AUC to PP	6.8×10^{6}	8.6×10^{6}	8.4×10^{6}	8.2×10^{6}
ln curve parameters				
k	1.64×10^{-4}	2.09×10^{-4}	2.35×10^{-4}	2.40×10^{-4}
Intercept (ln value)	2.90	2.72	2.68	2.80
Intercept (antiln value)	18.17	15.18	14.59	16.44
R^2	0.9998	0.9998	0.9992	0.9995

Table 4.28 Basic shape analysis parameters and parameters derived from logarithmically transformed p-t curves of FV1-artificial spiked with *E. faecium*. .

The three curves (**Figure 4.36**) containing *E. faecium* looked very reproducible and distinctively different from that of the control curve. Quantitative parameters presented in **Table 4.28** (there were no mean values or SD values available as these were single experiments with no repeats) showed that the more *E. faecium* present the faster the time

to PP, this trend however, was not observed in the control, which was more in line with 10µL *E. faecium*. Another example of systematic differences was notable in AUC to PP where the lowest *E. faecium* content at inoculation produces largest AUC to PP with a regular interval decrease (2 x10^5) for the other two *E. faecium* inoculation volumes whilst the control AUC to PP was significantly different from all three samples containing *E. faecium*.

4.3.6.4 Discussion

Whilst PPs showed good reproducibility (1.53%, see **Table 4.26**), times to reach PP were less consistent between the two series 527 and 535. One of the reasons for less consistency was perhaps the fact that there were double peaks, and these were different (the first peak in 527 series did not represent PP of this series, however it occurred at the time when the PP of the second series 535 was observed; furthermore, the reverse phenomenon was observed for PP of 527 series; *i.e.*, the second peak was the PP) (see **Figure 4.37**). The mean time difference between the two series to reach PP was 2633 seconds (527 mean time to reach PP minus 535 mean time to reach PP). This meant that AUCs was significantly different (**Table 4.26**). One explanation why double peaks were close to each other in both series, but in reverse order, when the two series were compared, could be perhaps minimal medium composition differences. Two batches of MRS were used as mentioned earlier in **4.3.6.1**; even though the fundamentals were declared the same; *i.e.*, both MRS batches were made from the same bottle of dehydrated MRS powder, using the same protocol. In these experiments a surprisingly high sensitivity to medium composition was discovered. It was known that there were two batches of MRS when these were made for the experiments and this was later seen in the results. Consequently, what was regarded as a reference would only be a reference for the particular batch of MRS. Therefore, each time a batch of MRS was changed, a reference must be recreated as well (this is not a problem in any setting because doing just 4 experiments in a 4-channel instrument would be sufficient for a particular batch of MRS as was demonstrated with 503 series in **4.3.1**).

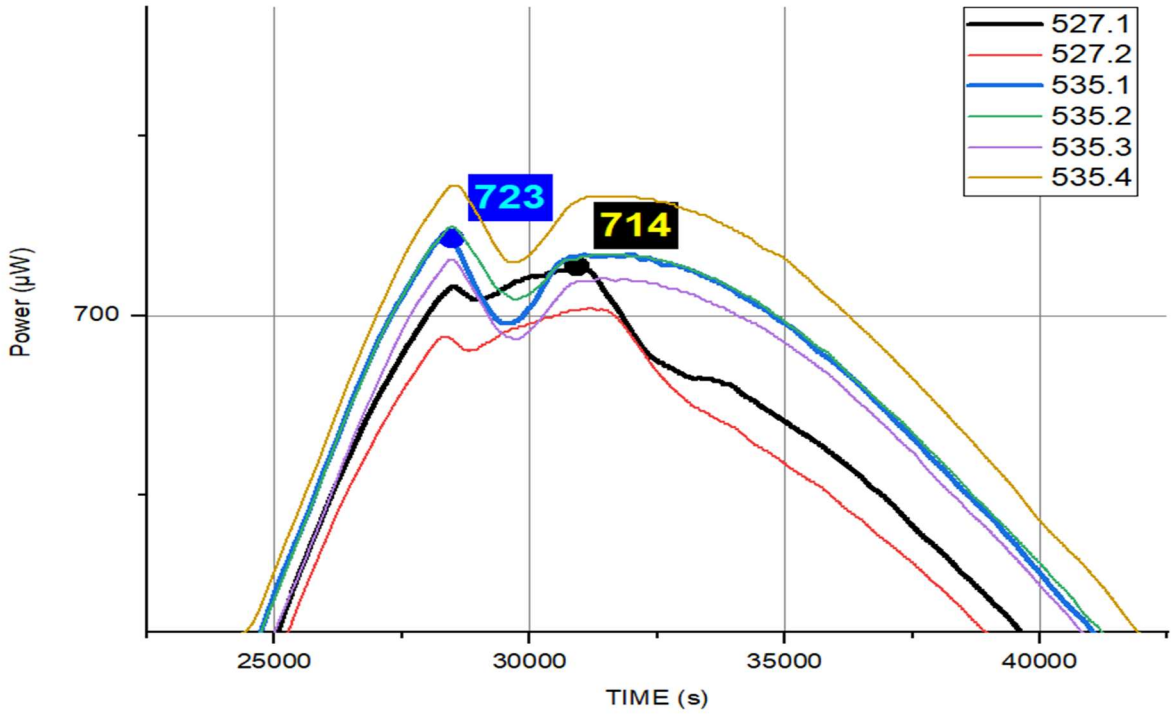

Figure 4.37 Times to reach PP detail for 527 and 535 series (zoom of **Figure 4.35**). PPs_{527} are time distant from PPs_{535}. $PP_{535.1}$ (723µW –blue rectangle) and $PP_{527.1}$ (714 µW –black rectangle)

It seemed, considering the p-t shapes only, that *L. rhamnosus* was more dominant in co-culture with *L. acidophilus*, although PP of *L. rhamnosus* was affected most likely by *L. acidophilus*. Having made the comparison of the individual parameters of *L. rhamnosus*, *L. acidophilus* and FV1-artificial (**Table 4.29** and **Table 4.30**), PP in FV1-artificial was down from *L. rhamnosus* PP, but consistent with *L. acidophilus* PP. The higher PP of *L. rhamnosus* when individually tested might be impeded by the presence of *L. acidophilus*, therefore the PP was lower for *L. rhamnosus* when in pair with *L. acidophilus*. Interestingly, time to PP was shortest when the two organisms were together, which could be a consequence of their competition for nutrients, and this could also be a reason why *L. rhamnosus* produced higher PP when on its own. If AUC to PP was considered as an indicator of the extent of growth of an organism, then the two organisms together produced the lowest AUC to PP, which would indicate there were some interaction (competition for nutrients, some inhibition of growth, metabolites build up) between them.

Experiment	*L. rhamnosus* pure *	*L. acidophilus* pure *	FV1-artificial *
p-t curve parameters			
Mean PP [µW]	790	723	719
SD (reproducibility)	12 (1.52%)	18 (2.49%)	11 (1.53%)
Mean Time to PP [s]	33208	45754	29307
SD (reproducibility) [s]	317 (0.95%)	905 (1.98%)	1244 (4.24%)
Mean AUC to PP	9.83×10^6	8.20×10^6	7.99×10^6
SD (reproducibility)	1.61×10^5 (1.64%)	1.50×10^5 (1.83%)	7.37×10^5 (9.21%)

Table 4.29 Quantitative data (p-t curve derived) for the individual organisms *L. rhamnosus*, *L. acidophilus* and FV1-artificial. *Mean of six individual experiments.

Experiment	*L. rhamnosus* pure *	*L. acidophilus* pure *	FV1-artificial *
ln curve parameters			
Mean *k*	1.87×10^{-4}	2.03×10^{-4}	1.62×10^{-4}
SD *k* (reproducibility)	1.46×10^{-6} (0.78%)	3.44×10^{-6} (1.69%)	1.07×10^{-6} (0.66%)
Intercept (ln value)	2.14	-0.99	2.78
SD (reproducibility)	0.030 (1.40%)	0.09 (9.09%)	0.007 (0.25%)
Mean Intercept (antilog value)	8.49	0.37	16.17
SD (reproducibility)	0.26 (3.06%)	0.03 (8.11%)	0.12 (0.74%)
Mean AUC to PP	1.65×10^5	1.83×10^5	1.49×10^5
SD (reproducibility)	1.90×10^3 (1.15%)	2.11×10^3 (1.15%)	7.91×10^3 (5.30%)
Mean R^2	0.9997	0.9999	0.9994
SD (reproducibility)	2.10×10^{-4} (0.02%)	7.64×10^{-5} (0.008%)	1.57×10^{-4} (0.02%)

Table 4.30 Quantitative data (logarithmically transformed curve derived) for the individual organisms *L. rhamnosus*, *L. acidophilus* and FV1-artificial. *Mean of six individual experiments.

The analysis of FV1-artificial contaminated with *E. faecium* (**Table 4.28**) revealed that PPs were essentially the same regardless of the contaminant concentration. It was plausible that the extent of growth of the FV1-artificial was unaffected by the presence of *E. faecium*, hence

the PPs were the same. However, times to PP were different. There was discrimination in times to PP and it seemed the more *E. faecium* present, the faster time to reach PP. There were no significant differences, however, between the times to PP to conclude any effects of *E. faecium* on *L. acidophilus* regarding this parameter. The AUCs were not very different when *E. faecium* was present in any concentration (there was a slight trend downwards with increased concentration of *E. faecium*), however, these were significantly different from the AUC of FV1-artificial without *E. faecium* (544.1). The growth rate was increasing with increased concentration of *E. faecium* and was significantly lower when *E. faecium* was absent. At the same time, the response of the intercept was not consistent. All linear fits were with high R^2.

It was discovered that there were some interactions between *L. rhamnosus* and *L. acidophilus* when these two organisms were tested together (1:1 ratio) in MRS. For example, the rate of growth of *L. rhamnosus* was affected by the presence of *L. acidophilus* and vice versa. The observed consequences of the interactions between the two organisms were for example, fastest time to reach PP when they were in co-culture, however, at the expense of lower PP and much lower AUC to PP when compared with *L. rhamnosus* on its own. The rate of growth *k* of FV1-artificial showed to be slower than that of *L. rhamnosus* or *L. acidophilus*. These interactions should be considered when co-culturing the two organisms because the resulting parameters (FV1-artificial) were not just sums of the two organisms when grown individually.

Assuming heat/cell was constant, for both *L. acidophilus* and *L. rhamnosus*, it would be expected that more cells produce more heat, therefore lower PP would indicate there were fewer cells produced in FV1-artificial compared with *L. rhamnosus* on its own.

Whilst there was no overall consistency in all parameters, the growth rate constants in all experiments (with no contaminants) were consistent and highly reproducible. When *E. faecium* contaminant was added into FV1-artificial, it did affect the growth rate significantly enough to be detected by IMC. The results were encouraging because IMC proved to be robust even though MRS was not a specific medium for its detection in a highly complex system (FV1-artificial).

It was plausible that the slight variations in medium composition had significant effects on the resulting p-t curves. This was not dealt with in detail in this thesis as it was beyond its scope. It formed, however, in a limited way, the next section where FV1-real (produced in

full scale equipment using barley wort) was investigated. Finally, it is important to note that every change (medium, new stock of bacteria) must result in re-examination of the reference reactions.

The theoretical development so far described that analysis of the quantitative data (analysis via the equations for the rate constant and the intercept) may be useful (as demonstrated with *L. rhamnosus*, *L. acidophilus* and FV1-artificial studies) if the reproducibility in the FV1-real merited that kind of analysis. And it merited that kind of analysis only if the images were reproducible. And if that was true, then it was worth applying this kind of quantitative analysis. The equations may offer more insights into the nature of Symprove but would also offer the possibility of having, as indicated earlier, when looking at FV1-artificial for example, a capacity for quantitative analysis which would allow for a better insight and more secure judgement about proceeding to bottle. This is demonstrated in the next section.

4.3.7 FV1-real tested in MRS

"Real" in the context of this section meant that samples tested were taken directly from fermenting vessels after the fermentation was completed. The six experiments reported in this section represented six unique FV1-real batches. The same protocol (see **2.2.3** and **2.2.4**) was followed. Samples of FV1-real were taken directly from full-scale fermenting vessels (1000 L) after the fermentation was completed. The FV1-real resulted from pure organisms inoculated into a medium which could be very variable. The control of the fermentation was not as precise as in the laboratory conditions. Consequently, the outcome was not obvious despite that the previous systems (controlled experiments with high reproducibility) showed excellent outcomes. The purpose of the work reported in this section was to determine what was the behaviour (performance in a calorimeter, and reproducibility) of FV1-real with respect to *L. rhamnosus* and *L. acidophilus*, separately as well as FV1-artificial.

In order to facilitate the interpretation of the, prospectively, complex FV1-real the following tables display the quantitative data for the individual organisms and their combination in FV1-artificial as comparators and best outcome targets when comparing these with FV1-real.

Experiment	***L. rhamnosus* pure ***	***L. acidophilus* pure ***	**FV1-artificial ***
p-t curve parameters			
Mean PP [μW]	790	723	719
SD (reproducibility)	12 (1.52%)	18 (2.49%)	11 (1.53%)
Mean Time to PP [s]	33208	45754	29307
SD (reproducibility) [s]	317 (0.95%)	905 (1.98%)	1244 (4.24%)
Mean AUC to PP	9.83×10^6	8.20×10^6	7.99×10^6
SD (reproducibility)	1.61×10^5 (1.64%)	1.50×10^5 (1.83%)	7.37×10^5 (9.21%)

Table 4.31 Quantitative data (p-t curve derived) for the individual organisms *L. rhamnosus*, *L. acidophilus* and FV1-artificial. *Mean of six individual experiments.

Experiment	*L. rhamnosus* pure *	*L. acidophilus* pure *	FV1-artificial *
ln curve parameters			
Mean *k*	1.87 x10^{-4}	2.03 x10^{-4}	1.62 x10^{-4}
SD *k* (reproducibility)	1.46 x10^{-6} (0.78%)	3.44 x10^{-6} (1.69%)	1.07 x10^{-6} (0.66%)
Intercept (ln value)	2.14	-0.99	2.78
SD (reproducibility)	0.030 (1.40%)	0.09 (9.09%)	0.007 (0.25%)
Mean Intercept (antilog value)	8.49	0.37	16.17
SD (reproducibility)	0.26 (3.06%)	0.03 (8.11%)	0.12 (0.74%)
Mean AUC to PP	1.65 x10^{5}	1.83 x10^{5}	1.49 x10^{5}
SD (reproducibility)	1.90 x10^{3} (1.15%)	2.11 x10^{3} (1.15%)	7.91 x10^{3} (5.30%)
Mean R^2	0.9997	0.9999	0.9994
SD (reproducibility)	2.10 x10^{-4} (0.02%)	7.64 x10^{-5} (0.008%)	1.57 x10^{-4} (0.02%)

Table 4.32 Quantitative data (logarithmically transformed curve derived) for the individual organisms *L. rhamnosus*, *L. acidophilus* and FV1-artificial. *Mean of six individual experiments.

It was surprising but encouraging to see high reproducibility in p-t curves (**Figure 4.38**), and their quantitative parameters (**Table 4.33**) and this therefore encouraged the application of the equations to derive parameters presented in **Table 4.34**. The consistency seen in the p-t curves of FV1-real batches meant that the production led to a consistent product –at least in terms of cell numbers and identities. Each experiment represented a different batch of FV1-real (i.e., six individual, independent and unique FV1-real batches).

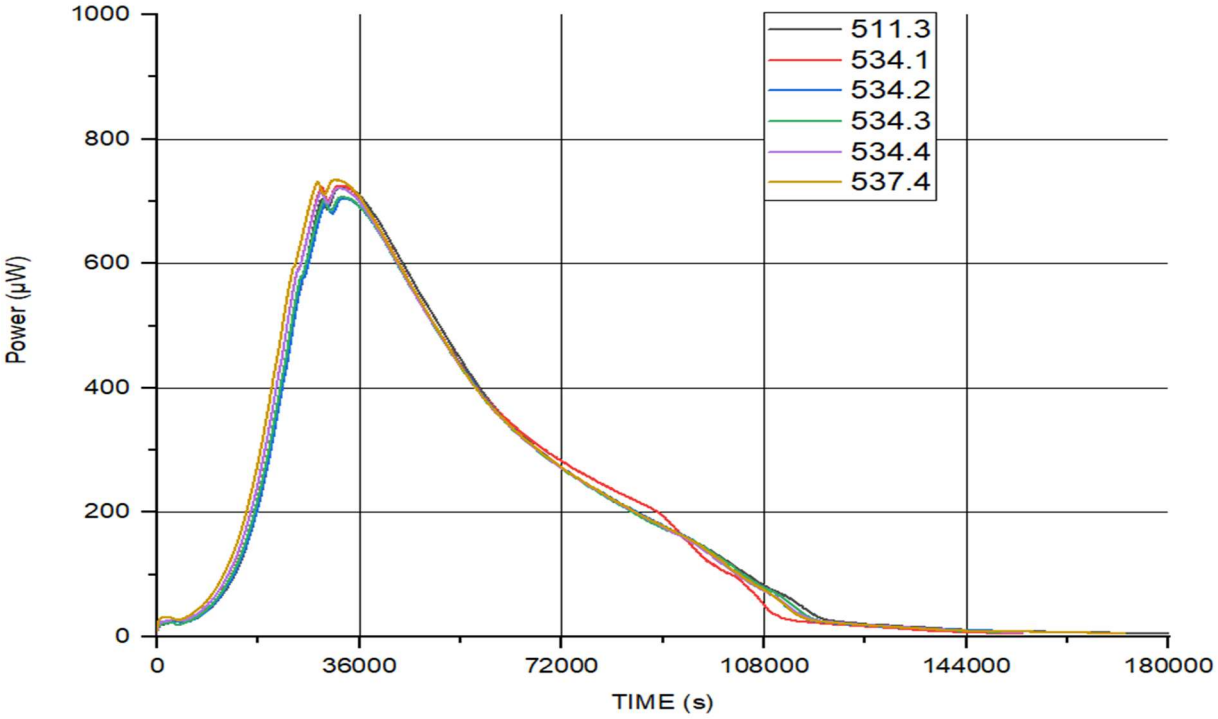

Figure 4.38 P-t curves of FV1-real tested in MRS. Each curve (experiment) represents a different batch of FV1-real.

Experiment no	511.3	534.1	534.2	534.3	534.4	537.4
p-t curve parameters						
PP [µW]	724	726	705	708	721	735
Mean PP	720					
SD (reproducibility)	10 (1.39%)					
Time to PP [s]	33742	32912	33502	32882	32242	31542
Mean time to PP [s]	32804					
SD (reproducibility) [s]	741 (2.26%)					
AUC to PP	9.64×10^6	9.76×10^6	9.32×10^6	9.14×10^6	9.26×10^6	9.40×10^6
Mean AUC to PP	9.42×10^6					
SD (reproducibility)	2.3×10^5 (2.44%)					

Table 4.33 Basic shape analysis parameters (PP, time to PP and AUC to PP). FV1-real tested in MRS.

Experiment no	511.3	534.1	534.2	534.3	534.4	537.4
ln curve parameters						
k	1.76×10^{-4}	1.76×10^{-4}	1.75×10^{-4}	1.76×10^{-4}	1.74×10^{-4}	1.75×10^{-4}
Mean *k*	1.75×10^{-4}					
SD *k* (reproducibility)	7.45×10^{-7} (0.43%)					
Intercept (log value)	2.18	2.37	2.20	2.25	2.40	2.53
Mean intercept	2.32					
SD (reproducibility)	0.12 (5.17%)					
Intercept (antilog value)	8.85	10.70	9.03	9.49	11.02	12.55
Mean intercept	10.27					
SD (reproducibility)	1.30 (12.66%)					
AUC to PP	1.68×10^{5}	1.67×10^{5}	1.67×10^{5}	1.63×10^{5}	1.63×10^{5}	1.61×10^{5}
Mean AUC to PP	1.65×10^{5}					
SD (reproducibility)	5.0×10^{3} (3%)					
R^2	0.9998	0.9998	0.9997	0.9996	0.9995	0.9998
Mean R^2	0.9997					
SD (reproducibility)	0.0001 (0.01%)					

Table 4.34 Parameters derived from the application of **Eq. 3.12**, *i.e.*, analysis of the logarithmically transformed p-t curves. FV1-real tested in MRS

4.3.7.1 Growth rate constant

Data presented in **Table 4.34** showed again excellent reproducibility (0.43%) in the growth rate constant. The capacity of the medium –wort to support growth of the two bacteria in FV1-real– was essentially the same as indicated by PPs derived from both p-t curves as well as logarithmically transformed curves. This suggested that the batches of medium used for producing the individual FV1 batches tested here were highly consistent. Additionally, it was likely that the growth in wort prior to testing in MRS preconditioned the bacteria so they would grow to the same extent.

4.3.7.2 Intercept

It was expected that the reproducibility of the intercept values of FV1-real could be different, but consistent, from those of carefully controlled laboratory scale experiments (FV1-artificial). This expectation was observed to be true. The differences could have been caused by the variations in inoculum cell density as the inoculum was taken directly from the production line without any control of organism density.

4.3.7.3 Contaminant detection

Acetobacter cibinongensis chosen for this study was a contaminating organism isolated from the regular product during a routine testing. The purpose of this study was to determine, whether it was possible to detect *A. cibinongensis* in co-culture of FV1-real by using IMC. Three different volumes (*i.e.*, 5, 10 and 15 µL; these were selected to see the sensitivity of IMC to detect low levels of contaminants) of *A. cibinongensis* were directly added to 30 µL of three FV1-real samples and these were then compared with the working reference of FV1-real (mean of 6 independent experiments –**Figure 4.38**).

A limited number of experiments were performed to see whether it was possible to detect a contaminating organism *Acetobacter cibinongensis*. The results (**Figure 4.39** and **Table 4.35**) were encouraging because even though MRS was not a specific medium for detection of *A. cibinongensis*, some parameters of the control (**Table 4.33** and **Table 4.34**) were affected enough to determine that the contaminated samples were out of the expected range. PP, AUC to PP and *k* were significantly different for all three *A. cibinongensis* inoculum volumes compared with the control even when ± 2SD was applied (**Figure 4.39**, green dash dotted and green dotted lines).

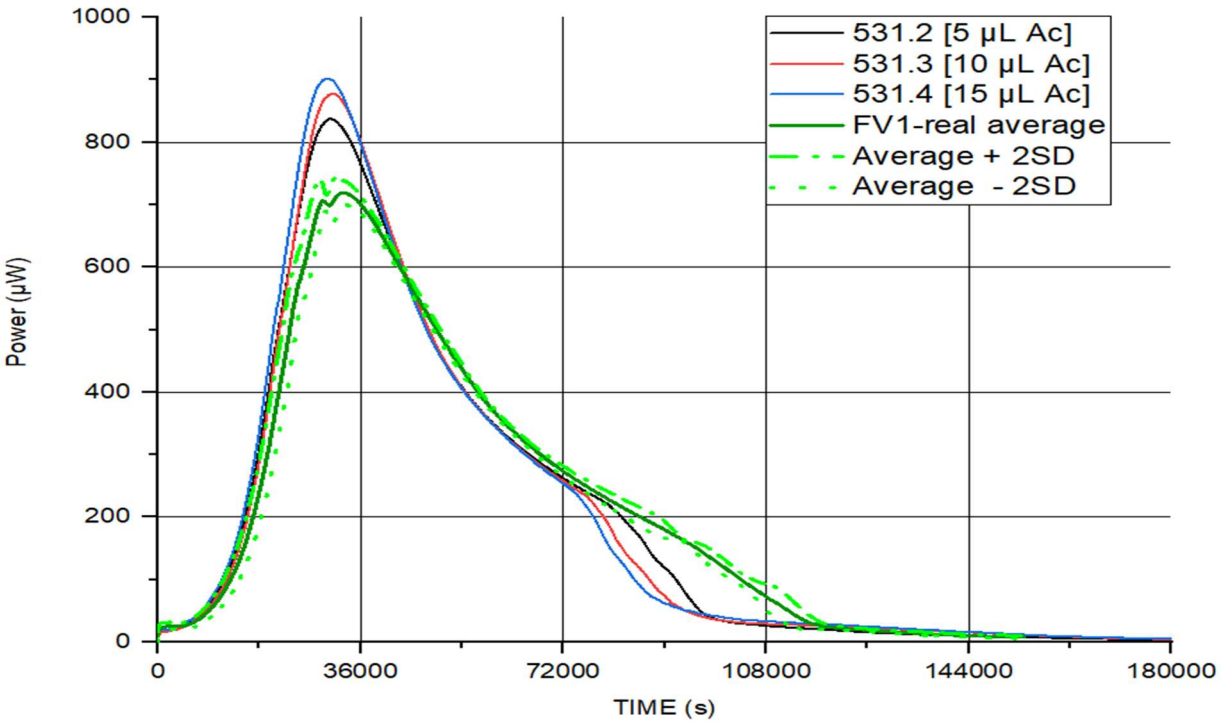

Figure 4.39 FV1-real without contamination (green solid curve) and the same FV1-real spiked with three different concentrations of A. cibinongensis; tested in MRS.

Experiment number	Control*	531.2	531.3	531.4
A. cibinongensis inoculum volume (µL/ampoule)	0	5	10	15
p-t curve parameters				
Time to PP [s]	32804	30662	31322	30062
PP [µW]	720	839	878	902
AUC to PP	9.42×10^{6}	9.60×10^{6}	1.01×10^{7}	9.96×10^{6}
ln curve parameters				
k	1.75×10^{-4}	1.80×10^{-4}	1.86×10^{-4}	1.85×10^{-4}
Intercept (ln value)	2.32	2.49	2.32	2.50
Intercept (antiln value)	10.18	12.06	10.18	12.18
R^2	0.9997	0.9998	0.9998	0.9997

Table 4.35 Basic shape analysis parameters and parameters derived from logarithmically transformed p-t curves. * Control parameters are means of the parameters from **Table 4.33** and **Table 4.34**.

The three curves (**Figure 4.39**, blue, red and black curve) containing *A. cibinongensis* looked quite reproducible considering that 15 µL produces a higher peak than 10 µL and higher than 5 µL. This order, blue, red, black, continued to approximately 35000 seconds when it started to change slowly resulting in, black, red, blue order, at approximately 72000 seconds; *i.e.*, the lowest trace was for 15µL, little higher for 10 µL and the highest was for 5

µL. In other words, they got inverted. There was something about more rapid metabolism, more rigorous metabolism in the early stages and then they changed order. It seemed that there was an interaction between the organisms and some metabolic products may inhibited the growth or stimulated the organisms, however, this was not an exhaustive study (where biochemistry of organism's metabolism could be examined, for example), but only analysing the overall behaviour in the medium which was demanding by Symprove's production. If a functional dependence could be established, there was an indication that 15 µL was higher than 10 µL and it was higher than 5µL, it would be reasonable that these seemed dose related.

There was some distinction in the parameters presented in **Table 4.35**. For example, systematic differences in times to PP between the control and 5, 10, 15µL; AUCs between the control and 5, 10, 15µL; and most notably differences in PP and *k* between the control and the rest. What was also striking was the closest agreement in some of the parameters, for example the intercepts, between 5µL and 15µL and between the control and 10µL.

Finally, the three curves reached much higher PP than the mean of six (green solid curve; the control) and its ± 2SD (green dash-dotted and green dotted curve respectively) of non-contaminated batches therefore were clearly distinguishable from non-contaminated batches.

4.3.7.4 Discussion

Note that where differences were assigned, it was demonstrated that the mean values ± 2SD did not overlap.

FV1-real p-t curves showed two distinct peaks (see **Figure 4.38**). The highest power reading was observed at the second distinct peak (in all six experiments) and this value was taken as peak power (PP) for all analysis. A mean PP of the six experiments was calculated and compared with the mean PPs of *L. rhamnosus* pure (**4.3.1**), *L. acidophilus* pure (**4.3.5**) and FV1-artificial (**4.3.6**). There was a clear distinction between FV1-real and *L. rhamnosus* pure (see **Figure 4.42**). The error bars were calculated for each mean and their respective ± 2 SD . However, there was an overlap of mean PPs (± 2SD) between FV1-real, *L. acidophilus* pure and FV1-artificial which did not allow to discriminate between them based on mean PPs only.

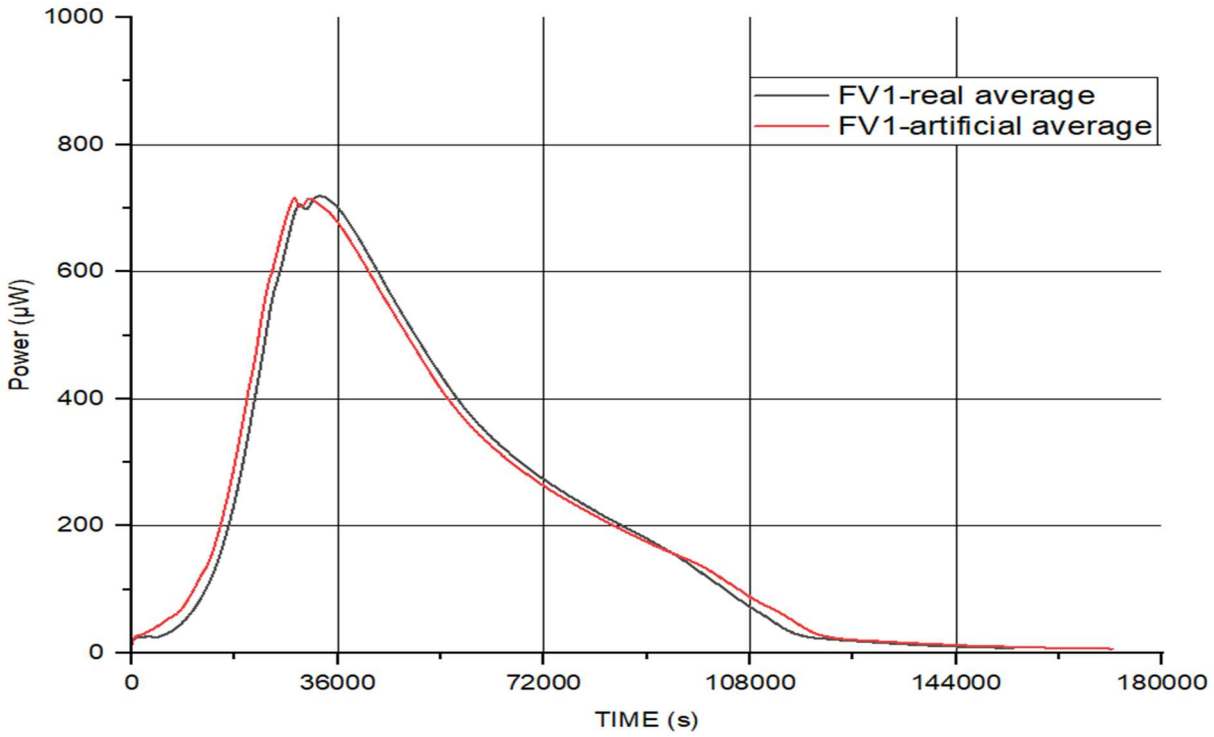

Figure 4.40 Comparison of mean p-t curves of FV1-real and FV1-artificial. Each mean curve was calculated from six independent p-t curves (data from **4.7** –FV1-real, and **4.6** – FV1-artificial).

The p-t curves of FV1-real and FV1-artificial looked very similar. Both curves showed double peak and their general shapes were similar (**Figure 4.40**). However, it was consistently observed that the first peak in FV1-real was lower than its second peak and this situation was reversed in FV1-artificial (the first peak was the PP and the second peak was lower). The reason as to what might have caused these reversed peaks could be a consequence of, for example, differences in the growth media in which the FV1 bacteria were grown (barley wort in FV1-real and MRS in FV1-artificial) before they were calorimetrically tested in MRS.

The organisms constituting FV1 produced distinctively different p-t curves when they were tested individually as *L. rhamnosus* pure (section **4.3.1**) and *L. acidophilus pure* (section **4.3.5**). Comparing these to FV1-real or FV1-artificial (**Figure 4.41**),also showed a clear distinction. Each curve was a mean of 6 individual experiments from the previous sections **4.3.1**, **4.3.5**, **4.3.6** and **4.3.7**.

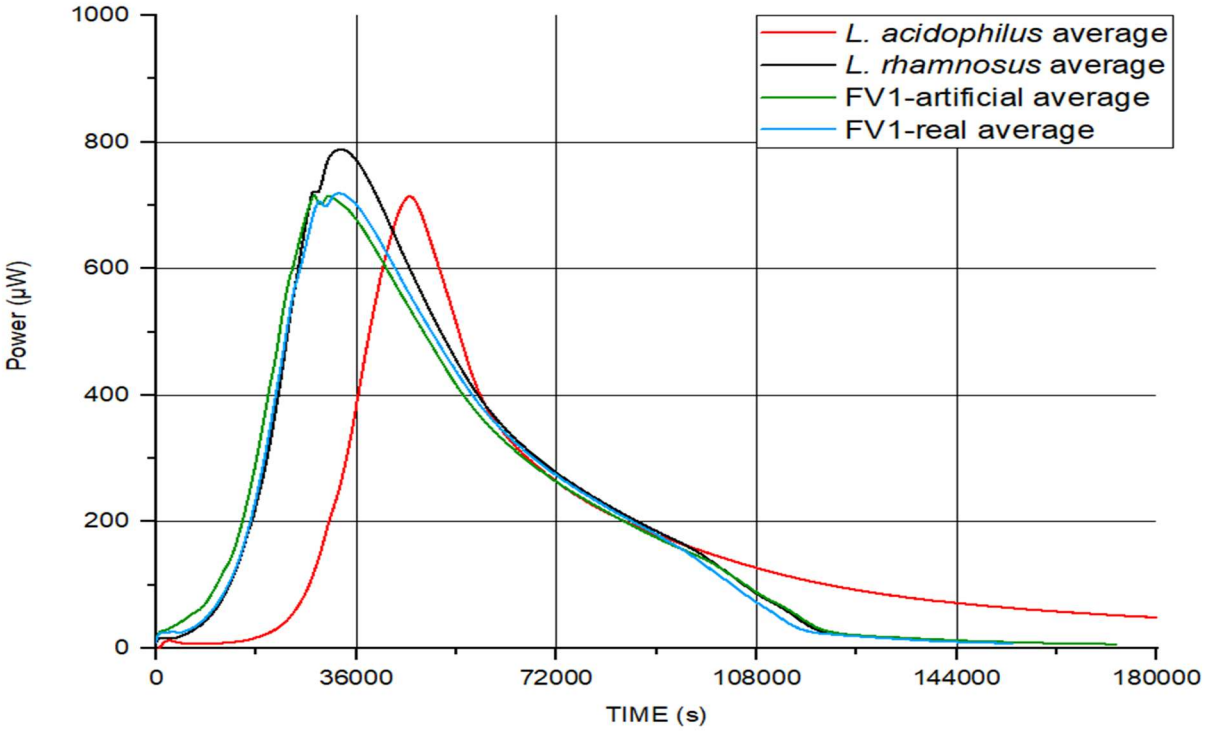

Figure 4.41 Comparison of mean p-t curves (*L. acidophilus* pure, *L. rhamnosus* pure, FV1-artificial and FV1-real).

In FV1-artificial model experiments the total number and the ratios of inoculating organisms was the same as in FV1-real which was inoculated with equal parts (1:1) of the individual bacteria (according to **1.4.1**). Hence the expectation was that FV1-real and FV1 artificial should be very closely comparable if the medium had no effect. Therefore, if an observable change was detected the medium –wort was most likely producing the difference (*i.e.*, different peaks).

The effects of *L. acidophilus* on *L. rhamnosus*, when these two were in co-culture as FV1-real or FV1-artificial, were more obvious such as lower PP and longer time to reach PP. It appeared that the *L. acidophilus* had some retardation effect, on the growth of *L. rhamnosus* when co-cultured. There could be several reasons why PP of FV1-real was lower than that of *L. rhamnosus* pure such as faster nutrient exhaustion and/or *L. acidophilus*' metabolic byproducts interference with *L. rhamnosus* metabolism. It was also plausible that there were some effects of *L. rhamnosus* on *L. acidophilus,* however, not clearly observable as *L. rhamnosus* was much faster growing than *L. acidophilus*.

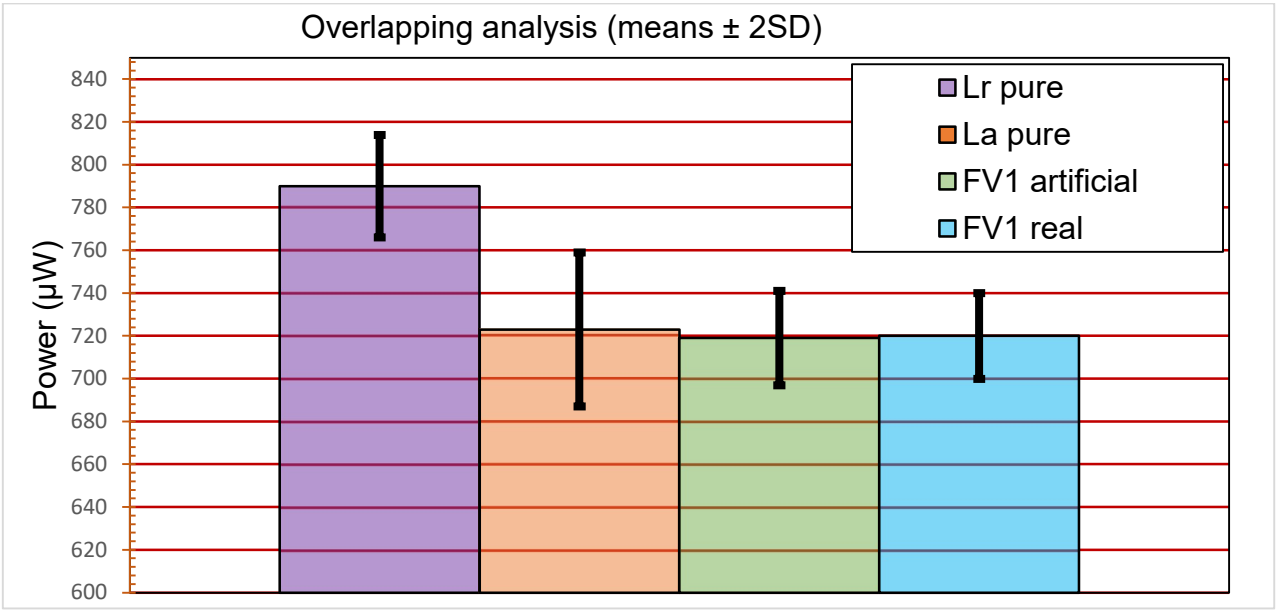

Figure 4.42 Analysis of peak powers (PP). Each column represents a mean of six experiments (*i.e.*, purple column *L. rhamnosus* experiments in section **4.3.1**; orange column *L. acidophilus* experiments in section **4.5**; green column FV1-artificial experiments in section **4.6**; blue column FV1-real experiments in the current section **4.7**). ±

The analysis of times to reach PP revealed that FV1-real was clearly distinguished from *L. acidophilus* only, whereas it could not be distinguished from *L. rhamnosus* or FV1-artificial (see **Figure 4.43**) It was also clear (**Table 4.36**) that the combination of *L. rhamnosus* and *L. acidophilus* constituting either FV1-artificial or FV1-real resulted in faster times to reach PP than their growth individually in pure forms.

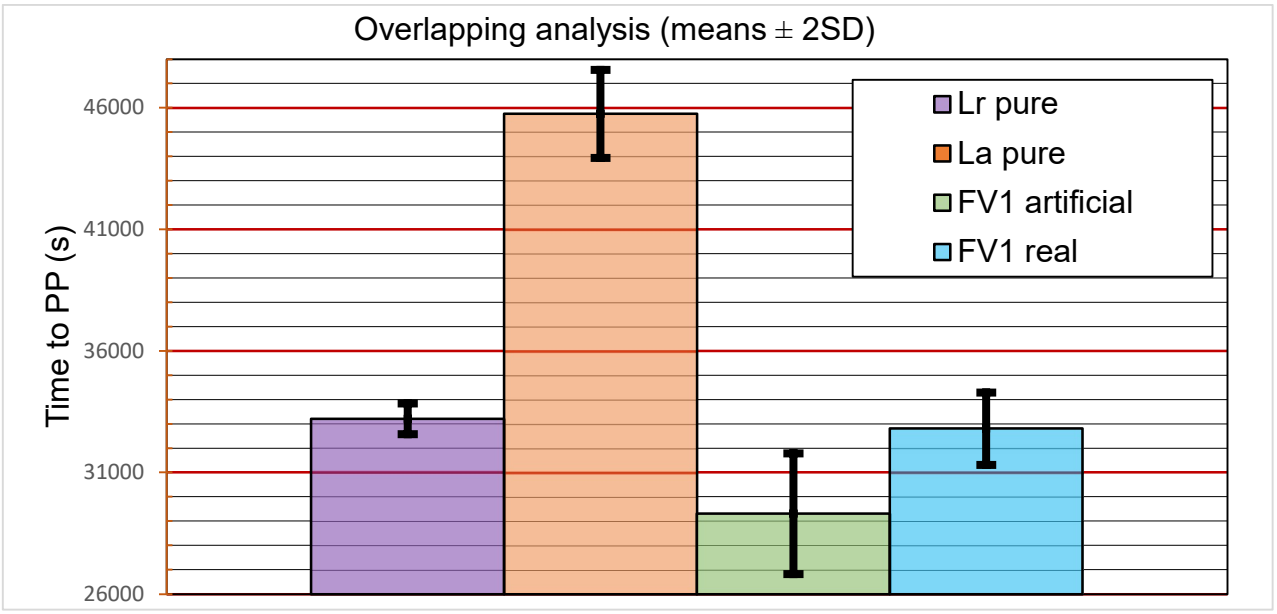

Figure 4.43 Analysis of times to PP. (Same detail as **Figure 4.42**.)

FV1-real's mean area under the curve (p-t curve) was distinguished from *L. acidophilus* pure only. There was a clear difference between *L. rhamnosus* and *L. acidophilus*. *L. rhamnosus* could also be distinguished from FV1-artificial (**Figure 4.44**). These differences had to reflect complex organismal responses to respective media, and in mixed growths the presence of the other organism(s).

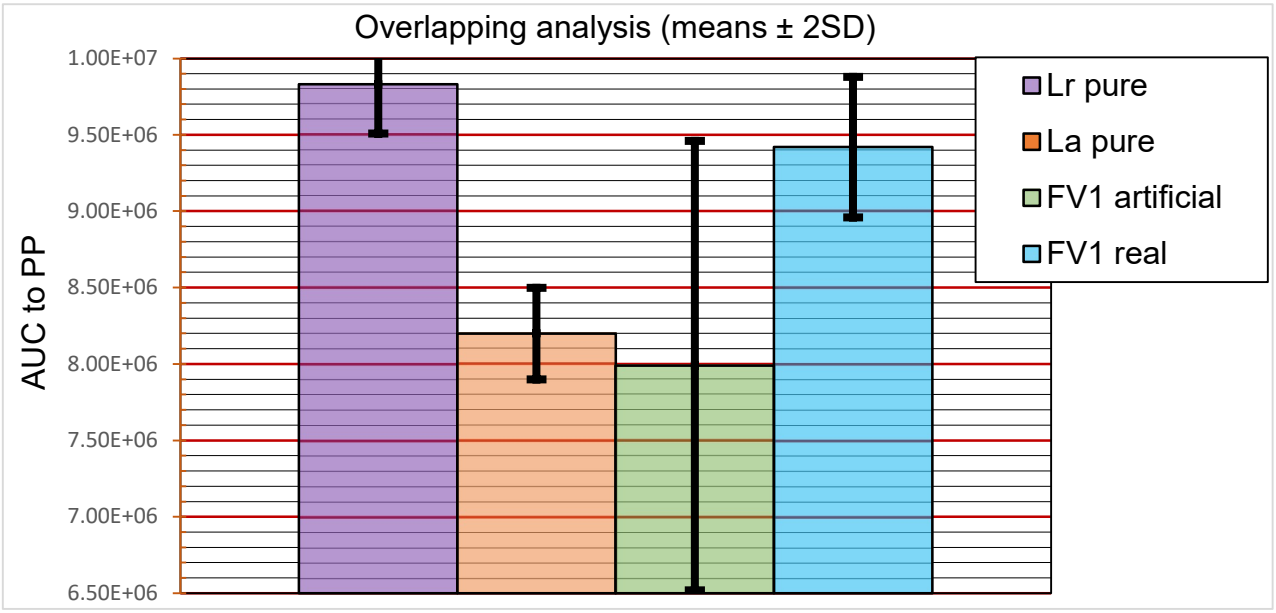

Figure 4.44 Analysis of AUC to PP. (Same detail as **Figure 4.42**.)

Firstly, there was the difference that the organisms had with respect to different media (MRS growth was not the same as wort growth).

Secondly, and this was not possible to distinguish here, it was the case of a mixed growth (*i.e.*, *L. rhamnosus* and *L. acidophilus* together) where the consequences of having the metabolism of the latter was affecting the growth of the former, for example.

It was clear that in whichever medium were the two organisms presented the response was different from simply looking at the two organisms together. They were not simply additive, they represented the consequences of having the two organisms together, their interactions and whatever that depended upon, whether it was the medium or produced metabolites.

The rate of growth *k* of FV1-real (1.75 x10^{-4}) was faster than that of FV1-artificial (1.62 x10^{-4}). When *L. rhamnosus* was grown in wort the rate of growth was slower (1.70 x10^{-4}) and when *L. rhamnosus* was grown in DLW the rate of growth was faster (2.07 x10^{-4}) than that of *L. rhamnosus* pure (1.87 x10^{-4}). The consequence of these different rates as well as other

interspecies interactions (Fredua-Agyeman *et al*., 2017b) might have contributed to a much slower rate of growth of FV1-artificial (1.62 x10^{-4}), or indeed when it came to FV1-real (see **Table 4.37**). Furthermore, it was observed that the start of the linear fit in *L. acidophilus* pure data starts on average at about 22000 seconds which would leave approximately 11000 seconds to *L. rhamnosus* before it would naturally reach its PP (when grown on its own). This could mean that the faster growth rate of *L. acidophilus* could interfere with the slower rate of growth of *L. rhamnosus*.

If the same trend was true for *L. acidophilus* as it was shown for *L. rhamnosus* (grown in 2 worts) –it could be extrapolated that the rate of growth of *L. acidophilus* in wort would be slower and in DLW would be faster than its rate of growth when in pure form. Therefore, the same could be observed in FV1-real *i.e.*, *L. acidophilus* might have some inhibitory effect on *L. rhamnosus* (**Figure 4.41**), (or it affects the extent of growth of *L. rhamnosus* - lower PP, when in co-culture.

Experiment	***L. rhamnosus* pure**	***L. rhamnosus* grown in wort***	***L. rhamnosus* grown in DLW****	***L. acidophilus* pure**	**FV1 artificial**	**FV1-real**
p-t curve parameters						
Mean PP [µW]	790	771	1062	723	719	720
SD (reproducibility)	12 (1.52%)	11 (1.42%)	10 (0.94%)	18 (2.49%)	11 (1.53%)	10 (1.39%)
Mean Time to PP [s]	33208	35982	33164	45754	29307	32804
SD (reproducibility) [s]	317 (0.95%)	631 (1.75%)	193 (0.58%)	905 (1.98%)	1244 (4.24%)	741 (2.26%)
Mean AUC to PP	9.83 x10^6	9.58 x10^6	8.83 x10^6	8.20 x10^6	7.99 x10^6	9.42 x10^6
SD (reproducibility)	1.61 x10^5 (1.64%)	2.55 x10^5 (2.66%)	1.03 x10^5 (1.17%)	1.50 x10^5 (1.83%)	7.37 x10^5 (9.21%)	2.3 x10^5 (2.44%)

Table 4.36 Comparison matrix of p-t curve derived parameters for all *L. rhamnosus*, *L. acidophilus*, FV1-artificial and FV1-real.

* Mean of 2 experiments (wort produced onsite).
** Mean of 4 experiments (Dohler wort (DLW)).

Experiment	*L. rhamnosus* pure	*L. rhamnosus* grown in wort*	*L. rhamnosus* grown in DLW**	*L. acidophilus* pure	FV1 artificial	FV1-real
ln curve parameters						
Mean *k*	1.87×10^{-4}	1.70×10^{-4}	2.07×10^{-4}	2.03×10^{-4}	1.62×10^{-4}	1.75×10^{-4}
SD *k* (reproducibility)	1.46×10^{-6} (0.78%)	0 (0%)	1.22×10^{-6} (0.59%)	3.44×10^{-6} (1.69%)	1.07×10^{6} (0.66%)	7.45×10^{-7} (0.43%)
Intercept (ln value)	2.14	1.81	0.93	-0.99	2.78	2.32
SD (reproducibility)	0.030 (1.40%)	0.14 (7.73%)	0.04 (4.30%)	0.09 (9.09%)	0.007 (0.25%)	0.12 (5.17%)
Mean Intercept (antilog value)	8.49	6.11	2.53	0.37	16.17	10.27
SD (reproducibility)	0.26 (3.06%)	0.14 (2.29%)	0.11 (4.35%)	0.03 (8.11%)	0.12 (0.74%)	1.30 (12.66%)
Mean AUC to PP	1.65×10^{5}	1.72×10^{5}	1.49×10^{5}	1.83×10^{5}	1.49×10^{5}	1.65×10^{5}
SD (reproducibility)	1.90×10^{3} (1.15%)	5.00×10^{2} (0.29%)	1.00×10^{3} (0.67%)	2.11×10^{3} (1.15%)	7.91×10^{3} (5.30%)	5.0×10^{3} (3%)
Mean R^2	0.9997	0.9995	0.9998	0.9999	0.9994	0.9997
SD (reproducibility)	2.10×10^{-4} (0.02%)	0 (0%)	8.29×10^{-5} (0.008%)	7.64×10^{-5} (0.008%)	1.57×10^{-4} (0.02%)	0.0001 (0.01%)

Table 4.37 Comparison matrix of the logarithmically transformed p-t curves derived parameters for all *L. rhamnosus*, *L. acidophilus*, FV1-artificial and FV1-real.

Each experiment reported was from one production growth only (as well as only one run in the calorimeter, there were no repeats of the same batch to choose the best data). It was demonstrated that the behaviour of FV1-real in the calorimeter was distinguishable based on the growth rate constant *k* from that of FV1-artificial, *L. rhamnosus* pure as well as *L. acidophilus* pure (see **Figure 4.45**). It was remarkable that highly reproducible data was obtained from such a complex and potentially rather variable system.

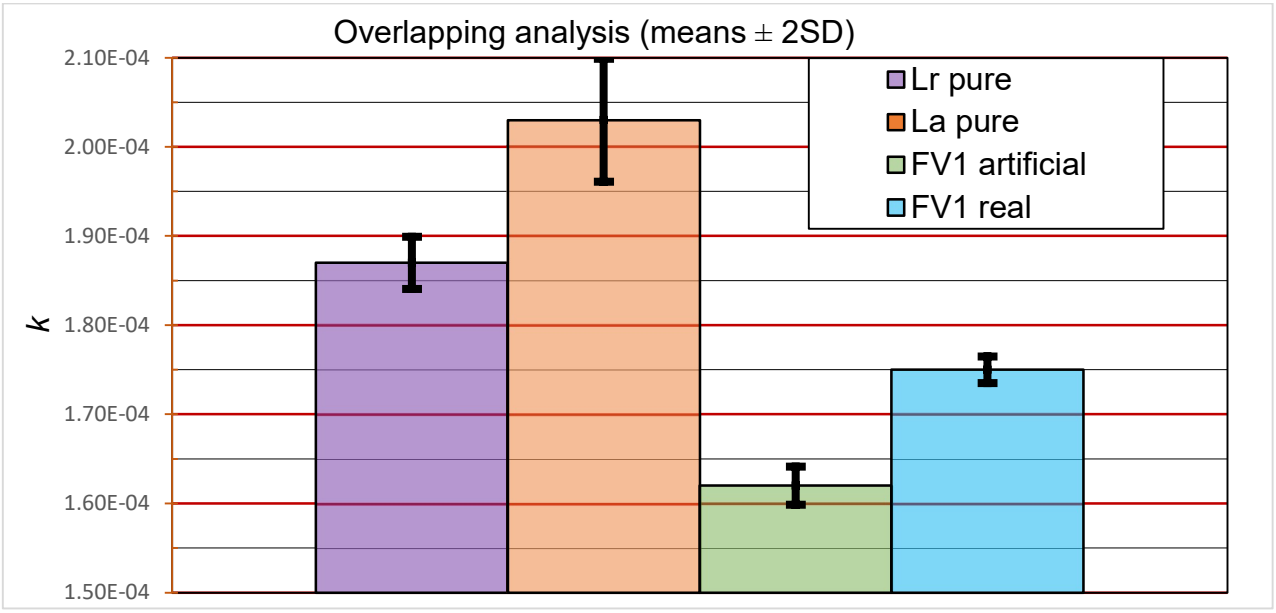

Figure 4.45 Slope *k* analysis. (Same detail as **Figure 4.42**.) Data derived from logarithmically transformed p-t curves.

It was remarkable, given the instrument (four channel) available with limited capacity for experiments, to see differences which were indicative of medium effects or metabolic effects but each individual experiment taking 30 µL from 1000L had produced astonishingly reproducible data.

It was highly surprising, also, to obtain such a high reproducibility (especially *k*) when taking 30µL samples from six separate batches of 1000L. Despite the challenges of a real-world production (variable medium, sample size representation of a whole vessel, *etc*.) a surprising consistency was found (because not the same 30µL sample was taken each time but any random 30µL sample was taken from six different 1000L vessels, and additionally not one of these six samples was a repeat). Therefore, these 30µL samples appeared to be highly representative of the whole 1000L system.

There was no observable difference between FV1-real, FV1-artificial or *L. acidophilus* based on PP. *L. rhamnosus* pure had produced significantly higher PP in comparison with the aforementioned three. Equally, it proved to be difficult to use AUC as a means to distinguish between FV1-real and *L. rhamnosus*.

FV1-real data were also compared with the traditional microbiological analysis results obtained from the commercial laboratory. Whilst all the results were within specification (no failed batch or conflicting results between IMC and microbiological results), testing the same

batches, the mean time to get IMC results was 9 hours (**Table 4.36** – 32804 seconds) and the mean time to get the microbiological results from the laboratory was 7 days. This yet again demonstrated how much faster IMC was in comparison with the traditional microbiology.

4.4 Chapter conclusion

A successful industrial application of IMC was presented. It was demonstrated that a useful and practical set of standard references for Symprove bacteria (FV1 components) was simple and fast to establish with surprisingly high repeatability for such complex systems. It was detected that they (FV1 bacterial components individually and in pairs) were different and that meant, in the absence of other information, a known sample of for example *L. rhamnosus* in Symprove and a known but anonymous sample of another organism from Symprove's collection could be studied and identified as either *L. rhamnosus*, *L. acidophilus*, *L. plantarum* or indeed *E. faecium*. This was quite important because within this limited world (within Symprove species) it was possible to distinguish between the four organisms present in Symprove using exclusively IMC. Only very basic laboratory provisions were needed and a simple protocol for setting up experiments, with minimal sample preparation, was required. This part of the project was successful because the organisms could be identified, could be seen and could be distinguished from each other within hours (see **Figure A5**).

The logical progress from the simplest best case scenario (*L. rhamnosus* in MRS) to the complexity of FV1-real (two bacteria in a variable wort medium), was confirmed to be practical as the differences in obtained parameters were easy to attribute to either of the bacteria or their co-culture.

Added benefits of using IMC included revelations that calorimetry had the capacity to investigate the effects of growth media on the studied bacteria (**4.3.2**), including the cultivation history of the organisms (**4.3.3**).

Data processing, and performance parameter extraction which was difficult when done manually can be automated and streamlined in order to make this procedure operator independent and applicable to an industrial setting; essentially a BB.

It was also shown that IMC detected contaminants with a high degree of reliability, significantly faster, than traditional microbiological plating methods. This points to the

availability of characterisation process (identification of good growth and deciphering contaminants) based on calculated results. The case of *E. faecium* cross-contamination (**4.3.6.3**) showed that whilst it was not a risk to health, IMC was robust and fast in detecting it. Hence it had the capacity to identify the presence of contamination and was practically demonstrated in **4.3.7.3** with *A. cibinongensis*.

The presence of a contaminant would lead to abandonment of that growth, destruction of that growth. Among the advantages in using IMC with its potential for shortening the testing times was not only to cut the time to bottling but cutting out the waste of time storing something which was later to be abandoned. Additionally, if it was known early that there was a contamination in a batch, the batch would be abandoned and that would change the work schedule for the following days (critically important in an industrial setting) because what would have to be done was to sterilise the plant and make up for the lost batch. It would also save time waiting for another number of batches before the problem was detected by traditional microbiology and potentially spoil the next batches. The whole exercise could aid in improving/changing operating procedures and optimising production timings.

In summary, therefore, the work presented here established confidence in the potential (realised here in Symprove production/product authentication) of the use of ICM in managing/controlling/evaluating industrial production in complex (biologically based) system.

Chapter 5 Conclusions and future work

5.1 Conclusions

The project just presented was initially conceived to explore whether it was possible to use calorimetry for an industrial process management *i.e.*, Symprove production, and to determine whether the calorimeter can act as a batch-to-batch release tool for Symprove quality assurance.

The approach taken to complete the goals outlined was twofold; pragmatic and theoretical. The pragmatic approach detailed in **Chapter 2** was primarily concerned with whether it was possible to establish a satisfactory reproducibility that could be used in achieving the project's objectives. In other words, is the reproducibility of the calorimeter at least as good as and, optimistically, better than classical microbiological methods used by Symprove for their quality assurance? It turned out that the reproducibility of p-t curves was more than satisfactory, in fact better than the traditional microbiological plating methods. Two major outcomes were derived as a consequence of this success. One was significantly shortened testing time (a matter of hours rather than days) and the other one was improved sensitivity and accuracy of testing. At this point, one could argue, that calorimetry worked for the purpose of the project. Therefore, if the project stopped here, the evaluation of calorimetry in the context of Symprove's purpose would only be concerned with comparing shapes of the p-t curves. It would be very well to simply look at the shapes as it has been typically done in the biological calorimetry before (Boling *et al*., 1973; Beezer *et al*., 1979; Newell, 1980; von Ah *et al*., 2008), but it would be more successful and quantitatively more desirable to be able to analyse the curves in a more formal way—the theoretical approach. Whilst automatic shape reading could, in principle, be established it was felt that more useful and important *quantitative* data was available, *i.e.*, from mathematical analysis of p-t curves. Moreover, the potential for developing coding for this analysis suggests immediately the prospect of a black-box technician management of such a procedure.

Necessary practices and regulations in industrial processes require that reference protocols be established that ensure the consistency over time of; core materials (medium, inocula and other critical materials and instrumentation: the IMC, associated equipment and related analytical aspects). It was practically demonstrated, in **Chapter 2**, that the IMC is: a reliable indicator of for example a good product; very successful in identifying a bad product *e.g.*, seemingly-good product (reported as good by the contracted microbiological laboratory

following anomalous IMC results to find to be contaminated and was hence abandoned); a bad product; and a reliable tool to determine bacterial strain quality and purity. The p-t curves obtained via IMC are highly reproducible and consistency in the experimental method was shown. This allowed the establishment of working reference curves. Furthermore, IMC revealed that contaminating organisms either in the final product or in the individual ingredients (bacteria) can be detected and with greater sensitivity, much faster than a contract microbiological laboratory. These initial achievements exceeded expectations (it was not expected that there would be instances, prompted by anomalous IMC results, where extra analysis was required, and not prompted by routine, conventional microbiological testing as shown in **2.6.1**, **2.6.2** and **2.6.3**). This outcome more than satisfied the initial goal of the project. Additionally, a system in which samples can be tested without any treatment and for which only a few simple laboratory procedures are required was derived.

Another, particularly important, practical outcome of the initial experimentation was that Symprove decided to use pure inocula in their production, after IMC revealed contamination in the stock of bacteria of a lower purity previously used in their process.

The theoretical approach presented in **Chapter 3** was an attempt to develop a formal quantitative analysis, with simple-to-assess parameters of exponential growth. Hence equations were developed which allowed, in principle, to extract quantitative parameters of bacterial growth including slope and intercept obtained from **Eq. 3.12**.

These two approaches were fused together and gave a basis for the work reported in **Chapter 4**, where theory and practice complement each other. The industrial application of this project meant that, it was necessary to know whether the instrument behaved/functioned in a consistent way. In order to do these internal standard references were established to check the performance of the calorimeter over time

It was discovered that establishing internal references (see **4.3.1**) was straightforward, and simple . The quantitative parameters (PP, AUC, slope, intercept) derived from the reference-establishment work allowed for the understanding of not just how the shapes were reproducible but how the quantitative data was reproducible. With quantitative data available a black-box data processing solution could be easily developed

There was an attempt to develop coding and automation of data processing and interpretation (pass/fail), essentially a BB (see Cabadaj *et al*., 2021), however, the unfortunate death of the code developer prevented a fully functional system to be completed.

The small piece of work that was done however, demonstrated that it would be straightforward to create an algorithm which would enable fast and technician independent data processing.

This project achieved over and above the initial goals. The strategy to first analyse FV1 organisms individually, then as pairs in FV1-artificial and FV1-real was successful. The analytic outcomes, the matrices of data (**Table 4.36** and **Table 4.37**), with a rich variety of shape analysis parameters and quantitative data analysis parameters (for example, PP, time to PP, AUC to PP, growth rate, intercept) resulted in reproducible data which is a significant achievement given the highly complex biological environment; *i.e.*, industrial production of FV1. Having these data available will allow to make a judgement of not only about a good product, but that richness of data will also enable to detect if something has gone wrong (*e.g.*, batch was contaminated). In other words, it is believed that this real analytical procedure has the very real capacity to determine a good product outcome enabling to make decisions of whether to bottle if there is a detectable anomaly. In addition, it can give an indication that there is a contaminant present but not identified. Now it is reasonable to say that implementing this strategy into the real world of an industrial production process is possible, given that a reproducible system was developed, internal references commissioned and simple laboratory procedures derived. It was necessary to have microbiologically based references because the performance of the calorimeter (no drift over time) should be guaranteed over the time of the experiments reported here (*e.g.*, 24-48 hours). Furthermore, IMC method is faster, simpler to perform and easier to interpret the results than conventional detection methods (Fricke *et al.*, 2019). Operating costs of the experiments and related consumables are low once an appropriate instrument is in place. It can be concluded with confidence that similar outcomes will be found in FV2 and the full product if this analysis would be extended to those.

5.2 Future work

There are several areas where the work described in this thesis could significantly contribute to the industrial process management where microbial activities are of interest. However, the immediate practical tasks in the future work would be implementing the same strategy to investigate the second component of the Symprove product –FV2 (individual organisms separately, FV2-artificial and FV2-real) and subject the full product (FV1-real + FV2-real) to the same procedure. The above extensions to the work presented would be desirable because the work done so far was to take the organisms directly from FV1 after fermentation, test those via IMC, and say at that point, which was a good growth and one that could go ahead and be bottled. It would give a greater confidence in using IMC as a standalone method for quality assurance purposes should these extensions be completed.

Naturally, if IMC can be used to identify a good product, the next important question is how long the good product can be used for *i.e.*, investigating the shelf life as indicated in **Figure 4.2**. Work reported in this thesis refers only to the original product (without flavouring) of its first component FV1-real and it will be important to understand the effects, if any, of additives (flavours, preservatives and vitamins) and the consequences on the product's shelf life. It is possible that the bacterial balance could be affected by different additives, hence the stability and efficacy of the final products might be affected. Simplicity of the IMC experiments and their high repeatability offers an excellent opportunity to investigate all of the above significantly faster and would result in money saved compared with the traditional microbiological methods.

Although enumeration of bacteria was not attempted in this thesis, it could be attempted and its use evaluated in future. For example, Fricke *et al*., (2019) have done enumeration experiments using IMC. However, it is possible to enumerate much faster than reported by Fricke *et al*., (2019). For example, a 24-channel or 48-channel instrument could be used doing the same experiments as described in this thesis, supplemented by experiments in which the product (FV1-real, FV2-real, full product) would be inoculated into buffered glucose using a flow through cell. This would be simple and is a well established method of counting bacteria (Beezer *et al*., 1974b; Beezer and Chowdhry, 1980). In a multichannel instrument it would be possible to give a number of channels to just counting bacteria and once it was established what a count for a good product was, it would be possible to determine that the objective of a good count was met. This would add an extra parameter to a future matrix of good growth parameters. Consequently, doing experiments on FV1,

FV2 and the full product would not only show that all the current parameters (*e.g.*, rate constant, intercept, AUC, PP, time to PP) are good, but in addition, the total number of organisms falls within a determined range for a good product. Importantly the same principle could be applied to investigate shelf life to see how many bacteria are still alive at different time points (a week, a month or other specified time point). The smart part of the buffered glucose method is that the bacteria will not grow, they will not multiply, just respire, and so it would be known how many bacteria are alive at a specific time point of storage.

What was described in this thesis was directly applied to Symprove. The utility of IMC, as demonstrated in this project (and the matrices of quantitative data developed), has a scope of applications, for example, if new formulations (*e.g.*, new flavours, bacteria, vitamins added) were to be developed. It is not satisfactory to just test if the organisms grow (in a new medium or matrix), but if they grow properly and their metabolism proceeds according to quantitative parameters *e.g.*, rate constant, intercept, PP, time to PP, AUC, to show that it is a normal growth (no inhibitory interactions, degradation of product's quality, efficacy). Therefore, it would be possible to actively investigate aspects that add value to an industrial process (*e.g.*, Symprove).

Given that clinical evidence indicates that Symprove has some contribution to improvements in symptoms of IBS (Sisson *et al*., 2014), inflammatory bowel diseases (Bjarnason *et al*., 2019; Ghyselinck *et al*., 2020), Parkinson's disease (Ghyselinck *et al*., 2021) and, that Symprove has not been optimised for these conditions it would be worth exploring a specific formulation that might assist specific disease conditions instead of having just the 4 original organisms. It is probable that different formulations would produce different metabolites which would better promote synthesis with better effect to PD, for example (this would be done together with other methods depending on a particular application as demonstrated by Sancandi *et al*., 2023). This would mean that suitability of possible new organisms and new media combinations could be explored via IMC. Quantitative data available from the analysis of p-t curves could serve as medium comparators (which medium is better in supporting growth and sustaining the shelf life) or indicators of suitability when multi-strain combinations (Fredua-Agyeman *et al.*, 2017b) are considered for a new product.

Detection of contaminants as demonstrated in **4.3.5.3**, **4.3.6.3** and **4.3.7.3** could involve investigations of causes for failed batches, for example identifying the sources of contamination. This could be done by pre-screening raw materials and sampling from different stages of the production process itself using IMC. For example, the case reported

in **Figure 4.6** demonstrated that the viability of new batches of inocula could be determined from a simple IMC experiment, *i.e.*, a pre-production quality control test. It would be necessary to do this so that consistency of inoculation in production can be established, *i.e.*, not just product test but frozen inocula pre-production quality control test. Such pre-production inocula quality control test could be also done every time a new inocula batch is produced. The inocula ought to be examined for performance in a standard test. Thereafter what might be expected from the test result is the possibility to gauge the inoculum density from zero viability to what is expected, hence the same effective number of organisms is inoculated into the production vessel, therefore controlling the production process even further. Hence IMC could be used not just to discover the deleterious effects of the contaminants (a batch is spoiled), but in principle could be used to investigate the root cause (see **Figure 4.6**) or source of the contamination (as exemplified in **2.6.3**). This would also offer a possibility to intervene during or after the fermentation stage much faster than waiting for the results of the traditional microbiological methods.

In this context, for example, the extent to which a 30 µL sample is representative of the 1000L FV1 could be elucidated. The instrument used for the work reported here could only take 4 samples. With a 24-channel instrument the sampling could be done, for example 24 times (taking a sample every 1 minute whilst stirring the 1000L and this would be more representative than one 30 µL sample). Once established that one sample is sufficiently representative of the whole vessel, or not, the testing protocol could be tailored to any specific scenario. However, bearing in mind that the six experiments reported in **4.3.7** were from six different batches of FV1-real, and yet an acceptable reproducibility was observed, that work suggests there is confidence in taking a very small sample from a big vessel to get uniform sampling.

Getting the highly reproducible quantitative data found for FV1-real from the 24 hours period study it is reasonable to imagine that it would be possible to use a shorter analytical time (perhaps five or ten hours) to develop confidence in assuring a good product through prediction from early time data to confidently expected outcome. It is likely that it would require growth in multiple media *e.g.*, one for lactic acid bacteria to see they grow well, one for general contaminants with lactic acid bacteria suppressed or eliminated, one for slow growing contaminants, one just sterile medium from FV1 before bacteria are added (sterility test). There are other options for testing if there is a multi-channel instrument, for example a long-term degradation of medium, a long-term stability of the final product, one channel dedicated to just keeping the product as is in an ampoule at storage temperature and see

whether there are any activities on storage. Additionally, if there was a calorimetric probe incorporated directly in a fermenting vessel, this would offer even faster data capture and these data could be analysed in real time.

Further research should also focus on investigating growth media using IMC. The system developed here is very sensitive to medium. Differences can be detected in the same medium; *e.g.*, TSB from different manufacturers, and that is really quite important. For example, studies that publish evidence from growing organisms and doing experiments with them on TSB might do so without knowing there is a detectable difference between TSB batches and TSB manufactures.

A question whether IMC has the capacity for identification, and more precisely distinguishing between perhaps just a small defined number of known microorganisms, should be explored in future. For example, could it be possible to say from two experiments that one is *E. faecium* and the second one *L. acidophilus*? In fact, from an extremely limited number of experiments (see **Appendix 5**) there is an illustration of a possibility of differentiating between the four organisms in Symprove using one testing medium only. This is suggestive of careful experiments using selective substrate utilisation by the product organisms (*e.g.*, as described in, for example, Ludwig *et al*., 2009). Designing selective media could be used to start a process of even species identification firstly of known organisms in a sample and extended to unknown samples.

Developing a fully functional and operator independent data processing and data interpretation tool; *i.e.*, a black box would be desirable in order to streamline the IMC testing method and roll it into the industry.

The equations developed in **Chapter 3** are perfectly general and describe any exponential growth in organisms. But because the equations were written from the perspective of microbiological theory, there will be some additional outcomes which could enhance microbiological theory and contribute to interpretation of microbial metabolism. The evidence for that is in **Chapter 4,** where it was noted that despite the equations only referring strictly to the exponential growth, because these are first order processes, it was observed that there were four other linear portions (**Figure 4.10**), revealed in the overall calorimetric experiment.

These other four unexplored linear periods offer the possibility to investigate these processes. Since the linear periods were observed in the growth of the organisms, these

periods indicate, in real time, where there are significant changes in metabolism. This was not the province of this thesis but being able to observe and record these changes is very suggestive of the capacity to employ calorimetry to understand much more about the metabolism of organisms. The process and progress of the metabolic changes (linear periods 2-5, **Figure 4.10**) so recorded were not related directly to exponential growth (linear period 1, **Figure 4.10**) but are related to other limiting factors in that particular system. It would be the first portion of each linear period that would be investigated to see what was being eliminated or becoming a critical element, for example substrate concentration or metabolite concentration using other methods (spectroscopic, chromatographic or wet chemical).

This study was not a biochemical one and there was no attempt made to speculate about the other linear portions observed in the logarithmically transformed p-t curve. However, it can be seen, in real time, that these other first order periods are giving information which, in principle, could be for example exhaustion of a component in the medium, build-up of metabolites, some other limiting factor or critical parameter. IMC does uniquely offer the means, should there be an interest in studying these other processes in future.

In medical settings, determining antibiotic susceptibility or resistance is a major concern. The capacity to deal with the microbial growth and getting quantitative data of interactions out as described in this project suggests the possibility of discovering quantitative data on a number of other growing organisms in other media and other conditions.. IMC has not yet become a widely used method to investigate for example urinary tract infections despite a lot of work done regarding the most common causal microorganisms with their specific growth characteristics in a variety of growth media (Beezer *et al.*, 1974; Bonkat *et al.*, 2013; Sigg *et al.*, 2022). Another example is the work done on IMC and sepsis where detection of bacterial or viral agents that are likely to cause the infection could, in principle, be quickly determined and appropriate treatment started (Kragh *et al.*, 2021). As IMC becomes more established method, this could lead to an early identification and targeted antibiotic intervention, whilst susceptibility or resistance of a particular microorganism to an antibiotic could be determined (Tellapragada *et al.*, 2020; Christensen *et al.*, 2024). The same principle, determining growth characteristics of microorganisms via IMC, could be used in intensive care settings where, for example, infective agents could be screened for resistance to antibiotic treatments with some antimicrobial susceptibility testing devices already containing a calorimeter (Shanmugakani *et al.*, 2020; Yamin *et al.*, 2023).

One example of a wider IMC application for the pharmaceutical industries could consist in checking the sterility of medical devices *e.g.*, swabs from any surfaces placed in an ampoule containing growth medium or analysis of coatings and materials proof of concept of which was done by Symcel company (Symcel, 2024). Sterility of medical formulations (sera or other injectables) using IMC was previously demonstrated advantageous compared with visual inspection by Brueckner *et al.*, (2017). In principle, there should be no growth (p-t curve should be a straight line closely parallel to zero power) if no microorganisms are present.

Isothermal calorimeters have the capacity to study these live and active products or their production processes. One of the major outcomes that is being advanced in this thesis is the capacity to take a sample from a fermentor directly to a calorimeter and get quantitative data out in order to gain insights into the processes in question. These applications are not purely about positive inoculations (do the organisms that were added to the process grow?). This was previously demonstrated, for example by Xiufang *et al.*, 1997; Miyake *et al.*, 2016; Fricke *et al.*, 2020), but they are also about negative inoculations hinting a contaminant presence by deviation from the expected p-t trace (Trampuz *et al.*, 2007; Maskow *et al.*, 2012; Ruchti *et al.*, 2024), hence a warning can be issued early. It needs to be appreciated that in between the analysis of the industrial applications and their extensions is the notion that the calorimeter itself can be multichannel, can be different sizes, it can in principle be adapted to particular circumstances. For example, as a part of the initial exploration of IMC suitability for this project was an attempt of flowthrough experiments (a viable prototype was developed), and that is important to mention because in some industries, like for example Symprove, it may be possible to continuously monitor the microbial growth directly in line from the fermentor vessel in real time.

It was shown that calorimetry has a significant potential for an industrial production control and it is not just a research tool. Calorimetry offers a qualitative as well as quantitative outcome, derived from the capacity to study sample as is, without any treatment but also in a simplified way.

References

Aguilera, J.M. (2019). The food matrix: Implications in processing, nutrition and health. *Critical Reviews in Food Science and Nutrition*, 59 (22), pp. 3612-3629. https://doi.org/10.1080/10408398.2018.1502743

Ahmed, G.K., Ramadan, H.K.A., Elbeh, K. and Haridy, N.A. (2024). Bridging the gap: Associations between gut microbiota and psychiatric disorders. *Middle East Current Psychiatry*, 31, 2 (14pp). https://doi.org/10.1186/s43045-024-00395-9

Almeida e Sousa, L., Beezer, A.E., Hansen, L.D., Clapham, D., Connor, J.A. and Gaisford, S. (2012). Calorimetric determination of rate constants and enthalpy changes for zero-order reactions. *Journal of Physical Chemistry B*, 116 (22), pp. 6356-6360. https://doi.org/10.1021/jp302933f

Aminov, R. and Aminova, L. (2023). The role of the glycome in symbiotic host-microbe interactions. *Glycobiology*, 33 (12), pp. 1106-1116. https://doi.org/10.1093/glycob/cwad073

Allegretti, J.R., Fischer, M., Sagi, S.V., Bohm, M.E., Fadda, H.M., Ranmal, S.R., Budree, S., Basit, A.W., Glettig, D.L., Eva, L. and Gentile, A. (2019). Fecal microbiota transplantation capsules with targeted colonic versus gastric delivery in recurrent *Clostridium difficile* infection: A comparative cohort analysis of high and lose dose. *Digestive Diseases and Sciences*, 64 (6), pp. 1672-1678. https://doi.org/10.1007/s10620-018-5396-6

Arboleya, S., Solís, G., Fernández, N., de los Reyes-Gavilán, C.G. and Gueimonde, M. (2012). Facultative to strict anaerobes ratio in the preterm infant microbiota: a target for intervention? *Gut microbes*, 3 (6), pp. 583-588. https://doi.org/10.4161/gmic.21942

Ashby, L.J. and Beezer, A.E. (1996). Calorimetry of Whole Yeast Cells. in Evans, I.H. (ed.) *Yeast Protocols. Methods in Molecular Biology*™, 53, Humana Press, pp. 376-382. https://doi.org/10.1385/0-89603-319-8:367

Astasov-Frauenhoffer, M., Braissant, O., Hauser-Gerspach, I., Daniels, A.U., Wirz, D., Weiger, R. and Waltimo, T. (2011). Quantification of vital adherent *Streptococcus sanguinis* cells on protein-coated titanium after disinfectant treatment. *Journal of Materials Science: Materials in Medicine*, 22 (9), pp. 2045-2051. https://doi.org/10.1007/s10856-011-4377-5

Bader, F.G. (1978). Analysis of double-substrate limited growth. *Biotechnology and bioengineering*, 20 (2), pp. 183-202. https://doi.org/10.1002/bit.260200203

Baker, J.L., Mark Welch, J.L., Kauffman, K.M., McLean, J.S. and He, X. (2024). The oral microbiome: diversity, biogeography and human health. *Nature Reviews Microbiology*, 22, pp. 89-104. https://doi.org/10.1038/s41579-023-00963-6

Bakken, J.S. (2009). Fecal bacteriotherapy for recurrent *Clostridium difficile* infection. *Anaerobe*, 15 (6), pp. 285-289. https://doi.org/10.1016/j.anaerobe.2009.09.007

Bajaj, J.S., Ng, S.C. and Schnabl, B. (2022). Promises of microbiome-based therapies. *Journal of Hepatology*, 76 (6), pp. 1379-1391. https://doi.org/10.1016/j.jhep.2021.12.003

Banik, A., Ghosh, K., Pal, S., Halder, S.K., Ghosh, C. and Mondal, K.C. (2020). Biofortification of multi-grain substrates by probiotic yeast. *Food Biotechnology*, 34 (4), pp. 283-305. https://doi.org/10.1080/08905436.2020.1833913

Barisas, B.G. and Gill, S.J. (1978). Microcalorimetry of biological systems. *Annual Review of Physical Chemistry*, 29 (1), pp. 141-166. https://doi.org/10.1146/annurev.pc.29.100178.001041

Battley, E.H., Putnam, R.L. and Boerio-Goates, J. (1997). Heat capacity measurements from 10 to 300 K and derived thermodynamic functions of lyophilized cells of *Saccharomyces cerevisiae* including the absolute entropy and the entropy of formation at 298.15 K. *Thermochimica Acta*, 298 (1-2), pp. 37-46. https://doi.org/10.1016/S0040-6031(97)00108-1

Battley, E.H. (1998). Augustin Pierre Dubrunfaut. *Thermochimica Acta*, 309 (1-2), pp. 1-3. https://doi.org/10.1016/S0040-6031(97)83271-6

Battley, E.H. (2013). A theoretical study of the thermodynamics of microbial growth using *Saccharomyces cerevisiae* and a different free energy equation. *The Quarterly Review of Biology*, 88 (2), pp. 69-96. https://doi.org/10.1086/670529

Beezer, A.E. and Tyrrell, H.J.V. (1972). Applications of flow microcalorimetry to biological problems: Part I theoretical aspects. *Science Tools, The LKB Instrument Journal*, 19 (1), pp. 13-16.

Beezer, A.E., Steenson, T.I. and Tyrrell, H.J.V. (1974a). Kinetic studies in a flow microcalorimeter: The acid-catalysed hydrolysis of methyl acetate at 25° C. *Thermochimica Acta*, 9 (4), pp. 447-449. https://doi.org/10.1016/0040-6031(74)80043-2

Beezer, A.E., Bettelheim, K.A., Newell, R.D. and Stevens, J. (1974b). The diagnosis of *bacteriuria* by flow microcalorimetry. A preliminary investigation. *Science Tools, The LKB Instrument Journal*, 21, pp. 13–16.

Beezer, A.E., Newell, R.D. and Tyrrell, H.J.V. (1976). Application of flow microcalorimetry to analytical problems: The preparation, storage and assay of frozen inocula of *Saccharomyces cerevisiae*. *Journal of Applied Bacteriology,* 41 (2), pp. 197-207. https://doi.org/10.1111/j.1365-2672.1976.tb00620.x

Beezer, A.E. (1977). Microcalorimetric studies of micro-organisms. in Lamprecht, I. and Schaarschmidt, B. (eds.) *Proceedings of the international conference in Berlin, August 2–3, 1976*. Berlin, Boston: De Gruyter, pp. 109-118. https://doi.org/10.1515/9783110860719

Beezer, A.E., Newell, R.D. and Tyrrell, H.J.V. (1979). Characterisation and metabolic studies of *Saccharomyces cerevisiae* and *Kluyveromyces fragilis* by flow microcalorimetry. *Antonie van Leeuwenhoek*, 45, pp. 55-63. https://doi.org/10.1007/BF00400779

Beezer, A.E. (1980). *Biological microcalorimetry*. London: Academic Press.

Beezer, A.E. and Chowdhry, B.Z. (1980). Microcalorimetric investigations of drugs, in A.E. Beezer (ed.) *Biological microcalorimetry*. London: Academic Press, pp. 195–246.

Beezer, A.E., Gaisford, S., Hills, A.K., Richard, J. and Mitchell, J.C. (1999). Pharmaceutical microcalorimetry: Applications to long-term stability studies. *International Journal of Pharmaceutics*, 179 (2), pp. 159-165. https://doi.org/10.1016/S0378-5173(98)00336-6

Beezer, A.E. (2001). An outline of new calculation methods for the determination of both thermodynamic and kinetic parameters from isothermal heat conduction microcalorimetry. *Thermochimica Acta*, 380 (2), pp. 205-208. https://doi.org/10.1016/S0040-6031(01)00673-6

Beezer, A.E., Morris, A.C., O'Neill, M.A., Willson, R.J., Hills, A.K., Mitchell, J.C. and Connor, J.A. (2001). Direct determination of equilibrium thermodynamic and kinetic parameters from isothermal heat conduction microcalorimetry. *The Journal of Physical Chemistry B*, 105 (6), pp. 1212-1215. https://doi.org/10.1021/jp003539s

Belaich, J.P. (1980). Growth and metabolism in bacteria, in Beezer, A.E. (ed.) *Biological microcalorimetry*. London: Academic Press, pp. 1-42.

Berg, G., Rybakova, D., Fischer, D., Cernava, T., Vergès, M.C., Charles, T., Chen, X., Cocolin, L., Eversole, K., Corral, G.H., Kazou, M., Kinkel, L., Lange, L., Lima, N., Loy, A., Macklin, J.A., Maguin, E., Mauchline, T., McClure, R., Mitter, B., Ryan, M., Sarand, I., Smidt, H., Schelkle, B., Roume, H., Kiran, G.S., Selvin, J., Souza, R.S.C., van Overbeek, L., Singh, B.K., Wagner, M., Walsh, A., Sessitsch, A. and Schloter, M. (2020). Microbiome definition re-visited: Old concepts and new challenges. *Microbiome*, 8, 103 (22pp). https://doi.org/10.1186/s40168-020-00875-0

Binda, S., Hill, C., Johansen, E., Obis, D., Pot, B., Sanders, M.E., Tremblay, A. and Ouwehand, A.C. (2020). Criteria to qualify microorganisms as "probiotic" in foods and dietary supplements. *Frontiers in Microbiology,* 11, 1662 (9pp). https://doi.org/10.3389/fmicb.2020.01662

Bjarnason, I., Sission, G. and Hayee, B. (2019). A randomised, double-blind, placebo-controlled trial of a multi-strain probiotic in patients with asymptomatic ulcerative colitis and Crohn's disease. *Inflammopharmacology*, 27 (3), pp. 465-473. https://doi.org/10.1007/s10787-019-00595-4

Boling, E., Blanchard, G. and Russell, W. (1973). Bacterial identification by microcalorimetry. *Nature*, 241, pp. 472–473. https://doi.org/10.1038/241472a0

Bonkat, G., Braissant, O., Widmer, A.F., Frei, R., Rieken, M., Wyler, S., Gasser, T.C., Wirz, D., Daniels, A.U. and Bachmann, A. (2012). Rapid detection of urinary tract pathogens using microcalorimetry: Principle, technique and first results. *BJU International*, 110 (6) pp. 892-897. https://doi.org/10.1111/j.1464-410X.2011.10902.x

Bonsack, B., Jiang, R.H. and Borlongan, C.V. (2020). A gut feeling about stroke reveals gut-brain axis' active role in homeostasis and dysbiosis. *Journal of Cerebral Blood Flow & Metabolism*, 40 (5), pp. 1132-1134. https://doi.org/10.1177/0271678X19900037

Bourdichon, F., Casaregola, S., Farrokh, C., Frisvad, J.C., Gerds, M.L., Hammes, W.P., Harnett, J., Huys, G., Laulund, S., Ouwehand, A., Powell, I.B., Prajapati, J.B., Seto, Y., Ter Schure, E., Van Boven, A., Vankerckhoven, V., Zgoda, A., Tuijtelaars, S. and Hansen, E.B. (2012). Food fermentations: Microorganisms with technological beneficial use. *International Journal of Food Microbiology,* 154 (3), pp. 87-97. https://doi.org/10.1016/j.ijfoodmicro.2011.12.030

Boyte, M.-E., Benkowski, A., Pane, M. and Shehata, H.R. (2023). Probiotic and postbiotic analytical methods: A perspective of available enumeration techniques. *Frontiers in Microbiology*. 14, 1304621 (15pp). https://doi.org/10.3389/fmicb.2023.1304621

Braissant, O., Wirz, D., Göpfert, B. and Daniels, A.U. (2010a). Biomedical use of isothermal microcalorimeters. *Sensors*, 10 (10), pp. 9369-9383. https://doi.org/10.3390/s101009369

Braissant, O., Wirz, D., Göpfert, B. and Daniels, A.U. (2010b). Use of isothermal microcalorimetry to monitor microbial activities. *FEMS Microbiology Letters*, 303 (1), pp. 1-8. https://doi.org/10.1111/j.1574-6968.2009.01819.x

Braissant, O., Bonkat, G., Wirz, D. and Bachmann, A. (2013). Microbial growth and isothermal microcalorimetry: Growth models and their application to microcalorimetric data. *Thermochimica Acta*, 555, pp. 64-71. http://dx.doi.org/10.1016/j.tca.2012.12.005

Braissant, O., Bachmann, A. and Bonkat, G. (2015a). Microcalorimetric assays for measuring cell growth and metabolic activity: Methodology and applications. *Methods*, 76, pp. 27-34. https://doi.org/10.1016/j.ymeth.2014.10.009

Braissant, O., Chavanne, P., de Wild, M., Pieles, U., Stevanovic, S., Schumacher, R., Straumann, L., Wirz, D., Gruner, P., Bachmann, A. and Bonkat, G. (2015b). Novel microcalorimetric assay for antibacterial activity of implant coatings: The cases of silver-doped hydroxyapatite and calcium hydroxide. *Journal of Biomedical Materials Research Part B: Applied Biomaterials*, 103 (6), pp. 1161-1167. https://doi.org/10.1002/jbm.b.33294

Braissant, O., Astasov-Frauenhoffer, M., Waltimo, T. and Bonkat, G. (2020). A review of methods to determine viability, vitality, and metabolic rates in microbiology. *Frontiers in Microbiology*. 11, 547458 (25pp). https://doi.org/10.3389/fmicb.2020.547458

Brown, H.D. (1969). *Biochemical microcalorimetry*. London: Academic Press.

Brueckner, D., Krähenbühl, S., Zuber, U., Bonkat, G. and Braissant, O. (2017). An alternative sterility assessment for parenteral drug products using isothermal microcalorimetry. *Journal of applied microbiology*, 123 (3), pp.773-779. https://doi.org/10.1111/jam.13520

Burlett, D.J. (2008). Quality Control. in Brown, M.E. and Gallagher, P.K. (eds.) *Handbook of thermal analysis and calorimetry: Recent advances, techniques and applications, Volume 5*. Elsevier Science B.V., pp. 695-732.

Buttó, L.F., Schaubeck, M. and Haller, D. (2015). Mechanisms of microbe–host interaction in Crohn's disease: Dysbiosis vs. pathobiont selection. *Frontiers in Immunology*, 6, 555 (20pp). https://doi.org/10.3389/fimmu.2015.00555

Byndloss, M.X. and Bäumler, A.J. (2018). The germ-organ theory of non-communicable diseases. *Nature Reviews Microbiology*, 16 (2), pp. 103-110. https://doi.org/10.1038/nrmicro.2017.158

Cabadaj, M., Bashir, S., Haskins, D., Said, J., Gaisford, S. and Beezer, A. (2021). Kinetic analysis of microcalorimetric data derived from microbial growth: Basic theoretical, practical and industrial considerations. *Journal of Microbiological Methods*, 187, 106276 (7pp). https://doi.org/10.1016/j.mimet.2021.106276

Callaghan, B.L., Fields, A., Gee, D.G., Gabard-Durnam, L., Caldera, C., Humphreys, K.L., Goff, B., Flannery, J., Telzer, E.H., Shapiro, M. and Tottenham, N. (2020). Mind and gut: Associations between mood and gastrointestinal distress in children exposed to adversity. *Development and Psychopathology*, 32 (1), pp.309-328. https://doi:10.1017/S0954579419000087

Calvet, E. and Prat, H. (1963). *Recent progress in microcalorimetry*. Oxford, UK: Pergamon Press.

Cammarota, G., Ianiro, G., Bibbo, S. and Gasbarrini, A. (2014). Gut microbiota modulation: Probiotics, antibiotics or fecal microbiota transplantation? *Internal and Emergency Medicine*, 9 (4), pp. 365-373. https://doi.org/10.1007/s11739-014-1069-4

Cani, P.D. (2012). Crosstalk between the gut microbiota and the endocannabinoid system: Impact on the gut barrier function and the adipose tissue. *Clinical Microbiology and Infection,* 18 (s4)*,* pp. 50-53. https://doi.org/10.1111/j.1469-0691.2012.03866.x

Cani, P.D., Plovier, H., Van Hul, M., Geurts, L., Delzenne, N.M., Druart, C. and Everard, A. (2016). Endocannabinoids—at the crossroads between the gut microbiota and host metabolism. *Nature Reviews Endocrinology*, 12 (3), pp. 133-143. https://doi.org/10.1038/nrendo.2015.211

Capozzi, V., Fragasso, M. and Russo, P. (2020). Microbiological safety and the management of microbial resources in artisanal foods and beverages: The need for a transdisciplinary assessment to conciliate actual trends and risks avoidance. *Microorganisms*, 8 (2) 306 (9pp). https://doi.org/10.3390/microorganisms8020306

Carr, R.W. (ed.) (2007). Modeling of chemical reactions. Volume 42, in Green, N.J.B. (ed.) *Comprehensive chemical kinetics*, Amsterdam, Oxford: Elsevier, pp. 1-6. https://doi.org/10.1016/S0069-8040(07)42001-5

Carroll, B. and Manche, E.P. (1972). Kinetic analysis of chemical reactions for non-isothermal procedures. *Thermochimica Acta*, 3 (6), pp. 449-459. https://doi.org/10.1016/0040-6031(72)85004-4

Castelli, V., d'Angelo, M., Quintiliani, M., Benedetti, E., Cifone, M.G. and Cimini, A. (2021). The emerging role of probiotics in neurodegenerative diseases: New hope for Parkinson's disease? *Neural Regeneration Research*, 16 (4), pp. 628-634. https://doi.org/10.4103/1673-5374.295270

Chakraborty, P., Majumder, P., Banerjee, D. and Sarkar, J. (2024). Gut microbiota nexus: Exploring the interactions with the brain, heart, lungs, and skin axes and their effects on health. *Medicine in Microecology*, 20, 100104 (11pp). https://doi.org/10.1016/j.medmic.2024.100104

Chaluvadi, S., Hotchkiss, A.T. and Yam, K.L. (2015). Gut microbiota: Impact of probiotics, prebiotics, synbiotics, pharmabiotics, and postbiotics on human health. in Watson, R.R. and Preedy, V.R. (eds.) *Probiotics, Prebiotics, and Synbiotics: Bioactive Foods in Health Promotion,* USA, Academic Press, pp. 515-523.

Chang-Li, X., Hou-Kuhan, T., Zhau-Hua, S., Song-Sheng, Q., Yao-Ting, L. and Hai-Shui, L. (1988). Microcalorimetric study of bacterial growth. *Thermochimica Acta*, 123, pp. 33-41. https://doi.org/10.1016/0040-6031(88)80007-8

Chetty, A. and Blekhman, R. (2024). Multi-omic approaches for host-microbiome data integration. *Gut Microbes*, 16 (1), 2297860 (22pp). https://doi.org/10.1080/19490976.2023.2297860

Chevalier, G., Siopi, E., Guenin-Macé, L., Pascal, M., Laval, T., Rifflet, A., Boneca, I.G., Demangel, C., Colsch, B., Pruvost, A., Chu-Van, E., Messager, A., Leulier, F., Lepousez, G., Eberl, G. and Lledo, P.-M. (2020). Effect of gut microbiota on depressive-like behaviors in mice is mediated by the endocannabinoid system. *Nature Communications*, 11 (1), 6363 (15pp). https://doi.org/10.1038/s41467-020-19931-2

Clemente, J.C., Ursell, L.K., Parfrey, L.W. and Knight, R. (2012). The impact of the gut microbiota on human health: An integrative view. *Cell*, 148 (6), pp. 1258-1270. https://doi.org/10.1016/j.cell.2012.01.035

Codex Alimentarius Commission, (2018). *Joint FAO/WHO Food Standards Programme. Codex Committee on Nutrition and Foods for Special Dietary Uses. Proposal for new work on international prebiotic guidelines for use in foods and dietary supplements*. pp. 1-14. Available at: https://www.fao.org/fao-who-codexalimentarius/sh-proxy/en/?lnk=1&url=https%253A%252F%252Fworkspace.fao.org%252Fsites%252Fcodex%252FMeetings%252FCX-720-40%252FCRD%252FCRD04%2B%2528prepared%2Bby%2BSudan%2529.pdf (Accessed: 15 February, 2024).

Collado, M.C., Vinderola, G. and Salminen, S. (2019). Postbiotics: Facts and open questions. A position paper on the need for a consensus definition. *Beneficial Microbes*, 10 (7), pp. 711-719. https://doi.org/10.3920/BM2019.0015

Contois, D.E. (1959). Kinetics of bacterial growth: Relationship between population density and specific growth rate of continuous cultures. *Microbiology*, 21 (1), pp. 40-50. https://doi.org/10.1099/00221287-21-1-40

Corning, B., Copland, A.P. and Frye, J.W. (2018). The esophageal microbiome in health and disease. *Current Gastroenterology Reports*, 20, 39 (7pp). https://doi.org/10.1007/s11894-018-0642-9

Cornish-Bowden, A. (2012). *Fundamentals of enzyme kinetics*. 4th edn. Weinheim: John Wiley & Sons.

Corry, J.E., Jarvis, B., Passmore, S. and Hedges, A., (2007). A critical review of measurement uncertainty in the enumeration of food micro-organisms. *Food Microbiology*, 24 (3), pp. 230-253. https://doi.org/10.1016/j.fm.2006.05.003

Corvec, S., Seiler, E., Wang, L., Moreno, M.G. and Trampuz, A. (2020). Characterization of medical relevant anaerobic microorganisms by isothermal microcalorimetry. *Anaerobe*, 66, 102282 (6pp). https://doi.org/10.1016/j.anaerobe.2020.102282

Costea, P.I., Hildebrand, F., Arumugam, M., Bäckhed, F., Blaser, M.J., Bushman, F.D., De Vos, W.M., Ehrlich, S.D., Fraser, C.M., Hattori, M. and Huttenhower, C. (2018). Enterotypes in the landscape of gut microbial community composition. *Nature microbiology,* 3 (1), pp. 8-16. https://doi.org/10.1038/s41564-017-0072-8

Cryan, J.F., O'Riordan, K.J., Cowan, C.S., Sandhu, K.V., Bastiaanssen, T.F., Boehme, M., Codagnone, M.G., Cussotto, S., Fulling, C., Golubeva, A.V. and Guzzetta, K.E., Jaggar, M., Long-Smith, C.M., Lyte, J.M., Martin, J.A., Molinero-Perez, A., Moloney, G., Morelli, E., Morillas, E., O'Connor, R., Cruz-Pereira, J.S., Peterson, V.L., Rea, K., Ritz, N.L., Sherwin, E., Spichak, S., Teichman, E.M., van de Wouw, M., Ventura-Silva, A.P., Wallace-Fitzsimons,

S.E., Hyland, N., Clarke, G. and Dinan, T.G. (2019). The microbiota-gut-brain axis. *Physiological Reviews*, 99 (4), pp. 1877-2013. https://doi.org/10.1152/physrev.00018.2018

Curtis, M.A., Zenobia, C. and Darveau, R.P. (2011). The relationship of the oral microbiotia [*sic*] to periodontal health and disease. *Cell Host & Microbe*, 10 (4), pp. 302-306. https://doi.org/10.1016/j.chom.2011.09.008

Cusick, S.E. and Georgieff, M.K. (2016). The role of nutrition in brain development: The golden opportunity of the "first 1000 days". *The Journal of Pediatrics*, 175, pp. 16-21. https://doi.org/10.1016/j.jpeds.2016.05.013

Cutting, S.M. (2011). *Bacillus* probiotics. *Food Microbiology,* 28 (2)*,* pp. 214-220. https://doi.org/10.1016/j.fm.2010.03.007

Czerucka, D., Piche, T. and Rampal, P. (2007). Yeast as probiotics–*Saccharomyces boulardii*. *Alimentary Pharmacology & Therapeutics*, 26 (6), pp. 767-778. https://doi.org/10.1111/j.1365-2036.2007.03442.x

de Buruaga, I.S., Echevarría, A., Armitage, P.D., De la Cal, J.C., Leiza, J.R. and Asua, J.M. (1997). On-line control of a semibatch emulsion polymerization reactor based on calorimetry. *AIChE Journal*, 43 (4), pp. 1069-1081. https://doi.org/10.1002/aic.690430420

Deleu, S., Machiels, K., Raes, J., Verbeke, K. and Vermeire, S. (2021). Short chain fatty acids and its producing organisms: An overlooked therapy for IBD? *EBioMedicine*, 66, 103293 (8pp). https://doi.org/10.1016/j.ebiom.2021.103293

Di Domenico, M., Ballini, A., Boccellino, M., Scacco, S., Lovero, R., Charitos, I.A. and Santacroce, L. (2022). The intestinal microbiota may be a potential theranostic tool for personalized medicine. *Journal of Personalized Medicine*, 12 (4), 523 (26pp). https://doi.org/10.3390/jpm12040523

Di Pilato, V., Freschi, G., Ringressi, M.N., Pallecchi, L., Rossolini, G.M. and Bechi, P. (2016). The esophageal microbiota in health and disease. *Annals of the New York Academy of Sciences*, 1381 (1), pp. 21-33. https://doi.org/10.1111/nyas.13127

Dietert, R.R. and Dietert, J.M. (2015). The microbiome and sustainable healthcare. *Healthcare*, 3 (1), pp. 100-129. https://doi.org/10.3390/healthcare3010100

Dieterich, W., Schink, M. and Zopf, Y. (2018). Microbiota in the gastrointestinal tract. *Medical Sciences*, 6 (4), 116 (15pp). https://doi.org/10.3390/medsci6040116

Dodoo, C.C., Stapleton, P., Basit, A.W. and Gaisford, S. (2019). Use of a water-based probiotic to treat common gut pathogens. *International Journal of Pharmaceutics,* 556, pp. 136-141. https://doi.org/10.1016/j.ijpharm.2018.11.075

Dominguez-Bello, M.G., Costello, E.K., Contreras, M., Magris, M., Hidalgo, G., Fierer, N. and Knight, R. (2010). Delivery mode shapes the acquisition and structure of the initial microbiota across multiple body habitats in newborns. *Proceedings of the National Academy of Sciences,* 107 (26), pp. 11971-11975. https://doi.org/10.1073/pnas.1002601107

Droop, M.R. (1983). 25 years of algal growth kinetics a personal view. *Botanica Marina*, 26, pp. 99-112. https://doi.org/10.1515/botm.1983.26.3.99

Egli, T. (2009). Growth kinetics, bacterial. in Schaechter, M. (ed.) *Encyclopedia of Microbiology*. Oxford: Elsevier, pp. 180-193.

European Commission. (2005). Regulation (EC) No 2073/2005 on microbiological criteria for foodstuffs. *Official Journal of European Union,* 02005R2073 — EN — 08.03.2020 — 009.001, pp. 1-32. http://data.europa.eu/eli/reg/2005/2073/2020-03-08

European parliament and the Council. (2015). Regulation EU 2015/2283 on novel foods, amending Regulation (EU) No 1169/ 2011 of the European Parliament and of the Council and repealing Regulation (EC) No 258/ 97 of the European Parliament and of the Council and Commission Regulation (EC) No 1852/ 2001, *EUR-Lex*, pp. 21. http://data.europa.eu/eli/reg/2015/2283/2021-03-27

FAO, WHO, 2002. Food and Agriculture Organization (FAO), World Health Organization (WHO). (2002). *Report of a Joint FAO/WHO working group on drafting guidelines for the evaluation of probiotics in food. Guidelines for the evaluation of probiotics in food*. Available at: https://www.mhlw.go.jp/file/05-Shingikai-11121000-Iyakushokuhinkyoku-Soumuka/0000197343.pdf (Accessed: 22 February 2024)

Fassarella, M., Blaak, E.E., Penders, J., Nauta, A., Smidt, H. and Zoetendal, *E.G.* (2021). Gut microbiome stability and resilience: elucidating the response to perturbations in order to modulate gut health. *Gut,* 70 (3), pp. 595-605. https://doi.org/10.1136/gutjnl-2020-321747

Feher, J.J. (2012). *Quantitative human physiology: An introduction*. USA: Academic press. https://doi.org/10.1016/C2009-0-64018-6

Feng, Y., Tian, X., Chen, Y. *et al*. Real-time and on-line monitoring of ethanol fermentation process by viable cell sensor and electronic nose. (2021). *Bioresources and Bioprocessing*. 8, 37 (10pp). https://doi.org/10.1186/s40643-021-00391-5

Ferreira, R.D.S., Mendonça, L.A.B.M., Ribeiro, C.F.A., Calças, N.C., Guimarães, R.D.C.A., Nascimento, V.A.D., Gielow, K.D.C.F., Carvalho, C.M.E., Castro, A.P.D. and Franco, O.L. (2022). Relationship between intestinal microbiota, diet and biological systems: An integrated view. *Critical Reviews in Food Science and Nutrition*, 62 (5), pp.1166-1186. https://doi.org/10.1080/10408398.2020.1836605

Fessas, D., Schiraldi, A. (2017). Isothermal calorimetry and microbial growth: Beyond modeling. *Journal of Thermal Analysis and Calorimetry*, 130, pp. 567–572. https://doi.org/10.1007/s10973-017-6515-x

Foddai, A.C.G. and Grant, I.R. (2020). Methods for detection of viable foodborne pathogens: Current state-of-art and future prospects. *Applied Microbiology and Biotechnology*, 104, pp. 4281-4288. https://doi.org/10.1007/s00253-020-10542-x

Fredua-Agyeman, M. and Gaisford, S. (2015). Comparative survival of commercial probiotic formulations: tests in biorelevant gastric fluids and real-time measurements using microcalorimetry. *Beneficial Microbes,* 6 (1), pp. 141-151. https://doi.org/10.3920/BM2014.0051

Fredua-Agyeman, M., Stapleton, P., Basit, A.W., Beezer, A.E. and Gaisford, S. (2017a). *In vitro* inhibition of *Clostridium difficile* by commercial probiotics: A microcalorimetric study. *International Journal of Pharmaceutics*, 517 (1-2), pp. 96-103. https://doi.org/10.1016/j.ijpharm.2016.12.005

Fredua-Agyeman, M., Stapleton, P., Basit, A.W. and Gaisford, S. (2017b). Microcalorimetric evaluation of a multi-strain probiotic: Interspecies inhibition between probiotic strains. *Journal of Functional Foods*, 36, pp. 357-361. https://doi.org/10.1016/j.jff.2017.07.018

Fredua-Agyeman, M., Gaisford, S. and Beezer, A.E. (2018). Observation with microcalorimetry: Behaviour of *P. aeruginosa* in mixed cultures with *S. aureus* and *E. coli*. *Thermochimica Acta*, 663, pp. 93-98. https://doi.org/10.1016/j.tca.2018.03.009

Freeman, E.S. and Carroll, B. (1958). The application of thermoanalytical techniques to reaction kinetics: The thermogravimetric evaluation of the kinetics of the decomposition of calcium oxalate monohydrate. *The Journal of Physical Chemistry*, 62 (4), pp. 394-397. https://doi.org/10.1021/j150562a003

Freitas, C.A., Rodrigues, D., Sousa, S., Gomes, M.A. and Pintado, M.M. (2014). Food as vehicles of probiotics. in Sousa e Silva, J.P. and Freitas, A.C. (eds.) *Probiotic bacteria: Fundamentals, therapy, and technological aspects*, USA: Pan Stanford Publishing, pp. 95-169.

Fricke, C., Harms, H. and Maskow, T. (2019). Rapid calorimetric detection of bacterial contamination: Influence of the cultivation technique. *Frontiers in Microbiology*, 10, 2530 (12pp). https://doi.org/10.3389/fmicb.2019.02530.

Fricke, C., Xu, J., Jiang, F.L., Liu, Y., Harms, H. and Maskow, T. (2020). Rapid culture-based detection of *Legionella pneumophila* using isothermal microcalorimetry with an improved evaluation method. *Microbial Biotechnology*, 13 (4), pp. 1262-1272. https://doi.org/10.1111/1751-7915.13563

Fujiki, J. and Schnabl, B. (2023). Phage therapy: Targeting intestinal bacterial microbiota for treatment of liver diseases. *JHEP Reports*, 5 (12), 100909 (13pp). https://doi.org/10.1016/j.jhepr.2023.100909

Fujita, T., Monk, P.R. and Wadsö, I. (1978). Calorimetric identification of several strains of lactic acid bacteria. *Journal of Dairy Research*. 45 (3), pp. 457-463. https://doi.org/10.1017/S0022029900016678

Funkhouser LJ, Bordenstein SR. (2013). Mom knows best: The universality of maternal microbial transmission. *PLoS Biology*, 11 (8), e1001631 (9pp). https://doi.org/10.1371/journal.pbio.1001631.

Gaisford, S., Hills, A.K., Beezer, A.E. and Mitchell, J.C. (1999). Thermodynamic and kinetic analysis of isothermal microcalorimetric data: Applications to consecutive reaction schemes. *Thermochimica Acta*, 328 (1-2), pp. 39-45. https://doi.org/10.1016/S0040-6031(98)00622-4

Gaisford, S. and O'Neill, M.A.A. (2006). *Pharmaceutical isothermal calorimetry*. New York: Informa Healthcare.

Gaisford, S., O'Neill, M.A.A. and Beezer, A.E. (2009). Shelf life prediction of complex food systems by quantitative interpretation of isothermal calorimetric data. in Kaletunc, G. (ed.) *Calorimetry in food processing: Analysis and design of food systems*. Wiley-Blackwell. pp. 201-236.

Gao, J., Yi, X. and Wang, Z. (2023). The application of multi-omics in the respiratory microbiome: Progresses, challenges and promises. *Computational and Structural Biotechnology Journal*, 21, pp. 4933-4943. https://doi.org/10.1016/j.csbj.2023.10.016

Gao, Y., Yao, Q., Meng, L., Wang, J. and Zheng, N. (2024). Double-side role of short chain fatty acids on host health via the gut-organ axes. *Animal Nutrition*, 18, pp. 322-339. https://doi.org/10.1016/j.aninu.2024.05.001

Garcia, A.H., Herrmann, A.M. and Håkansson, S. (2017). Isothermal microcalorimetry for rapid viability assessment of freeze-dried *Lactobacillus reuteri*. *Process Biochemistry*, 55, pp. 49-54. https://doi.org/10.1016/j.procbio.2017.01.012

Gardikis, K., Signorelli, M., Ferrario, C., Schiraldi, A., Fortina, M.G., Hatziantoniou, S., Demetzos, C. and Fessas, D. (2017). Microbial biosensors to monitor the encapsulation effectiveness of doxorubicin in chimeric advanced drug delivery nano systems: A calorimetric approach. *International Journal of Pharmaceutics*, 516 (1-2), pp. 178-184. https://doi.org/10.1016/j.ijpharm.2016.11.033

Ghyselinck, J., Verstrepen, L., Moens, F., Van den Abbeele, P., Said, J., Smith, B., Bjarnason, I., Basit, A.W. and Gaisford, S. (2020). A 4-strain probiotic supplement influences gut microbiota composition and gut wall function in patients with ulcerative colitis. *International Journal of Pharmaceutics*, 587, 119648 (9pp). https://doi.org/10.1016/j.ijpharm.2020.119648

Ghyselinck, J., Verstrepen, L., Moens, F., Van Den Abbeele, P., Bruggeman, A., Said, J., Barker, L.A., Jordan, C., Leta, V., Chaudhuri, K.R., Basit, A.W. and Gaisford, S. (2021). Influence of probiotic bacteria on gut microbiota composition and gut wall function in an in-vitro model in patients with Parkinson's disease. *International Journal of Pharmaceutics: X*, 3, 100087 (12pp). https://doi.org/10.1016/j.ijpx.2021.100087

Gibson, G.R. and Roberfroid, M.B. (1995). Dietary modulation of the human colonic microbiota: Introducing the concept of prebiotics. *The Journal of nutrition*, 125 (6), pp. 1401-1412. https://doi.org/10.1093/jn/125.6.1401

Gibson, G.R., Probert, H.M., Van Loo, J., Rastall, R.A. and Roberfroid, M.B. (2004). Dietary modulation of the human colonic microbiota: Updating the concept of prebiotics. *Nutrition Research Reviews*, 17 (2), pp. 259-275. https://doi.org/10.1079/NRR200479

Gibson, G.R., Hutkins, R., Sanders, M.E., Prescott, S.L., Reimer, R.A., Salminen, S.J., Scott, K., Stanton, C., Swanson, K.S., Cani, P.D. and Verbeke, K. (2017). Expert consensus document: The International Scientific Association for Probiotics and Prebiotics (ISAPP) consensus statement on the definition and scope of prebiotics. *Nature Reviews Gastroenterology & Hepatology,* 14 (8), pp. 491-502. https://doi.org/10.1038/nrgastro.2017.75

GMI. (2023). *Probiotic Strains Market Size. Report ID: GMI7272*. Available at: https://www.gminsights.com/industry-analysis/probiotic-strains-market (Accessed: 17 February 2024).

Gogineni, V.K., Morrow, L.E., Gregory, P.J. and Malesker, M.A. (2013). Probiotics: History and evolution. *Journal of Infectious Diseases and Preventive Medicine*, 1 (2), 1000107 (7pp). https://doi.org/10.4172/2329-8731.1000107

Gogokhia, L., Buhrke, K., Bell, R., Hoffman, B., Brown, D.G., Hanke-Gogokhia, C., Ajami, N.J., Wong, M.C., Ghazaryan, A., Valentine, J.F. and Porter, N. (2019). Expansion of bacteriophages is linked to aggravated intestinal inflammation and colitis. *Cell Host & Microbe*, 25 (2), pp. 285-299. https://doi.org/10.1016/j.chom.2019.01.008

Gomes, J., Chopda, V. and Rathore, A.S. (2019). Monitoring and control of bioreactor: Basic concepts and recent advances. in Komives, C. and Zhou, W. (eds.) *Bioprocessing Technology for Production of Biopharmaceuticals and Bioproducts*. USA, John Wiley & Sons, Inc. pp. 201-237.

Gompertz, B. (1825). On the nature of the function expressive of the law of human mortality, and on a new mode of determining the value of life contingencies. *Philosophical Transactions of the Royal Society of London*, 115, pp. 513-585. https://doi.org/10.1098/rstl.1825.0026

Goodarzi, A., Mozafarpoor, S., Bodaghabadi, M. and Mohamadi, M. (2020). The potential of probiotics for treating acne vulgaris: A review of literature on acne and microbiota. *Dermatologic therapy*, 33 (3), e13279 (6pp). https://doi.org/10.1111/dth.13279

Gorkiewicz, G. and Moschen, A. (2018). Gut microbiome: A new player in gastrointestinal disease. *Virchows Archiv*, 472 (1), pp. 159-172. https://doi.org/10.1007/s00428-017-2277-x

Gram, L. and Søgaard, H. (1985). Microcalorimetry as a rapid method for estimation of bacterial levels in ground meat. *Journal of Food Protection*, 48 (4), pp. 341-345. https://doi.org/10.4315/0362-028X-48.4.341

Gray, H. (1977). Anatomy, descriptive and surgical: The organs of digestion. in Pickering Pick, T. and Howden, R. (eds.) *Gray's anatomy*. New York: Bounty Books, pp. 869-954.

Green, L.A., Loscombe, S.M., Wood, S.L. and Barker, K.A. (2013). *Tests for microbial examination of probiotic products – microbial enumeration tests, total lactobacillus count and total enterococcus count - pre-poured plate method*. SOP No: MM154-00. Fareham: Wickham Laboratories Limited. (Available upon request)

Grigg, J.B. and Sonnenberg, G.F. (2017). Host-microbiota interactions shape local and systemic inflammatory diseases. *The Journal of Immunology,* 198 (2), pp. 564-571. https://doi.org/10.4049/jimmunol.1601621

Grime, J.K., (1980). Biochemical and clinical analysis by enthalpimetric measurements—a realistic alternative approach? *Analytica Chimica Acta*, 118 (2), pp.191-225. https://doi.org/10.1016/S0003-2670(01)93597-4

Guo, W.L., Du, Y.P., Zhou, Y.C., Yang, S., Lu, J.H., Zhao, H.Y., Wang, Y. and Teng, L.R. (2012). At-line monitoring of key parameters of nisin fermentation by near infrared spectroscopy, chemometric modeling and model improvement. *World Journal of Microbiology and Biotechnology*. 28, pp.993-1002. https://doi.org/10.1007/s11274-011-0897-x

Guo, Y., Kitamoto, S. and Kamada, N. (2020). Microbial adaptation to the healthy and inflamed gut environments. *Gut Microbes*, 12 (1), pp. 1-14. https://doi.org/10.1080/19490976.2020.1857505

Gupta, S., Mullish, B.H. and Allegretti, J.R. (2021). Fecal microbiota transplantation: The evolving risk landscape. *Official Journal of the American College of Gastroenterology*, 116 (4), pp. 647-656. https://doi.org/10.14309/ajg.0000000000001075

Handbook of Microbiological Criteria for Foods. (2020). 2nd edn. London: Institute of Food Science & Technology.

Hassan, H.O.T. (2020). *Improving the reporting of death and investigating the role of probiotics in mucositis and infections in children with cancer*. Thesis. University of Leeds. Available at: https://etheses.whiterose.ac.uk/28137/ (Accessed: 19 February 2024).

Hey, G.E., Vedam-Mai, V., Beke, M., Amaris, M. and Ramirez-Zamora, A. (2023). The interface between inflammatory bowel disease, neuroinflammation, and neurological disorders. *Seminars in Neurology*, 43 (4), pp. 572-582. https://doi.org/10.1055/s-0043-1771467.

Hill, C., Guarner, F., Reid, G., Gibson, G.R., Merenstein, D.J., Pot, B., Morelli, L., Canani, R.B., Flint, H.J., Salminen, S. and Calder, P.C. (2014). Expert consensus document: The International Scientific Association for Probiotics and Prebiotics consensus statement on the scope and appropriate use of the term probiotic. *Nature Reviews Gastroenterology & Hepatology,* 11 (8), pp. 506-514. https://doi.org/10.1038/nrgastro.2014.66

Hills, A. (2011). Isothermal calorimetric analysis, in Storey, R.A. and Ymén, I. (eds.) *Solid state characterization of pharmaceuticals*. Chichester: John Wiley & Sons, pp. 207-231.

Hinshelwood, C.N. (1946). *The chemical kinetics of the bacterial cell*. Oxford: The Clarendon Press.

Hu, W.-S. (2018). *Engineering principles in biotechnology*. Chichester: John Wiley & Sons.

Hu, S., Fang, Y., Ng, C.H. and Mann, J.J. (2019). Involvement of neuro-immune mechanism and brain–gut axis in pathophysiology of mood disorders. *Frontiers in psychiatry*, 10, 403 (2pp). https://doi.org/10.3389/fpsyt.2019.00403

Hunt, R.H., Camilleri, M., Crowe, S.E., El-Omar, E.M., Fox, J.G., Kuipers, E.J., Malfertheiner, P., McColl, K.E.L., Pritchard, D.M., Rugge, M. and Sonnenberg, A. (2015). The stomach in health and disease. *Gut,* 64 (10), pp. 1650-1668. https://doi.org/10.1136/gutjnl-2014-307595

Iebba, V., Totino, V., Gagliardi, A., Santangelo, F., Cacciotti, F., Trancassini, M., Mancini, C., Cicerone, C., Corazziari, E., Pantanella, F. and Schippa, S. (2016). Eubiosis and dysbiosis: The two sides of the microbiota. *New Microbiologica,* 39 (1), pp. 1-12. Available at: https://newmicrobiologica.org/PUB/allegati_pdf/2016/1/1.pdf (Accessed: 22 February 2024).

Itoh, S. and Takahashi, K. (1984). Calorimetric studies of microbial growth: Kinetic analysis of growth thermograms observed for bakery yeast at various temperatures. *Agricultural and Biological Chemistry*, 48 (2), pp. 271–275. https://doi.org/10.1080/00021369.1984.10866155

Jackson, S.A., Schoeni, J.L., Vegge, C., Pane, M., Stahl, B., Bradley, M., Goldman, V.S., Burguière, P., Atwater, J.B. and Sanders, M.E. (2019). Improving end-user trust in the

quality of commercial probiotic products. *Frontiers in Microbiology*, 10, 739 (15pp). https://doi.org/10.3389/fmicb.2019.00739

James, A.M. (1987). *Thermal and energetic studies of cellular biological systems*. Bristol, UK: IOP Publishing Limited.

Jannasch, H.W. and Egli, T. (1993). Microbial growth kinetics: A historical perspective. *Antonie van Leeuwenhoek*, 63, pp. 213-224. https://doi.org/10.1007/BF00871219

Jansma, J., Brinkman, F., van Hemert, S. and El Aidy, S. (2021). Targeting the endocannabinoid system with microbial interventions to improve gut integrity. *Progress in Neuro-Psychopharmacology and Biological Psychiatry*, 106, 110169 (8pp). https://doi.org/10.1016/j.pnpbp.2020.110169

Jarvis, B., Hedges, A.J. and Corry, J.E. (2007). Assessment of measurement uncertainty for quantitative methods of analysis: comparative assessment of the precision (uncertainty) of bacterial colony counts. *International Journal of Food Microbiology*, 116 (1), pp. 44-51. https://doi.org/10.1016/j.ijfoodmicro.2006.12.037

Jarvis, B., Hedges, A.J. and Corry, J.E. (2012). The contribution of sampling uncertainty to total measurement uncertainty in the enumeration of microorganisms in foods. *Food Microbiology*, 30 (2), pp. 362-371. https://doi.org/10.1016/j.fm.2012.01.002

Kahm, M., Hasenbrink, G., Lichtenberg-Fraté, H., Ludwig, J. and Kschischo, M. (2010). Grofit: Fitting biological growth curves. *Journal of Statistical Software*, 33 (7), pp. 1-21. https://doi.org/10.18637/jss.v033.i07

Kaletunc, G. (2009). Calorimetric methods as applied to food: An overview. in Kaletunc, G. (ed.) *Calorimetry in food processing: Analysis and design of food systems*. Wiley-Blackwell. pp. 5-13.

Kennedy, M.S. and Chang, E.B. (2020). The microbiome: Composition and locations. *Progress in molecular biology and translational science*, 176, pp. 1-42. https://doi.org/10.1016/bs.pmbts.2020.08.013

Kennedy, K.M., de Goffau, M.C., Perez-Muñoz, M.E., Arrieta, M., Bäckhed, F., Bork, P., Braun, T., Bushman, F.D., Dore, J., de Vos, W.M., Earl, A.M., Eisen, J.A., Elovitz, M.A., Ganal-Vonarburg, S., Gänzle, M.G., Garrett, W.S., Hall, L.J., Hornef, M.W., Huttenhower, C., Konnikova, L., Lebeer, S., Macpherson, A.J., Massey, R.C., McHardy, A.C., Koren, O., Lawley, T.D., Ley, R.E., O'Mahony, L., O'Toole, P.,W., Pamer, *E.G.*, Parkhill, J., Raes, J., Rattei, T., Salonen, A., Segal, E., Segata, N., Shanahan, F., Sloboda, D.M., Smith, G.C.S., Sokol, H., Spector, T.D., Surette, M.G., Tannock, G.W., Walker, A.W., Yassour, M. and Walter, J. (2023). Questioning the fetal microbiome illustrates pitfalls of low-biomass microbial studies. *Nature*, 613 (7945), pp. 639-649. https://doi.org/10.1038/s41586-022-05546-8

Kitzinger, C. and Benzing, T.H. (1960). Principle and method of heatburst microcalorimetry and the determination of free energy, enthalpy, and entropy changes. in Glick, D. (ed.) *Methods of Biochemica1 Analysis*, Volume 8, Interscience Publishers, pp. 309-360.

Klippenstein, S.J., Pande, V.S. and Truhlar, D.G. (2014). Chemical kinetics and mechanisms of complex systems: A perspective on recent theoretical advances. *Journal of the American Chemical Society*, 136 (2), pp. 528-546. https://doi.org/10.1021/ja408723a

Koenig, J.E., Spor, A., Scalfone, N., Fricker, A.D., Stombaugh, J., Knight, R., Angenent, L.T. and Ley, R.E. (2011). Succession of microbial consortia in the developing infant gut microbiome. *Proceedings of the National Academy of Sciences,* 108 (Supplement 1)*,* pp. 4578-4585. https://doi.org/10.1073/pnas.1000081107

Koutsoumanis, K., Allende, A., Alvarez-Ordóñez, A., Bolton, D., Bover-Cid, S., Chemaly, M., Davies, R., De Cesare, A., Hilbert, F., Lindqvist, R., Nauta, M., Peixe, L., Ru, G., Simmons, M., Skandamis, P., Suffredini, E., Cocconcelli, P.S., Fernández Escámez, P.S., Maradona, M.P., Querol, A., Suarez, J.E., Sundh, I., Vlak, J., Barizzone, F., Correia, S. and Herman, L. (2020). Scientific Opinion on the update of the list of QPS-recommended biological agents intentionally added to food or feed as notified to EFSA (2017–2019). *EFSA Journal*, 18 (2), e05966 (56pp). https://doi.org/10.2903/j.efsa.2020.5966

Koutsoumanis, K., Allende, A., Alvarez-Ordóñez, A., Bolton, D., Bover-Cid, S., Chemaly, M., Davies, R., De Cesare, A., Hilbert, F., Lindqvist, R., Nauta, M., Peixe, L., Ru, G., Simmons, M., Skandamis, P., Suffredini, E., Cocconcelli, P.S., Fernández Escámez, P.S., Maradona, M.P., Querol, A., Sijtsma, L., Suarez, J.E., Sundh, I., Vlak, J., Barizzone, F., Hempen, M. and Herman, L. (2022). Update of the list of QPS-recommended biological agents intentionally added to food or feed as notified to EFSA 15: suitability of taxonomic units notified to EFSA until September 2021. *EFSA Journal*, 20 (1), e07045 (40pp). https://doi.org/10.2903/j.efsa.2022.7045

Kovárová-Kovar, K. and Egli, T. (1998). Growth kinetics of suspended microbial cells: From single-substrate-controlled growth to mixed-substrate kinetics. *Microbiology And Molecular Biology Reviews*, 62 (3), pp. 646-666. https://doi.org/10.1128/mmbr.62.3.646-666.1998

Kvasnovsky, C.L., Bjarnason, I., Donaldson, A.N., Sherwood, R.A. and Papagrigoriadis, S. (2017). A randomized double-blind placebo-controlled trial of a multi-strain probiotic in treatment of symptomatic uncomplicated diverticular disease. *Inflammopharmacology*, 25 (5), pp. 499-509. https://doi.org/10.1007/s10787-017-0363-y

Laursen, M.F., Andersen, L.B., Michaelsen, K.F., Mølgaard, C., Trolle, E., Bahl, M.I. and Licht, T.R. (2016). Infant gut microbiota development is driven by transition to family foods independent of maternal obesity. *mSphere*, 1 (1), e00069-15 (16pp). https://doi.org/10.1128/msphere.00069-15

Laursen, M.F., Bahl, M.I., Michaelsen, K.F. and Licht, T.R. (2017). First foods and gut microbes. *Frontiers in Microbiology,* 8*,* 356 (8pp). https://doi.org/10.3389/fmicb.2017.00356

Lavoisier, A.-L. and De Laplace, P.S. ([1783] 1994). Memoir on Heat read to the Royal Academy of Sciences, 28 June 1783. *Obesity Research*, 2 (2), pp. 189-202. https://doi.org/10.1002/j.1550-8528.1994.tb00646.x

Law, A.T., Robertson, B.R., Dunker, S.S. and Button, D.K. (1975). On describing microbial growth kinetics from continuous culture data: Some general considerations, observations, and concepts. *Microbial Ecology*, 2, pp. 261-283. https://doi.org/10.1007/BF02011647

Law, D. and Zhou, D. (2017). Solid-state characterization and techniques. in Qiu, Y., Chen, Y., Zhang, G.G.Z., Yu, L. and Mantri, R.V. (eds.) *Developing solid oral dosage forms*. Academic Press. pp. 59-84.

Le Parlouër, P. and Benoist, L. (2009). Methods and applications of microcalorimetry in food. in Kaletunc, G. (ed.) *Calorimetry in food processing: Analysis and design of food systems*. Wiley-Blackwell. pp. 15-49.

Lee, S.M., Donaldson, G.P., Mikulski, Z., Boyajian, S., Ley, K. and Mazmanian, S.K. (2013). Bacterial colonization factors control specificity and stability of the gut microbiota. *Nature,* 501 (7467), pp. 426-429. https://doi.org/10.1038/nature12447

Leiza, J.R. and McKenna, T. (2014). Calorimetry, conductivity, densimetry, and rheological measurements. in Reed, W.F. and Alb, A.M. (eds.) *Monitoring polymerization reactions: From fundamentals to applications*. Hoboken, New Jersey: John Wiley & Sons, pp. 135-150.

Leme, J., Fernández Núñez, *E.G.*, de Almeida Parizotto, L., Chagas, W.A., Salla dos Santos, E., Caricati, T.P.A., Gonçalves de Rezende, A., Labate Vale da Costa, B., Ventini Monteiro, D.C., Lopes Boldorini, V.L., Calil Jorge, S.A., Mancini Astray, R., Pereira, C.A., Pereira Caricati, C. and Tonso, T. (2014). A multivariate calibration procedure for UV/VIS spectrometric monitoring of BHK-21 cell metabolism and growth. *Biotechnology Progress*, 30 (1), pp. 241-248. https://doi.org/10.1002/btpr.1847

Levy, M., Kolodziejczyk, A.A., Thaiss, C.A. and Elinav, E. (2017). Dysbiosis and the immune system. *Nature Reviews Immunology*, 17 (4), pp. 219-232. https://doi.org/10.1038/nri.2017.7

Li, H., Limenitakis, J.P., Fuhrer, T., Geuking, M.B., Lawson, M.A., Wyss, M., Brugiroux, S., Keller, I., Macpherson, J.A., Rupp, S., Stolp, B., Stein, J.V., Stecher, B., Sauer, U., McCoy, K.D. and Macpherson, A.J. (2015). The outer mucus layer hosts a distinct intestinal microbial niche. *Nature Communications,* 6 (1)*,* pp. 1-13. https://doi.org/10.1038/ncomms9292

Litvak, Y., Byndloss, M.X. and Bäumler, A.J. (2018). Colonocyte metabolism shapes the gut microbiota. *Science*, 362 (6418), pp. 1-6. https//doi.org/10.1126/science.aat9076

Likotrafiti, E. and Rhoades, J. (2016). Probiotics, prebiotics, synbiotics, and foodborne illness. in Watson, R.R. and Preedy, V.R. (eds.) *Probiotics, Prebiotics, and Synbiotics: Bioactive Foods in Health Promotion,* USA, Academic Press, pp. 469-476. https://doi.org/10.1016/B978-0-12-802189-7.00032-0

Liu, Y., Tran, D.Q. and Rhoads, J.M. (2018). Probiotics in disease prevention and treatment. *The Journal of Clinical Pharmacology*, 58 (S10), pp. S164-S179. https://doi.org/10.1002/jcph.1121

Liu, L., Yang, M., Dong, W., Liu, T., Song, X., Gu, Y., Wang, S., Liu, Y., Abla, Z., Qiao, X. and Liu, W. (2021). Gut dysbiosis and abnormal bile acid metabolism in Colitis-associated cancer. *Gastroenterology Research and Practice*, 2021, 6645970 (12pp). https://doi.org/10.1155/2021/6645970

Lopetuso, L.R., Scaldaferri, F., Franceschi, F. and Gasbarrini, A. (2014). The gastrointestinal microbiome–functional interference between stomach and intestine. *Best Practice & Research Clinical Gastroenterology*, 28 (6), pp. 995-1002. https://doi.org/10.1016/j.bpg.2014.10.004

Ludwig, W., Schleifer, K.-H. and Whitman, W.B. (2009). *Lactobacillales*. in Vos, P., Garrity, G., Jones, D., Krieg, N.R., Ludwig, W., Rainey, F.A., Schleifer, K.H. and Whitman, W.B.

(eds.). *Bergey's manual of systematic bacteriology: Volume 3: The Firmicutes*. Second edition. Springer Science & Business Media, pp. 464-607.

Ma, T., Jin, H., Kwok, L.Y., Sun, Z., Liong, M.T. and Zhang, H. (2021). Probiotic consumption relieved human stress and anxiety symptoms possibly via modulating the neuroactive potential of the gut microbiota. *Neurobiology of Stress*, 14, 100294 (10pp). https://doi.org/10.1016/j.ynstr.2021.100294

Macaloney, G., Draper, I., Preston, J., Anderson, K.B., Rollins, M.J., Thompson, B.G., Hall, J.W. and McNeil, B. (1996). At-line control and fault analysis in an industrial high cell density *Escherichia coli* fermentation, using NIR spectroscopy. *Food and Bioproducts Processing*, 74 (4), pp. 212-220. https://doi.org/10.1205/096030896531217

Maciel-Fiuza, M.F., Muller, G.C., Campos, D.M.S., do Socorro Silva Costa, P., Peruzzo, J., Bonamigo, R.R., Veit, T. and Vianna, F.S.L. (2023). Role of gut microbiota in infectious and inflammatory diseases. *Frontiers in Microbiology*, 14, 1098386 (18pp). https://doi.org/10.3389/fmicb.2023.1098386

Madigan, M.T., Martinko, J.M., Bender, K.S., Buckley, D.H. and Stahl, D.A. (2015). *Brock biology of microorganisms.* 14th edn. Harlow: Pearson Education Limited.

Malagón-Rojas, J.N., Mantziari, A., Salminen, S. and Szajewska, H. (2020). Postbiotics for preventing and treating common infectious diseases in children: A systematic review. *Nutrients*, 12 (2), 389 (14pp). https://doi.org/10.3390/nu12020389

Maleki, D., Homayouni, A., Khalili, L. and Golkhalkhali, B. (2016). Probiotics in cancer prevention, updating the evidence. in Watson, R.R. and Preedy, V.R. (eds.) *Probiotics, Prebiotics, and Synbiotics: Bioactive Foods in Health Promotion,* USA, Academic Press, pp. 781-791. https://doi.org/10.1016/B978-0-12-802189-7.00059-9

Manoj, D., Shanmugasundaram, S. and Anandharamakrishnan, C. (2021). Nanosensing and nanobiosensing: Concepts, methods, and applications for quality evaluation of liquid foods. *Food Control*, 126, 108017 (18pp). https://doi.org/10.1016/j.foodcont.2021.108017

Marinova, V.Y., Rasheva, I.K., Kizheva, Y.K., Dermenzhieva, Y.D. and Hristova, P.K. (2019). Microbiological quality of probiotic dietary supplements. *Biotechnology & Biotechnological Equipment*, 33 (1), pp. 834-841. https://doi.org/10.1080/13102818.2019.1621208

Marison, I.W. and Von Stockar, U. (1988). Fermentation control and the use of calorimetry. *Biochemical Society Transactions*, 16 (6), pp. 1091–1093. https://doi-org.libproxy.ucl.ac.uk/10.1042/bst0161091

Market Watch. (2021). *Global probiotics market size 2021-2026*. Available at: https://www.marketwatch.com/press-release/global-probiotics-market-size-2021-2026-with-top-countries-data-industry-research-share-trend-industry-size-price-future-analysis-regional-outlook-to-research-report-with-covid-19-analysis-2021-02-22 (Accessed 19 March 2021).

Marzorati, M., Van den Abbeele, P., Ghyselinck, J., Moens, F. and De Blaiser, A. (2018) Modulatory effect of Symprove™ on the gut microbiota of multiple patients. Symprove internal report: 2015059/D667/Colonic simulation. pp. 1-43. (available upon request)

Marzorati, M., Van den Abbeele, P., Verstrepen, L., Ghyselinck, J., De Medts, J., Steppé, E. and De Munck, J. (2020) Investigation of the effect of Symprove on a healthy microbiota using ProDigest's short-term single-stage colonic simulation and cell assays. Symprove internal report: 2015059/D1556/P443. Unpublished. pp. 1-41. (available upon request)

Maskow, T. and Harms, H. (2006). Real time insights into bioprocesses using calorimetry: State of the art and potential. *Engineering in Life Sciences*, 6 (3), pp. 266-277. https://doi.org/10.1002/elsc.200520123

Maskow, T., Wolf, K., Kunze, W., Enders, S. and Harms, H. (2012). Rapid analysis of bacterial contamination of tap water using isothermal calorimetry. *Thermochimica acta*, 543, pp.273-280. http://dx.doi.org/10.1016/j.tca.2012.06.002

Maskow, T. (2013). Calorimetry and biothermodynamics for biotechnology, medicine and environmental sciences: Current status and advances. *Engineering in Life Sciences*, 13 (6), pp. 508-509. https://doi.org/10.1002/elsc.201370064

Mauerhofer, L.M., Pappenreiter, P., Paulik, C., Seifert, A.H., Bernacchi, S. and Simon, K.M.R. (2019). Methods for quantification of growth and productivity in anaerobic microbiology and biotechnology. *Folia Microbiologica*, 64 (3), pp. 321-360. https://doi.org/10.1007/s12223-018-0658-4

Mayorgas, A., Dotti, I. and Salas, A. (2021). Microbial metabolites, postbiotics, and intestinal epithelial function. *Molecular Nutrition & Food Research*, 65 (5), 2000188 (17pp). https://doi.org/10.1002/mnfr.202000188

McCallum, G. and Tropini, C. (2024). The gut microbiota and its biogeography. *Nature Reviews Microbiology*, 22, pp. 105-118. https://doi.org/10.1038/s41579-023-00969-0

Michels, N., Van de Wiele, T., Fouhy, F., O'Mahony, S., Clarke, G. and Keane, J. (2019). Gut microbiome patterns depending on children's psychosocial stress: Reports versus biomarkers. *Brain, Behavior and Immunity,* 80, pp. 751-762. https://doi.org/10.1016/j.bbi.2019.05.024

Mihhalevski, A., Sarand, I., Viiard, E., Salumets, A. and Paalme, T. (2011). Growth characterization of individual rye sourdough bacteria by isothermal microcalorimetry. *Journal of Applied Microbiology*, 110 (2), pp. 529-40. https://doi.org/10.1111/j.1365-2672.2010.04904.x

Milani, C., Duranti, S., Bottacini, F., Casey, E., Turroni, F., Mahony, J., Belzer, C., Palacio, S.D., Montes, S.A., Mancabelli, L. and Lugli, G.A., Rodriguez, J.M., Bode, L., de Vos, W., Gueimonde, M., Margolles, A., van Sinderen, D. and Ventura, M. (2017). The first microbial colonizers of the human gut: Composition, activities, and health implications of the infant gut microbiota. *Microbiology and Molecular Biology Reviews,* 81 (4), pp. 1-67. https://doi.org/10.1128/mmbr.00036-17

Miyake, H., Maeda, Y., Ishikawa, T. and Tanaka, A. (2016). Calorimetric studies of the growth of anaerobic microbes. *Journal of Bioscience and Bioengineering*, 122 (3), pp. 364-369. https://doi.org/10.1016/j.jbiosc.2016.02.006

Moens, F., Van den Abbeele, P., Basit, A.W., Dodoo, C., Chatterjee, R., Smith, B. and Gaisford, S. (2019). A four-strain probiotic exerts positive immunomodulatory effects by

enhancing colonic butyrate production *in vitro*. *International Journal of Pharmaceutics*, 555, pp. 1-10. https://doi.org/10.1016/j.ijpharm.2018.11.020

Monk, P. and Wadsö, I. (1968). A flow micro reaction calorimeter. *Acta Chemica Scandinavica*, 22, pp. 1842-1852.

Monod, J. (1949). The growth of bacterial cultures. *Annual Review of Microbiology*, 3, pp. 371-394. https://doi.org/10.1146/annurev.mi.03.100149.002103

Moradi, M., Kousheh, S.A., Almasi, H., Alizadeh, A., Guimarães, J.T., Yılmaz, N. and Lotfi, A. (2020). Postbiotics produced by lactic acid bacteria: The next frontier in food safety. *Comprehensive Reviews in Food Science and Food Safety*, 19 (6), pp. 3390-3415. https://doi.org/10.1111/1541-4337.12613

Moradi, M., Guimarães, J.T. and Sahin, S. (2021). Current applications of exopolysaccharides from lactic acid bacteria in the development of food active edible packaging. *Current Opinion in Food Science*, 40, pp. 33-39. https://doi.org/10.1016/j.cofs.2020.06.001

Morniroli, D., Vizzari, G., Consales, A., Mosca, F. and Gianni, M.L. (2021). Postbiotic Supplementation for Children and Newborn's Health. *Nutrients*, 13 (3), 781 (11pp). https://doi.org/10.3390/nu13030781

Morozova, K., Andreotti, C., Armani, M., Cavani, L., Cesco, S., Cortese, L., Gerbi, V., Mimmo, T., Spena, P.R. and Scampicchio, M. (2017). Indirect effect of glyphosate on wine fermentation studied by microcalorimetry. *Journal of Thermal Analysis and Calorimetry*, 127, pp. 1351–1360. https://doi.org/10.1007/s10973-016-5891-y

Morozova, K., Armani, M. and Scampicchio, M. (2020). Isothermal calorimetry for monitoring of grape juice fermentation with yeasts immobilized on nylon-6 nanofibrous membranes. *Journal of Thermal Analysis and Calorimetry*, 139, pp. 375–382. https://doi.org/10.1007/s10973-019-08370-x

Mortimer, M. and Taylor, P. (eds.). (2002). *Chemical kinetics and mechanism*. Milton Keynes: The Open University, pp. 24-78.

Mosca, A., Leclerc, M. and Hugot, J.P. (2016). Gut microbiota diversity and human diseases: Should we reintroduce key predators in our ecosystem? *Frontiers in Microbiology*, 7, 455 (12pp). https://doi.org/10.3389/fmicb.2016.00455

Mowat, A.M. (2021). Historical Perspective: M*etch*nikoff and the intestinal microbiome. *Journal of Leukocyte Biology*, 109 (3), pp. 513-517. https://doi.org/10.1002/JLB.4RI0920-599

Muccioli, G.G., Naslain, D., Bäckhed, F., Reigstad, C.S., Lambert, D.M., Delzenne, N.M. and Cani, P.D. (2010). The endocannabinoid system links gut microbiota to adipogenesis. *Molecular Systems Biology*, 6 (1), 392 (15pp). https://doi.org/10.1038/msb.2010.46

Mukhopadhya, I., Hansen, R., El-Omar, E.M. and Hold, G.L. (2012). IBD—what role do Proteobacteria play? *Nature Reviews Gastroenterology & Hepatology*, 9 (4), pp. 513-517. https://doi.org/10.1038/nrgastro.2012.14

Murphy, K., Curley, D., O'Callaghan, T.F., O'Shea, C.A., Dempsey, E.M., O'Toole, P.W., Ross, R.P., Ryan, C.A. and Stanton, C. (2017). The composition of human milk and infant

faecal microbiota over the first three months of life: A pilot study. *Scientific reports*, 7, 40597 (10pp). https://doi.org/10.1038/srep40597

Nagpal, R., Tsuji, H., Takahashi, T., Nomoto, K., Kawashima, K., Nagata, S. and Yamashiro, Y. (2017). Ontogenesis of the gut microbiota composition in healthy, full-term, vaginally born and breast-fed infants over the first 3 years of life: A quantitative bird's-eye view. *Frontiers in Microbiology*, 8, 1388 (9pp). https://doi.org/10.3389/fmicb.2017.01388

Newell, R.D. (1980). The identification and characterization of microorganisms by microcalorimetry, in A.E. Beezer (ed.) *Biological microcalorimetry*. London: Academic Press, pp. 163–186.

Nguyen, T.T., Kosciolek, T., Maldonado, Y., Daly, R.E., Martin, A.S., McDonald, D., Knight, R. and Jeste, D.V. (2019). Differences in gut microbiome composition between persons with chronic schizophrenia and healthy comparison subjects. *Schizophrenia Research*, 204, pp. 23-29. https://doi.org/10.1016/j.schres.2018.09.014

Nie, H.Y., Ge, J., Huang, G.X., Liu, K.G., Yue, Y., Li, H., Lin, H.G., Zhang, T., Yan, H.F., Xu, B.X. and Sun, H.W. (2024). New insights into the intestinal barrier through "gut-organ" axes and a glimpse of the microgravity's effects on intestinal barrier. *Frontiers in Physiology*, 15, 1465649 (22pp). https://doi.org/10.3389/fphys.2024.1465649

Notay, M., Foolad, N., Vaughn, A.R. and Sivamani, R.K. (2017). Probiotics, prebiotics, and synbiotics for the treatment and prevention of adult dermatological diseases. *American Journal of Clinical Dermatology*, 18 (6), pp. 721-732. https://doi.org/10.1007/s40257-017-0300-2

Novik, G. and Savich, V. (2020). Beneficial microbiota. Probiotics and pharmaceutical products in functional nutrition and medicine. *Microbes and Infection*, 22 (1), pp. 8-18. https://doi.org/10.1016/j.micinf.2019.06.004

Nunomura, K. and Fujita, T. (1981). Calorimetric study of the endogenous metabolism of yeast. *The Journal of General and Applied Microbiology*, 27 (5), pp. 357-364. https://doi.org/10.2323/jgam.27.357

Nutrition Division FAO/WHO. (2006). *Probiotics in food. Health and nutritional properties and guidelines for evaluation*. Available at: https://www.fao.org/publications/card/en/c/7c102d95-2fd5-5b22-8faf-f0b2e68dfbb6/ (Accessed: 15 February 2024).

Nykyri, J., Herrmann, A.M. and Håkansson, S. (2019). Isothermal microcalorimetry for thermal viable count of microorganisms in pure cultures and stabilized formulations. *BMC Microbiology*, 19, 65 (10pp). https://doi.org/10.1186/s12866-019-1432-8

O'Hara, A.M. and Shanahan, F. (2006). The gut flora as a forgotten organ. *EMBO Reports*, 7 (7), pp. 688-693. https://doi.org/10.1038/sj.embor.7400731

Okada, F., Kobayashi, A., Fujiwara, N. and Takahashi, K. (1998). Microbial calorimetry of supported cultures and its application to the study of antimicrobial action. *Biocontrol Science*, 3 (2), pp. 79-85. https://doi.org/10.4265/bio.3.79

Okereke, I., Hamilton, C., Wenholz, A., Jala, V., Giang, T., Reynolds, S., Miller, A. and Pyles, R. (2019). Associations of the microbiome and esophageal disease. *Journal of Thoracic Disease*, 11 (Supplement 12), pp. S1588-S1593. http://dx.doi.org/10.21037/jtd.2019.05.82

Olteanu, G., Ciucă-Pană, M.A., Busnatu, Ș.S., Lupuliasa, D., Neacșu, S.M., Mititelu, M., Musuc, A.M., Ioniță-Mîndrican, C.B. and Boroghină, S.C. (2024). Unraveling [sic] the microbiome–human body axis: A comprehensive examination of therapeutic strategies, interactions and implications. *International Journal of Molecular Sciences*, 25 (10), 5561 (50pp). https://doi.org/10.3390/ijms25105561

O'Neill, M.A.A., Beezer, A.E., Labetoulle, C., Nicolaides, L., Mitchell, J.C., Orchard, J.A., Connor, J.A., Kemp, R.B. and Olomolaiye, D. (2003). The base catalysed hydrolysis of methyl paraben: A test reaction for flow microcalorimeters used for determination of both kinetic and thermodynamic parameters. *Thermochimica Acta*, 399 (1-2), pp. 63-71. https://doi.org/10.1016/S0040-6031(02)00401-X

O'Neill, M.A.A., Beezer, A.E., Mitchell, J.C., Orchard, J. and Connor, J.A. (2004). Determination of Michaelis–Menten parameters obtained from isothermal flow calorimetric data. *Thermochimica Acta*, 417 (2), pp. 187-192. https://doi.org/10.1016/j.tca.2003.07.019

Ozawa, T. (1970). Kinetic analysis of derivative curves in thermal analysis. *Journal of Thermal Analysis*, 2, pp. 301-324. https://doi.org/10.1007/BF01911411

Padilha, M., Danneskiold-Samsøe, N.B., Brejnrod, A., Hoffmann, C., Cabral, V.P., Iaucci, J. de M., Sales, C.H., Fisberg, R.M., Cortez, R.V., Brix, S., Taddei, C.R., Kristiansen, K. and Saad, S.M.I. (2019). The human milk microbiota is modulated by maternal diet. *Microorganisms*, 7 (11), 502 (18pp). https://doi.org/10.3390/microorganisms7110502

Palade, C.-M., Vulpoi, G.-A., Vulpoi, R.-A., Drug, V.L., Barboi, O.-B. and Ciocoiu, M. (2022). The biotics family: Current knowledge and future perspectives in metabolic diseases. *Life*, 12 (8), 1263 (21pp). https://doi.org/10.3390/life12081263

Pandey, K.R., Naik, S.R. and Vakil, B.V. (2015). Probiotics, prebiotics and synbiotics - a review. *Journal of Food Science and Technology*, 52 (12), pp. 7577-7587. https://doi.org/10.1007/s13197-015-1921-1

Park, C.H., Hong, C., Lee, A.R., Sung, J. and Hwang, T.H. (2022). Multi-omics reveals microbiome, host gene expression, and immune landscape in gastric carcinogenesis. *iScience*, 25 (3), 103956 (19pp). https://doi.org/10.1016/j.isci.2022.103956

Parker, C.T., Tindall, B.J. and Garrity, G.M. (2019). International code of nomenclature of prokaryotes: Prokaryotic code (2008 revision). *International Journal of Systematic and Evolutionary Microbiology*, 69 (1A), pp. S1-S111. https://doi.org/10.1099/ijsem.0.000778

Patro, J.N., Ramachandran, P., Barnaba, T., Mammel, M.K., Lewis, J.L. and Elkins, C.A. (2016). Culture-independent metagenomic surveillance of commercially available probiotics with high-throughput next-generation sequencing. *mSphere*, 1 (2). https://doi.org/10.1128/mSphere.00057-16

Perry, B.F., Beezer, A.E. and Miles, R.J. (1979). Flow microcalorimetric studies of yeast growth: Fundamental aspects. *Journal of Applied Bacteriology*, 47 (3), pp. 527-537. https://doi.org/10.1111/j.1365-2672.1979.tb01214.x

Perry, B.F., Beezer, A.E., and Miles, R. J. (1981). Microcalorimetry as a tool for evaluation of complex media: Molasses. *Microbios*, 32 (129-130), pp. 163–171.

Perry, B.F., Miles, R.J. and Beezer, A.E. (1990). Calorimetry for yeast fermentation monitoring and control. in Spencer, J.F.T. and Spencer, D.M. *Yeast technology*., Berlin: Springer-Verlag, pp. 276-347.

Person, H. and Keefer, L. (2021). Psychological comorbidity in gastrointestinal diseases: Update on the brain-gut-microbiome axis. *Progress in Neuro-Psychopharmacology and Biological Psychiatry*, 107, 110209 (12pp). https://doi.org/10.1016/j.pnpbp.2020.110209

Petersen, C. and Round, J.L. (2014). Defining dysbiosis and its influence on host immunity and disease. *Cellular Microbiology*, 16 (7), pp. 1024-1033. https://doi.org/10.1111/cmi.12308

Pickard, J.M. and Chervonsky, A.V. (2015). Intestinal fucose as a mediator of host–microbe symbiosis. *The Journal of Immunology*, 194 (12), pp. 5588-5593. https://doi.org/10.4049/jimmunol.1500395

Pinapati, K.K., Vidya, S., Khan, M.F., Mandal, D. and Banerjee, S. (2024). Gut bacteria, endocannabinoid system, and marijuana addiction: Novel therapeutic implications. *Health Sciences Review*, 10, 100144 (12pp). https://doi.org/10.1016/j.hsr.2023.100144

Pineiro, M., Asp, N-G., Reid, G., Macfarlane, S., Morelli, L., Brunser, O. and Tuohy, K. (2008). FAO Technical meeting on prebiotics. *Journal of Clinical Gastroenterology*, 42, pp. S156-S159, https://doi.org/10.1097/MCG.0b013e31817f184e

Prakash, S., Rodes, L., Coussa-Charley, M. and Tomaro-Duchesneau, C. (2011). Gut microbiota: Next frontier in understanding human health and development of biotherapeutics. *Biologics: Targets and Therapy*, 5, pp. 71-86. https://doi.org/10.2147/BTT.S19099

Pirt, S.J. (1965). The maintenance energy of bacteria in growing cultures. *Proceedings of the Royal Society of London. Series B. Biological Sciences*, 163 (991), pp. 224-231. Available at: https://www.jstor.org/stable/75569 (Accessed: 8 April 2021).

Purdel, C., Ungurianu, A., Adam-Dima, I. and Margină, D. (2023). Exploring the potential impact of probiotic use on drug metabolism and efficacy. *Biomedicine & Pharmacotherapy*, 161, 114468 (14pp). https://doi.org/10.1016/j.biopha.2023.114468

Qi, D., Nie, X.-L. and Zhang, J.J. (2020). The effect of probiotics supplementation on blood pressure: A systemic review and meta-analysis. *Lipids in Health and Disease*, 19, 79 (11pp). https://doi.org/10.1186/s12944-020-01259-x

Qin, J., Li, R., Raes, J., Arumugam, M., Burgdorf, K.S., Manichanh, C., Nielsen, T., Pons, N., Levenez, F., Yamada, T., Mende, D.R., Li, J., Xu, J., Li, S., Li, D., Cao, J., Wang, B., Liang, H., Zheng, H., Xie, Y., Tap, J., Lepage, P., Bertalan, M., Batto, J-M., Hansen, T., Le Paslier, D., Linneberg, A., Nielsen, H.B., Pelletier, E., Renault, P., Sicheritz-Ponten, T., Turner, K., Zhu, H., Yu, C., Li, C., Jian, M., Zhou, Y., Li, Y., Zhang, X., Li, S., Qin, N., Yang, H., Wang, J., Brunak, S., Doré, J., Guarner, F., Kristiansen, K., Pedersen, O., Parkhill, J., Weissenbach, J., MetaHIT Consortium, Peer Bork, Ehrlich, S.D. and Wang, J. (2010). A human gut microbial gene catalogue established by metagenomic sequencing. *Nature*, 464 (7285), pp. 59-65. https://doi.org/10.1038/nature08821

R and M report. (2018). Probiotics Market: Global industry perspective, comprehensive analysis and forecast, 2018-2025. Report ID: 4854530. Available at: https://www.researchandmarkets.com/reports/4854530/probiotics-market-global-industry-perspective#rela4-4438669 (Accessed 18 March 2021).

R and M report. (2021). Probiotics Dietary Supplements - Global Market Trajectory & Analytics. Report ID: 5304212. Available at: https://www.researchandmarkets.com/reports/5304212/probiotics-dietary-supplements-global-market (Accessed: 18 March 2021).

R and M report. (2024). Probiotics dietary supplements - Global strategic business report. Report ID: 5304212. Available at: https://www.researchandmarkets.com/reports/5304212/probiotics-dietary-supplements-global (Accessed: 17 February 2024).

Raemy, A., Nouzille, C.A., Lambelet, P. and Marabi, A. (2009). Overview of calorimetry as a tool for efficient and safe food-processing design. in Kaletunc, G. (ed.) *Calorimetry in food processing: Analysis and design of food systems*. Wiley-Blackwell. pp. 201-236.

Ralli, T., Saifi, Z., Rathee, A., Aeri, V. and Kohli, K. (2023). Decoding the bidirectional relationship between gut microbiota and COVID-19. *Heliyon*, 9 (3), pp. 1-9. https://doi.org/10.1016/j.heliyon.2023.e13801

Ramesh, V. (ed.). (2019). *Biomolecular and bioanalytical techniques: Theory, methodology and applications*. Hoboken, NJ: John Wiley & Sons.

Ratsika, A., Codagnone, M.C., O'Mahony, S., Stanton, C. and Cryan, J.F. (2021). Priming for life: Early life nutrition and the microbiota-gut-brain axis. *Nutrients*, 13 (2), 423 (33pp). https://doi.org/10.3390/nu13020423

Rea, K., O'Mahony, S. and Cryan, J.F. (2021). High and mighty? Cannabinoids and the microbiome in pain. *Neurobiology of Pain*, 9, 100061 (7pp). https://doi.org/10.1016/j.ynpai.2021.100061

Rebollo, I., Wolpert, N. and Tallon-Baudry, C. (2021). Brain-stomach coupling: anatomy, functions, and future avenues of research. *Current Opinion in Biomedical Engineering*, 18, 100270 (7pp). https://doi.org/10.1016/j.cobme.2021.100270

Reyes, A., Haynes, M., Hanson, N., Angly, F.E., Heath, A.C., Rohwer, F. and Gordon, J.I. (2010). Viruses in the faecal microbiota of monozygotic twins and their mothers. *Nature*, 466 (7304), pp. 334-338. https://doi.org/10.1038/nature09199

Riedel, U.C., Schwiertz, A. and Egert, M. (2014). The stomach and small and large intestinal microbiomes. in Marchesi, J.R. (ed.) *The Human Microbiota and Microbiome.* Croydon: CABI, pp. 1-19.

Riva, M. and Schiraldi, A. (1993). Kinetic parameterization of transitions and reactions in food systems from isothermal and non-isothermal DSC traces. *Thermochimica Acta*, 220, pp. 117-130. https://doi.org/10.1016/0040-6031(93)80459-N

Roberfroid, M. (2007). Prebiotics: The concept revisited. *The Journal of Nutrition*, 137 (3), pp. 830S-837S. https://doi.org/10.1093/jn/137.3.830S

Robertson, R.C., Manges, A.R., Finlay, B.B. and Prendergast, A.J. (2019). The human microbiome and child growth–first 1000 days and beyond. *Trends in Microbiology*, 27 (2), pp. 131-147. https://doi.org/10.1016/j.tim.2018.09.008

Romano, N., Tymczyszyn, E., Mobili, P. and Gómez-Zavaglia, A. (2016). Prebiotics as protectants of lactic acid bacteria. in Watson, R.R. and Preedy, V.R. (eds.) *Probiotics, Prebiotics, and Synbiotics: Bioactive Foods in Health Promotion,* USA, Academic Press, pp. 155-163.

Saboury, A.A., Miroliae, M., Nemat-Gorgani, M. and Moosavi-Movahedi, A.A. (1999). Kinetics denaturation of yeast alcohol dehydrogenase and the effect of temperature and trehalose. An isothermal microcalorimetry study. *Thermochimica Acta*, 326 (1-2), pp. 127-131. https://doi.org/10.1016/S0040-6031(98)00588-7

Sadler, R., Cramer, J.V., Heindl, S., Kostidis, S., Betz, D., Zuurbier, K.R., Northoff, B.H., Heijink, M., Goldberg, M.P., Plautz, E.J. and Roth, S. (2020). Short-chain fatty acids improve poststroke recovery via immunological mechanisms. *Journal of Neuroscience*, 40 (5), pp. 1162-1173. https://doi.org/10.1523/JNEUROSCI.1359-19.2019

Sadowsky, M.J. and Khoruts, A. (2016). Faecal microbiota transplantation is promising but not a panacea. *Nature Microbiology*, 1 (3), 16015 (2pp). https://doi.org/10.1038/nmicrobiol.2016.15

Said, J.F.S. (2014). *The application of static and flow-through isothermal microcalorimetry to the antimicrobial analysis of medical materials and devices*. Thesis. University College London. Available at: https://discovery.ucl.ac.uk/id/eprint/1451950/ (Accessed: 14 February 2020)

Salminen, S., Collado, M.C., Endo, A., Hill, C., Lebeer, S., Quigley, E.M., Sanders, M.E., Shamir, R., Swann, J.R., Szajewska, H. and Vinderola, G. (2021). The International Scientific Association of Probiotics and Prebiotics (ISAPP) consensus statement on the definition and scope of postbiotics. *Nature Review Gastroenterology & Hepatology*, 18 (9), pp. 649–667. https://doi.org/10.1038/s41575-021-00440-6

Sancandi, M., De Caro, C., Cypaite, N., Marascio, N., Avagliano, C., De Marco, C., Russo, E., Constanti, A. and Mercer, A. (2023). Effects of a probiotic suspension Symprove™ on a rat early-stage Parkinson's disease model. *Frontiers in Aging Neuroscience*, 14, 986127 (16pp). https://doi.org/10.3389/fnagi.2022.986127

Sardaro, A., Castagnolo, M., Trotta, M., Italiano, F., Milano, F., Cosma, P., Agostiano, A. and Fini, P. (2013). Isothermal microcalorimetry of the metabolically versatile bacterium *Rhodobacter sphaeroides*. *Journal of Thermal Analysis and Calorimetry*, 112, pp. 505–511. https://doi.org/10.1007/s10973-012-2895-0

Sarge, S.M., Höhne, G.W. and Hemminger, W. (2014). *Calorimetry: Fundamentals, instrumentation and applications*. Weinheim, Germany: Wiley-VCH Verlag.

Saxami, G., Kerezoudi, E.N., Eliopoulos, C., Arapoglou, D. and Kyriacou, A. (2023). The gut–organ axis within the human body: gut dysbiosis and the role of prebiotics. *Life*, 13 (10), pp. 1-41. https://doi.org/10.3390/life13102023

Schaarschmidt, B., Zotin, A.I. and Lamprecht, I. (1976). Quantitative relation between heat production and weight during growth of microbial cultures. in Lamprecht, I. and

Schaarschmidt, B. (eds.) *Proceedings of the international conference in Berlin, August 2–3, 1976*. Berlin, Boston: De Gruyter, pp. 139-148. https://doi.org/10.1515/9783110860719

Schäffer, B., Szakály, S. and Lőrinczy, D. (2004). Examination of the growth of probiotic culture combinations by the isoperibolic batch calorimetry. *Thermochimica Acta*, 415 (1-2), pp. 123-126. https://doi.org/10.1016/j.tca.2003.07.017

Schäffer, B. and Lőrinczy, D. (2005). Isoperibol calorimetry as a tool to evaluate the impact of the ratio of exopolysaccharide-producing microbes on the properties of sour cream. *Journal of Thermal Analysis and Calorimetry*, 82, pp. 537–541 (2005). https://doi.org/10.1007/s10973-005-0929-6

Schiraldi, A. (1995). Microbial growth and metabolism: Modelling and calorimetric characterization. *Pure and Applied Chemistry*, 67 (11), pp. 1873-1878. https://doi.org/10.1351/pac199567111873

Schroeder, B.O. and Bäckhed, F. (2016). Signals from the gut microbiota to distant organs in physiology and disease. *Nature Medicine*, 22 (10), pp. 1079-1089. https://doi.org/10.1038/nm.4185

Sender, R., Fuchs, S. and Milo, R. (2016). Revised estimates for the number of human and bacteria cells in the body. *PLoS Biology*, 14 (8), pp. 1-14. doi:10.1371/journal.pbio.1002533.t001

Sfriso, R., Egert, M., Gempeler, M., Voegeli, R. and Campiche, R. (2020). Revealing the secret life of skin-with the microbiome you never walk alone. *International Journal of Cosmetic Science*, 42 (2), pp. 116-126. https://doi.org/10.1111/ics.12594

Shanmugakani, R.K., Srinivasan, B., Glesby, M.J., Westblade, L.F., Cárdenas, W.B., Raj, T., Erickson, D. and Mehta, S. (2020). Current state of the art in rapid diagnostics for antimicrobial resistance. *Lab on a Chip*, 20 (15), pp. 2607-2625. https://doi:10.1039/d0lc00034e

Shao, X., Xu, B., Chen, C., Li, P. and Luo, H. (2021). The function and mechanism of lactic acid bacteria in the reduction of toxic substances in food: A review. *Critical Reviews in Food Science and Nutrition*, 62 (21), pp. 5950-5963. https://doi.org/10.1080/10408398.2021.1895059

Sharma, R. and Padwad, Y. (2020). Plant-polyphenols based second-generation synbiotics: Emerging concepts, challenges, and opportunities. *Nutrition*, 77, 110785 (6pp). https://doi.org/10.1016/j.nut.2020.110785

Sharma, R., Gupta, D., Mehrotra, R. and Mago, P. (2021). Psychobiotics: The next-generation probiotics for the brain. *Current Microbiology*, 78, pp. 449-463. https://doi.org/10.1007/s00284-020-02289-5

Shaw, L.P., Smith, A.M. and Roberts, A.P. (2017). The oral microbiome. *Emerging Topics in Life Sciences*, 1 (4), pp. 287-296. https://doi.org/10.1042/ETLS20170040

Sheng, L., Zhang, Z., Su, L., Zhang, H., Zhang, H., Li, K., Fang, Y. and Ye, W. (2021). A calibration calorimetry method to investigate the thermal characteristics of a cylindrical lithium-ion battery. *International Journal of Thermal Sciences*, 165, 106891 (8pp). https://doi.org/10.1016/j.ijthermalsci.2021.106891

Sethi, S. and Anurag, R.K. (2021). Probiotic and prebiotic plant milk dairy foods. in da Cruz, A.G., Ranadheera, C.S., Nazzaro, F. and Mortazavian, A. (eds.) *Probiotics and prebiotics in foods: Challenges, innovations, and advances*. Academic Press, pp. 153-177. https://doi.org/10.1016/B978-0-12-819662-5.00017-3

Siddiqui, K.S., Poljak, A., Ertan, H. and Bridge, W. (2022). The use of isothermal titration calorimetry for the assay of enzyme activity: Application in higher education practical classes. *Biochemistry and Molecular Biology Education*, 50 (5), pp. 519-526. https://doi.org/10.1002/bmb.21657

Sigg, A.P., Mariotti, M., Grütter, A.E., Lafranca, T., Leitner, L., Bonkat, G. and Braissant, O. (2022). A method to determine the efficacy of a commercial phage preparation against uropathogens in urine and artificial urine determined by isothermal microcalorimetry. *Microorganisms*, 10 (5), 845 (13pp). https://doi.org/10.3390/microorganisms10050845

Sigma-Aldrich. (2013) *69966 MRS Broth (Lactobacillus Broth acc. to De Man, Rogosa and Sharpe)*. https://www.sigmaaldrich.com/deepweb/assets/sigmaaldrich/product/documents/158/568/69966dat.pdf (Accessed 10 April 2024)

Singh, R.P., Bashir, H. and Kumar, R. (2021). Emerging role of microbiota in immunomodulation and cancer immunotherapy. *Seminars in Cancer Biology*, 70, pp. 37-52. https://doi.org/10.1016/j.semcancer.2020.06.008

Sisson, G., Ayis, S., Sherwood, R.A. and Bjarnason, I. (2014). Randomised clinical trial: A liquid multi-strain probiotic vs. placebo in the irritable bowel syndrome–a 12 week double-blind study. *Alimentary Pharmacology & Therapeutics*, 40 (1), pp. 51-62. https://doi.org/10.1111/apt.12787

Sisson, G., Hayee, B. and Bjarnason, I. (2015). Assessment of a Multi Strain Probiotic (Symprove) in IBD. *Gastroenterology*, 148 (4), S-531. https://doi.org/10.1016/S0016-5085(15)31779-0

Slouka, C., Wurm, D.J., Brunauer, G., Welzl-Wachter, A., Spadiut, O., Fleig, J. and Herwig, C. (2016). A novel application for low frequency electrochemical impedance spectroscopy as an on-line process monitoring tool for viable cell concentrations. *Sensors*, 16 (11), 1900 (12pp). https://doi.org/10.3390/s16111900

Snider, E.J., Compres, G., Freedberg, D.E., Giddins, M.J., Khiabanian, H., Lightdale, C.J., Nobel, Y.R., Toussaint, N.C., Uhlemann, A.C. and Abrams, J.A. (2018). Barrett's esophagus is associated with a distinct oral microbiome. *Clinical and Translational Gastroenterology*, 9 (3), e135 (9pp). https://doi.org/10.1038/s41424-018-0005-8

Soares, M. B., Almada, C. N., Pereira, E. P. R., Ferreira, B. M., Balthazar, C. F., Khorshidian, N., Rocha, R. S., Xavier-Santos, D., Cruz, A. G., Ranadheera, C. S., Mortazavian, A. M., Gómez-Zavaglia, A., Martinez, R. C. R., and Sant'Ana, A. S. (2023). Review - Sporeforming probiotic bacteria: Characteristics, health benefits, and technological aspects for their applications in foods and beverages. *Trends in Food Science & Technology*, 138, pp. 453–469. https://doi.org/10.1016/j.tifs.2023.06.029

Spink, C. and Wadsö, I. (1976). Calorimetry as an analytical tool in biochemistry and biology. in Glick, D. (ed.) *Methods of Biochemical Analysis*. Volume 23. New York: John Wiley & Sons, pp. 1-159.

Stulova, I., Kabanova, N., Kriščiunaite, T., Adamberg, K., Laht, T.M. and Vilu, R. (2015). Microcalorimetric study of the growth of *Streptococcus thermophilus* in renneted milk. *Frontiers in Microbiology*, 6, 79 (13pp). https://doi.org/10.3389/fmicb.2015.00079

Suez, J., Zmora, N., Zilberman-Schapira, G., Mor, U., Dori-Bachash, M., Bashiardes, S., Zur, M., Regev-Lehavi, D., Brik, R.B.Z., Federici, S. and Horn, M., M., Cohen, Y., Moor, A. E., Zeevi, D., Korem, T., Kotler, E., Harmelin, A., Itzkovitz, S., Maharshak, N., Shibolet, O., Pevsner-Fischer, M., Shapiro, H., Sharon, I., Halpern, Z., Segal, E. and Elinav, E. (2018). Post-antibiotic gut mucosal microbiome reconstitution is impaired by probiotics and improved by autologous FMT. *Cell*, 174 (6), pp. 1406-1423. https://doi.org/10.1016/j.cell.2018.08.047

Suez, J., Zmora, N., Segal, E. and Elinav, E. (2019). The pros, cons, and many unknowns of probiotics. *Nature Medicine*, 25 (5), pp. 716-729. https://doi.org/10.1038/s41591-019-0439-x

Sung, H., Ferlay, J., Siegel, R.L., Laversanne, M., Soerjomataram, I., Jemal, A. and Bray, F. (2021). Global cancer statistics 2020: GLOBOCAN estimates of incidence and mortality worldwide for 36 cancers in 185 countries. *CA: A Cancer Journal for Clinicians*, 71 (3), pp. 209-249. https://doi.org/10.3322/caac.21660

Sutton, S. (2011). Accuracy of plate counts. *Journal of Validation Technology*, 17 (3), pp. 42-46. Available at: http://www.microbiologynetwork.com/content/file/JVT_2011_v17n3_Accuracy-of-Plate-Count.pdf (Accessed: 21 February 2024).

Suzzi, G. and Corsetti, A. (2020). Food microbiology: The past and the new challenges for the next 10 Years. *Frontiers in Microbiology*, 11, https://doi.org/10.3389/fmicb.2020.00237

Swanson, K.S., Gibson, G.R., Hutkins, R., Reimer, R.A., Reid, G., Verbeke, K., Scott, K.P., Holscher, H.D., Azad, M.B., Delzenne, N.M. and Sanders, M.E. (2020). The International Scientific Association for Probiotics and Prebiotics (ISAPP) consensus statement on the definition and scope of synbiotics. *Nature Reviews Gastroenterology & Hepatology*, 17 (11), pp. 687-701. https://doi.org/10.1038/s41575-020-0344-2

Symcel. (2024). Revolutionizing biofilm prevention: Microcalorimetric analysis of antimicrobial coatings and materials. Available at: https://symcel.com/application-notes/tag/biofilm (Accessed: 27 January 2025).

Symprove. (2021). Production process: Standard operating procedure. SOP No: WI-008. Farnham: Symprove Limited.

Tellapragada, C., Hasan, B., Antonelli, A., Maruri, A., de Vogel, C., Gijón, D., Coppi, M., Verbon, A., van Wamel, W., Rossolini, G.M. and Cantón, R. (2020). Isothermal microcalorimetry minimal inhibitory concentration testing in extensively drug resistant Gram-negative bacilli: A multicentre study. *Clinical Microbiology and Infection*, 26 (10), pp.1413-e1 – 1413-e7. https://doi.org/10.1016/j.cmi.2020.01.026

Thermometric. (1996). *2277 Thermal Activity Monitor: Instruction manual*. Thermometric AB and Scitech Software AB, Sweden.

Thriene, K. and Michels, K.B. (2023). Human gut microbiota plasticity throughout the life course. *International Journal of Environmental Research and Public Health*. 20 (2), 1463 (14pp). https://doi.org/10.3390/ijerph20021463

Thurlby, T. (2006). *Metabolically active micro organisms [sic] and methods for their production*. World Intellectual Property Organisation Patent no. WO2006035218A1. Available at: https://patents.google.com/patent/WO2006035218A1/en?oq=WO%2f2006%2f035218 (Accessed: 20 February 2024)

Tilg, H., Zmora, N., Adolph, T.E. and Elinav, E. (2020). The intestinal microbiota fuelling metabolic inflammation. *Nature Reviews Immunology*, 20 (1), pp. 40-54. https://doi.org/10.1038/s41577-019-0198-4

Todd, M.J. and Gomez, J. (2001). Enzyme kinetics determined using calorimetry: A general assay for enzyme activity? *Analytical Biochemistry*, 296 (2), pp. 179-87. https://doi.org/10.1006/abio.2001.5218

Toubon, G., Butel, M-J., Rozé, J-C., Nicolis, I., Delannoy, J., Zaros, C., Ancel, P-Y., Aires, J. and Charles, M-A. (2023). Early life factors influencing children gut microbiota at 3.5 years from two French birth cohorts. *Microorganisms*. 11 (6), 1390 (18pp). https://doi.org/10.3390/microorganisms11061390

Trampuz, A., Salzmann, S., Antheaume, J. and Daniels, A.U. (2007). Microcalorimetry: A novel method for detection of microbial contamination in platelet products. *Transfusion*, 47 (9), pp.1643-1650. https:// doi: 10.1111/j.1537-2995.2007.01336.x

Tranah, T.H., Edwards, L.A., Schnabl, B. and Shawcross, D.L. (2021). Targeting the gut-liver-immune axis to treat cirrhosis. *Gut,* 70 (5), pp. 982-994.

Türker, M. (2004). Development of biocalorimetry as a technique for process monitoring and control in technical scale fermentations. *Thermochimica Acta*, 419 (1-2), pp. 73-81. https://doi.org/10.1016/j.tca.2004.01.036

Urdaneta, V. and Casadesús, J. (2017). Interactions between bacteria and bile salts in the gastrointestinal and hepatobiliary tracts. *Frontiers in medicine*, 4, 163 (13pp). https://doi.org/10.3389/fmed.2017.00163

Vaghef-Mehrabany, E., Maleki, V., Behrooz, M., Ranjbar, F. and Ebrahimi-Mameghani, M. (2020). Can psychobiotics “mood” ify [*sic*] gut? An update systematic review of randomized controlled trials in healthy and clinical subjects, on anti-depressant effects of probiotics, prebiotics, and synbiotics. *Clinical Nutrition*, 39 (5), pp. 1395-1410. https://doi.org/10.1016/j.clnu.2019.06.004

Van den Abbeele, P., Ghyselinck, J., Moens, F. and Marzorati, M. (2018). Evaluation of the effect of Symprove against *C. difficile* using the SHIME® technology platform. Symprove internal report: 2015059/D573/C.difficile. pp. 1-55. (available upon request)

Vasiliu, O. (2023). The current state of research for psychobiotics use in the management of psychiatric disorders–A systematic literature review. *Frontline in Psychiatry*, 14, 1074736 (22pp). https://doi.org/10.3389/fpsyt.2023.1074736

Vinderola, G. and Burns, P. (2021). The Biotics Family. in da Cruz, A.G., Ranadheera, C.S., Nazzaro, F. and Mortazavian, A. (eds.) *Probiotics and prebiotics in foods: Challenges, innovations, and advances*. Academic Press, pp. 1-11.

Vinderola, G., Sanders, M.E., Salminen, S. and Szajewska, H. (2022). Postbiotics: The concept and their use in healthy populations. *Frontiers in Nutrition*, 9, 1002213 (7pp). https://doi.org/10.3389/fnut.2022.1002213

Vogel, S.C., Brito, N.H. and Callaghan, B.L. (2020). Early life stress and the development of the infant gut microbiota: Implications for mental health and neurocognitive development. *Current Psychiatry Reports*, 22, 61 (9pp). https://doi.org/10.1007/s11920-020-01186-9

von Ah, U., Wirz, D. and Daniels, A.U. (2008). Rapid differentiation of methicillin-susceptible *Staphylococcus aureus* from methicillin-resistant *S. aureus* and MIC determinations by isothermal microcalorimetry. *Journal of Clinical Microbiology*, 46 (6), pp. 2083-2087. https://doi.org/10.1128/jcm.00611-08

von Stockar, U., Maskow, T., Liu, J., Marison, I.W. and Patino, R. (2006). Thermodynamics of microbial growth and metabolism: An analysis of the current situation. *Journal of Biotechnology*, 121 (4), pp. 517-533. https://doi.org/10.1016/j.jbiotec.2005.08.012

Vrieze, A., de Groot, P.F., Kootte, R.S., Knaapen, M., Van Nood, E. and Nieuwdorp, M. (2013). Fecal transplant: A safe and sustainable clinical therapy for restoring intestinal microbial balance in human disease? *Best Practice & Research Clinical Gastroenterology*, 27 (1), pp. 127-137. https://doi.org/10.1016/j.bpg.2013.03.003

Wadsö, I. (1979). Biocalorimetry: Past and present. Some views about the future. *熱測定 (Netsu Sokutei)*, 6 (2), pp. 66-77. https://doi.org/10.11311/jscta1974.6.66

Wadsö, I. (1986). Bio-calorimetry. *Trends in Biotechnology*, 4 (2), pp. 45-51. https://doi.org/10.1016/0167-7799(86)90153-8

Wadsö, I. (2002). Isothermal microcalorimetry in applied biology. *Thermochimica Acta*, 394 (1-2), pp. 305-311. https://doi.org/10.1016/S0040-6031(02)00263-0

Wadsö, I. (2009). Characterization of microbial activity in soil by use of isothermal microcalorimetry. *Journal of Thermal Analysis and Calorimetry*, 95 (3), pp. 843–850. https://doi.org/10.1007/s10973-008-9467-3

Wadsö, L. and Galindo, F.G. (2009). Isothermal calorimetry for biological applications in food science and technology. *Food Control*, 20 (10), pp. 956-961. https://doi.org/10.1016/j.foodcont.2008.11.008

Wadsö, L., Salamanca, Y. and Johansson, S. (2011). Biological applications of a new isothermal calorimeter that simultaneously measures at four temperatures. *Journal of Thermal Analysis and Calorimetry*, 104 (1), pp. 119-126. https://doi.org/10.1007/s10973-010-1140-y

Walter, J. and Ley, R. (2011). The human gut microbiome: Ecology and recent evolutionary changes. *Annual Review of Microbiology*, 65, pp. 411-429. https://doi.org/10.1146/annurev-micro-090110-102830

Wang, Y., Wang, G., Moitessier, N. and Mittermaier, A.K. (2020). Enzyme kinetics by isothermal titration calorimetry: Allostery, inhibition, and dynamics. *Frontiers in Molecular Biosciences*, 7, 583826 (19pp). https://doi.org/10.3389/fmolb.2020.583826

Weerth, C. de, Aatsinki, A.K., Azad, M.B., Bartol, F.F., Bode, L., Collado, M.C., Dettmer, A.M., Field, C.J., Guilfoyle, M., Hinde, K. and Korosi, A. (2023). Human milk: From complex tailored nutrition to bioactive impact on child cognition and behavior. *Critical Reviews in Food Science and Nutrition*, 63 (26), pp. 7945-7982. https://doi.org/10.1080/10408398.2022.2053058

Weitzel, M.L.J., Vegge, C.S., Pane, M., Goldman, V.S., Koshy, B., Porsby, C.H., Burguière, P. and Schoeni, J.L. (2021). Improving and comparing probiotic plate count methods by analytical procedure lifecycle management. *Frontiers in Microbiology*, 12, 693066 (17pp). https://doi.org/10.3389/fmicb.2021.693066

Wernli, L., Bonkat, G., Gasser, T.C., Bachmann, A. and Braissant, O. (2013). Use of isothermal microcalorimetry to quantify the influence of glucose and antifungals on the growth of *Candida albicans* in urine. *Journal of Applied Microbiology*, 115 (5), pp. 1186-1193. https://doi.org/10.1111/jam.12306

Whiting, C., Abdel Azim, S. and Friedman, A. (2024). the skin microbiome and its significance for dermatologists. *American Journal of Clinical Dermatology*, 25 (2), pp. 169–177. https://doi.org/10.1007/s40257-023-00842-z

Willson, R.J., Beezer, A.E., Mitchell, J.C. and Loh, W. (1995). Determination of thermodynamic and kinetic parameters from isothermal heat conduction microcalorimetry: Applications to long-term-reaction studies. *The Journal of Physical Chemistry*, 99 (18), pp. 7108-7113. https://doi-org.libproxy.ucl.ac.uk/10.1021/j100018a051

Willson, R.J., Beezer, A.E. and Mitchell, J.C. (1996). Solid state reactions studied by isothermal microcalorimetry: The solid state oxidation of ascorbic acid. *International Journal of Pharmaceutics*, 132 (1-2), pp. 45-51. https://doi.org/10.1016/0378-5173(95)04339-X

Willson, R.J. and Beezer, A.E. (2003). A mathematical approach for the calculation of reaction order for common solution phase reactions. *Thermochimica Acta*, 402 (1-2), pp. 75-80. https://doi.org/10.1016/S0040-6031(02)00534-8

Wiredu Ocansey, D.K., Hang, S., Yuan, X., Qian, H., Zhou, M., Olovo, C. V., Zhang, X. and Mao, F. (2023). The diagnostic and prognostic potential of gut bacteria in inflammatory bowel disease. *Gut Microbes*, 15 (1), 2176118 (28pp). https://doi.org/10.1080/19490976.2023.2176118

Wu, J., Singleton, S.S., Bhuiyan, U., Krammer, L. and Mazumder, R. (2024). Multi-omics approaches to studying gastrointestinal microbiome in the context of precision medicine and machine learning. *Frontiers in Molecular Biosciences*, 10, 1337373 (8pp). https://doi.org/10.3389/fmolb.2023.1337373

Xiufang, Y., Honglin, Z., Zhiping, L., Hu, H., Maosun, L. and Jiurong, Y. (1997). Determination of power-time curves of *Staphylococcus aureus* growth and study of promoter action of a ginseng. *Journal of Thermal Analysis and Calorimetry*, 50 (3), pp. 499-503. https://doi.org/10.1007/bf01980509

Yamin, D., Uskoković, V., Wakil, A.M., Goni, M.D., Shamsuddin, S.H., Mustafa, F.H., Alfouzan, W.A., Alissa, M., Alshengeti, A., Almaghrabi, R.H. and Fares, M.A.A. (2023). Current and future technologies for the detection of antibiotic-resistant bacteria. *Diagnostics*, 13 (20), 3246 (43pp). https://doi.org/10.3390/diagnostics13203246

Ying, G., Zhang, S., Hu, Y., Yang, M., Chen, P., Wu, X., Guo, W. and Kong, W. (2017). Antibacterial evaluation of *Salvia miltiorrhizae* on *Escherichia coli* by microcalorimetry coupled with chemometrics. *AMB Express*, 7 (1), pp. 1-11. https://doi.org/10.1186/s13568-017-0359-4

Yu, Y., Wang, W. and Zhang, F. (2023). The next generation fecal microbiota transplantation: To transplant bacteria or virome. *Advanced Science*, 10 (35), 2301097 (17pp). https://doi.org/10.1002/advs.202301097

Zaura, E., Koopman, J. E., Fernandez y Mostajo, M. and Crielaard, W. (2014). The Oral Microbiome. in Marchesi, J.R. (ed.) *The Human Microbiota and Microbiome.* Croydon: CABI, pp. 20-31.

Zawistowska-Rojek, A., Zareba, T. and Tyski, S. (2022). Microbiological testing of probiotic preparations. *International Journal of Environmental Research and Public Health*, 19 (9), 5701 (19pp). https://doi.org/10.3390/ijerph19095701

Zhang, W., Zhang, K., Zhang, P., Zheng, J., Min, C. and Li, X. (2021). Research Progress of Pancreas-Related Microorganisms and Pancreatic Cancer. *Frontiers in Oncology*, 10, 604531 (12pp). https://doi.org/10.3389/fonc.2020.604531

Zimehl, R., Drews, J. and Fischer-Brandies, H. (2002). Thermometric monitoring of setting biomaterials. *Thermochimica Acta*, 382 (1-2), pp. 161-168. https://doi.org/10.1016/S0040-6031(01)00726-2

Ziyaina, M., Rasco, B. and Sablani, S.S. (2020). Rapid methods of microbial detection in dairy products. *Food Control*, 110, 107008 (8pp). https://doi.org/10.1016/j.foodcont.2019.107008

Zou, Q., Feng. L., Cai, X., Qian, Y. and Xu, L. (2023). Esophageal microflora in esophageal diseases. *Frontiers in Cellular and Infection Microbiology*. 13, 1145791 (11pp). https://doi.org/10.3389/fcimb.2023.1145791

Zwietering, M.H., Jongenburger, I., Rombouts, F.M. and Van't Riet, K. (1990). Modeling of the bacterial growth curve. *Applied and Environmental Microbiology*, 56 (6), pp. 1875-1881. https://doi.org/10.1128/aem.56.6.1875-1881.1990

Appendices

Appendix Chapter 4

$t_{peak} = t_{lag} + nt_g$

Thus;

$t_{peak(0.3)} = t_{lag} + n_{(0.3)}t_g$

and;

$t_{peak(3)} = t_{lag} + n_{(3)}t_g$

eliminating t_{lag} yields;

$t_{peak(0.3)} - n_{(0.3)}t_g = t_{peak(3)} - n_{(3)}t_g$

rearranging;

$n_{(0.3)} - n_{(3)} = \frac{\text{tpe} \quad (0.3) - \text{tpeak}(3)}{tg}$

repeating for;

$t_{peak(30)} = t_{lag} + n_{(30)}t_g$

$t_{peak(300)} = t_{lag} + n_{(300)}t_g$

gives;

$$\boldsymbol{n_{(0.3)} - n_{(3)}} = \frac{tpeak(0.3) - tpeak(3)}{tg} = \frac{(55713+229\ ) - (44503+2290)}{4125} = \frac{11210}{4125} = \quad \mathbf{2.7}$$

$$\boldsymbol{n_{(3)} - n_{(30)}} = \frac{tpeak(3) - tpeak(30)}{tg} = \frac{(44503+2290) - (33952+2290)}{4125} = \frac{10551}{4125} = \quad \mathbf{2.6}$$

$$\boldsymbol{n_{(30)} - n_{(300)}} = \frac{tpeak(30) - tpeak(300)}{tg} = \frac{(33952+229\ ) - (22442+229\ )}{4125} = \frac{11510}{4125} = \quad \mathbf{2.8}$$

503.1 run

1. No transformation = raw data;

2. Logarithmic transformation = first order process indicator;
3. Integration = cumulative heat;
4. Logarithmic transformation of integrated p-t curve;
5. Q (J) heat signal data directly from TAM.

1. No transformation;
    a. AUC_{PP} = 9.97×10^{6}
    b. AUC_{exact} = 1.14×10^{6} = 11.42% of AUC_{PP}

2. Logarithmically transformed p-t curve;
    a. AUC_{PP} = 1.65×10^{5}
    b. AUC_{exact} = 5.10×10^{4} = 30.88% of AUC_{PP}

3. Integrated p-t curve;
    a. AUC_{PP} = 7.94×10^{10}
    b. AUC_{exact} = 5.92×10^{9} = 7.46% of AUC_{PP}

4. Logarithmic transformation of integrated p-t curve;
    a. AUC_{PP} = 4.47×10^{5}
    b. AUC_{exact} = 1.50×10^{5} = 33.57% of AUC_{PP}
5. Raw TAM data for Q (J);
    a. AUC_{PP} = 5.96×10^{4}
    b. AUC_{exact} = 5.93×10^{3} = 9.93% of AUC_{PP}

Appendix Chapter 5

The graph below (**Figure A5**), illustrates that each of the individual organisms in the Symprove product shows very different outcome upon IMC examination. This is suggestive of the possibility to distinguish between them from a single set of four experiments in under 11 hours.

The matrix (**Table A5**) is an example of distinction between organisms. Whilst some parameters are similar, they are similar but not precise, other parameters are completely different. For example, AUCs to PP for *L. rhamnosus* and *L. plantarum* are similar as are their times to PP, however, their PPs, intercepts and growth rates (*k*) are completely different

It is not claimed here that any random organisms can be identified like this, but in this closely defined world (limited world of Symprove –four known microorganisms) it was possible to differentiate the organisms from one another. If enough work was done, (because it was possible to discriminate between three species of *Lactobacilli*) it is plausible that discrimination between more organisms (to even strain level) not yet included in this matrix and from different environments is attainable. It also appears that shape analysis on its own is inadequate in a way, it is important, but it is not detailed enough. Although the complexity of what was shown here suggests the prospect of discrimination perhaps only in limited worlds, it would be worthwhile to explore these possibilities in future work.

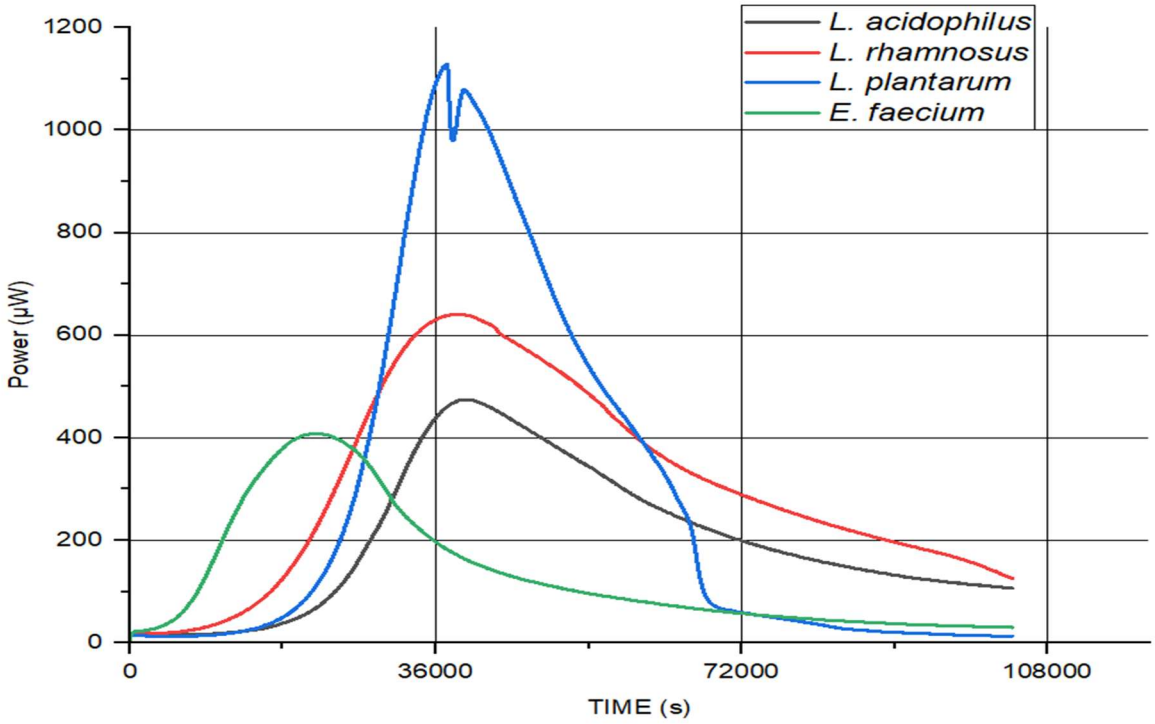

Figure A5 P-t curves of the individual Symprove organisms (*L. acidophilus*, *L. rhamnosus*, *L. plantarum* and *E. faecium*) tested in a batch of MRS (without Tween).

Experiment number	**387.1**	**387.2**	**387.3**	**387.4**
	L. acidophilus	*L. rhamnosus*	*L. plantarum*	*E. faecium*
p-t curve parameters				
Time to PP [s]	39042	38142	37252	22161
PP [µW]	474	640	1129	408
AUC to PP	5.25×10^{6}	9.29×10^{6}	9.42×10^{6}	4.59×10^{6}
ln curve parameters				
k (slope)	1.69×10^{-4}	1.58×10^{-4}	2.06×10^{-4}	2.84×10^{-4}
Intercept (ln value)	0.53	1.99	0.19	2.33
Intercept (antiln value)	1.70	7.32	1.21	10.28
R^2	0.9998	0.9999	0.9999	0.9998

Table A5 P-t curve shape analysis parameters (PP, time and AUC to PP) and logarithmic transformation parameters (slope, intercept) of the individual Symprove organisms, tested in MRS.